The Pennsylvania State University

The Graduate School

Eberly College of Science

# FUNCTIONAL ASSESSMENT OF TRANSCRIPTIONAL REGULATION IN THE METHANOGEN, METHANOSARCINA ACETIVORANS

A Dissertation in

Biochemistry, Microbiology and Molecular Biology

by

Matthew James Reichlen

© 2010 Matthew James Reichlen

Submitted in Partial Fulfillment
of the Requirements
for the Degree of

Doctor of Philosophy

May 2010

The dissertation of Matthew James Reichlen was reviewed and approved* by the following:

James G. Ferry
Stanley Person Professor and Director, Center for Microbial Structural Biology
Dissertation Co-Advisor
Co-Chair of Committee

Katsuhiko Murakami
Associate Professor of Biochemistry and Molecular Biology
Dissertation Co-Advisor
Co-Chair of Committee

Sarah Ades
Associate Professor of Biochemistry and Molecular Biology

Philip C. Bevilacqua
Professor of Chemistry

B. Franklin Pugh
Willaman Professor of Molecular Biology

Scott B. Selleck
Professor and Head of the Department of Biochemistry and Molecular Biology

*Signatures are on file in the Graduate School

# Abstract

The methanogenic archaea play an essential role in the biosphere by controlling the flux of carbon between oxic and anoxic environments. Yet much of the basic the physiology of these organisms is poorly understood. This dissertation strives to further the understanding of gene regulation in the methanogenic archaea using the model organism, *Methanosarcina acetivorans*. The first two chapters provide overviews of the methanogens and of the current understanding on archaeal transcription. The final four chapters describe the experimental work performed. A functional investigation of the three TATA-binding protein (TBP) homologs in *M. acetivorans* is described in chapter 3. TBP1 was found to function as the primary general transcription factor (GTF) and was essential for *M. acetivorans* growth. The minor TBPs, TBP2 and TBP3 were dispensable for growth but required for optimal fitness during culturing with acetate likely due to a role in the optimization of gene expression. Chapter 4 analyzes the transcriptional response of *M. acetivorans* diauxic growth with methanol and acetate. This analysis of a metabolic transition, the first of its kind for a methanogen, significantly contributed to the understanding of *M. acetivorans* physiology and ascribed potential biological roles to numerous previously uncharacterized or poorly characterized genes. The fifth chapter describes a functional investigation of MA3302, a member of a widespread yet uncharacterized family of euryarchaeal transcription factors. MA3302 expression was elevated during acetoclastic growth, was required for optimal growth on this substrate and was highly conserved in acetotrophic methanogens consistent with an involvement in transcriptional regulation during growth on acetate. Future investigations will seek to identify target genes for regulation by MA3302 and to overexpress, purify and characterize the recombinant MA3302 protein. Ongoing investigations addressing the roles of the three *M. acetivorans* TBP homologs are presented in the final chapter. Unresolved issues under investigation include assessments of why *tbp1* is essential for *M. acetivorans* growth and of physiological consequence resulting from the simultaneous deletion of *tbp2* and *tbp3* and to identify DNA-binding loci for each TBP isomer on the *M. acetivorans* chromosome.

# Table of Contents

# List of Figures

# List of Tables

# List of Abbreviations

| | |
|---|---|
| **TBP** | TATA-binding protein |
| **TFB,E,S** | Archaeal transcription factor B, E or S |
| **TFIIA,B,D,E,F,H** | Eukaryotic RNA polymerase II transcription initiation factor A,B, D, E, F or H |
| **TFIIIA,B,C** | Eukaryotic RNA polymerase III transcription initiation factor A,B or C |
| **$TAF_{I,II,III}$** | TBP-associated factor for RNA polymerase I, II or III |
| **$BRE_{u,d}$** | TFB/TFIIB recognition element upstream or downstream of the TATA box |
| **GTF** | General transcription factor |
| **PIC** | Preinitiation complex |
| **TRF** | TBP-related factor |
| **TSS** | Transcription start site |
| **TMA** | Trimethylamine |
| **qRT-PCR** | Quantitative real time reverse transcriptase polymerase chain reaction |
| **Pur** | Puromycin |
| **8ADP** | 8-aza-2,6-diaminopurine |
| **TrmB** | Thermococcus regulator of maltose binding |

# Acknowledgements

I extend my thanks and appreciation to all the people who have helped to enrich my graduate career at Penn State. My deepest gratitude goes out to my advisors, Drs. James G. Ferry and Katsuhiko Murakami for their invaluable training and constant encouragement. They have fostered my love of science and my development as an independent thinker. I thank the remaining members of my committee Drs. Sarah Ades, Philip Bevilacqua and Frank Pugh for their thoughtful suggestions to guide the direction of my research. Thanks go out to all the past and present members of the Ferry and Murakami research groups for their help and support. I am grateful to have had the opportunity to work with such a diverse collection of individuals. Too many people have come and gone to mention everyone. I will say with confidence that everyone brought a unique quality to the table. It has made the day to day life in the lab interesting if nothing else. Lastly, I would like to thank my family especially my parents for their support, encouragement and mostly importantly, their patience with me throughout this process.

# Chapter 1

# Methanogens: Ecology, Physiology and Metabolism

## Overview

Methanogenesis is the biological process by which simple carbon compounds are converted into methane gas ($CH_4$). Virtually all methanogenesis is carried out by a group of strictly anaerobic microorganisms from the *Archaea* domain known as methanogens. On an annual basis, methanogens are responsible for the production of approximately one billion metric tons of $CH_4$ gas. An approximately equal amount is released abioticly from the melting of methane hydrates. To put this number into its proper perspective, it is estimated that roughly 70 billion tons of $CO_2$ are fixed into biomass annually. Therefore, approximately two percent of the biomass synthesized annually eventually becomes converted to $CH_4$ (46). Most of the $CH_4$ produced is oxidized to $CO_2$ by methanotrophic microorganisms. However, around 400 million metric tons of $CH_4$ per year eventually escapes into the atmosphere. This can be viewed as both an enormous quantity and virtually untapped source of renewable energy, $CH_4$ which is the primary component of natural gas and as a frighteningly large release of a potent greenhouse gas with roughly 30 times the greenhouse capacity of $CO_2$. This of particular relevance in light of the fact that human activities (i.e. increased populations of ruminate animals) are thought to have

attributed to an increase in the atmospheric concentration of $CH_4$ over the past century (52).

Methanogens represent the largest and most well-studied group of organisms in the *Archaea* domain (52). The *Archaea,* the so called third domain of life, are distinct from the *Eukarya* and the *Bacteria*, as dictated by the unique sequence of their small subunit ribosomal RNA (50). Like the *Bacteria,* all members of the *Archaea* are single cellular prokaryotes, and while they possess several superficial characteristics that also persist across the *Bacteria* (i.e. cell size, genome size, gross morphology), the *Archaea* are distinguished from *Bacteria* in several key aspects. For instance, the polar and non-polar groups of archaeal membranes are bound by an ether linkage, while in the membranes of bacterial and eukaryotic species, lipid bilayers contain phospholipids with a polar glycerol linked a non-polar fatty acid by an ester linkage. In many cases, particularly in thermophilic archaea, the cellular membranes are further distinguished by a lipid monolayer with two polar ends which is thought to increase its stability (23). Archaeal species also differ from the *Bacteria* in cell wall structure. Unlike bacterial species, the cell walls in archaeal species are devoid of peptidoglycan, although some species do produce a related compound called pseudomurein (21), and are typically composed of a proteinaceous S layer. In addition, the archaeal cellular machinery for gene expression including DNA replication, transcription (described in detail in Chapter 2), and translation has much greater similarity to that in *Eukarya* than to that in *Bacteria*.

A diverse array of anaerobic environments are occupied by methanogens, including the lower intestinal tract of ruminate animals, freshwater and marine sediments, rice paddies, hydrothermal vents, the subsurface layer, sewage digesters and landfills (13,

52). Methanogens also occupy wide ranges of temperature (5-120$^{o}$C), salinity (fresh water to brine) and pH (~3-10) (13, 52). Complex organics that collect in these environments require the action of a consortium of three different groups of anaerobic microorganisms for sequential conversion into $CO_2$ and $CH_4$ – a process that is essential to the global carbon cycle (Fig. 1-1). The first group is comprised of fermentative bacteria, which break down the complex organic material to acetate, $H_2$, $CO_2$ and volatile fatty acids. The second group, $H_2$-producing acetogenic bacteria, metabolizes the volatile fatty acids into acetate, $H_2$ and $CO_2$. Lastly, the methanogens convert these metabolites to $CH_4$ and $CO_2$ gasses, which can then escape to the aerobic environment. The $CH_4$ produced by this metabolic sequence can then, in turn, have several possible outcomes: it can be aerobically oxidized to $CO_2$ by methanotrophic bacteria with $O_2$ as a terminal electron acceptor (19), anaerobically oxidized to $CO_2$ by a consortium of methanotrophic archaea and sulfate-reducing bacteria which utilize $SO_4^{2-}$ as a terminal electron acceptor (6, 42), or it can escape into the atmosphere where it eventually becomes photo-oxidized to $CO_2$ by UV radiation.

Approximately two thirds of the world's biologically produced methane originates from the methyl moiety of acetate (11-13), while the remaining one third originates from the reduction of $CO_2$ to methane with $H_2$ or formate providing the reducing equivalents (45). Smaller amounts of $CH_4$ also originate from the dismutation of C-1 compounds such as methanol, methylamines and methylthiols to $CH_4$ and $CO_2$ (7, 8, 22).

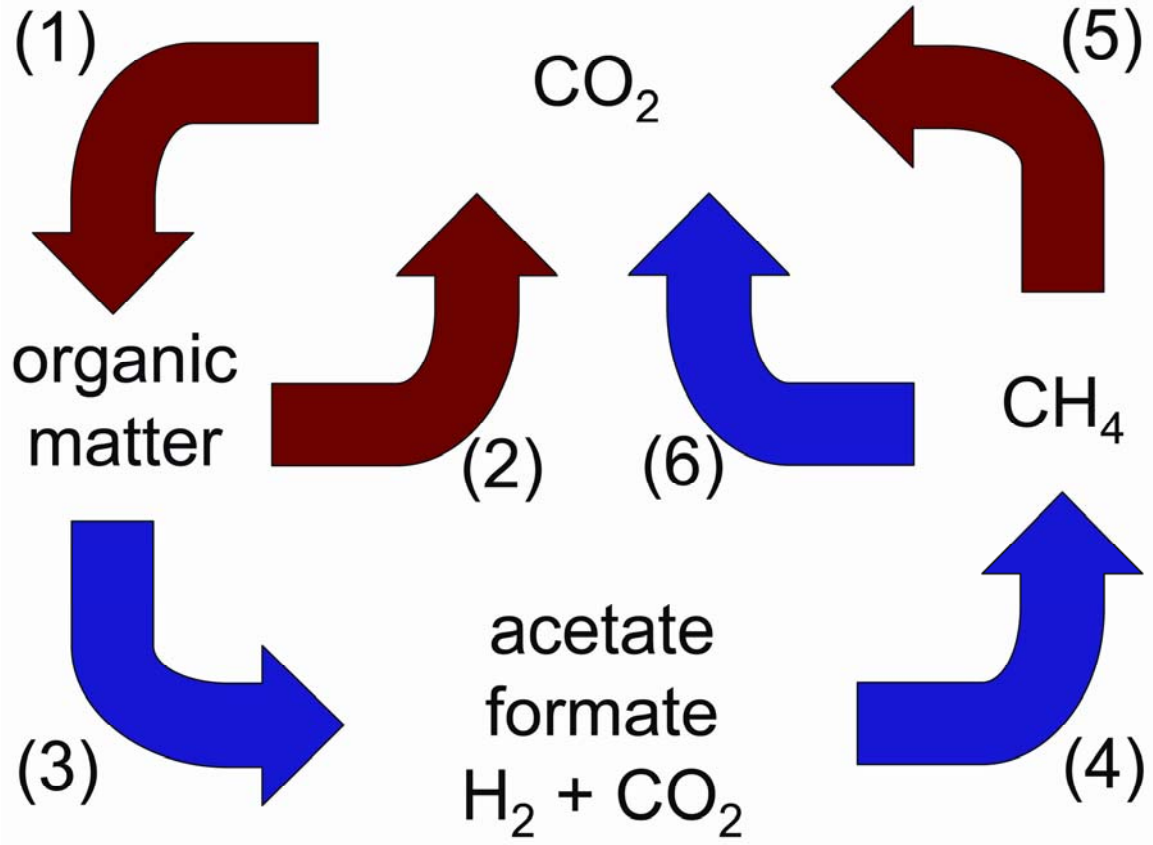


**Figure 1-1. The steps involved in the global carbon cycle.** Modified from (13). Steps colored red occur aerobically. Steps colored blue occur anaerobically. In step 1 organic matter is generated from $CO_2$ fixation and aerobically metabolized back to $CO_2$ in step 2. Organic matter sequestered in anoxic zones is broken down by fermentative and acetogenic bacteria in step 3, and the by-products of this metabolism are used as substrates for methangenesis in step 4. $CH_4$ produced can be oxidized back to $CO_2$ aerobically methanotrophic bacteria or photo-oxidation in step 5, or it can anaerobically oxidized to $CO_2$ by anaerobic oxidation of methane (AOM) in step 6.

It should be pointed out that all known methanogens are metabolic specialists. All are obligate methanogens, and most are only capable of growth on a very narrow range of substrates all of which are very simple carbon compounds. In order to conserve energy necessary for growth during the stepwise reduction of these substrates to methane, protons are translocated across the cellular membrane creating an electrochemical gradient which is used to drive ATP synthesis using an $A_1A_0$-type ATP synthase (8). It is not entirely understood why methanogens cannot utilize more complex catabolites such as sugars. One leading view is that because of the complexity of the machinery required for methanogenesis, methanogens are simply out-competed for these substrates by more specialized fermentative organisms (52).

## Pathways of Methanogenesis

Presently, there are three known pathways of the methanogenesis: 1) the acetoclastic pathway in which the methyl-moiety of acetate is reduced to $CH_4$ and the carboxyl group is oxidized to $CO_2$, 2) the $CO_2$-reducing pathway in which $CO_2$ is reduced to $CH_4$ with electrons supplied typically from $H_2$ or formate, and 3) the methylotrophic pathway in which the methyl groups from C-1 compounds such as methanol and methylamines are dismuted to $CH_4$ and $CO_2$ in a 3:1 ratio with the electrons derived from the oxidation of one methyl group being used to reduce the remaining three to $CH_4$. The balanced equations for each of theses reactions are as follows:

$$CH_3COO^- + H^+ \rightarrow CH_4 + CO_2 \quad (1)$$

$$CO_2 + 4H_2 \rightarrow CH_4 + 2H_2O \quad (2)$$

$$CH_3OH + H_2O \rightarrow CO_2 + 6\ e^- \quad (3)$$

$$3CH_3OH + 6\ e^- \rightarrow 3CH_4 + 3H_2O \quad (4)$$

The steps involved in each of these pathways are depicted in Fig. 1-2, and the free energy availability from each of the net reactions is listed in Table 1-1. There are three steps which are common to both the acetoclastic and $CO_2$-reducing pathways (reaction 5-7), and two which are common to all three pathways (reaction 6-7). The first (reaction 5) is the transfer of a methyl group from the cofactor tetrahydromethanopterin (THMPT) to the cofactor coenzyme M (HS-CoM) catalyzed by the eight subunit membrane-bound $Na^+$ translocating $^5$*N*-methyl-THMPT:CoM methyltransferase (Mtr) (16). This is followed the reduction of the methyl group to $CH_4$. catalyzed by the enzyme complex methyl-CoM reductase (Mcr), which is highly conserved among methanogens (reaction 6). Electrons for this reaction are derived from a covalent reaction between HS-CoM and coenzyme B (HS-CoB) in which they generate a heterodisulphide: CoMS-SCoB (THMPT, Hs-CoM and HS-CoB are unique cofactors in methanogenic archaea). The final step (reaction 7) is the regeneration of the sulfhydryl forms of HS-CoM and HS-CoB catalyzed heterodisulfide reductase (Hdr). In order to drive ATP synthesis, the formation of a proton gradient is coupled to the reduction of CoMS-SCoB (34).

**Table 1-1. Standard free energy availability for common methanogenic substrates.** Modified from (33).

| Substrate | Reaction | $\Delta G^o$ kJ $mol^{-1}$ $CH_4$ |
|---|---|---|
| $H_2$ and $CO_2$ | $4H_2 + CO_2 \rightarrow CH_4 + 2H_2O$ | -130 |
| Formate | $4HCOOH \rightarrow 3CO_2 + CH_4$ | -119 |
| Acetate | $CH_3COO^- + H^+ \rightarrow CH_4 + H_2O$ | -36 |
| Methanol | $4CH_3OH \rightarrow 3CH_4 + CO_2$ | -106 |
| Trimethylamine[a] | $4(CH_3)_3NH^+ + 6H_2O \rightarrow 9CH_4 + 3CO_2 + 4NH_4^+$ | -76 |

[a] Other methylamines, momo- and dimethylamine can also be utilized

$$CH_3\text{-THMPT} + \text{HS-CoM} \rightarrow CH_3\text{-S-CoM} + \text{THMPT} \quad (5)$$

$$CH_3\text{-S-CoM} + \text{HS-CoB} \rightarrow \text{CoMS-SCoB} + CH_4 \quad (6)$$

$$\text{CoMS-SCoB} + 2e^- + 2H^+ \rightarrow \text{HS-CoM} + \text{HS-CoB} \quad (7)$$

The acetoclastic and $CO_2$-reducing pathways are distinguished by how acetate and $CO_2$ are converted to $CH_3$-THMPT, and the methylotrophic pathway is distinguished from both by how C-1 compounds are converted to $CH_3$-S-CoM.

The conversion of acetate to $CH_3$-THMPT first requires the activation of acetate to acetyl-CoA catalyzed by acetate kinase (Ack) and phosphotransacetylase (Pta), two enzymes which are common to many pathogenic gram negative bacteria. Ack first converts acetate to acetyl-phosphate at the expense of one ATP molecule. Pta then transfers the acetyl group to coenzyme A (HS-CoA) generating acetyl-CoA and inorganic phosphate. The acetoclastic splitting of the C-C and C-S bonds of acetyl-CoA is catalyzed by the five subunit CO dehydrogenase/acetyl-CoA synthase (Cdh/Acs) complex. This liberates the methyl moiety to be transferred to THMPT, and the carbonyl

group is oxidized to $CO_2$ with the electrons being used to reduce ferredoxin (Fd). The γ-class carbonic anhydrase (Cam) catalyzes the hydrolysis of the released $CO_2$ to $HCO_3$- facilitating the removal of $HCO_3$- from the cell.

In the conversion of $CO_2$ to $CH_3$-THMPT, $CO_2$ is first attached to the cofactor methanofuran (MF), another cofactor unique to methanogens, and is reduced to formyl-MF by formyl-MF dehydrogenase with electrons being supplied by $Fd^{red}$. The formyl group is transferred to THMPT by formyl-MF:THMPT formyltransferase generating $N^5$-formyl-THMPT. $N^5$-formyl-THMPT is reduced to $N^5$, $N^{10}$-methenyl-THMPT by methenyl-THMPT cyclohydrolase (Mch). $N^5$, $N^{10}$-methenyl-THMPT is reduced $N^5$, $N^{10}$-methylene-THMPT by $N^5$, $N^{10}$-methylene-THMPT dehydrogenase with electrons supplied by either $H_2$ or $F_{420}H_2$, a flavin-containing cofactor also unique to methanogens. Finally $N^5$, $N^{10}$-methylene-THMPT is reduced to $N^5$-methyl-THMPT by $N^5$, $N^{10}$-methylene-THMPT reductase with electrons donated by $F_{420}H_2$.

In the dismutation of C-1 compounds to $CH_4$, the methyl moiety is transferred to HS-CoM by two substrate-specific methyltransferase designated MT1 and MT2. MT1 consists of two polypeptides. The first is the methyltransferase, and it catalyzes the transfer of the methyl group of the C-1 compound to a corrinoid cofactor on the second polypeptide. This corrinoid cofactor is the substrate for MT2 which then transfers the methyl group to HS-CoM generating $CH_3$-S-CoM. The $CH_3$-S-CoM is dismuted in a 3:1 ratio with one methyl group being oxidized to $CO_2$ in a reversal of the steps for reduction of $CO_2$ to $CH_3$-S-CoM. This oxidation supplies the 6 e- necessary for the reduction three methyl groups to $CH_4$.

## Substrate Usage Among the Major Methanogenic Groups

The methanogens are represented by five phylogenetically distinct orders within the Kingdom, *Euryarchaeota* which are the *Methanobacteriales,* the *Methanococcales,* the *Methanomicrobiales,* the *Methanopyrales* and the *Methanosarcinales* (Fig. 1-2). The former four groups derive their energy primarily from the reduction of $CO_2$ to $CH_4$ using electrons supplied by either $H_2$ or formate in most cases or occasionally with primary or secondary alcohols serving as electron donors (13, 52). Reduction of methanol with $H_2$ has been documented as well (13, 52). Many species from these groups are capable of directly fixing $CO_2$ into biomass. However, numerous other species are heterotrophic and require a secondary carbon source such as acetate or yeast extract for cell growth (13, 52). The *Methanosarcinales,* on the other hand, have a more diversified substrate range. This Order is sub-divided into two families, the *Methanosaetaceae* and the *Methanosarcinaceae*. Members of the *Methanosaetaceae* are only capable of growth and methanogenesis using acetate. This group is distinguished from all other methanogenic groups as being the only obligate acetotrophs (13). The family *Methanosarcinaceae*, in particular, the genus *Methanosarcina* is by far the most metabolically diverse group among the methanogenic archaea. All members of this family are capable of growth by the dismutation of various C-1 compounds such as methanol, methylamines, and, in some cases, methylthiols. In addition, most species in the *Methanosarcina* genus also have the capacity to reduce $CO_2$ to $CH_4$ using $H_2$ and to reduce to the methyl group of acetate to $CH_4$ making this the only genus capable of utilizing all three of the known pathways of methanogenesis (13, 52).

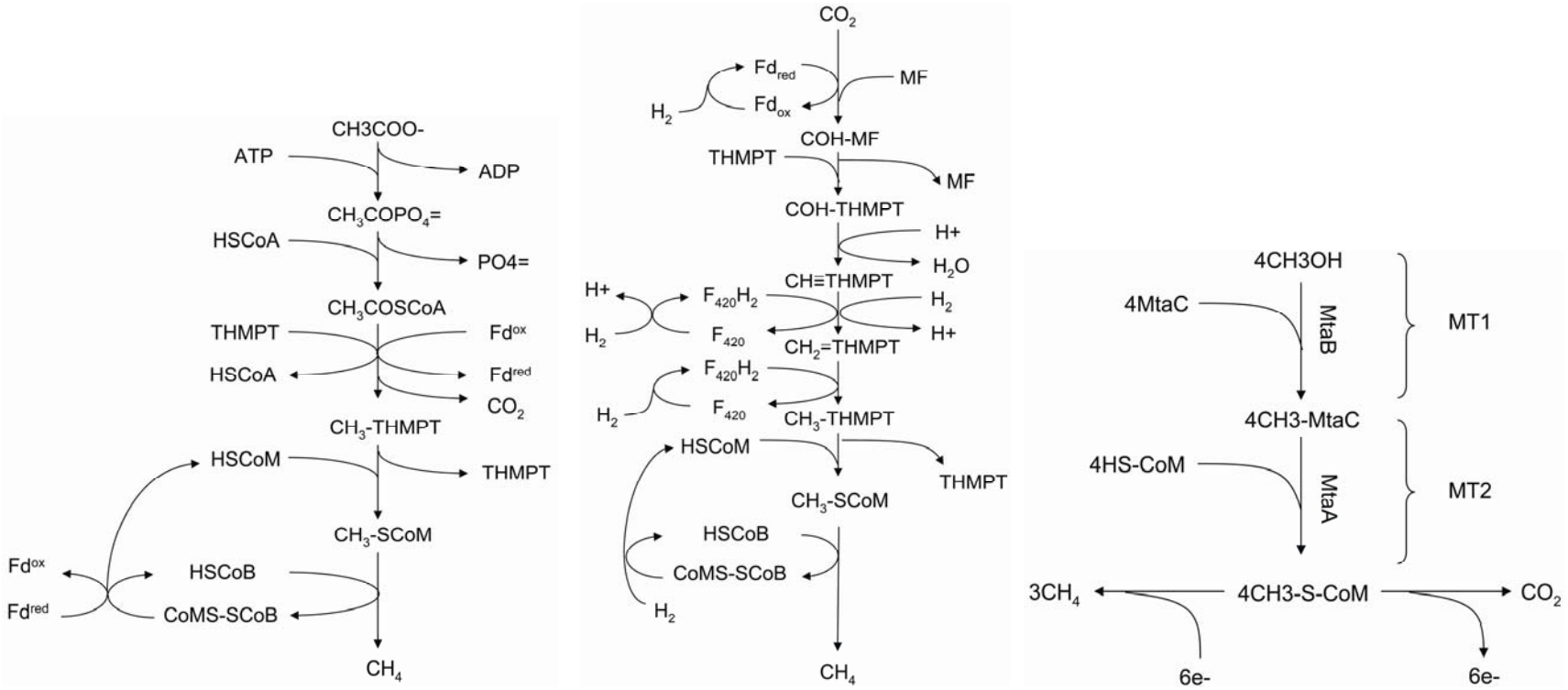


**Figure 1-2. Steps involved in the one carbon reactions for the three major methanogenic pathways.** Modified from (13). The acetoclastic pathway is shown on the left, the CO2-reducing pathway is shown in the middle, and the methylotrophic pathway (using methanol as the substrate) is shown on the right.

## *Methanosarcina* Species as Model Organisms

Although a wealth of information pertaining to the basic biochemistry of methanogenesis is known, there are still large gaps in the basic understanding of the overall physiology of the methanogenic archaea and for most archaeal species in general. For instance, very little is known about the mechanisms of gene expression regulation in these organisms. Despite the presence of numerous annotated putative transcription regulatory proteins on the genomes of most methanogens, only a handful has been experimentally investigated. Many of these investigations were performed in cell free *in vitro* transcription systems using a very limited number of promoters leaving the question of if the extent of the role these regulators have on the cell unresolved (47).

In most methanogens that are capable of growth utilizing only a single methanogenic pathway, the enzymes required for methanogenesis are essential for growth and not subject to differential regulation in response to growth substrate. This does not appear to be the case for *Methanosarcina* species. Due to their considerable metabolic flexibility compared to other methanogens, *Methanosarcina* species make ideal candidates for the investigation of the regulation of the different methanogenic pathways. Because there are substantial differences in the chemical reactions and the enzymes involved in these reactions for the different methanogenic pathways (Fig. 1-2), it has been hypothesized that genes encoding the enzymes each different pathway will be differentially regulated in response to growth substrate. Experimental evidence in support of this hypothesis has been reported on numerous occasions for *Methanosarcina*

*acetivorans, Methanosarcina mazei* and *Methanosarcina thermophila* (3, 5, 10, 20, 24, 26-29, 35, 44).

Completed genome sequences, which enable comparative genomic studies, are also available for three species in this genus: *M. acetivorans* (14), *M. mazei* (9) and *Methanosarcina barkeri* (www.tigr.org). The genomes of these organisms are among the largest in the *Archaea* (at 5.7 MB, *M. acetivorans* is in fact the largest). One striking feature about the genomes for these organisms is the large number of multigene families. *M. acetivorans,* for instance,contains 539 mutligene families which accounts for roughly half of its total genes (14). This feature might be a reflection of the versatility of these organisms.

Perhaps the most useful feature about the *Methanosarcina* species is that the genetic tools are available for these organisms (in particular for *M. acetivorans* and *M. barkeri*) are some of the most advanced in the *Archaea*. The tools available include specialized media for growth in single celled morphology (43), high efficiency plating (31, 43), high efficiency transformation (30), plasmid shuttle vectors (30), random *in vivo* transposon mutagenesis (51), directed mutagenesis (32), multiple selected antibiotic resistance markers (2, 15), multiple reporter genes (1, 37), markerless exchange tools (37, 40), high efficiency site-specific chromosomal integration (18) and conditional gene inactivation (18, 38). Development of these tools has been carried out primarily in the laboratory of Dr. William Metcalf at the University of Illinois at Urbana-Champaign. These tools have greatly aided the study of all facets of *Methanosarcina* physiology. In particular, they have enabled the study of the genetic requirements of individual enzymes in for the different pathways of methanogenesis. Such studies are only possible in

*Methanosarcina* species since mutants defective in one pathway are still capable of growth using an alternative pathway (4, 17, 25, 32, 36, 39, 41, 48, 49). Yet despite these advances, there are still three major obstacles to using these techniques. The first is that because these organisms are strict anaerobes, all growth and manipulation requires the use of specialized and often very expensive equipment as well as a considerable amount of skill on the part of the researcher. Second, because of the slow growth of these organisms, the time frame required for these experiments can be frustratingly long. Colony formation on solid media, for instance, takes approximately two weeks (30). Finally, at the present time, there are only two selectable markers available for these species (one of which is not commercially available) preventing multiple rounds mutagenesis. This problem can be circumvented with the use of markerless exchange techniques (37, 40). However, this process is time consuming (requiring 6 weeks for a single mutant under ideal circumstances), and requires extensive screening because of the high frequency of spontaneously resistant mutants to the drug used in counter selection (37).

## References

1. **Apolinario, E. E., K. M. Jackson, and K. R. Sowers.** 2005. Development of a plasmid-mediated reporter system for in vivo monitoring of gene expression in the archaeon Methanosarcina acetivorans. Appl Environ Microbiol **71:**4914-8.
2. **Boccazzi, P., J. K. Zhang, and W. W. Metcalf.** 2000. Generation of dominant selectable markers for resistance to pseudomonic acid by cloning and mutagenesis

of the ileS gene from the archaeon Methanosarcina barkeri fusaro. J Bacteriol **182:**2611-8.

3. **Bose, A., G. Kulkarni, and W. W. Metcalf.** 2009. Regulation of putative methyl-sulphide methyltransferases in Methanosarcina acetivorans C2A. Mol Microbiol **74:**227-38.
4. **Bose, A., M. A. Pritchett, and W. W. Metcalf.** 2008. Genetic analysis of the methanol- and methylamine-specific methyltransferase 2 genes of Methanosarcina acetivorans C2A. J Bacteriol **190:**4017-26.
5. **Bose, A., M. A. Pritchett, M. Rother, and W. W. Metcalf.** 2006. Differential Regulation of the Three Methanol Methyltransferase Isozymes in Methanosarcina acetivorans C2A. J Bacteriol **188:**7274-83.
6. **Caldwell, S. L., J. R. Laidler, E. A. Brewer, J. O. Eberly, S. C. Sandborgh, and F. S. Colwell.** 2008. Anaerobic oxidation of methane: mechanisms, bioenergetics, and the ecology of associated microorganisms. Environ Sci Technol **42:**6791-9.
7. **Deppenmeier, U.** 2004. The membrane-bound electron transport system of Methanosarcina species. J Bioenerg Biomembr **36:**55-64.
8. **Deppenmeier, U.** 2002. The unique biochemistry of methanogenesis. Prog Nucleic Acid Res Mol Biol **71:**223-83.
9. **Deppenmeier, U., A. Johann, T. Hartsch, R. Merkl, R. A. Schmitz, R. Martinez-Arias, A. Henne, A. Wiezer, S. Baumer, C. Jacobi, H. Bruggemann, T. Lienard, A. Christmann, M. Bomeke, S. Steckel, A. Bhattacharyya, A. Lykidis, R. Overbeek, H. P. Klenk, R. P. Gunsalus, H. J. Fritz, and G.**

**Gottschalk.** 2002. The genome of Methanosarcina mazei: evidence for lateral gene transfer between bacteria and archaea. J Mol Microbiol Biotechnol **4:**453-61.

10. **Ding, Y. H., S. P. Zhang, J. F. Tomb, and J. G. Ferry.** 2002. Genomic and proteomic analyses reveal multiple homologs of genes encoding enzymes of the methanol:coenzyme M methyltransferase system that are differentially expressed in methanol- and acetate-grown Methanosarcina thermophila. FEMS Microbiol Lett **215:**127-32.
11. **Ferry, J. G.** 1997. Enzymology of the fermentation of acetate to methane by Methanosarcina thermophila. Biofactors **6:**25-35.
12. **Ferry, J. G.** 1992. Methane from acetate. J Bacteriol **174:**5489-95.
13. **Ferry, J. G., and K. A. Kastead.** 2007. Methanogenesis, p. 288-314. *In* R. Cavicchioli (ed.), Archaea: Molecular and Cellular Biology. ASM Press, Washington, DC.
14. **Galagan, J. E., C. Nusbaum, A. Roy, M. G. Endrizzi, P. Macdonald, W. FitzHugh, S. Calvo, R. Engels, S. Smirnov, D. Atnoor, A. Brown, N. Allen, J. Naylor, N. Stange-Thomann, K. DeArellano, R. Johnson, L. Linton, P. McEwan, K. McKernan, J. Talamas, A. Tirrell, W. Ye, A. Zimmer, R. D. Barber, I. Cann, D. E. Graham, D. A. Grahame, A. M. Guss, R. Hedderich, C. Ingram-Smith, H. C. Kuettner, J. A. Krzycki, J. A. Leigh, W. Li, J. Liu, B. Mukhopadhyay, J. N. Reeve, K. Smith, T. A. Springer, L. A. Umayam, O. White, R. H. White, E. Conway de Macario, J. G. Ferry, K. F. Jarrell, H. Jing, A. J. Macario, I. Paulsen, M. Pritchett, K. R. Sowers, R. V. Swanson, S. H. Zinder, E. Lander, W. W. Metcalf, and B. Birren.** 2002. The genome of M.

acetivorans reveals extensive metabolic and physiological diversity. Genome Res **12:**532-42.

15. **Gernhardt, P., O. Possot, M. Foglino, L. Sibold, and A. Klein.** 1990. Construction of an integration vector for use in the archaebacterium Methanococcus voltae and expression of a eubacterial resistance gene. Mol Gen Genet **221:**273-9.

16. **Gottschalk, G., and R. K. Thauer.** 2001. The Na(+)-translocating methyltransferase complex from methanogenic archaea. Biochim Biophys Acta **1505:**28-36.

17. **Guss, A. M., B. Mukhopadhyay, J. K. Zhang, and W. W. Metcalf.** 2005. Genetic analysis of mch mutants in two Methanosarcina species demonstrates multiple roles for the methanopterin-dependent C-1 oxidation/reduction pathway and differences in H(2) metabolism between closely related species. Mol Microbiol **55:**1671-80.

18. **Guss, A. M., M. Rother, J. K. Zhang, G. Kulkarni, and W. W. Metcalf.** 2008. New methods for tightly regulated gene expression and highly efficient chromosomal integration of cloned genes for Methanosarcina species. Archaea **2:**193-203.

19. **Hakemian, A. S., and A. C. Rosenzweig.** 2007. The biochemistry of methane oxidation. Annu Rev Biochem **76:**223-41.

20. **Hovey, R., S. Lentes, A. Ehrenreich, K. Salmon, K. Saba, G. Gottschalk, R. P. Gunsalus, and U. Deppenmeier.** 2005. DNA microarray analysis of

Methanosarcina mazei Go1 reveals adaptation to different methanogenic substrates. Mol Genet Genomics **273:**225-39.

21. **Kandler, O., and H. Konig.** 1998. Cell wall polymers in Archaea (Archaebacteria). Cell Mol Life Sci **54:**305-8.

22. **Keltjens, J. T., and G. D. Vogels.** 1993. Conversion of Methanol and Methylamines to Methane and Carbon Dioxide, p. 253-303. *In* J. G. Ferry (ed.), Methanogenesis: Ecology, Physiology, Biochemistry and Genetics, vol. I. Chapman and Hall, New York, NY.

23. **Kletzin, A.** 2007. General Characteristics and Important Model Organisms, p. 14-92. *In* R. Cavicchioli (ed.), Archaea: Molecular and Cellular Biology. ASM Press, Washington, DC.

24. **Kratzer, C., P. Carini, R. Hovey, and U. Deppenmeier.** 2009. Transcriptional profiling of methyltransferase genes during growth of Methanosarcina mazei on trimethylamine. J Bacteriol **191:**5108-15.

25. **Kulkarni, G., D. M. Kridelbaugh, A. M. Guss, and W. W. Metcalf.** 2009. Hydrogen is a preferred intermediate in the energy-conserving electron transport chain of Methanosarcina barkeri. Proc Natl Acad Sci U S A **106:**15915-20.

26. **Lessner, D. J., L. Li, Q. Li, T. Rejtar, V. P. Andreev, M. Reichlen, K. Hill, J. J. Moran, B. L. Karger, and J. G. Ferry.** 2006. An unconventional pathway for reduction of CO2 to methane in CO-grown Methanosarcina acetivorans revealed by proteomics. Proc Natl Acad Sci U S A **103:**17921-6.

27. **Li, L., Q. Li, L. Rohlin, U. Kim, K. Salmon, T. Rejtar, R. P. Gunsalus, B. L. Karger, and J. G. Ferry.** 2007. Quantitative proteomic and microarray analysis

of the archaeon Methanosarcina acetivorans grown with acetate versus methanol. J Proteome Res **6:**759-71.

28. **Li, Q., L. Li, T. Rejtar, B. L. Karger, and J. G. Ferry.** 2005. Proteome of Methanosarcina acetivorans Part II: comparison of protein levels in acetate- and methanol-grown cells. J Proteome Res **4:**129-35.

29. **Li, Q., L. Li, T. Rejtar, D. J. Lessner, B. L. Karger, and J. G. Ferry.** 2006. Electron transport in the pathway of acetate conversion to methane in the marine archaeon Methanosarcina acetivorans. J Bacteriol **188:**702-10.

30. **Metcalf, W. W., J. K. Zhang, E. Apolinario, K. R. Sowers, and R. S. Wolfe.** 1997. A genetic system for Archaea of the genus Methanosarcina: liposome-mediated transformation and construction of shuttle vectors. Proc Natl Acad Sci U S A **94:**2626-31.

31. **Metcalf, W. W., J. K. Zhang, and R. S. Wolfe.** 1998. An anaerobic, intrachamber incubator for growth of Methanosarcina spp. on methanol-containing solid media. Appl Environ Microbiol **64:**768-70.

32. **Meuer, J., H. C. Kuettner, J. K. Zhang, R. Hedderich, and W. W. Metcalf.** 2002. Genetic analysis of the archaeon Methanosarcina barkeri Fusaro reveals a central role for Ech hydrogenase and ferredoxin in methanogenesis and carbon fixation. Proc Natl Acad Sci U S A **99:**5632-7.

33. **Muller, V., M. Blaut, and G. Gottschalk.** 1993. Bioenergetics of Methanogenesis, p. 360-406. *In* J. G. Ferry (ed.), Methanogenesis: Ecology, Physiology, Biochemistry and Genetics, vol. I. Chapman and Hall, New York, NY.

34. **Muller, V., C. Ruppert, and T. Lemker.** 1999. Structure and function of the A1A0-ATPases from methanogenic Archaea. J Bioenerg Biomembr **31:**15-27.

35. **Oelgeschlager, E., and M. Rother.** 2009. Influence of carbon monoxide on metabolite formation in Methanosarcina acetivorans. FEMS Microbiol Lett **292:**254-60.

36. **Pritchett, M. A., and W. W. Metcalf.** 2005. Genetic, physiological and biochemical characterization of multiple methanol methyltransferase isozymes in Methanosarcina acetivorans C2A. Mol Microbiol **56:**1183-94.

37. **Pritchett, M. A., J. K. Zhang, and W. W. Metcalf.** 2004. Development of a markerless genetic exchange method for Methanosarcina acetivorans C2A and its use in construction of new genetic tools for methanogenic archaea. Appl Environ Microbiol **70:**1425-33.

38. **Rother, M., P. Boccazzi, A. Bose, M. A. Pritchett, and W. W. Metcalf.** 2005. Methanol-dependent gene expression demonstrates that methyl-coenzyme M reductase is essential in Methanosarcina acetivorans C2A and allows isolation of mutants with defects in regulation of the methanol utilization pathway. J Bacteriol **187:**5552-9.

39. **Rother, M., and W. W. Metcalf.** 2004. Anaerobic growth of Methanosarcina acetivorans C2A on carbon monoxide: an unusual way of life for a methanogenic archaeon. Proc Natl Acad Sci U S A **101:**16929-34.

40. **Rother, M., and W. W. Metcalf.** 2005. Genetic technologies for Archaea. Curr Opin Microbiol **8:**745-51.

41. **Rother, M., E. Oelgeschlager, and W. M. Metcalf.** 2007. Genetic and proteomic analyses of CO utilization by Methanosarcina acetivorans. Arch Microbiol **188:**463-72.

42. **Shima, S., and R. K. Thauer.** 2005. Methyl-coenzyme M reductase and the anaerobic oxidation of methane in methanotrophic Archaea. Curr Opin Microbiol **8:**643-8.

43. **Sowers, K. R., J. E. Boone, and R. P. Gunsalus.** 1993. Disaggregation of Methanosarcina spp. and Growth as Single Cells at Elevated Osmolarity. Appl Environ Microbiol **59:**3832-3839.

44. **Sowers, K. R., T. T. Thai, and R. P. Gunsalus.** 1993. Transcriptional regulation of the carbon monoxide dehydrogenase gene (cdhA) in Methanosarcina thermophila. J Biol Chem **268:**23172-8.

45. **Thauer, R. K., R. Hedderich, and R. Fischer.** 1993. Reactions and Enzymes Involved in Methanogenesis from CO2 and H2, p. 209-252. *In* J. G. Ferry (ed.), Methanogenesis: Ecology, Physiology, Biochemistry and Genetics, vol. I. Chapman and Hall, New York, NY.

46. **Thauer, R. K., A. K. Kaster, H. Seedorf, W. Buckel, and R. Hedderich.** 2008. Methanogenic archaea: ecologically relevant differences in energy conservation. Nat Rev Microbiol **6:**579-91.

47. **Thomm, M.** 2007. Transcription: Mechanism and Regulation, p. 139-157. *In* R. Cavicchioli (ed.), Archaea: Molecular and Cellular Biology. ASM Press, Washington, DC.

48. **Welander, P. V., and W. W. Metcalf.** 2005. Loss of the mtr operon in Methanosarcina blocks growth on methanol, but not methanogenesis, and reveals an unknown methanogenic pathway. Proc Natl Acad Sci U S A **102:**10664-9.

49. **Welander, P. V., and W. W. Metcalf.** 2008. Mutagenesis of the C1 oxidation pathway in Methanosarcina barkeri: new insights into the Mtr/Mer bypass pathway. J Bacteriol **190:**1928-36.

50. **Woese, C. R., O. Kandler, and M. L. Wheelis.** 1990. Towards a natural system of organisms: proposal for the domains Archaea, Bacteria, and Eucarya. Proc Natl Acad Sci U S A **87:**4576-9.

51. **Zhang, J. K., M. A. Pritchett, D. J. Lampe, H. M. Robertson, and W. W. Metcalf.** 2000. In vivo transposon mutagenesis of the methanogenic archaeon Methanosarcina acetivorans C2A using a modified version of the insect mariner-family transposable element Himar1. Proc Natl Acad Sci U S A **97:**9665-70.

52. **Zinder, S. H.** 1993. Physiological Ecology of Methanogens, p. 128-206. *In* J. G. Ferry (ed.), Methanogenesis: Ecology, Physiology, Biochemistry and Genetics, vol. I. Chapman and Hall, New York, NY.

# Chapter 2

# Transcription in the *Archaea* and *Eukarya* domains

## Overview

On striking feature of the *Archaea* is that they possess a high degree of similarity to eukaryotes in the proteins utilized for gene expression. This includes proteins involved in coordinating DNA replication, translation and transcription, and it is reflective of the common ancestry shared by the two groups (109). This chapter will summarize the commonalities and differences in transcription initiation between the two domains of life with greatest emphasis on a comparison of the functional roles for the TATA-binding proteins (TBP) in the two domains.

TBP is a highly conserved protein found in all known species of *Archaea* and *Eukarya*, but not in *Bacteria* (1, 4, 7, 9, 14, 26, 29, 34, 82, 102, 103, 106). TBP orthologs are general transcription factors (GTF) essential for the transcription of most genes in the *Archaea* and *Eukarya* domains (82, 103). TBP binds promoter DNA along the minor groove at an AT-rich TATA-box sequence located approximately 25 bp upstream of the transcription start site and causes a sharp bend (~67-90$^0$) in the DNA backbone (57, 60, 76). The distortion of the DNA backbone is thought to assist in the recruitment of other general transcription factors to the promoter (82, 103). Archaeal TBPs and the C-

terminal domain of the eukaryal TBPs are approximately 180 amino acids in length, and they consist of two domains which are direct imperfect repeats approximately 40 and 30% identical in the archaeal and eukaryotic lineages respectively. Archaeal TBPs and the eukaryal TBP C-terminal core domain (TBPc) have approximately 30-40% amino acid sequence identity (98) and have close similarity in terms of 3-D structure (8, 57, 60, 76) (Fig 2-1). The TBPs from eukaryotes differ from their archaeal counterparts in that they contain a non conserved N-terminal domain of variable length that is absent in the archaeal molecule (98, 106). Additionally, eukaryotic TBPs generally have an overall basic charge whereas archaeal TBPs tend to be acidic (106).

Early biochemical investigations into the mechanism of eukaryotic transcription led to the discovery of TBP. These studies revealed that four additional subcellular protein fractions designated A,B,C and D were required to reconstitute transcriptional activity of purified RNA polymerase II (pol II) *in vitro* (70, 91). The D fraction, designated TFIID was found to be the fraction capable of binding the AT-rich TATA box motif common to many known eukaryotic promoters, and it was postulated that TFIID functioned as a scaffold for the other components of the pre-initiation complex (PIC) (101). It was later discovered that a single 27 kDa peptide from yeast was capable of binding a mammalian TATA box and could functionally replace the 750 kDa TFIID complex to support basal pol II transcriptional activity *in vitro* from the human Adenovirus-2 major late promoter (11, 12, 47). However, it was later demonstrated that this protein was not sufficient for specificity protein 1 (Sp1)-mediated activated transcription which required the complete TFIID complex (83). The protein, designated as the TATA-binding protein or TBP, was soon found to be conserved across all

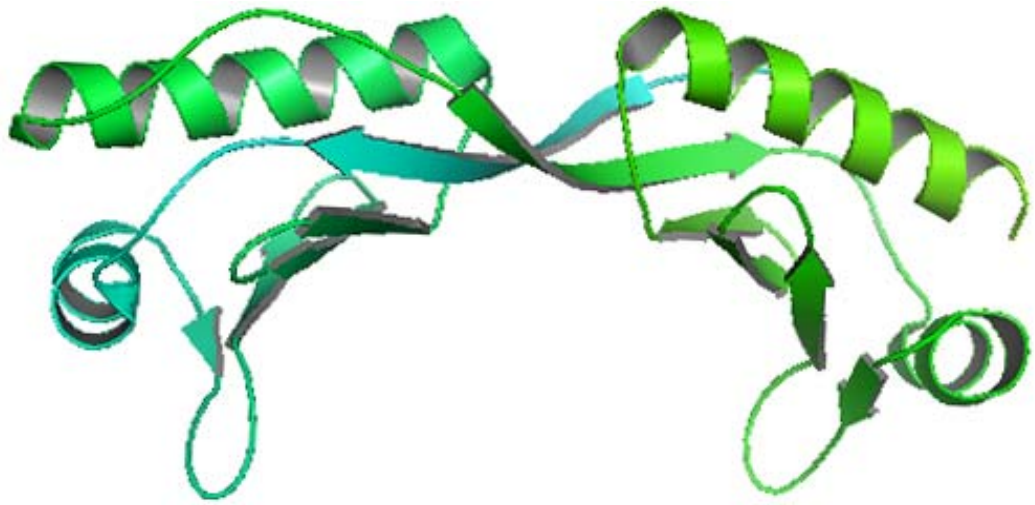

**Fig 2-1. X-ray crystal structure of *Methanocaldococcus janaschii* TBP (PDB:2Z8U).** The TBP molecule is shown as a ribbon diagram. All TBPs have a characteristic saddle shape which straddles the DNA backbone along the minor groove. The two imperfect repeat domains each have two α-helices and five anti-parallel β-strands. The arrow denotes the DNA-binding surface. This figure was prepared in PyMol.

eukaryotes and to be required for transcription of all three multi-subunit RNA polymerases (101). Homologs of TBP were later identified in three species of hyperthermophic archaea, *Pyrococcus woesei, Methanococcus thermolithotrophicus* and *Thermococcus celer* leading to the hypothesis that an ancestral TBP functioned as a GTF for the progenitor of all archaeal and eukaryotic RNA polymerases (30, 38, 88).

Aside from TBP, a multi-subunit RNA polymerase homologous to eukaryotic pol II is shared between the *Archaea* and *Eukarya* as is a second general transcription factor called transcription initiation factor B (TFB) in archaea and transcription initiation factor II B (TFIIB) in eukaryotes (2, 4, 6, 8, 9, 29, 42, 78, 82, 84, 98, 102, 103). Archaeal species also possess less well characterized homologs to the N-terminal domain of the α-subunit of eukaryotic TFIIE designated TFE (3, 103) and to the C-terminal domain of the eukaryotic elongation factor, TFIIS designated TFS (37, 62, 103). There have been no

identified archaeal homologs to eukaryotic TFIIA, TFIIF or TFIIH nor have there been any identified archaeal homologs to any of the myriad of eukaryotic TBP associated factors (TAF) which are found in TFIID (103).

## Multi-subunit cellular RNA polymerases

The central player in the transcription process for all cellular organisms is a DNA-dependent RNA polymerase (RNAP) which catalyzes the *de novo* synthesis of RNA molecules from a DNA template (Fig 2-2). All eukaryotic organisms contain three distinct multi-subunit RNAPs: RNA polymerase I (pol I) which contains 14 subunits and is responsible for the transcription of the 18S and 28S rRNAs, pol II which has 12 subunits and catalyzes the transcription of mRNAs, and RNA polymerase III (pol III) which has 17 subunits and is responsible for the transcription of tRNAs, 5S rRNA and other small non-coding RNAs (Fig. 2-3) (86, 87, 101). Five RNAP subunits, Rpb5, Rpb6, Rpb8, Rpb10 and Rpb12 (using the pol II nomenclature) are shared between all three (Fig. 2-3) (34, 107). Some eukaryotes contain additional RNAPs, pol IV and pol V which are not shared across the domain (40, 53, 61, 77). In contrast to the *Eukarya*, species from the *Bacteria* and *Archaea* domains each contain a single multi-subunit RNAP that transcribes all cellular genes. The archaeal RNAP contains 11 to 13 subunits (42, 43, 59, 103), and the bacterial RNAP core enzyme contains 5 subunits, and the holoenzyme, which includes a σ-factor, has six (Fig.2-2; Fig. 2-3) (71, 72).

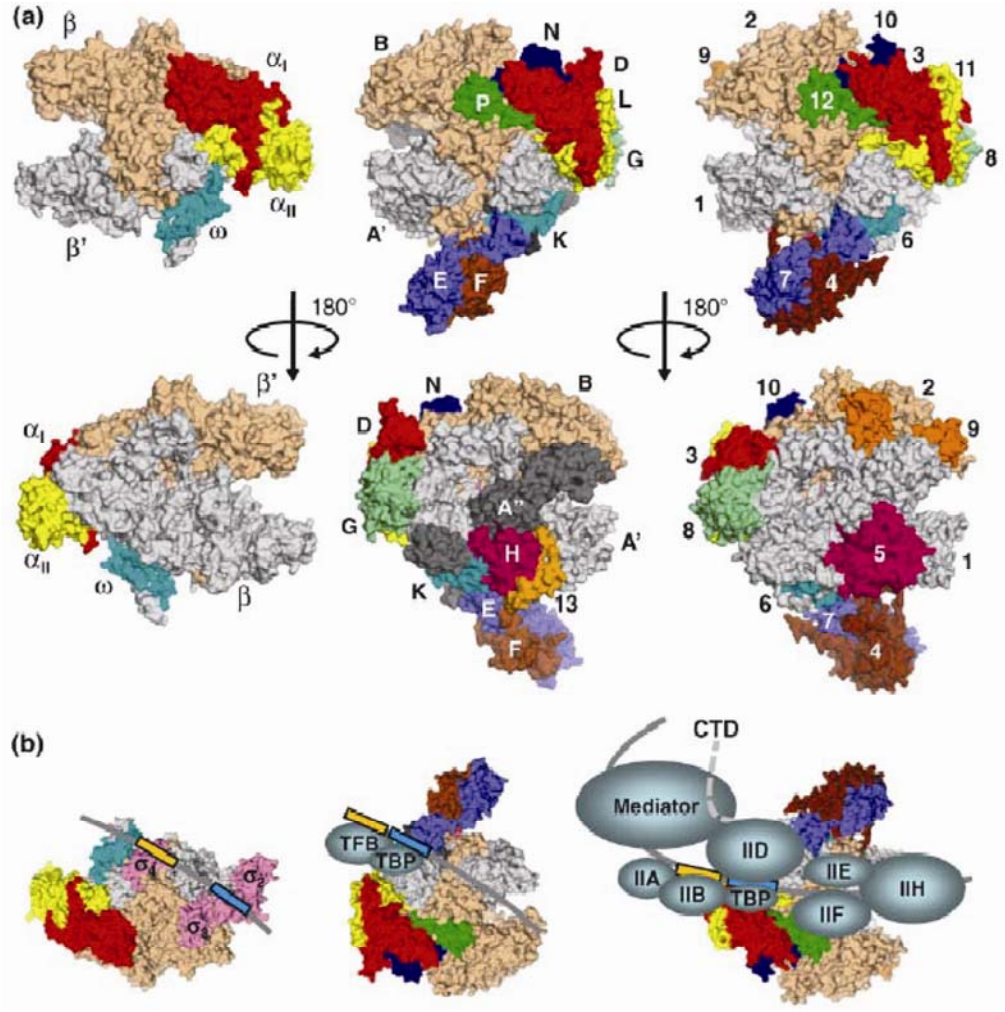


**Fig 2-2. Cellular RNAP structures and transcription preinitiation complexes from three domains of life.** Reproduced from original source[1]. **(a)** Surface representations of cellular RNAP structures from bacteria (left, *T. aquaticus* core enzyme), archaea (center, *S. Solfataricus* RNAP), and eukaryote (right, *S. cerevisiae* Pol II). Each subunit is denoted by a unique color and labeled. Orthologous subunits are depicted with the same color. **(b)** Models of PIC in bacteria (left), archaea (center), and eukaryote (right). Bacterial σ factor is colored pink and its three domains are labeled. DNA is depicted with a gray line (transcription start site is at the right side). Promoter −10 and −35 elements in bacterial transcription and TATA-box and BRE in archaeal and eukaryotic transcriptions are shown as light blue and light orange boxes, respectively. The Pol II CTD is disordered in the X-ray crystal structure and is depicted as a dashed line.

[1] **Hirata, A. and K.S. Murakami.** 2009. Archaeal RNA polymerase. Curr Opin Struct Biol. **19:**724-31.

Comparative analyses reveal that the archaeal RNAP is highly similar to eukaryotic pol II in terms of sequence, subunit composition and 3-D structure (Fig. 2-2; Fig. 2-3) (42, 59). Homologs to 10 of the 12 pol II subunits are found in all archaeal RNAPs (Fig. 2-2). However, the pol II subunit Rpb8 is absent in the *Euryarchaea* (59), and the Rbp9 homolog in *Archaea,* TFS does not appear to be a component of the archaeal RNAP (42, 58). The *Crenarchaea* have one additional RNAP subunit, Rpo13 which is unique to that kingdom (58). Significant homology also exists between archaeal RNAP and eukaryotic pol I and pol III, although the degree of similarity is less than that for pol II. None of subunits unique to either pol I or pol III among eukaryotes are present in archaeal RNAP (Fig 2-2). There is much less homology between archaeal RNAP and all the three eukaryotic RNAPs to the bacterial RNAP. Although homologs to each of the 5 subunits from the bacterial core enzyme are conserved across all three domains including the two largest subunits, β and β' which comprise the catalytic core (58), 5 subunits from the archaeal RNAP, 9 from pol I, 7 from pol II and 12 from pol III are absent from the bacterial enzyme. Furthermore, neither archaea nor eukaryotes utilize σ-factors in promoter selection although some archaeal and eukaryotic GTFs do have partial sequence homology to σ-factors (i.e. TFIIF, TFIIEα, TFE) (101).

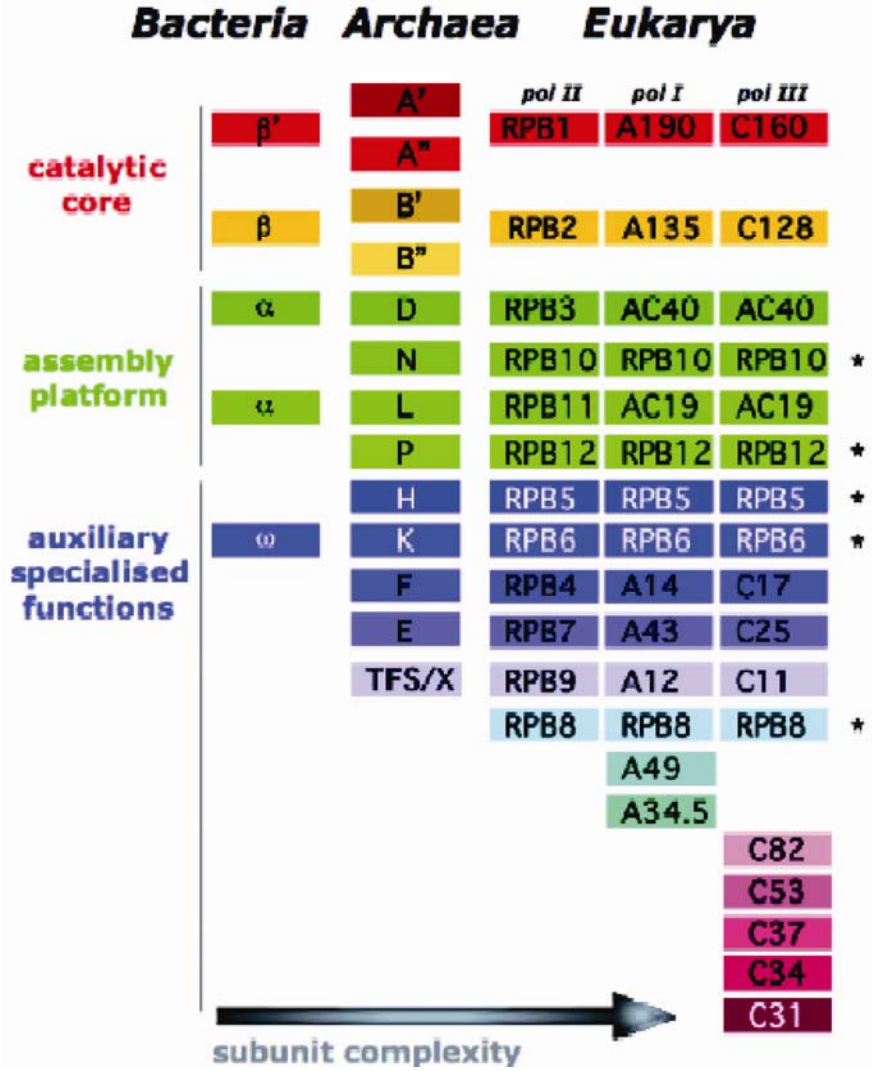


**Fig 2-3. RNA polymerase composition in the three domains of life.** Reproduced from original source[2]. The subunits are organized according to function rather than size and homologous subunits are color coded. Moving towards the right denotes increasing subunit complexity. Subunits marked with an asterisk are conserved throughout the three eukaryotic RNAPI, II and III. Some *Archae*a make use of a fused B subunit (B"–B').

[2] **F. Werner.** 2007. Structure and function of archaeal RNA polymerases. Mol Microbiol. **65**(6):1395-1404.

## Functional roles for TBP in eukaryotic transcription initiation

Despite their capacity for *de novo* transcription without a primer, multi-subunit RNAPs are incapable of sequence-specific promoter recognition. Thus, they require the aid of additional transcription factors to properly position them at the transcription start site (TSS) before engaging in transcription. The core promoter elements as well as the GTFs involved in RNAP recruitment differ substantially between each of the three eukaryotic RNAPs. However, TBP is unique in that it functions with all three eukaryotic RNAPs (21, 22, 39, 90).

TBP is most well known for its role in PIC formation during pol II-mediated transcription of protein coding genes (Fig 2-2). During pol II-mediated transcription, TBP functions as an integral component of the GTF TFIID. The ~750 kDa TFIID protein complex contains 13 or 14 $TAF_{II}$s in addition to TBP. TFIID functions primarily in promoter selection in order to accurately position machinery of the PIC at the TSS. TBP carries out this function at promoters containing a bona fide TATA box (82, 101). Other $TAF_{II}$s carry out this role at promoters lacking a TATA box generally through interactions with alternative core promoter elements such as the initiator (Inr) or the downstream promoter element (DPE) (52, 96). PIC complex formation can proceed via one of two pathways. In the sequential assembly pathway, PIC formation begins with TFIID promoter binding followed by the binding of the GTFs TFIIA to the TFIID complex and TFIIB to TFIID and to the promoter DNA. Both TFIIA and the TFIIB C-terminal domain function to stabilize the TBP-DNA or TFIID-DNA binary complex. TFIIB also plays a role in determining the transcriptional polarity by binding to TBP and

to DNA at two core promoter elements flanking the TATA box known as the upstream and downstream TFIIB recognition elements ($BRE^u$ and $BRE^d$ respectively). Next, the TFIIB NTD recruits pol II to the TFIIA-TFIIB-TFIID-DNA complex through interactions the polymerase and with TFIIF which is already associated with pol II. This followed by recruitment of TFIIE by TFIIF and TFIIH by the combined action of TFIIE and TFIIF. The TFIIB NTD along with TFIIE, TFIIF and TFIIH all play a role in the early steps of transcription initiation assisting in promoter DNA melting, stabilization of transcription bubble, substrate binding and pol II promoter clearance (52, 101).

The second pathway for PIC formation is called the pol II holoenzyme pathway. This pathway begins with TFIID promoter binding along with TFIIA to stabilize the TBP-DNA binary complex. Next, a preassembled pol II holoenzyme containing pol II in complex with TFIIB, TFIIE, TFIIF, TFIIH and several other proteins of functional significance to pol II (i.e. chromatin remodeling factors, transcriptional co-activators) is recruited to the promoter through interactions between TFIID to TFIIB and TFIIF. Following PIC assembly, pol II can initiate transcription. The biochemistry of pol II-mediated transcription has been intensely studied and is the subject of several extensive reviews (34, 52, 97, 101).

In pol I PIC formation, TBP functions as a component of the GTF selectivity factor 1 (SL1) which in addition to TBP, contains four $TAF_I$s (25, 32, 90). SL1 binds to the rDNA promoter core element and recruits pol I to the promoter through an interaction with the pol I associated factor RRN3 (90). SL1 alone is sufficient to support basal pol I transcription (90). However, activated transcription of pol I requires an additional activator, upstream bridging factor (UBF) that binds to a promoter element upstream of

SL1 called the upstream core element (UCE) (25). UBF appears to stabilize SL1 binding to the core promoter. The rDNA core promoter does not contain a TATA-box. Therefore, the role of TBP1 in SL1 may not involve DNA binding, but instead, it likely mediates protein-protein interactions between UBF, SL1 and pol I.

TBP interacts with a third set of proteins during pol III PIC formation. As it does for pol II promoters, TBP is required for pol III PIC formation at both TATA-containing and TATA-less promoters. Here TBP along with two additional $TAF_{III}$s form the pol III GTF TFIIIB (21, 48, 70, 79). Functions for the two TFIIIB $TAF_{III}$s, B" and the TFIIB-related factor (Brf) include stabilization of the TBP-DNA binary complex, pol III recruitment and interaction with a second pol III GTF, TFIIIC (21). Brf is an ortholog of TFIIB. Like TFIIB, the C-terminal domain of Brf interacts with TBP, and the N-terminal domain of Brf interacts with pol III. Although TFIIB and Brf carry out similar functions with pol II and pol III respectively, they are not functionally interchangeable (49). TFIIIB recruitment is mediated by the five to six subunit TFIIIC complex which is bound to pol III promoters downstream of the TSS (21, 48, 79). TFIIIC is important for pol III TSS selection at promoters lacking a TATA box. However, at pol III promoters containing a TATA box, TFIIIB alone is sufficient for pol III-mediated transcription *in vitro* (21, 48, 79). A third pol III gene specific transcription factor TFIIIA is required for transcription of the 5S rRNA gene (21, 48, 79).

## Functional roles of TBP in archaeal transcription initiation

The archaeal transcriptional machinery is orthologous to eukaryotic pol II machinery but considerably more simplified (Fig 2-2). The formation of the archaeal PIC begins with TBP binding to the promoter at an archaeal TATA box. The TBP-DNA binary complex serves as a scaffold for the binding of the C-terminal domain of TFB. TFB binds to the solvent exposed surface of TBP, to the promoter DNA at a TFB recognition element (BRE) located directly upstream of the TATA-box and to a second site on the promoter directly downstream of the TATA-box (2). No consensus archaeal BRE[d] has been identified. The binding of TFB to the BRE is important for proper orientation of the PIC and for stabilization of the TBP-DNA binary complex (5). The extent of the conservation of the TATA box and BRE is unclear since only a handful of promoters have been experimentally identified for most archaeal species. RNAP recruitment is carried out by the Zn ribbon domain on the TFB N-terminal domain which was suggested to interact with RNAP through subunit K (66). A second domain on the TFB NTD, the B-finger extends into the RNAP active site near the TSS where it is presumed to play a role in abortive initiation (Fig. 2-5) (85, 108).

In cell free *in vitro* transcription, archaeal RNAP requires only TBP and TFB to initiate transcription from most promoters, but it is unclear whether any additional factors are involved *in vivo* (103). A third archaeal GTF, TFE an ortholog of the NTD of the α-subunit of TFIIE, has been shown to enhance transcription under a variety of circumstances *in vitro* such as at weak promoters, under TBP-limiting conditions or with

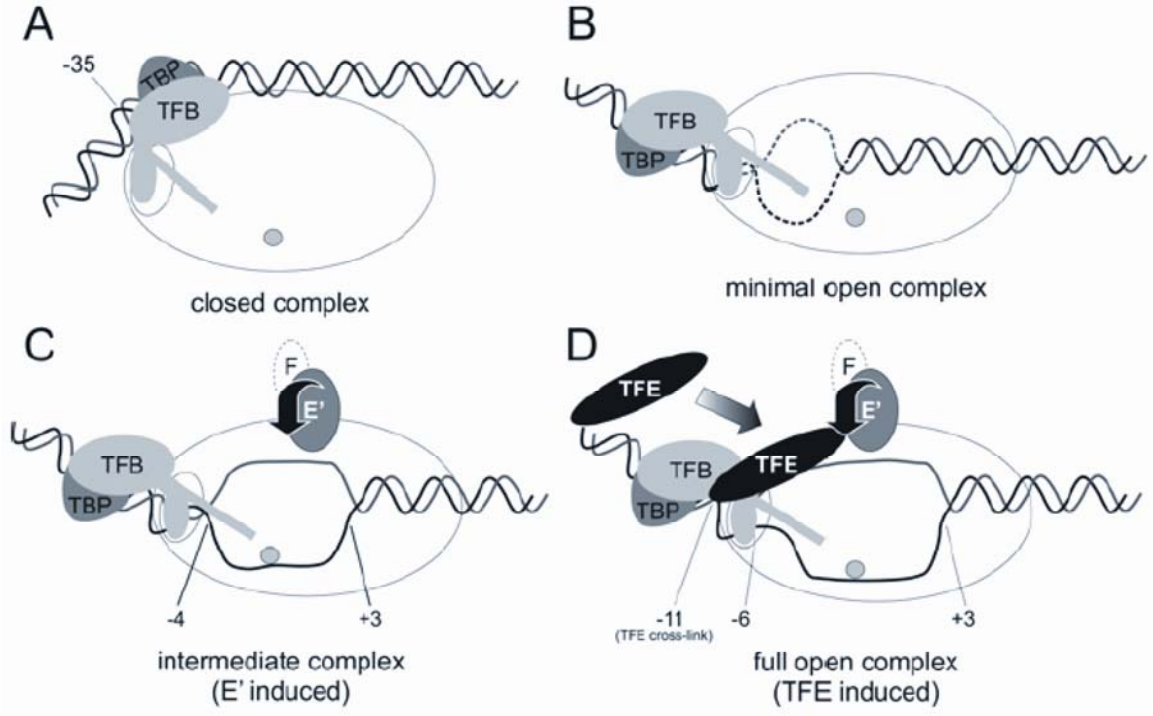


**Fig 2-4. Schematic view of the different steps during initiation.** Reproduced from original source[3]. (**A**) The core enzyme (large oval) is recruited to the promoter platform formed by promoter-bound transcription factors TBP and TFB. (**B**) After reorganization of the binary complex, the core enzyme is able to form a minimal open complex. (**C**) Binding of the E′–F heterodimer to the core enzyme induces an extension of the transcription bubble in the direction of the RNAPs active centre. (**D**) TFE interacts with the non-coding strand upstream of the catalytic centre, resulting in a stabilization of the bubble.

TFB mutants with impaired RNAP recruitment (3, 36, 103, 108). Transcription from strong promoters is apparently unaffected by TFE (3). It has been suggested that TFE is involved in stabilizing the RNAP open complex formation by enhancing DNA melting and DNA loading, and that this activity is dependent upon the RpoE subunit of RNAP (73, 104). It has also been demonstrated that unlike TFIIE, TFE remains associated with RNAP during elongation (Fig. 2-4) (33).

[3] **Thomm, M., Reich, C., Grunberg, S. and S. Naji.** 2009. Mutational studies of archaeal RNA polymerase and analysis of hybrid RNA polymerases. Biochem Soc Trans. **37:**18-22.

Although no archaeal homologs to any eukaryotic TAFs have been identified, one protein, designated TBP-interacting protein 26 (TIP26) has been identified in *Thermococcus kodakaraensis* KOD1 which can bind TBP and inhibit it from binding DNA (68, 69, 110). Although TIP26 homologs are not widespread in the *Archaea*, its finding gives rise to the possibility that other proteins with analogous functions might exist in other archaeal species.

Despite its greater identity to the pol II machinery, the complexity of the archaeal PIC is much more similar to the bacterial RNAP PIC in which only σ-factor is required for promoter selection and accurate initiation at many promoters. Furthermore, the majority of the gene specific transcription factors identified and characterized within the *Archaea* are both homologous and functionally similar to bacterial transcription factors (9, 103). These characteristics illustrate how in many ways, the *Archaea* can been seen as a mosaic of both bacterial and eukaryotic features.

## TBP-related factors

Because of its involvement in PIC formation for all three cellular RNAPs, it was postulated that TBP might be a universal requirement for the transcription of all genes. Doubt was cast upon this idea with the discovery of a *Drosophila* protein homologous to TBP that was designated the TBP-related factor (TRF; later TRF1) (16). Subsequently three additional TRF-family members were identified in eukaryotes: TRF2 (aka TBP-like

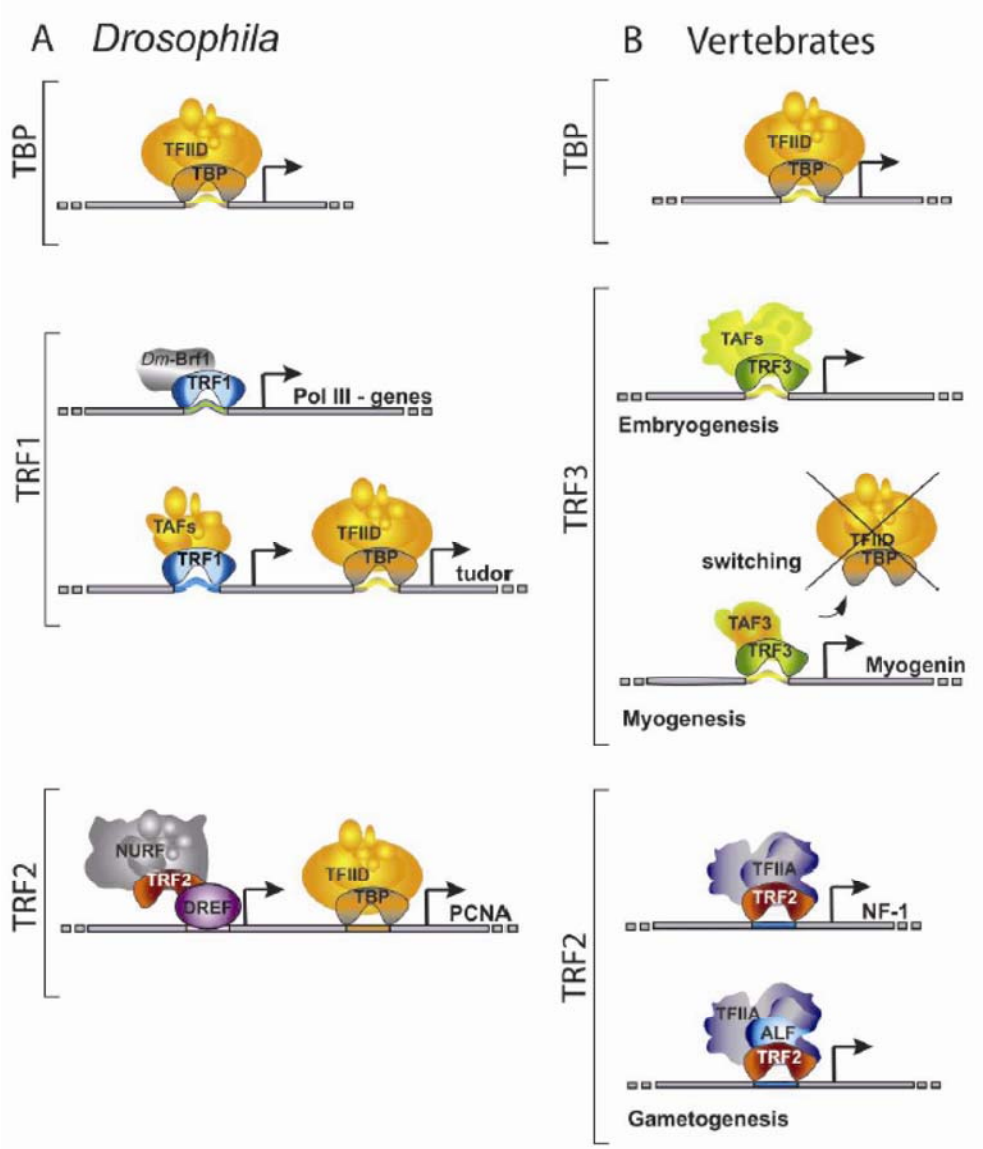


**Figure 2-5. Targets of TBP and TRFs in *Drosophila* and vertebrates.** Reproduced from original source[4]. (*A*) Schematic depiction of various promoters in *Drosophila*. (TBP panel) A pol II promoter containing a *TATA-box* (yellow) with bound TFIID upstream of the transcription start site (arrow). (TRF1 panel, *top* model) A pol III promoter with the TRF1–Brf1 complex bound to a region (green) upstream of the start site (binding to this region is mediated by accessory factors such as TFIIIA and/or TFIIIC, not shown here). (TRF1 panel, *bottom* model) The *tudor* gene tandem promoters with a TRF1–TAFs complex bound to a TC-rich element (blue) to direct transcription from an upstream start site, and TFIID bound to a *TATA-box* to direct transcription from the downstream start site. (TRF2 panel) The tandem *PCNA* promoters with DREF associated with TRF2 and other polypeptides—in particular, some subunits also present in the NURF complex, bound to a *DRE* (purple) to direct transcription from an upstream start site, and TFIID bound to the *TATA-less* downstream promoter to direct transcription from a downstream site. (*B*) Schematic depiction of various promoters in vertebrates. (TBP panel) A pol II promoter containing a *TATA-box* (yellow) with bound TFIID upstream of the transcription start site. (TRF3 panel, *top* model) A promoter from a gene involved in embryogenesis with the TRF3–TAFs complex bound to a *TATA-box* (yellow). (TRF3 panel, *bottom* model) A promoter from a gene such as myogenin required for muscle differentiation bound by a TRF3–TAF3 complex, which replaces TFIID during myogenesis. (TRF2 panel, *top* model) The TATA-less *NF-1* promoter with a TRF2–TFIIA complex containing perhaps additional polypeptides bound to an undefined promoter element (blue). (TRF2 panel, *bottom* model) A promoter from a gene involved in gametogenesis with a TRF2–TFIIA/ALF complex containing perhaps additional polpeptides bound to an undefined promoter element (blue).

[4] **Reina, J.H. and N. Hernandez.** 2007. On a roll for new TRF targets. Genes Dev. **21:**2855-60.

factor or TLF and TBP-related protein or TRP) which is found in all metazoans (17); TRF3 (aka TBP2) which is found exclusively in vertebrates (81); and TRF4 found in the unicellular parasite, *Trypanosoma brucei* (89). TBP and TRF1 share 63% sequence identity in the C-terminal core domains including most of the amino acids shown to be important for DNA-, TFIIB- and TFIIA-binding, but they are less conserved in the NTD. TRF1 can bind to the TATA box and has the capacity to replace TBP from numerous TATA containing promoters *in vitro* (35). *In vivo* and *in vitro* studies have demonstrated that TRF1 expression is specific to the embryonic tissue, adult neuronal tissues and the male germ cells were it directs transcription of pol III genes by replacing TBP in the TFIIIB complex (Fig. 2-5) (45). TRF1 directs pol II-mediated transcription of the *Drosophila* Tudor gene by interacting with a specialized set of $TAF_{II}$s known as neuronal TAFs (nTAFs) and by binding an alternative TC-rich DNA sequence not recognized by TBP (Fig. 2-5) (46).

The TRF2 protein bears less identity to TBP than does TRF1 (approximately 40% identity and 60% similarity in the TBP C-terminal core domain), but sequence alignments suggest that TRF2 does form the characteristic saddle-shape configuration of TBP (10, 18, 45). The binding sequences for TFIIA and TFIIB are conserved in TRF2 enabling interactions with these GTFs (101). However, unlike TRF1, the DNA binding surface of TBP is not conserved in TRF2 and thus, TRF2 lacks the capacity to associate with TATA sequences or to replace TBP during *in vitro* transcription with any of the three RNAPs. In fact, TRF2 has the capacity to inhibit TBP-supported transcription *in vitro* at TATA containing promoters by sequestering TFIIA (10, 13). TRF2 has been implicated in embryogenesis in for *Caenorhabhitis elegans, Xenopus laevis* and zebrafish where TRF2

depletion leads to developmental arrest and impaired expression of developmental specific genes (Fig. 2-5) (18). TRF2 is not essential in mice although TRF2$^{-/-}$ male mice are sterile (67, 111). In *Drosophila*, TRF2 was co-immunopurified with the nucleosome remodeling factor complex (NURF). Together these proteins were found to drive transcription of the proliferating cell nuclear antigen (PCNA) promoter (Fig. 2-5) (44).

The third member, TRF3 has by far the most sequence similarity to TBP among the TRF family. This vertebrate specific TRF has greater than 90% sequence identity to TBP in its C-terminal core including all of the residues involved in DNA-, TFIIA- and TFIIB-binding (101). TRF3 can functionally replace TBP *in vitro,* and in one case, TRF3 was shown to partially complement for TBP-depleted *Xenopus* embryos (51). Unlike TRF1 and TRF2 whose expression is restricted to either discreet tissues or developmental stages, TRF3 is expressed constitutively (81, 101) although TRF3 functionality appears to most important during embryogenesis. Specific inactivation of TRF3 in *Xenopus* and zebrafish embryos by RNA interference altered the transcription of roughly 60% their genes whereas TBP inactivation altered the transcription of only around 30% of their genes (Fig. 2-5) (24, 50). In adult mice, TFIID appears to be absent in muscle tissues whereas TRF3 is abundant. In these tissues, TRF3 has been found in a 200 kDa protein complex with TAF3 enriched at the Myogenin promoter suggesting that a functional replacement of TFIID by TRF3-TAF complex may be a widely used feature in vertebrates as a simple mechanism to alter gene expression program when necessary (Fig. 2-5) (19).

The final member of the TRF family is the TRF4 protein found in the human parasite *T. brucei* (89). Unlike higher eukaryotes, *T. brucei* and its relatives do not have a

classical TBP protein or orthologs of TFIIB, TFIIF or TFIIE. Instead, these organisms use TRF4 to direct transcription of all three cellular RNAPs by poorly understood mechanisms. TRF4 is the most divergent member of the TRF family to TBP. It bears only 31% sequence identity to the *Drosophila* TBP C-terminal core. It does not contain the residues required for TATA box recognition, but it does have the residues important for TFIIA- and TFIIB-binding which is curious due to the lack of TFIIB orthologs in *T. brucei* (89). TRF4 co-purifies in a complex with five additional proteins including three subunits of the small nuclear RNA-activating complex (SNAPc) and two TFIIA subunits. The binding of this complex to the spliced leader (SL) RNA promoter *in vitro* at DNA motif called the upstream sequence element (USE) was required for the transcription of this gene which is essential for essential role in *T. brucei* mRNA maturation (93).

## Multiple GTF homologs in *Archaea*

The presence of multiple TBP and TFIIB homologs is not unique to eukaryotes. Not long after the discovery of archaeal orthologs to TBP and TFIIB, it was discovered that some archaeal species possessed more than one gene for TBP and/or TFB consistent with the possibility that archaeal species might utilize these alternative GTF orthologs to differentially regulate gene expression. The sequencing of an extrachromosomal megaplasmid in the extreme halophile, *Halobacterium* sp. NRC-1 revealed four orfs encoding for putative TBPs located on this megaplasmid (74). Later, the sequencing of

the complete genome of this organism revealed two additional TBP orthologs and seven different TFB orthologs (1, 75). Subsequent genome sequencing projects revealed multiple TFB orthologs (15, 23, 27, 55, 56, 63, 94, 105) or multiple TBP orthologs (20, 28, 65) in several other archaeal species. It is now apparent that the presence of multiple archaeal GTF orthologs is not rare. The Institute for Genomic Research (TIGR) currently lists the completed genomes for 42 archaeal species on its database, and 29 of these species have at least two identified TBPs or TFBs (Table 2-1). Among those species with multiple GTF orthologs, there is a tendency towards multiple TFBs in the halophiles, hyperthermophiles and thermoacidophiles, whereas there is a tendency towards multiple TBPs in the methanogens. Whether or not this trend has any functional significance is unclear. However, in light of the important roles for TBP and TFB in DNA binding and DNA opening respectively, this trend could be an indication that for the halophiles and hyperthermophiles the DNA opening step is the major target for gene regulation whereas for the methanogens, the DNA binding step is the primary target for regultion.

The majority of the experimental investigations into the function of multiple archaeal GTFs have been carried out in *Halobacterium* sp. NRC-1. This has been due to the large number of unique GTF homologs (six TBPs and seven TFBs which is the most for any archaeal species) (Table 2-1) (1, 75), and because of the availability of facile genetic tools. These investigations have largely concluded that the individual GTF isomers in *Halobacterium* sp. NRC-1 function to differentially regulate gene expression.

Genetic analyses have established that at least 10 of its 13 GTF orthologs (4 TBPs and 6 TFBs) can be individually deleted under standard laboratory conditions without hindering cell vialbility (15, 23) although no investigations into the consequences of

**Table 2-1. Archaeal species with multiple annotated TBP or TFB genes.**

| Organism | Putative TBPs | Putative TFBs |
|---|---|---|
| *Aeropyrum pernix K1* | 1 | 2 |
| *Candidatus methanoregula boonei 6A8* | 3 | 1 |
| *Haloarcula marismortui ATCC 43049* | 1 | 9 |
| *Halobacterium sp. NRC-1* | 6 | 7 |
| *Haloquadratum walsbyi DSM 16790* | 2 | 9 |
| *Hyperthermus butylicus DSM 5456* | 1 | 2 |
| *Metallosphaera sedula DSM 5348* | 1 | 2 |
| *Methanococcus maripaludis C5* | 2 | 1 |
| *Methanocorpusculum labreanum Z* | 2 | 1 |
| *Methanoculleus marisnigri JR1* | 2 | 2 |
| *Methanosarcina acetivorans C2A* | 3 | 1 |
| *Methanosarcina barkeri fusaro* | 2 | 1 |
| *Methanosarcina mazei Goe1* | 3 | 1 |
| *Methanospirillum hungatei JF-1* | 2 | 1 |
| *Natronomonas pharaonis sp* | 1 | 9 |
| *Picrophilus torridus DSM 9790* | 1 | 2 |
| *Pyrobaculum aerophilum IM2* | 1 | 3 |
| *Pyrobaculum arsenaticum DSM 13514* | 1 | 2 |
| *Pyrobaculum islandicum DSM 4184* | 1 | 2 |
| *Pyrococcus furiosus DSM 3638* | 1 | 2 |
| *Pyrococcus horikoshii shinkaj OT3* | 1 | 2 |
| *Sulfolobus acidocaldarius DSM 639* | 1 | 2 |
| *Sulfolobus solfataricus P2* | 1 | 2 |
| *Sulfolobus tokodaii strain 7* | 1 | 2 |
| *Thermococcus kodakarensis KOD1* | 1 | 2 |
| *Thermofilum pendens Hrk 5* | 1 | 2 |
| *Thermoplasma acidophilum DSM 1728* | 1 | 3 |
| *Thermoplasma volcanium GSS1* | 1 | 3 |

deleting more than one GTF have been reported. One of the two TBPs that could not be deleted was *tbpE* which is located on the main chromosome of *Halobacterium* sp. NRC-1. Proteomics analysis and quantitative RT-PCR established that the *tbpE* is more robustly expressed than the other TBP genes, and it was suggested that TBPe is the primary TBP utilized during growth. It was proposed that the additional TBPs provide

added fitness based on defective growth of strains lacking the additional TBP genes (31, 100).

It is unclear if one TFB ortholog functions as the primary TFB during growth, although *tfbB* is the only TFB that could not be knocked out (15, 23). In a global analysis, a preliminary TFB regulatory network was deduced based on integrated data from ChIP-chip analysis, transcriptomic data and *in vivo* protein-protein interactions between the various TBP and TFB orthologs (23). In a separate report, one TBP, *tbpD* and one TFB, *tfbA* were shown to coordinately regulate roughly 10% of the *Halobacterim* sp. NRC-1 genome including several heat shock response genes suggesting that preferential pairings of TBP-TFB may be exploited to direct gene expression. Mutant strains with either *tbpD* or *tfbA* deleted elicited defective growth in response to heat shock (54). TFBb was shown to preferentially bind the heat shock inducible promoter $P_{hsp5}$ *in vitro* during incubation at 50$^{o}$C, but not during incubation at 37$^{o}$C. Furthermore, TFBg binding at $P_{hsp5}$ was not detected at either temperature consistent with a specific role for TFBb in the regulation of *hsp5* during *Halobacterium* sp. NRC-1 heat shock response (64). Consistent with these observations for *H. salinarum,* TFB orthologs from *Haloferax volcanii, Pyrococcus furiosus* and *Sulfolobus solfataricus* have been implicated in the heat shock response or UV irradiation response as well (80, 95, 105). This suggests that the use of alternative TFB orthologs to direct the regulation of stress response genes may be a common feature in archaeal species.

A functional assessment of the two TFB orthologs in the hyperthermophile, *T. kodakaraensis* suggested the possibility of functional redundancy for multiple TFBs (92). It was determined that either of the two TFB orthologs can be individually deleted

without hindering growth under optimal growth conditions. Furthermore, both TFB orthologs could support *in vitro* transcription equally well from several different promoters showing no difference in TSS selection (41). However, a separate investigation suggested that these two TFB orthologs may have a subtle difference in function. It was shown that recombinant TFB1 had a stronger association with the TBP-DNA binary complex *in vitro* than did TFB2. This tighter association increases the amount of abortive initiation products produced by RNAP prior to promoter escape. It was speculated that the excessive abortive initiation products may be detrimental under stress. Consistent with this prediction, *tfb2* elicited a greater increase in transcript abundance during heat shock than did *tfb1* suggesting that TFB2 may be utilized in preference to TFB1 under stress (99).

To date, no experimental investigations into the functional roles of multiple TBP orthologs in organisms with only a single TFB have been reported. Therefore, one of the primary objectives of this dissertation will be to address the functional roles of the three TBP orthologs in the mesophilic methanogen, *Methanosarcina acetivorans* in an effort to broaden the understanding of how the methanogenic archaea regulate their gene expression.

## References

1. **Baliga, N. S., Y. A. Goo, W. V. Ng, L. Hood, C. J. Daniels, and S. DasSarma.** 2000. Is gene expression in Halobacterium NRC-1 regulated by multiple TBP and TFB transcription factors? Mol Microbiol **36:**1184-5.

2. **Bartlett, M. S., M. Thomm, and E. P. Geiduschek.** 2004. Topography of the euryarchaeal transcription initiation complex. J Biol Chem **279:**5894-903.

3. **Bell, S. D., A. B. Brinkman, J. van der Oost, and S. P. Jackson.** 2001. The archaeal TFIIEalpha homologue facilitates transcription initiation by enhancing TATA-box recognition. EMBO Rep **2:**133-8.

4. **Bell, S. D., and S. P. Jackson.** 2001. Mechanism and regulation of transcription in archaea. Curr Opin Microbiol **4:**208-13.

5. **Bell, S. D., and S. P. Jackson.** 2000. The role of transcription factor B in transcription initiation and promoter clearance in the archaeon Sulfolobus acidocaldarius. J Biol Chem **275:**12934-40.

6. **Bell, S. D., and S. P. Jackson.** 1998. Transcription and translation in Archaea: a mosaic of eukaryal and bacterial features. Trends Microbiol **6:**222-8.

7. **Bell, S. D., and S. P. Jackson.** 1998. Transcription in Archaea. Cold Spring Harb Symp Quant Biol **63:**41-51.

8. **Bell, S. D., P. L. Kosa, P. B. Sigler, and S. P. Jackson.** 1999. Orientation of the transcription preinitiation complex in archaea. Proc Natl Acad Sci U S A **96:**13662-7.

9. **Bell, S. D., C. P. Magill, and S. P. Jackson.** 2001. Basal and regulated transcription in Archaea. Biochem Soc Trans **29:**392-5.

10. **Berk, A. J.** 2000. TBP-like factors come into focus. Cell **103:**5-8.

11. **Buratowski, S., S. Hahn, P. A. Sharp, and L. Guarente.** 1988. Function of a yeast TATA element-binding protein in a mammalian transcription system. Nature **334:**37-42.

12. **Cavallini, B., J. Huet, J. L. Plassat, A. Sentenac, J. M. Egly, and P. Chambon.** 1988. A yeast activity can substitute for the HeLa cell TATA box factor. Nature **334:**77-80.

13. **Chong, J. A., M. M. Moran, M. Teichmann, J. S. Kaczmarek, R. Roeder, and D. E. Clapham.** 2005. TATA-binding protein (TBP)-like factor (TLF) is a functional regulator of transcription: reciprocal regulation of the neurofibromatosis type 1 and c-fos genes by TLF/TRF2 and TBP. Mol Cell Biol **25:**2632-43.

14. **Cler, E., G. Papai, P. Schultz, and I. Davidson.** 2009. Recent advances in understanding the structure and function of general transcription factor TFIID. Cell Mol Life Sci **66:**2123-34.

15. **Coker, J. A., and S. DasSarma.** 2007. Genetic and transcriptomic analysis of transcription factor genes in the model halophilic Archaeon: coordinate action of TbpD and TfbA. BMC Genet **8:**61.

16. **Crowley, T. E., T. Hoey, J. K. Liu, Y. N. Jan, L. Y. Jan, and R. Tjian.** 1993. A new factor related to TATA-binding protein has highly restricted expression patterns in Drosophila. Nature **361:**557-61.

17. **Dantonel, J. C., J. M. Wurtz, O. Poch, D. Moras, and L. Tora.** 1999. The TBP-like factor: an alternative transcription factor in metazoa? Trends Biochem Sci **24:**335-9.

18. **Davidson, I.** 2003. The genetics of TBP and TBP-related factors. Trends Biochem Sci **28:**391-8.

19. **Deato, M. D., and R. Tjian.** 2007. Switching of the core transcription machinery during myogenesis. Genes Dev **21:**2137-49.

20. **Deppenmeier, U., A. Johann, T. Hartsch, R. Merkl, R. A. Schmitz, R. Martinez-Arias, A. Henne, A. Wiezer, S. Baumer, C. Jacobi, H. Bruggemann, T. Lienard, A. Christmann, M. Bomeke, S. Steckel, A. Bhattacharyya, A. Lykidis, R. Overbeek, H. P. Klenk, R. P. Gunsalus, H. J. Fritz, and G. Gottschalk.** 2002. The genome of Methanosarcina mazei: evidence for lateral gene transfer between bacteria and archaea. J Mol Microbiol Biotechnol **4:**453-61.

21. **Dieci, G., G. Fiorino, M. Castelnuovo, M. Teichmann, and A. Pagano.** 2007. The expanding RNA polymerase III transcriptome. Trends Genet **23:**614-22.

22. **Donohue, T. J., and C. M. Thomas.** 2004. Policy proposal for publication of papers with data sets from genome-wide studies. Int J Syst Evol Microbiol **54:**1915.

23. **Facciotti, M. T., D. J. Reiss, M. Pan, A. Kaur, M. Vuthoori, R. Bonneau, P. Shannon, A. Srivastava, S. M. Donohoe, L. E. Hood, and N. S. Baliga.** 2007. General transcription factor specified global gene regulation in archaea. Proc Natl Acad Sci U S A **104:**4630-5.

24. **Ferg, M., R. Sanges, J. Gehrig, J. Kiss, M. Bauer, A. Lovas, M. Szabo, L. Yang, U. Straehle, M. J. Pankratz, F. Olasz, E. Stupka, and F. Muller.** 2007. The TATA-binding protein regulates maternal mRNA degradation and differential zygotic transcription in zebrafish. Embo J **26:**3945-56.

25. **Friedrich, J. K., K. I. Panov, P. Cabart, J. Russell, and J. C. Zomerdijk.** 2005. TBP-TAF complex SL1 directs RNA polymerase I pre-initiation complex formation and stabilizes upstream binding factor at the rDNA promoter. J Biol Chem **280:**29551-8.

26. **Fuda, N. J., M. B. Ardehali, and J. T. Lis.** 2009. Defining mechanisms that regulate RNA polymerase II transcription in vivo. Nature **461:**186-92.

27. **Fukui, T., H. Atomi, T. Kanai, R. Matsumi, S. Fujiwara, and T. Imanaka.** 2005. Complete genome sequence of the hyperthermophilic archaeon Thermococcus kodakaraensis KOD1 and comparison with Pyrococcus genomes. Genome Res **15:**352-63.

28. **Galagan, J. E., C. Nusbaum, A. Roy, M. G. Endrizzi, P. Macdonald, W. FitzHugh, S. Calvo, R. Engels, S. Smirnov, D. Atnoor, A. Brown, N. Allen, J. Naylor, N. Stange-Thomann, K. DeArellano, R. Johnson, L. Linton, P. McEwan, K. McKernan, J. Talamas, A. Tirrell, W. Ye, A. Zimmer, R. D. Barber, I. Cann, D. E. Graham, D. A. Grahame, A. M. Guss, R. Hedderich, C. Ingram-Smith, H. C. Kuettner, J. A. Krzycki, J. A. Leigh, W. Li, J. Liu, B. Mukhopadhyay, J. N. Reeve, K. Smith, T. A. Springer, L. A. Umayam, O. White, R. H. White, E. Conway de Macario, J. G. Ferry, K. F. Jarrell, H. Jing, A. J. Macario, I. Paulsen, M. Pritchett, K. R. Sowers, R. V. Swanson, S. H. Zinder, E. Lander, W. W. Metcalf, and B. Birren.** 2002. The genome of M. acetivorans reveals extensive metabolic and physiological diversity. Genome Res **12:**532-42.

29. **Geiduschek, E. P., and M. Ouhammouch.** 2005. Archaeal transcription and its regulators. Mol Microbiol **56:**1397-407.

30. **Gohl, H. P., B. Grondahl, and M. Thomm.** 1995. Promoter recognition in archaea is mediated by transcription factors: identification of transcription factor aTFB from Methanococcus thermolithotrophicus as archaeal TATA-binding protein. Nucleic Acids Res **23:**3837-41.

31. **Goo, Y. A., E. C. Yi, N. S. Baliga, W. A. Tao, M. Pan, R. Aebersold, D. R. Goodlett, L. Hood, and W. V. Ng.** 2003. Proteomic analysis of an extreme halophilic archaeon, Halobacterium sp. NRC-1. Mol Cell Proteomics **2:**506-24.

32. **Gorski, J. J., S. Pathak, K. Panov, T. Kasciukovic, T. Panova, J. Russell, and J. C. Zomerdijk.** 2007. A novel TBP-associated factor of SL1 functions in RNA polymerase I transcription. Embo J **26:**1560-8.

33. **Grunberg, S., M. S. Bartlett, S. Naji, and M. Thomm.** 2007. Transcription factor E is a part of transcription elongation complexes. J Biol Chem **282:**35482-90.

34. **Hampsey, M.** 1998. Molecular genetics of the RNA polymerase II general transcriptional machinery. Microbiol Mol Biol Rev **62:**465-503.

35. **Hansen, S. K., S. Takada, R. H. Jacobson, J. T. Lis, and R. Tjian.** 1997. Transcription properties of a cell type-specific TATA-binding protein, TRF. Cell **91:**71-83.

36. **Hanzelka, B. L., T. J. Darcy, and J. N. Reeve.** 2001. TFE, an archaeal transcription factor in Methanobacterium thermoautotrophicum related to eucaryal transcription factor TFIIEalpha. J Bacteriol **183:**1813-8.

37. **Hausner, W., U. Lange, and M. Musfeldt.** 2000. Transcription factor S, a cleavage induction factor of the archaeal RNA polymerase. J Biol Chem **275:**12393-9.

38. **Hausner, W., and M. Thomm.** 1995. The translation product of the presumptive Thermococcus celer TATA-binding protein sequence is a transcription factor related in structure and function to Methanococcus transcription factor B. J Biol Chem **270:**17649-51.

39. **Hernandez, N.** 1993. TBP, a universal eukaryotic transcription factor? Genes Dev **7:**1291-308.

40. **Herr, A. J., M. B. Jensen, T. Dalmay, and D. C. Baulcombe.** 2005. RNA polymerase IV directs silencing of endogenous DNA. Science **308:**118-20.

41. **Hirata, A., T. Kanai, T. J. Santangelo, M. Tajiri, K. Manabe, J. N. Reeve, T. Imanaka, and K. S. Murakami.** 2008. Archaeal RNA polymerase subunits E and F are not required for transcription in vitro, but a Thermococcus kodakarensis mutant lacking subunit F is temperature-sensitive. Mol Microbiol **70:**623-33.

42. **Hirata, A., B. J. Klein, and K. S. Murakami.** 2008. The X-ray crystal structure of RNA polymerase from Archaea. Nature **452:**248.

43. **Hirata, A., and K. S. Murakami.** 2009. Archaeal RNA polymerase. Curr Opin Struct Biol.

44. **Hirose, F., M. Yamaguchi, H. Handa, Y. Inomata, and A. Matsukage.** 1993. Novel 8-base pair sequence (Drosophila DNA replication-related element) and specific binding factor involved in the expression of Drosophila genes for DNA polymerase alpha and proliferating cell nuclear antigen. J Biol Chem **268:**2092-9.

45. **Hochheimer, A., and R. Tjian.** 2003. Diversified transcription initiation complexes expand promoter selectivity and tissue-specific gene expression. Genes Dev **17:**1309-20.

46. **Holmes, M. C., and R. Tjian.** 2000. Promoter-selective properties of the TBP-related factor TRF1. Science **288:**867-70.

47. **Horikoshi, M., C. K. Wang, H. Fujii, J. A. Cromlish, P. A. Weil, and R. G. Roeder.** 1989. Purification of a yeast TATA box-binding protein that exhibits human transcription factor IID activity. Proc Natl Acad Sci U S A **86:**4843-7.

48. **Huang, Y., and R. J. Maraia.** 2001. Comparison of the RNA polymerase III transcription machinery in Schizosaccharomyces pombe, Saccharomyces cerevisiae and human. Nucleic Acids Res **29:**2675-90.

49. **Huang, Y., E. McGillicuddy, M. Weindel, S. Dong, and R. J. Maraia.** 2003. The fission yeast TFIIB-related factor limits RNA polymerase III to a TATA-dependent pathway of TBP recruitment. Nucleic Acids Res **31:**2108-16.

50. **Jacobi, U. G., R. C. Akkers, E. S. Pierson, D. L. Weeks, J. M. Dagle, and G. J. Veenstra.** 2007. TBP paralogs accommodate metazoan- and vertebrate-specific developmental gene regulation. Embo J **26:**3900-9.

51. **Jallow, Z., U. G. Jacobi, D. L. Weeks, I. B. Dawid, and G. J. Veenstra.** 2004. Specialized and redundant roles of TBP and a vertebrate-specific TBP paralog in embryonic gene regulation in Xenopus. Proc Natl Acad Sci U S A **101:**13525-30.

52. **Juven-Gershon, T., and J. T. Kadonaga.** 2009. Regulation of gene expression via the core promoter and the basal transcriptional machinery. Dev Biol.

53. **Kanno, T., B. Huettel, M. F. Mette, W. Aufsatz, E. Jaligot, L. Daxinger, D. P. Kreil, M. Matzke, and A. J. Matzke.** 2005. Atypical RNA polymerase subunits required for RNA-directed DNA methylation. Nat Genet **37:**761-5.

54. **Kaur, A., M. Pan, M. Meislin, M. T. Facciotti, R. El-Geweley, and N. S. Baliga.** 2006. A systems view of haloarchaeal strategies to withstand stress from transition metals. Genome Res.

55. **Kawarabayasi, Y., Y. Hino, H. Horikawa, S. Yamazaki, Y. Haikawa, K. Jin-no, M. Takahashi, M. Sekine, S. Baba, A. Ankai, H. Kosugi, A. Hosoyama, S. Fukui, Y. Nagai, K. Nishijima, H. Nakazawa, M. Takamiya, S. Masuda, T. Funahashi, T. Tanaka, Y. Kudoh, J. Yamazaki, N. Kushida, A. Oguchi, H. Kikuchi, and et al.** 1999. Complete genome sequence of an aerobic hyper-thermophilic crenarchaeon, Aeropyrum pernix K1. DNA Res **6:**83-101, 145-52.

56. **Kawarabayasi, Y., M. Sawada, H. Horikawa, Y. Haikawa, Y. Hino, S. Yamamoto, M. Sekine, S. Baba, H. Kosugi, A. Hosoyama, Y. Nagai, M. Sakai, K. Ogura, R. Otsuka, H. Nakazawa, M. Takamiya, Y. Ohfuku, T. Funahashi, T. Tanaka, Y. Kudoh, J. Yamazaki, N. Kushida, A. Oguchi, K. Aoki, and H. Kikuchi.** 1998. Complete sequence and gene organization of the genome of a hyper-thermophilic archaebacterium, Pyrococcus horikoshii OT3 (supplement). DNA Res **5:**147-55.

57. **Kim, J. L., and S. K. Burley.** 1994. 1.9 A resolution refined structure of TBP recognizing the minor groove of TATAAAAG. Nat Struct Biol **1:**638-53.

58. **Korkhin, Y., O. Littlefield, P. J. Nelson, S. D. Bell, and P. B. Sigler.** 2001. Preparation of components of archaeal transcription preinitiation complex. Methods Enzymol **334:**227-39.

59. **Korkhin, Y., U. M. Unligil, O. Littlefield, P. J. Nelson, D. I. Stuart, P. B. Sigler, S. D. Bell, and N. G. Abrescia.** 2009. Evolution of Complex RNA Polymerases: The Complete Archaeal RNA Polymerase Structure. PLoS Biol **7:**e102.

60. **Kosa, P. F., G. Ghosh, B. S. DeDecker, and P. B. Sigler.** 1997. The 2.1-A crystal structure of an archaeal preinitiation complex: TATA-box-binding protein/transcription factor (II)B core/TATA-box. Proc Natl Acad Sci U S A **94:**6042-7.

61. **Kravchenko, J. E., I. B. Rogozin, E. V. Koonin, and P. M. Chumakov.** 2005. Transcription of mammalian messenger RNAs by a nuclear RNA polymerase of mitochondrial origin. Nature **436:**735-9.

62. **Langer, D., and W. Zillig.** 1993. Putative tfIIs gene of Sulfolobus acidocaldarius encoding an archaeal transcription elongation factor is situated directly downstream of the gene for a small subunit of DNA-dependent RNA polymerase. Nucleic Acids Res **21:**2251.

63. **Lecompte, O., R. Ripp, V. Puzos-Barbe, S. Duprat, R. Heilig, J. Dietrich, J. C. Thierry, and O. Poch.** 2001. Genome evolution at the genus level: comparison of three complete genomes of hyperthermophilic archaea. Genome Res **11:**981-93.

64. **Lu, Q., J. Han, L. Zhou, J. A. Coker, P. Dassarma, S. Dassarma, and H. Xiang.** 2008. Dissection of the regulatory mechanism of a heat-shock responsive promoter in Haloarchaea: a new paradigm for general transcription factor directed archaeal gene regulation. Nucleic Acids Res.

65. **Maeder, D. L., I. Anderson, T. S. Brettin, D. C. Bruce, P. Gilna, C. S. Han, A. Lapidus, W. W. Metcalf, E. Saunders, R. Tapia, and K. R. Sowers.** 2006. The Methanosarcina barkeri genome: comparative analysis with Methanosarcina acetivorans and Methanosarcina mazei reveals extensive rearrangement within methanosarcinal genomes. J Bacteriol **188:**7922-31.

66. **Magill, C. P., S. P. Jackson, and S. D. Bell.** 2001. Identification of a conserved archaeal RNA polymerase subunit contacted by the basal transcription factor TFB. J Biol Chem **276:**46693-6.

67. **Martianov, I., G. M. Fimia, A. Dierich, M. Parvinen, P. Sassone-Corsi, and I. Davidson.** 2001. Late arrest of spermiogenesis and germ cell apoptosis in mice lacking the TBP-like TLF/TRF2 gene. Mol Cell **7:**509-15.

68. **Matsuda, T., M. Fujikawa, M. Haruki, X. F. Tang, S. Ezaki, T. Imanaka, M. Morikawa, and S. Kanaya.** 2001. Interaction of TIP26 from a hyperthermophilic archaeon with TFB/TBP/DNA ternary complex. Extremophiles **5:**177-82.

69. **Matsuda, T., M. Morikawa, M. Haruki, H. Higashibata, T. Imanaka, and S. Kanaya.** 1999. Isolation of TBP-interacting protein (TIP) from a hyperthermophilic archaeon that inhibits the binding of TBP to TATA-DNA. FEBS Lett **457:**38-42.

70. **Matsui, T., J. Segall, P. A. Weil, and R. G. Roeder.** 1980. Multiple factors required for accurate initiation of transcription by purified RNA polymerase II. J Biol Chem **255:**11992-6.

71. **Murakami, K. S., S. Masuda, E. A. Campbell, O. Muzzin, and S. A. Darst.** 2002. Structural basis of transcription initiation: an RNA polymerase holoenzyme-DNA complex. Science **296:**1285-90.

72. **Murakami, K. S., S. Masuda, and S. A. Darst.** 2002. Structural basis of transcription initiation: RNA polymerase holoenzyme at 4 A resolution. Science **296:**1280-4.

73. **Naji, S., S. Grunberg, and M. Thomm.** 2007. The RPB7 orthologue E' is required for transcriptional activity of a reconstituted archaeal core enzyme at low temperatures and stimulates open complex formation. J Biol Chem **282:**11047-57.

74. **Ng, W. V., S. A. Ciufo, T. M. Smith, R. E. Bumgarner, D. Baskin, J. Faust, B. Hall, C. Loretz, J. Seto, J. Slagel, L. Hood, and S. DasSarma.** 1998. Snapshot of a large dynamic replicon in a halophilic archaeon: megaplasmid or minichromosome? Genome Res **8:**1131-41.

75. **Ng, W. V., S. P. Kennedy, G. G. Mahairas, B. Berquist, M. Pan, H. D. Shukla, S. R. Lasky, N. S. Baliga, V. Thorsson, J. Sbrogna, S. Swartzell, D. Weir, J. Hall, T. A. Dahl, R. Welti, Y. A. Goo, B. Leithauser, K. Keller, R. Cruz, M. J. Danson, D. W. Hough, D. G. Maddocks, P. E. Jablonski, M. P. Krebs, C. M. Angevine, H. Dale, T. A. Isenbarger, R. F. Peck, M. Pohlschroder, J. L. Spudich, K. W. Jung, M. Alam, T. Freitas, S. Hou, C. J. Daniels, P. P. Dennis, A. D. Omer, H. Ebhardt, T. M. Lowe, P. Liang, M.**

**Riley, L. Hood, and S. DasSarma.** 2000. Genome sequence of Halobacterium species NRC-1. Proc Natl Acad Sci U S A **97:**12176-81.

76. **Nikolov, D. B., H. Chen, E. D. Halay, A. Hoffman, R. G. Roeder, and S. K. Burley.** 1996. Crystal structure of a human TATA box-binding protein/TATA element complex. Proc Natl Acad Sci U S A **93:**4862-7.

77. **Onodera, Y., J. R. Haag, T. Ream, P. C. Nunes, O. Pontes, and C. S. Pikaard.** 2005. Plant nuclear RNA polymerase IV mediates siRNA and DNA methylation-dependent heterochromatin formation. Cell **120:**613-22.

78. **Ouzounis, C., and C. Sander.** 1992. TFIIB, an evolutionary link between the transcription machineries of archaebacteria and eukaryotes. Cell **71:**189-90.

79. **Paule, M. R., and R. J. White.** 2000. Survey and summary: transcription by RNA polymerases I and III. Nucleic Acids Res **28:**1283-98.

80. **Paytubi, S., and M. F. White.** 2009. The crenarchaeal DNA damage-inducible transcription factor B paralogue TFB3 is a general activator of transcription. Mol Microbiol **72:**1487-99.

81. **Persengiev, S. P., X. Zhu, B. L. Dixit, G. A. Maston, E. L. Kittler, and M. R. Green.** 2003. TRF3, a TATA-box-binding protein-related factor, is vertebrate-specific and widely expressed. Proc Natl Acad Sci U S A **100:**14887-91.

82. **Pugh, B. F.** 2000. Control of gene expression through regulation of the TATA-binding protein. Gene **255:**1-14.

83. **Pugh, B. F., and R. Tjian.** 1990. Mechanism of transcriptional activation by Sp1: evidence for coactivators. Cell **61:**1187-97.

84. **Qureshi, S. A., and S. P. Jackson.** 1998. Sequence-specific DNA binding by the S. shibatae TFIIB homolog, TFB, and its effect on promoter strength. Mol Cell **1:**389-400.

85. **Renfrow, M. B., N. Naryshkin, L. M. Lewis, H. T. Chen, R. H. Ebright, and R. A. Scott.** 2004. Transcription factor B contacts promoter DNA near the transcription start site of the archaeal transcription initiation complex. J Biol Chem **279:**2825-31.

86. **Roeder, R. G., and W. J. Rutter.** 1969. Multiple forms of DNA-dependent RNA polymerase in eukaryotic organisms. Nature **224:**234-7.

87. **Roeder, R. G., and W. J. Rutter.** 1970. Specific nucleolar and nucleoplasmic RNA polymerases. Proc Natl Acad Sci U S A **65:**675-82.

88. **Rowlands, T., P. Baumann, and S. P. Jackson.** 1994. The TATA-binding protein: a general transcription factor in eukaryotes and archaebacteria. Science **264:**1326-9.

89. **Ruan, J. P., G. K. Arhin, E. Ullu, and C. Tschudi.** 2004. Functional characterization of a Trypanosoma brucei TATA-binding protein-related factor points to a universal regulator of transcription in trypanosomes. Mol Cell Biol **24:**9610-8.

90. **Russell, J., and J. C. Zomerdijk.** 2005. RNA-polymerase-I-directed rDNA transcription, life and works. Trends Biochem Sci **30:**87-96.

91. **Samuels, M., A. Fire, and P. A. Sharp.** 1982. Separation and characterization of factors mediating accurate transcription by RNA polymerase II. J Biol Chem **257:**14419-27.

92. **Santangelo, T. J., L. Cubonova, C. L. James, and J. N. Reeve.** 2007. TFB1 or TFB2 Is Sufficient for Thermococcus kodakaraensis Viability and for Basal Transcription in Vitro. J Mol Biol **367:**344-57.

93. **Schimanski, B., T. N. Nguyen, and A. Gunzl.** 2005. Characterization of a multisubunit transcription factor complex essential for spliced-leader RNA gene transcription in Trypanosoma brucei. Mol Cell Biol **25:**7303-13.

94. **She, Q., R. K. Singh, F. Confalonieri, Y. Zivanovic, G. Allard, M. J. Awayez, C. C. Chan-Weiher, I. G. Clausen, B. A. Curtis, A. De Moors, G. Erauso, C. Fletcher, P. M. Gordon, I. Heikamp-de Jong, A. C. Jeffries, C. J. Kozera, N. Medina, X. Peng, H. P. Thi-Ngoc, P. Redder, M. E. Schenk, C. Theriault, N. Tolstrup, R. L. Charlebois, W. F. Doolittle, M. Duguet, T. Gaasterland, R. A. Garrett, M. A. Ragan, C. W. Sensen, and J. Van der Oost.** 2001. The complete genome of the crenarchaeon Sulfolobus solfataricus P2. Proc Natl Acad Sci U S A **98:**7835-40.

95. **Shockley, K. R., D. E. Ward, S. R. Chhabra, S. B. Conners, C. I. Montero, and R. M. Kelly.** 2003. Heat shock response by the hyperthermophilic archaeon Pyrococcus furiosus. Appl Environ Microbiol **69:**2365-71.

96. **Smale, S. T.** 1997. Transcription initiation from TATA-less promoters within eukaryotic protein-coding genes. Biochim Biophys Acta **1351:**73-88.

97. **Smale, S. T., and J. T. Kadonaga.** 2003. The RNA polymerase II core promoter. Annu Rev Biochem **72:**449-79.

98. **Soppa, J.** 1999. Transcription initiation in Archaea: facts, factors and future aspects. Mol Microbiol **31:**1295-305.

99. **Tajiri, M.** 2008. Roles of Archaeal General Transcription Factors TFB1 and TFB2 in Thermococcus kodakaraensis During Heat Stress Response. The Pennsylvania State University, University Park, PA.

100. **Teufel, K., A. Bleiholder, T. Griesbach, and F. Pfeifer.** 2008. Variations in the multiple tbp genes in different Halobacterium salinarum strains and their expression during growth. Arch Microbiol **190:**309-18.

101. **Thomas, M. C., and C. M. Chiang.** 2006. The general transcription machinery and general cofactors. Crit Rev Biochem Mol Biol **41:**105-78.

102. **Thomm, M.** 1996. Archaeal transcription factors and their role in transcription initiation. FEMS Microbiol Rev **18:**159-71.

103. **Thomm, M.** 2007. Transcription: Mechanism and Regulation, p. 139-157. *In* R. Cavicchioli (ed.), Archaea: Molecular and Cellular Biology. ASM Press, Washington, DC.

104. **Thomm, M., C. Reich, S. Grunberg, and S. Naji.** 2009. Mutational studies of archaeal RNA polymerase and analysis of hybrid RNA polymerases. Biochem Soc Trans **37:**18-22.

105. **Thompson, D. K., J. R. Palmer, and C. J. Daniels.** 1999. Expression and heat-responsive regulation of a TFIIB homologue from the archaeon Haloferax volcanii. Mol Microbiol **33:**1081-92.

106. **Thomsen, J., A. De Biase, S. Kaczanowski, A. J. Macario, M. Thomm, P. Zielenkiewicz, R. MacColl, and E. Conway de Macario.** 2001. The basal transcription factors TBP and TFB from the mesophilic archaeon Methanosarcina

mazeii: structure and conformational changes upon interaction with stress-gene promoters. J Mol Biol **309:**589-603.

107. **Werner, F.** 2007. Structure and function of archaeal RNA polymerases. Mol Microbiol **65:**1395-404.

108. **Werner, F., and R. O. Weinzierl.** 2005. Direct modulation of RNA polymerase core functions by basal transcription factors. Mol Cell Biol **25:**8344-55.

109. **Woese, C. R., O. Kandler, and M. L. Wheelis.** 1990. Towards a natural system of organisms: proposal for the domains Archaea, Bacteria, and Eucarya. Proc Natl Acad Sci U S A **87:**4576-9.

110. **Yamamoto, T., T. Matsuda, T. Inoue, H. Matsumura, M. Morikawa, S. Kanaya, and Y. Kai.** 2006. Crystal structure of TBP-interacting protein (Tk-TIP26) and implications for its inhibition mechanism of the interaction between TBP and TATA-DNA. Protein Sci **15:**152-61.

111. **Zhang, D., T. L. Penttila, P. L. Morris, M. Teichmann, and R. G. Roeder.** 2001. Spermiogenesis deficiency in mice lacking the Trf2 gene. Science **292:**1153-5.

# Chapter 3

## Functional analysis of the three TBP homologs in *Methanosarcina acetivorans*

Portions of the work in this chapter have been published previously in *The Journal of Bacteriology*[1]. Published version is reproduced at the end of this chapter.

### Summary

The roles of TATA binding protein homologs (TBP1, TBP2 and TBP3) in the archaeon *Methanosarcina acetivorans* were investigated by genetic and molecular approaches. Although *tbp2* and *tbp3* deletion mutants were readily obtained, *tbp1* was not, and growth was tetracycline dependent for a conditional *tbp1* expression strain indicating that TBP1 is essential. Transcripts of *tbp1* were 20-fold more abundant than of *tbp2* and 100-200-fold more abundant than *tbp3* transcripts respectively, suggesting that

[1] **Reichlen, M.J., Murakami, K.S. and J.G. Ferry.** 2010. Functional analysis of the three TBP homologs in *Methanosarcina acetivorans.* J Bacteriol. **192**(6):1511-7.

TBP1 is the primary TBP utilized during growth. Accordingly, *tbp1* is strictly conserved in the genomes of *Methanosarcina* species. The Δ*tbp3* and Δ*tbp2* strains showed an extended lag phase *versus* wild-type, albeit the lag for Δ*tbp2* was less pronounced, when transitioning from growth on methylotrophic substrates to growth on acetate. Acetate-adapted Δ*tbp3* cells exhibited growth rates, final growth yields and lag times that were significantly impaired *versus* wild-type when cultured with growth-limiting concentrations of acetate, and the acetate-adapted Δ*tbp2* strain exhibited a reduced final growth yield *versus* wild-type when cultured with growth-limiting acetate concentrations. DNA microarray analyses identified 92 and 77 genes with altered transcription in the Δ*tbp2* and Δ*tbp3* strains respectively consistent with a role for TBP2 and TBP3 in optimizing gene expression. Together the results suggest that TBP2 and TBP3 are required for efficient growth in conditions similar to the native environment of this organism.

## Introduction

The basal transcription machinery of the *Archaea* resembles that of the RNA polymerase II system in the *Eukarya* domain that includes two essential general transcription factors, TBP (TATA Binding Protein) and TFB (Transcription Factor B) (3-5, 19, 30, 52). In order to establish promoter-directed transcription, TBP binds a TATA-box located ~25 bp upstream of the transcription start site. The binding of TBP to the promoter allows TFB to bind at sites both upstream and downstream of the TATA-box.

TFB then recruits RNA polymerase to the promoter to establish the pre-initiation complex followed by transcription (2).

Genes encoding multiple homologs of TBP and/or TFB have been identified in the genomes of several species in the *Archaea* domain. It is proposed that the homologs function to direct gene specific transcription in analogy to alternative σ-factors specific to the *Bacteria* domain (1). Experimental evidence in support of this hypothesis has been reported for the archaeal species *Halobacterium* sp. NRC-1 that contains six *tbp* and seven *tfb* genes (11, 15). A comprehensive systems approach provided evidence suggesting global gene regulation by specific TFB-TBP pairings (15). In another study, two different mutants with a deletion of either the *tbp*D or *tfb*A homolog showed the coordinate down regulation of 363 genes compared with the parental strain further supporting global gene regulation by specific TFB-TBP pairings (11). Many of the regulated genes are involved in the heat-shock response, and one of the TFB homologs binds specifically to the promoter of the heat shock protein gene *hsp5* (38). The functional roles for multiple TFB homologs have been investigated in various hyperthermophilic archaea species as well (40, 42, 45). Contrary to the reports for *Halobacterium*, none of these reports presented direct evidence for differentially gene regulation *in vivo* by the different TFB homologs. One matter complicating the study in *Halobacterium* sp. NRC-1 is multiple homologs of both TBP and TFB, presenting it with the opportunity to exploit as many as 42 different TBP/TFB combinations for recruitment of RNA polymerase to specific promoters. However, this is not the case for *Methanosarcina acetivorans* C2A, a genetically tractable methanogen with genome annotations for three homologs of TBP and only a single TFB (39, 48, 49), offering an

opportunity to study the role of multiple TBPs in the context of only a single TFB. *M. acetivorans* is the only acetotrophic methanogen isolated from a marine environment where it must compete for acetate with acetotrophic sulfate-reducing bacteria (27, 41, 46-48). The results of molecular and genetic approaches addressing roles for the three TBP homologs in *M. acetivorans* are reported here. The results illustrate that TBP1 is essential and that TBP2 and TBP3 are non essential although with specialized roles during adaptation to acetate and during growth with growth-limiting acetate concentrations.

## Results

### Analysis of *tbp1, tbp2* and *tbp3* gene expression

The genome of *M. acetivorans* is annotated with genes encoding three TBP homologs (18) distinguished by sequence identity (Table 3-1). In previous proteomics studies, peptides specific to TBP1, TBP2 and TBP3 were detected in cell lysates from methanol-, acetate- and CO-grown *M. acetivorans* (32, 36). Specific amplification products were detected for all three TBP transcripts in total RNA from methanol- and acetate-grown cells by non-quantitative reverse transcriptase PCR (RT-PCR) and sequencing of the amplified products (Fig. 3-1). Absolute transcript abundances were determined for each TBP gene by quantitative Real-Time Reverse Transcription PCR (qRT-PCR) at mid-exponential phase during growth with methanol, acetate, TMA (trimethylamine) and CO. Transcript abundances for *tbp1* were ~20-fold greater than

*tbp2* in cells cultured with any of the four growth substrates, ~100-fold more abundant than *tbp3* during growth on methanol, TMA or CO and ~200-fold more abundant than *tbp3* during growth on acetate (Table 3-2). Transcript abundances for *tbp2* were ~3-, 5-, 7- and 10-fold more abundant than *tbp3* during growth on methanol, TMA, CO and acetate respectively (Table 3-2). The transcript abundances of *tbp1*, *tbp2* and *tbp3* were also determined in early log phase and late log phase during growth on methanol. In each case, the relative proportion of *tbp2* and *tbp3* transcript abundance to *tbp1* remained the same (data not shown). Together, these results are consistent with undetermined physiological functions for each of the three TBPs.

Western blot analysis was implemented to measure the relative abundances of the TBP1, TBP2 and TBP3 peptides in *M. acetivorans* cell lysate. Polyclonal antisera were raised against purified recombinant TBP1 and TBP3. No antiserum was raised against recombinant TBP2 due to the formation inclusion bodies during over expression in *E. coli*. Both the anti-TBP1 and anti-TBP3 anitsera cross reacted with all three recombinant *M. acetivorans* TBPs (Fig. 3-2). Anti-TBP1 antisera reacted strongest with recombinant TBP1. However, the anti-TBP3 anitserum reacted strongest with recombinant TBP2. In an attempt to limit this cross reactivity, the anit-TBP1 anitserum was incubated with recombinant TBP2 and TBP3 and the anit-TBP3 antiserum was incubated with recombinant TBP1 prior to primary antibody treatment step. It was hypothesized that during this incubation step, the recombinant TBP proteins would act as an additional blocking agent. Indeed, this treatment did indeed increase the specificity of anti-TBP1 for recombinant TBP1 (Fig. 3-2A lanes 7-9) and the specificity of anti-TBP3 for recombinant TBP2 and TBP3 (Fig. 3-2B lanes 7-12).

**Table 3-1. Evolutionary relatedness of *Methanosarcina* TBPs.**

| | M.a. 1 (MA4331) | M.a. 2 (MA0179) | M.a. 3 (MA0278) | M.m. 1A (MM1028) | M.m. 1B (MM1027) | M.m. 3 (MM2184) | M.ba. 1 (MbarA0595) | M.ba. 3 (MbarA1062) | M.bu. 1 (Mbur1496) | M.t. 1 (Mthe0152) |
|---|---|---|---|---|---|---|---|---|---|---|
| **M.a. 1 (MA4331)** [a] | 100 [b] | 61 | 67 | 96 | 98 | 66 | 97 | 65 | 88 | 80 |
| **M.a. 2 (MA0179)** | 61 | 100 | 70 | 61 | 61 | 72 | 61 | 70 | 61 | 65 |
| **M.a. 3 (MA0278)** | 67 | 70 | 100 | 66 | 67 | 85 | 65 | 76 | 67 | 74 |
| **M.m. 1A (MM1028)** | 96 | 61 | 66 | 100 | 95 | 65 | 95 | 65 | 86 | 77 |
| **M.m. 1B (MM1027)** | 98 | 61 | 67 | 95 | 100 | 66 | 97 | 64 | 87 | 79 |
| **M.m. 3 (MM2184)** | 66 | 72 | 85 | 65 | 66 | 100 | 67 | 80 | 64 | 71 |
| **M.ba. 1 (MbarA0595)** | 97 | 61 | 65 | 95 | 97 | 67 | 100 | 65 | 89 | 79 |
| **M.ba. 3 (MbarA1062)** | 65 | 70 | 76 | 65 | 64 | 80 | 65 | 100 | 65 | 69 |
| **M.bu. 1 (Mbur1496)** | 88 | 61 | 67 | 86 | 87 | 64 | 89 | 65 | 100 | 78 |
| **M.t. 1 (Mthe0152)** | 80 | 65 | 74 | 77 | 79 | 71 | 79 | 69 | 78 | 100 |

[a] M.a. = *M. acetivorans*; M.m. = *M. mazei*; M.ba. = *M. barkeri*; M.bu. = *Methanococcoides burtonii*; M.t. = *Methanosaeta thermophila.*

[b] Percent amino acid sequence identity.

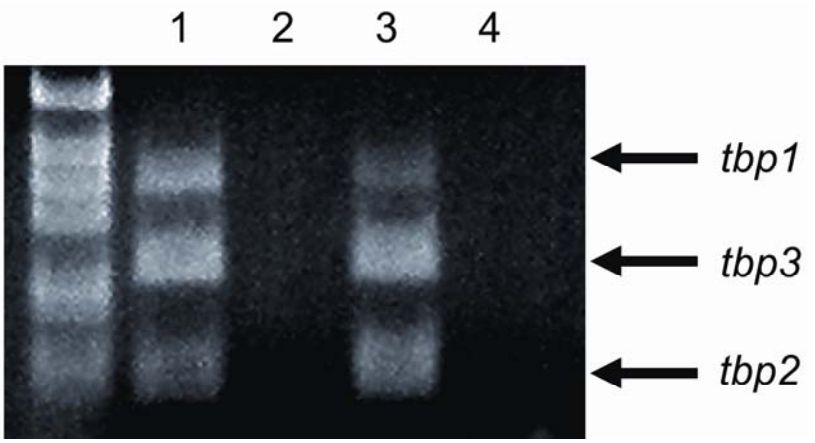


**Figure 3-1. Detection of *tbp1, tbp2* and *tbp3* transcripts by RT-PCR.** Lanes 1 and 3 show amplification products specific to each TBP transcript using total RNA from methanol- and acetate-grown cells respectively. Lanes 2 and 4 are negative controls using the same RNA as lanes 1 and 3 without the addition of reverse transcriptase. Arrows denote specific RT-PCR products for each TBP.

**Table 3-2. Abundance of *tbp1, tbp2* and *tbp3* transcripts in *M. acetivorans* cultured with various substrates.**

| | Growth substrate | | | |
|---|---|---|---|---|
| **Gene** | **Methanol** | **Acetate** | **TMA** | **CO** |
| ***tbp1*** | 390 ± 50 [a] | 380 ± 110 | 370 ± 20 | 140 ± 40 |
| ***tbp2*** | 13 ± 5 | 17 ± 5 | 21 ± 1 | 7.2 ± 2.5 |
| ***tbp3*** | 4.9 ± 0.8 | 1.7 ± 0.4 | 3.9 ± 0.4 | 1.1 ± 0.0 |

[a] Values are transcript copies per ng of total cellular RNA (x $10^{-3}$). Values represent the average and standard deviation of triplicate measurements. Absolute copy numbers were measured as described in the Materials and Methods using RNA from methanol-grown cells. Copy numbers for acetate- TMA- and CO-grown cells were inferred based on their relative abundances *versus* methanol-grown cells calculated using the $\Delta\Delta C_t$ method with the 16s rRNA gene used as an invariant control. The $\Delta C_t$ values for methanol-grown cells were used as the calibrator.

The anti-TBP1 and anit-TBP3 anitsera were probed against *M. acetivorans* whole cell lysates collected from cells growth on methanol, acetate, CO, TMA, DMA (dimethylamine), and MMA (monomethylamine). A single band of approximately equal intensity corresponding in size to the recombinant TBP proteins was detectible in the lysates from cells grown on each of the six substrates using either treated or untreated aniti-TBP1 anitsera (Fig. 3-2A) consistent with expression of TBP1 during growth on all six methanogenic substrates. Using untreated anit-TBP3 antiserum, a single band corresponding in size to the recombinant TBPs was also detected in lysate from methanol-, acetate-, TMA-, DMA-, MMA- and CO-grown cells. However, after treating anti-TBP3 with recombinant TBP1, this band was no longer detectible (Fig. 3-4B lanes 7-12) suggesting that TBP1 was the major protein in this band. In contrast, the reactivity of the anti-TBP3 to recombinant TBP2 and TBP3 was relatively unchanged following pre-incubation with recombinant TBP1 (Fig 3-2B). Thus, because TBP2 and TBP3 could not be detected in whole cell lysates by this method whereas TBP1 could be readily detected, it can be inferred that the abundance of these two proteins in the cell is considerably less than TBP1 consistent with qRT-PCR analysis.

**A.**

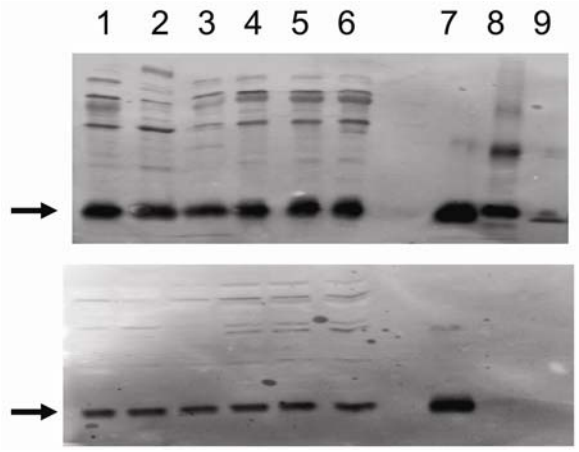


**B.**

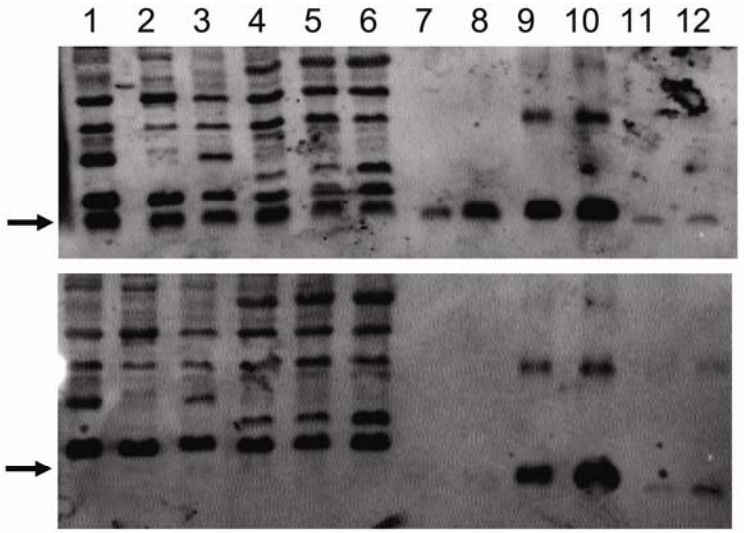


**Figure 3-2.** ***In vivo*** **TBP protein content determination by Western blot.** (A) Blots probed using anti-TBP1 antiserum. The blot on the top was probed with untreated anti-TBP1 antiserum. The blot on the bottom was probed with anti-TBP1 antiserum incubated overnight in the presence of 100 µg each of recombinant TBP2 and TBP3. Lanes 1-6: whole cell lysate from methanol-, acetate-, CO-, TMA-, DMA- and MMA-grown *M. acetivorans*. Lanes 7-9: 5 ng recombinant TBP1, TBP2 and TBP3 respectively. (B) Blots probed using anit-TBP3 antiserum. The blot on the top was probed with untreated anti-TBP3 antiserum. The blot on the bottom was probed with anti-TBP3 antibodies incubated overnight in the presence of 100 µg recombinant TBP1. Lanes 1-3: whole cell lysate from methanol-, acetate-, CO-, TMA-, DMA- and MMA-grown *M. acetivorans*. Lanes 7,8: 0.5 and 1 ng recombinant TBP1; lanes 9,10: 0.5 and 1 ng recombinant TBP2; lanes 11,12: 0.5 and 1 ng recombinant TBP3. Arrows denote the band corresponding in size to TBP.

## Transcriptional mapping of *tbp1, tbp2* and *tbp3*

Non-quantitative RT-PCR was used to assess the nature of the *tbp1, tbp2* and *tbp3* transcriptional units, and their transcription start sites (TSS) were mapped using RLM (RNA ligase mediated)-RT-PCR. A single RT-PCR product was detected spanning *tbp1* and MA4330 consistent with co-transcription of the two genes. Two transcription start sites were identified at 24 (start site 2) and 56 (start site 1) nucleotides upstream of the putative *tbp1* start codon (Fig. 3-6). Both of these TSSs were also identified by primer extension analysis. A more prominent band was identified corresponding to start site 2 suggesting that it is the primary TSS (Fig. 3-6B). Sequences closely resembling the consensus methanogen TATA box and BRE (VRAAANNTTTATATA) (26, 37, 51) were identified approximately 22 nucleotides upstream of both TSSs (Fig. 3-4A). A conserved 13-mer sequence, GCTTTATATACTG, was identified at the +1 nucleotide of start 2 and at the +2 nucleotide of start site 1 (Fig. 3-4A) although its functional significance is unclear. Additionally, the putative TATA box and BRE sequences for start site 2 are identical to those identified upstream of the TSS for the second GTF, *tfb* (Fig. 3-3) consistent with similar expression patterns for *tbp1* and *tfb*.

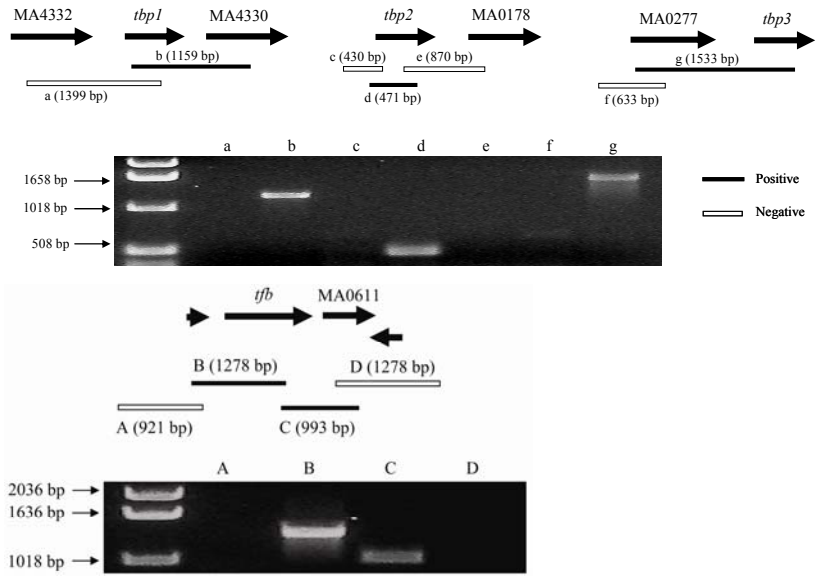


**Figure 3-3. Transcriptional mapping of *M. acetivorans tbp1, tbp2, tbp3* and *tfb* gene clusters by RT-PCR.** Arrows represent genes and direction of transcription. Predicted RT-PCR products are represented by lines under the genes and are labeled with lower case letters. Predicted RT-PCR product sizes are shown in parentheses. Letters above the gel lanes correspond to predicted RT-PCR products. RT-PCR was performed with total RNA from methanol-grown *M. acetivorans.*

RT-PCR analysis was consistent with monocistronic transcription of *tbp2* (Fig. 3-3), and a single transcription start site was identified 143 nucleotides upstream of the putative *tbp2* start codon (Fig. 3-4A). The nucleotide sequence from -22 to -33 upstream of this site resembled a methanogen TATA-box and BRE, but it was more divergent from the consensus methanogen TATA box/BRE than those identified upstream of the two *tbp1* TSSs suggesting a weaker promoter for *tbp2* than that for *tbp1* consistent with qRT-PCR analyses. A conserved 9-mer sequence motif, AAAAAANAG was identified at three sites within the *tbp2* 5' UTR consistent with a potential functional role in the regulation of *tbp2*.

**A.**

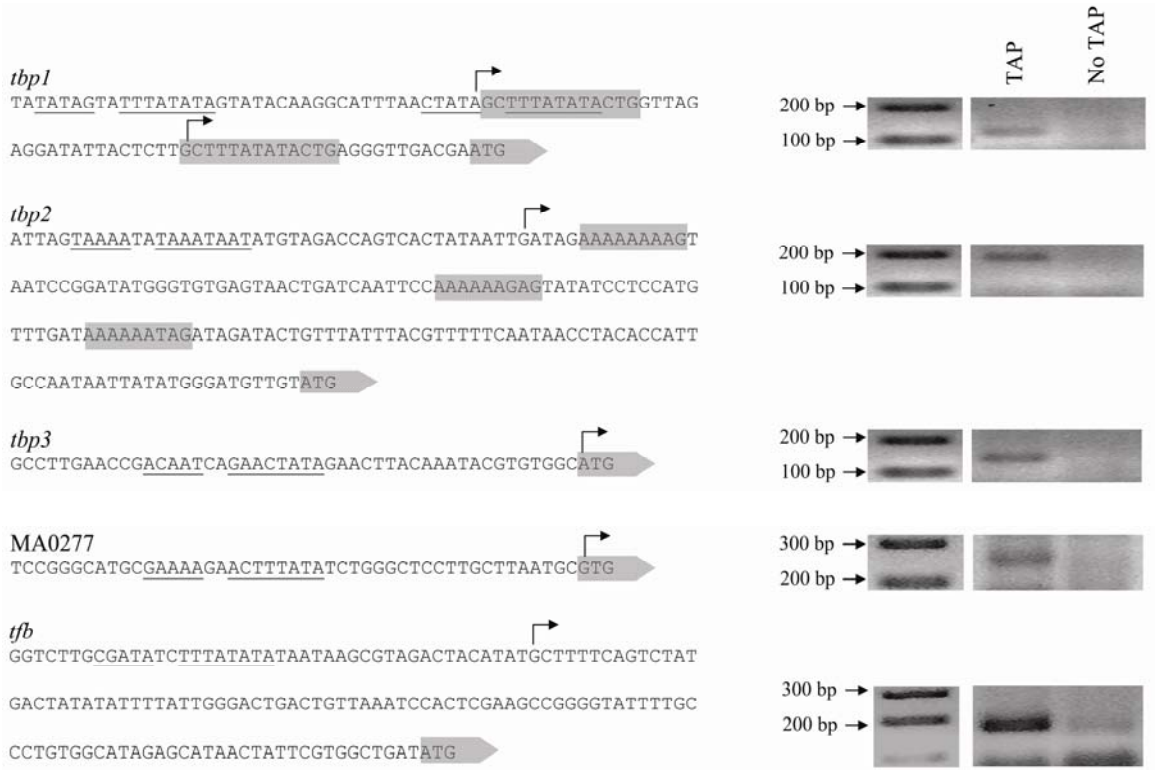
tbp1
TATATAGTATTTATATAGTATACAAGGCATTTAACTATAGCTTTATATACTGGTTAG
AGGATATTACTCTTGCTTTATATACTGAGGGTTGACGAATG
tbp2
ATTAGTAAAATATAAATAATATGTAGACCAGTCACTATAATTGATAGAAAAAAAAGT
AATCCGGATATGGGTGTGAGTAACTGATCAATTCCAAAAAAGAGTATATCCTCCATG
TTTGATAAAAAATAGATAGATACTGTTTATTTACGTTTTTCAATAACCTACACCATT
GCCAATAATTATATGGGATGTTGTATG
tbp3
GCCTTGAACCGACAATCAGAACTATAGAACTTACAAATACGTGTGGCATG
MA0277
TCCGGGCATGCGAAAAGAACTTTATATCTGGGCTCCTTGCTTAATGCGTG
tfb
GGTCTTGCGATATCTTTATATATAATAAGCGTAGACTACATATGCTTTTCAGTCTAT
GACTATATATTTTATTGGGACTGACTGTTAAATCCACTCGAAGCCGGGGTATTTTGC
CCTGTGGCATAGAGCATAACTATTCGTGGCTGATATG
TAP
No TAP
200 bp
100 bp
200 bp
100 bp
200 bp
100 bp
300 bp
200 bp
300 bp
200 bp

**B.**

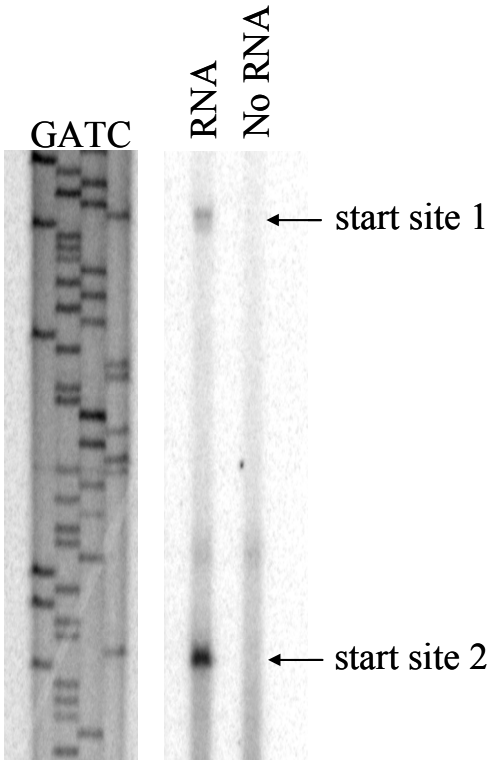
GATC
RNA
No RNA
start site 1
start site 2

**Figure 3-4. Transcription start site determination for *tbp1, tbp2, tbp3,* MA0277 and *tfb.*** (A) TSS determination by RLM-RT-PCR. Results for RT-PCR reactions performed with RNA templates treated and untreated with tobacco acid pyrophosphatase (TAP) are shown in the gels on the right of the panel in lanes labeled TAP and No TAP respectively. The products amplified exclusively in the TAP-treated RNA sample were isolated and sequenced. The junction site between the exogenous oligonucleotide sequence and *M. acetivorans* sequence identified the transcription start sites. The nucleotide sequences in the promoter regions for each gene are shown on the left side of the panel. The TSSs for each gene are denoted with hooked arrows above the corresponding nucleotide. The putative start codon for each corresponding protein denoted with a boxed arrow. Putative TATA-boxes and BREs are underlined. Repeated sequence motifs in the *tbp1* and *tbp2* transcripts are shaded in gray. (B) Primer extension analysis of *tbp1* promoter region. Products for the primer extension reactions performed with and without RNA are shown in lanes 1 and 2 respectively, and the bands representing transcription start sites are denoted with arrows. The results of sequencing reactions for the *tpb1* promoter region are shown in lanes labeled G, A, T and C.

Although separated by a large intergenic region of 336 bp, an RT-PCR product was detected spanning *tbp3* and the orf immediately upstream, MA0277 consistent with co-transcription of the two genes (Fig. 3-3). However, TSSs were identified at the putative TBP3 start codon and at the putative MA0277 start codon (Fig. 3-4A). The nucleotide sequences from -22 to -33 upstream these two TSSs did not closely resemble the consensus methanogen TATA-box and BRE suggestive of weak promoters. This is consistent with qRT-PCR analyses which revealed that *tbp3* transcript abundances were the lowest of the three TBP genes.

## Analysis of TBP mutant strains.

To assess the biological significance of each of the *M. acetivorans* TBP orthologs, individual deletion of the three encoding genes was attempted by homologous

recombination and selection for puromycin resistance in the presence of methanol in the growth medium. Mutant strains deleted for either the *tbp2* or *tbp3* (Δ*tbp2* and Δ*tbp3*) were obtained and confirmed by Southern hybridization (Fig. 3-5) and qRT-PCR (Table 3-3), indicating that *tbp2* and *tbp3* are dispensable during growth on methanol. Neither the *tbp2* nor the *tbp3* deletion significantly affected the transcription of either of the remaining TBP genes (Table 3-3). Attempts to delete *tbp1* by double cross over were unsuccessful. Therefore, a conditional mutant of *tbp1* was constructed using a previously described approach (21). As opposed to deleting the *tbp1* coding sequence, the promoter for *tbp1* was modified by replacing the native promoter (P*tbp1*) with a chimeric version of the *mcrB* promoter that contains an operator sequence for Tn*10* TetR protein (P*mcrB*(tetO1)) (Fig 3-5). The Tn*10* TetR is constitutively expressed from two remote sites on the chromosome. Transcription of P*mcrB*(tetO1) is repressed by the Tn*10* TetR in the absence of tetracycline. Thus in this strain (ΔP*tbp1*::P*mcrB*(tetO1)-*tbp1*), *tbp1* can only be expressed in the presence of tetracycline. Growth was comparable to the parental strain in the presence of 0.5-100 μg $mL^{-1}$ of tetracycline as was the transcript abundance of *tbp1* (Table 3-3). However, little growth was observed in the absence of tetracycline indicating that *tbp1* is essential for growth (Fig 3-6). In the presence of low levels of tetracycline (0.05 μg $mL^{-1}$), cell growth and transcription of *tbp1* were impaired (Fig. 3-6, Table 3-3).

To identify growth phenotypes associated with the deletion of either *tbp2* or *tbp3*, substrate-dependent cell growth was investigated by comparing growth parameters (initial growth rate, maximum $A_{600}$ and the lag time to reach mid-log phase) for the Δ*tbp2* and Δ*tbp3* strains *versus* wild-type when cultured with initial substrate concentrations of

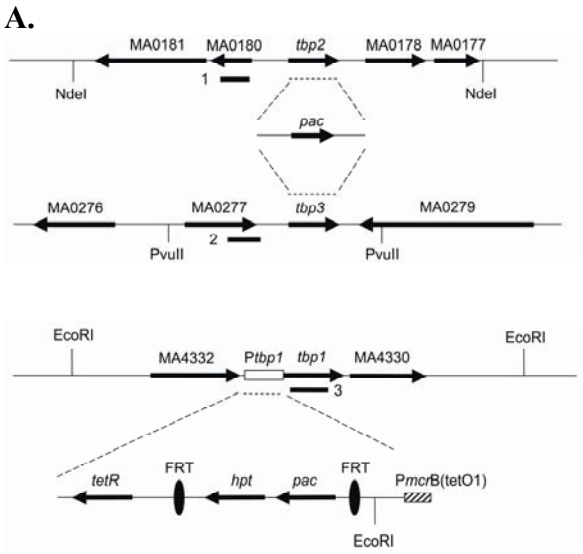


**Figure 3-5**. **Construction of *M. acetivorans* mutants with *tbp2* or *tbp3* deleted, or with the native P*tbp1* replaced with P*mcrB*(tetO1).** (A) Top half shows the *tbp2* and *tbp3* gene arrangements on the *M. acetivorans* C2A chromosome. Arrows denote genes and direction of transcription. Broken lines denote regions replaced with a *pac* (puromycin acetyltransferase) cassette in deletion mutant strains. The heavy lines labeled 1 and 2 identify the PCR products used as probes for Southern hybridizations depicted in panel B. NdeI and PvuII cut sites are indicated on the chromosome. The bottom half shows the *tbp1* gene arrangement on the *M. acetivorans* WWM75 chromosome. Arrows denote genes and direction of transcription. The boxes denote promoter sequences (P*tbp1* open; P*mcrB*(tetO1) striped). Broken lines denote regions replaced with the mutant strains. Ovals denote Flp recognition targets. The heavy line labeled 3 identifies the PCR products used as probes for Southern hybridizations depicted in panel B. EcoRI cut sites are indicated. (B) The genomic structures of Δ*tbp2*, Δ*tbp3* and ΔP*tbp1* were verified by Southern hybridizations of NdeI, PvuII or EcoRI digested genomic DNA from wild-type, WWM75, Δ*tbp2*, Δ*tbp3* or ΔP*tbp1 M. acetivorans* strains with DIG-labeled probes 1, 2 or 3. The molecular weight marker is shown in lane M with band sizes indicated on the left.

**Table 3-3. Relative abundance of *tbp1, tbp2* and *tbp3* transcripts in *M. acetivorans* wild-type and mutant strains.**

| Gene | Strain | | | | | | |
|---|---|---|---|---|---|---|---|
| | **C2A** | **Δ*tbp2*** | **Δ*tbp3*** | **WWM75** [b] | **WWM75** [c] | **ΔP*tbp1*::P*mcrB*(tetO1)-*tbp1*** [b] | **ΔP*tbp1*::P*mcrB*(tetO1)-*tbp1*** [d] |
| ***tbp1*** | 1.0 ± 0.1 [a] | 1.1 ± 0.0 | 1.1 ± 0.0 | 1.0 ± 0.1 | 1.3 ± 0.1 | 2.0 ± 0.1 | 0.077 ± 0.006 |
| ***tbp2*** | 1.0 ± 0.2 | Not detected | 0.67 ± 0.01 | 1.0 ± 0.1 | 0.93 ± 0.09 | 0.87 ± 0.17 | 1.5 ± 0.3 |
| ***tbp3*** | 1.0 ± 0.2 | 1.0 ± 0.1 | Not detected | 1.0 ± 0.1 | 1.3 ± 0.1 | 1.4 ± 0.3 | 0.49 ± 0.04 |

[a] Values represent the average and standard deviation of triplicate measurements. Relative transcript abundances were calculated using the $\Delta\Delta C_t$ method with the 16s rRNA gene used as an invariant control. The $\Delta C_t$ values for C2A cells were used as the calibrator for C2A (aka wild-type), Δ*tbp2* and Δ*tbp3*. The $\Delta C_t$ values for WWM75 were used as the calibrator for WWM75 and ΔP*tbp1*::P*mcrB*(tetO1)-*tbp1*.

[b] Grown in the presence of 100 μg $mL^{-1}$ Tetracycline

[c] Grown in the presence of 0 μg $mL^{-1}$ Tetracycline

[d] Grown in the presence of 0.050 μg $mL^{-1}$ Tetracycline

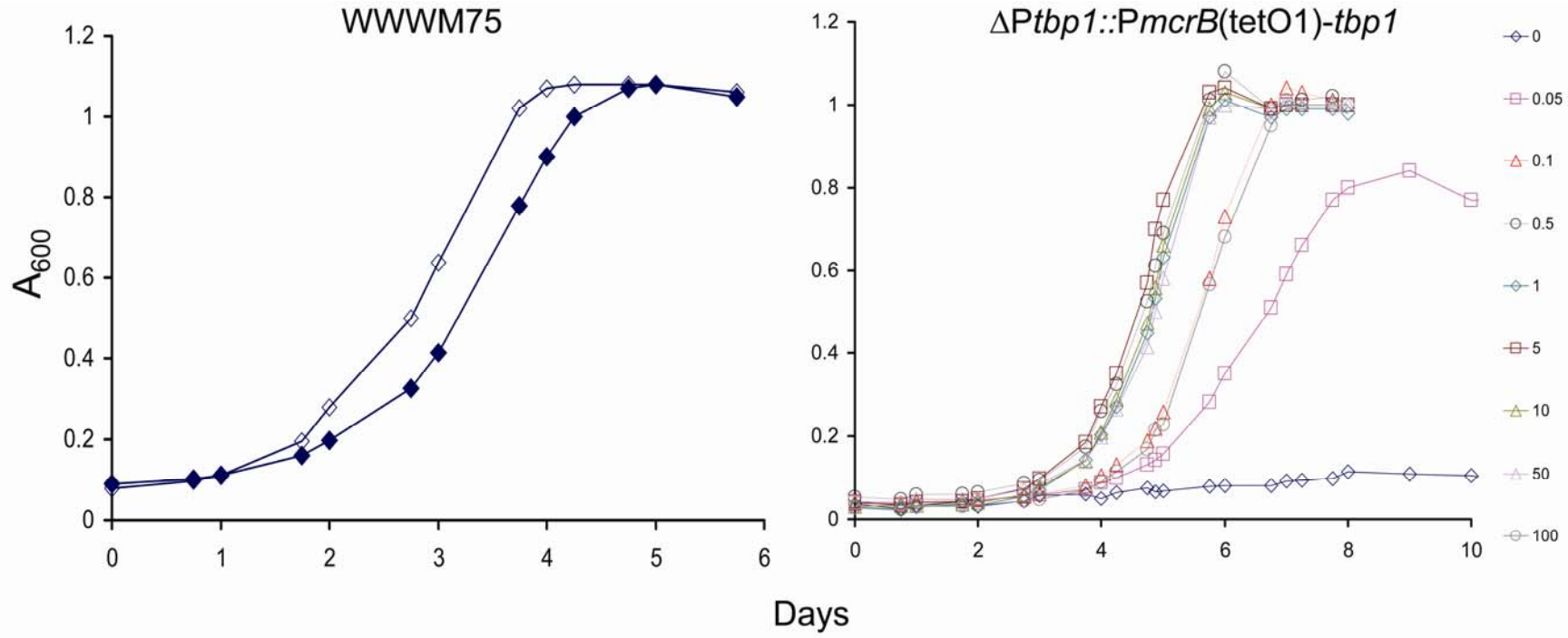


**Figure 3-6. Growth of ΔP*tbp1*::P*mcrB*(tetO1)-*tbp1* (right panel) and its parental strain, WWM75 (left panel).** Strains were cultured on 50 mM TMA. Growth of WWM75 is depicted in the presence (filled circles) or absence (open circles) of 100 μg $mL^{-1}$ of tetracycline. Growth of ΔP*tbp1*::P*mcrB*(tetO1)-*tbp1* is depicted in the absence or presence of 0.05-100 μg $mL^{-1}$ of tetracycline**.** Tetracycline concentration for each replicate culture is depicted in the legend

250 mM methanol, 100 mM TMA, 1.5 atm 100% CO headspace gas or 100 mM acetate. During culturing with acetate, the acetate concentration was maintained in the range of 75-100 mM by periodic supplementation with acetic acid. No robust differences in growth parameters were observed for the Δ*tbp2* and Δ*tbp3* strains *versus* the wild-type strain when cultured with the methylotrophic substrates, methanol or TMA (Fig. 3-7, Table 3-4). However, the lag time to reach mid-log phase for acetate-grown cultures of Δ*tbp3* (25.7 ± 6.1 n=30) inoculated with methanol-grown cells was 12 days longer on average than for wild-type (13.2 ± 3.7 n=30) (Fig. 3-8, Table 3-5). The Δ*tbp3* strain also showed a comparably longer lag when transitioning from growth on TMA to acetate (Fig 3-8). Once the mutant strains were fully adapted to growth on acetate (≥30 generations of growth on acetate), growth parameters were indistinguishable from wild-type strain during culturing with acetate maintained at 75-100 mM (Fig 3-9, Table 3-5). These results suggest that TBP3 has a role in the transition from growth on methylotrophic substrates to growth on acetate. Although not as robust as the phenotype observed for Δ*tbp3*, the Δ*tbp2* strain showed a trend towards a longer lag *versus* wild-type as well (18.4 ± 4.2 n=30) when transitioning from growth on methanol to growth on 75-100 mM acetate (Fig. 3-8, Table 3-5) and from TMA to 75-100 mM acetate (Fig. 3-8). Like the Δ*tbp3* strain, the Δ*tbp2* strain exhibited no significant difference in growth *versus* the wild-type after becoming fully adapted to growth on 75-100 mM acetate (Fig. 3-9, Table 3-5).

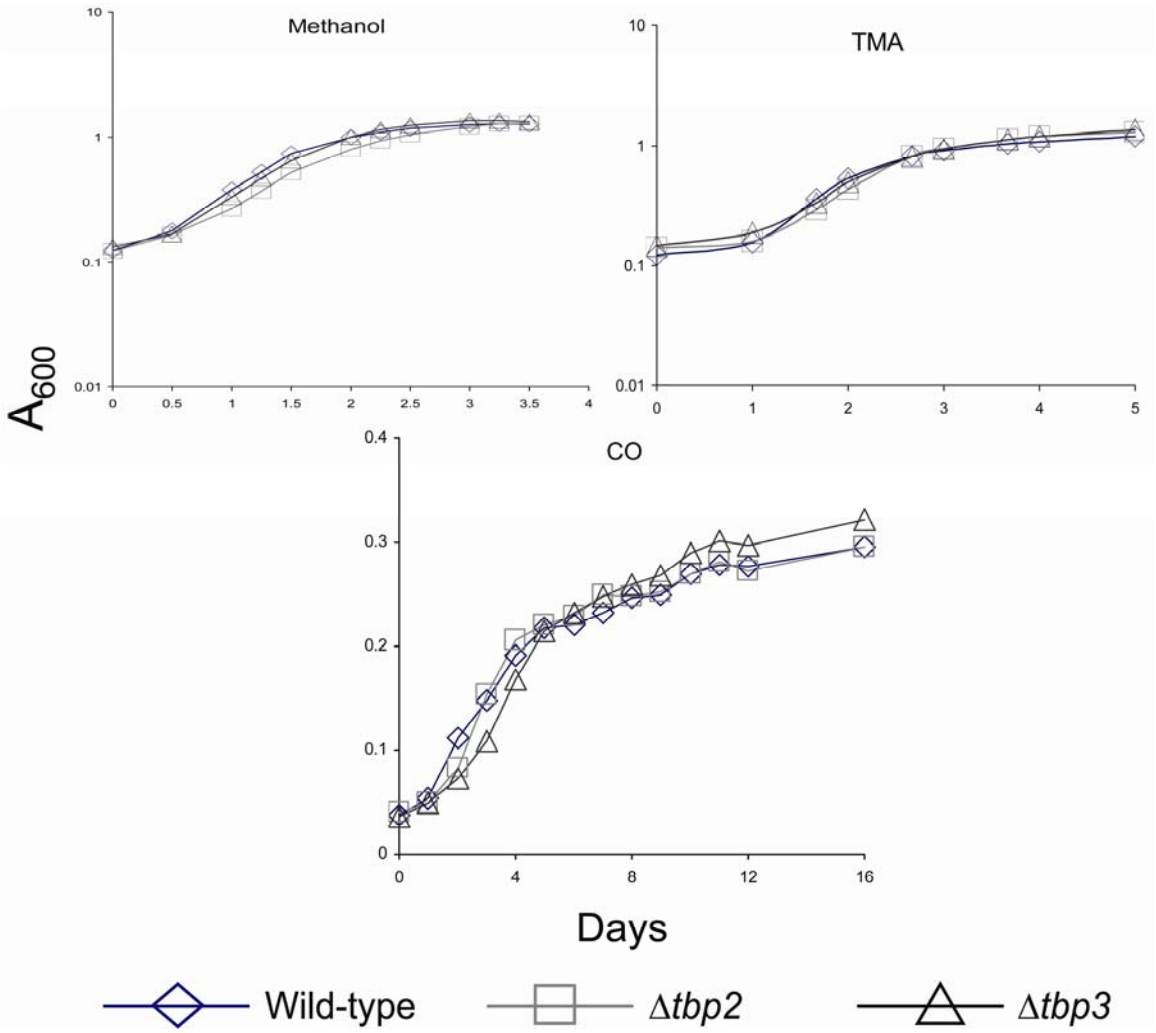


**Figure 3-7. Representative growth curves of wild-type, Δ*tbp2* and Δ*tbp3 M. acetivorans* strains on methanol, TMA and CO (single replicate).**

**Table 3-4. Growth parameters of *M. acetivorans* wild-type and mutant strains on various methanogenic substrates.**

| | wild-type | | | *Δtbp2* | | | *Δtbp3* | | |
|---|---|---|---|---|---|---|---|---|---|
| **Substrate** | **Generation Time (hours)** | **Maximum $A_{600}$** | **Lag [e] (days)** | **Generation Time (hours)** | **Maximum $A_{600}$** | **Lag (days)** | **Generation Time (hours)** | **Maximum $A_{600}$** | **Lag (days)** |
| **Methanol [a]** | 11.1 ± 1.4 [f] | 1.20 ± 0.07 | 1.6 ± 0.4 | 11.4 ± 2.2 | 1.23 ± 0.08 | 1.6 ± 0.4 | 11.1 ± 1.2 | 1.27 ± 0.07 | 1.6 ± 0.4 |
| **Methanol [b]** | 10.4 ± 0.8 | 1.21 ± 0.09 | 5.1 ± 1.8 | 10.4 ± 1.0 | 1.24 ± 0.07 | 5.1 ± 1.8 | 10.0 ± 1.6 | 1.27 ± 0.04 | 4.9 ± 1.9 |
| **TMA [c]** | 13.1 ± 1.6 | 1.28 ± 0.04 | 1.8 ± 0.3 | 12.8 ± 1.0 | 1.26 ± 0.04 | 1.9 ± 0.4 | 14.4 ± 1.9 | 1.36 ± 0.01 | 2.1 ± 0.2 |
| **TMA [a]** | 13.8 ± 0.9 | 1.33 ± 0.09 | 3.6 ± 0.1 | 13.9 ± 0.5 | 1.33 ± 0.09 | 3.2 ± 0.3 | 13.2 ± 0.1 | 1.34 ± 0.09 | 3.7 ± 0.2 |
| **CO [d]** | 27.2 ± 2.9 | 0.303 ± 0.016 | 4.0 ± 1.5 | 29.5 ± 2.8 | 0.277 ± 0.022 | 3.7 ± 0.5 | 36.7 ± 5.8 | 0.337 ± 0.015 | 6.2 ± 1.9 |

[a] Inocula adapted to growth on methanol.

[b] Inocula adapted to growth on acetate.

[c] Inocula adapted to growth on TMA.

[d] Inocula adapted to growth on CO.

[e] Time required to reach one half maximum $A_{600}$ value.

[f] All values represent the mean of 5-19 replicate cultures.

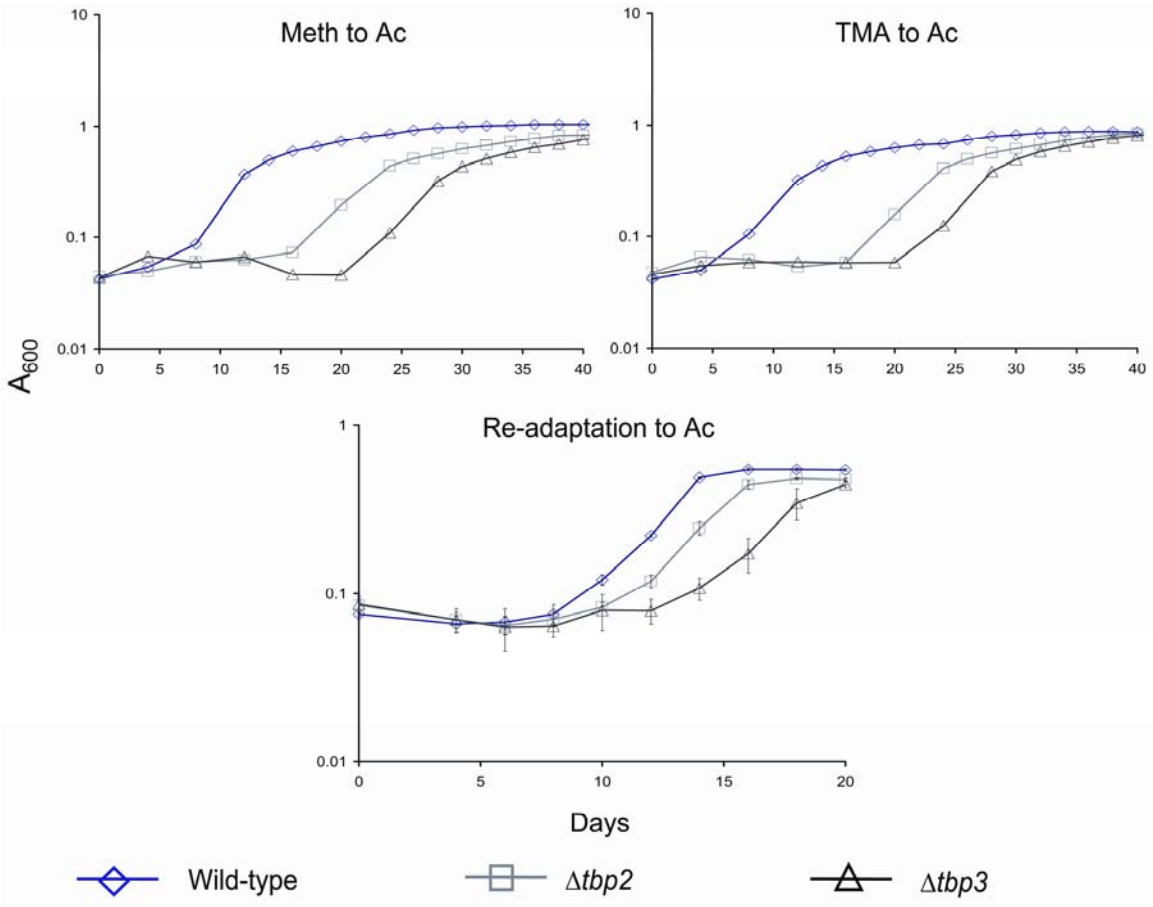


**Figure 3-8. Representative growth curves of wild-type, Δ*tbp2* and Δ*tbp3 M. acetivorans* strains during adaptation to growth on acetate.** The top two graphs depict adaptation to growth on acetate using inocula cultured on either methanol or TMA (single replicate). The bottom graph depicts re-adaptation to growth on acetate. The inocula which were cultured with methanol (250 mM) had been re-adapted to growth on methanol after previous culturing with acetate (75-100 mM). Error bars represent the standard deviation of triplicate cultures.

**Table 3-5. Growth parameters of *M. acetivorans* wild-type and mutant strains on acetate.**

| | wild-type | | | *Δtbp2* | | | *Δtbp3* | | |
|---|---|---|---|---|---|---|---|---|---|
| **Acetate (mM)** | **Generation Time (hours)** | **Maximum $A_{600}$** | **Lag [c] (days)** | **Generation Time (hours)** | **Maximum $A_{600}$** | **Lag (days)** | **Generation Time (hours)** | **Maximum $A_{600}$** | **Lag (days)** |
| **75-100** [a,e] | 48.9 ± 10.7 [d] | 0.90 ± 0.11 | 9.3 ± 1.6 | 51.6 ± 8.9 | 0.77 ± 0.07 | 11.6 ± 1.6 | 54.4 ± 11.1 | 0.84 ± 0.12 | 12.4 ± 3.0 |
| **75-100** [b,e] | 47.8 ± 9.5 | 0.92 ± 0.15 | 13.2 ± 3.7 | 56.5 ± 13.8 | 0.90 ± 0.13 | 18.4 ± 4.2 | 57.3 ± 13.5 | 0.90 ± 0.13 | 25.7 ± 6.1 |
| **100** [a,f] | 39.1 ± 0.6 | 0.69 ± 0.01 | 12.1 ± 0.5 | 44.3 ± 3.0 | 0.59 ± 0.01 | 13.6 ± 0.2 | 45.3 ± 2.5 | 0.53 ± 0.03 | 15.7 ± 1.6 |
| **50** [a,f] | 45.4 ± 3.9 | 0.45 ± 0.02 | 10.9 ± 1.5 | 51.8 ± 5.9 | 0.36 ± 0.02 | 12.9 ± 1.4 | 63.0 ± 8.8 | 0.30 ± 0.02 | 16.9 ± 1.6 |
| **20** [a,f] | 69.9 ± 5.1 | 0.18 ± 0.02 | 13.5 ± 2.9 | 73.8 ± 11.1 | 0.15 ± 0.02 | 14.4 ± 1.2 | 121 ± 37 [g] | 0.13 ± 0.02 [g] | 30.1 ± 2.9 [g] |

[a] Inocula adapted to growth on acetate.

[b] Inocula adapted to growth on methanol or TMA.

[c] Time required to reach one half maximum $A_{600}$ value.

[d] All values represent the mean and standard deviation of 3-30 replicate cultures.

[e] The acetate was maintained in this concentration range throughout growth.

[f] Initial acetate concentration. No additional acetate was added during growth.

[g] Measured in the four replicates that displayed growth. 3 of 7 replicates showed no measurable growth over a 2 month interval.

Because the prolonged lag phase between the Δ*tbp2* and Δ*tbp3* strains *versus* the wild-type when switching from growth on methanol to growth on 75-100 mM acetate diminished following adaptation, it called into question whether the growth on acetate in the mutants was the result of true adaptation or the acquisition of suppressor mutations. To test for this, acetate adapted wild-type and the Δ*tbp2* and Δ*tbp3* strains were re-adapted to growth on methanol and then subsequently re-adapted back to growth on acetate. It was assumed that if the strains had acquired suppressor mutations, they would no longer exhibit a prolonged lag phase relative to the wild-type upon subsequent re-adaptation to growth on acetate. In both cases, the mutant strain elicited a prolonged lag phase relative to the wild-type upon re-adaptation to 75-100 mM acetate (Fig 3-8), although the lag in the re-adaptation was shorter than in the initial adaptation. These results suggest that the diminished lag in the Δ*tbp2* and Δ*tbp3* strains fully adapted to 75-100 mM acetate cannot be solely attributed to acquisition of suppressor mutations (Fig 3-8) consistent with a reduced need for TBP2 and TBP3 following adaptation. However, the possibility that suppressor mutations facilitate growth on 75-100 mM acetate in the Δ*tbp2* and Δ*tbp2* cannot be ruled out.

To examine roles of TBPs in more ecologically relevant growth conditions, growth parameters of the Δ*tbp2* and Δ*tbp3* strains (Table 3-5) were determined with 20 or 50 mM acetate, concentrations nearer to the acetate concentrations (~1-2 mM) in the native environment of *M. acetivorans* (27, 47, 48). In this experiment, the inocula were fully adapted to growth on acetate and the cultures were not supplemented with acetic acid during their growth. Growth rates and lag times for the Δ*tbp2* strain were comparable to the wild-type strain. However, there was a ~20 % reduction of the

maximum $A_{600}$ obtained for the Δ*tbp2* strain *versus* the wild-type during growth with 50 mM acetate consistent with a role for TBP2 in efficient growth with growth-limiting acetate concentrations (Table 3-5, Fig 3-9). In the case of the Δ*tbp3* strain cultured with 50 mM acetate, growth rates and yields were ~40% and ~30% lower than wild-type, and the lag time was 6 days longer compared with the lag for of the wild-type strain (Table 3-5, Fig 3-9). Growth defects of the Δ*tbp3* strain were more profound when cultured with 20 mM acetate. There were 7 replicate cultures of Δ*tbp3* strain attempted all of which showed little detectible growth over the first three weeks of culturing (Fig 3-9). However, 4 of these cultures eventually initiated growth after this period. The growth rates and yields of these 4 cultures were significantly lower than wild-type, and the lag time was 17 days longer than wild-type (Table 3-5). There were no differences in any of the growth parameters for either mutant strain *versus* wild-type when cultured with limiting methanol concentrations of 25 or 50 mM (Fig 3-10). These results indicate that TBP3 is important for optimal growth with limiting concentrations of acetate.

In addition to methanol, TMA and acetate, growth of the Δ*tbp2* and Δ*tbp3* strains was compared to that of wild-type *M. acetivorans* with CO which is converted to methane by a pathway distinct from the methylotrophic and acetoclastic pathways (32, 43, 44). Growth parameters for the Δ*tbp2* were indistinguishable from wild-type (Table 3-4, Fig. 3-6) suggesting that *tbp2* is dispensable for CO metabolism. The Δ*tbp3* strain exhibited a small but significant decrease in growth rates *versus* the wild-type, but a small but significant increase in maximum $A_{600}$ (Table 3-4, Fig. 3-6). The decreased growth in the Δ*tbp3* strain is consistent with the trends observed on acetate, and it suggests that *tbp3* required for optimal growth under nutrient-limiting conditions.

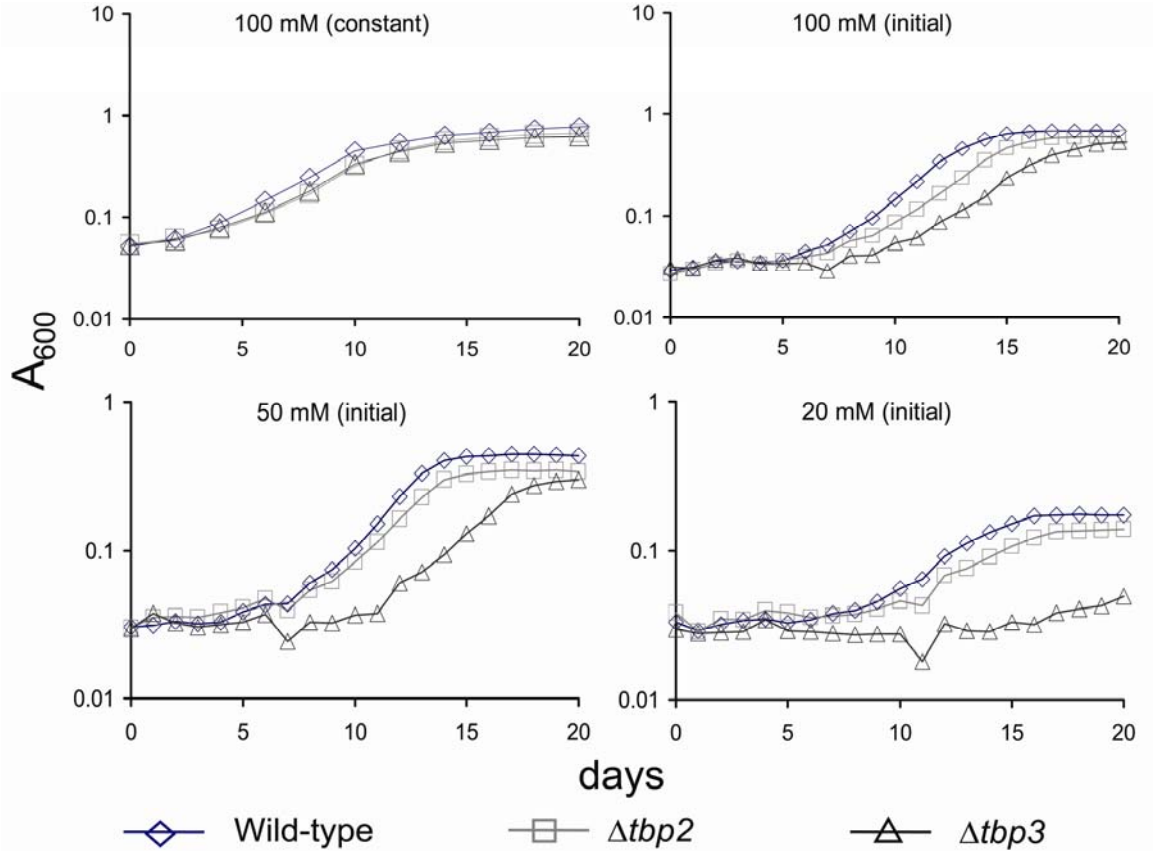


**Figure 3-9. Representative growth curves of wild-type, Δ*tbp2* and Δ*tbp3* strains of *M. acetivorans* cultured with various concentrations of acetate (single replicate).** The inocula were cultured with acetate (maintained at 75-100 mM). Cultures in the top left panel were maintained at 75-100 mM; all others were inoculated into to media with the indicated acetate concentrations and not supplemented further.

However, the significance for the increased total cell yield in the Δ*tbp3* strain *versus* the wild-type is not clear at the present time. The inherent difficulty in adapting even wild-type *M. acetivorans* to growth on CO prohibited a comparative analysis of this aspect of growth.

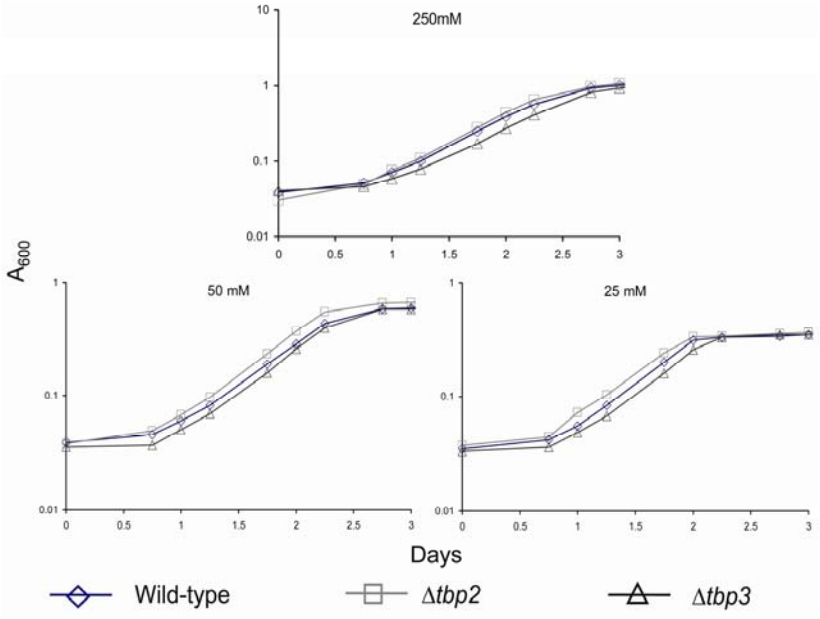


**Figure 3-10. Growth of wild-type, Δ*tbp2* and Δ*tbp3* strains of *M. acetivorans* cultured with various concentrations of methanol.** The inocula were cultured with methanol (250 mM). Error bars represent the standard deviation of triplicate cultures.

## Assessment of *Δtbp2* and *Δtbp3* competitive fitness

The marine isolate, *M. acetivorans* is distinguished from freshwater acetotrophic methanogens in that it must compete with sulfate-reducing bacteria for acetate consumption. In light of this, an assessment of the competitive fitness was made for the Δ*tbp2* and Δ*tbp3* strains *versus* that of wild-type *M. acetivorans* (Fig. 3-11). The fitness was evaluated in media containing either 250 mM methanol or acetate maintained between 75 and 100 mM. The medium was inoculated with an equal mixture of the mutant and wild-type cells, both fully adapted to growth on methanol. The relative proportion of wild-type cells and mutant cells in the total population was assessed

**A.**

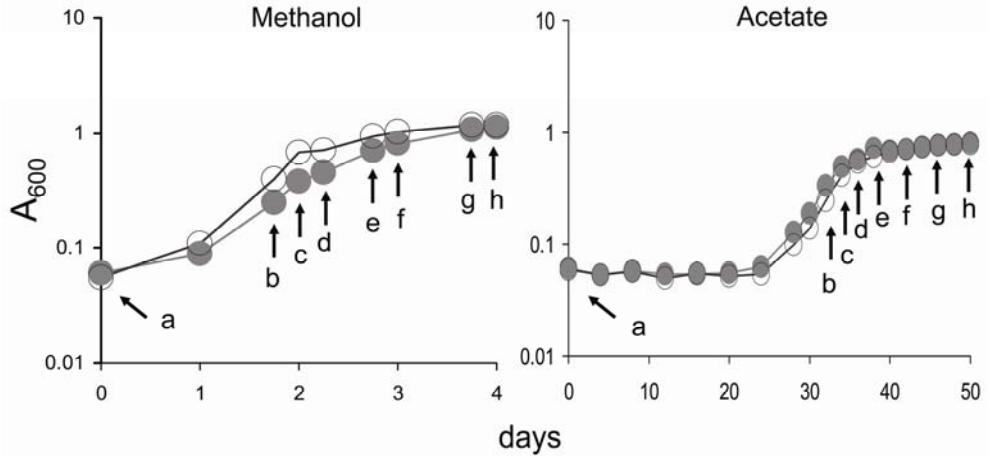


**B.**

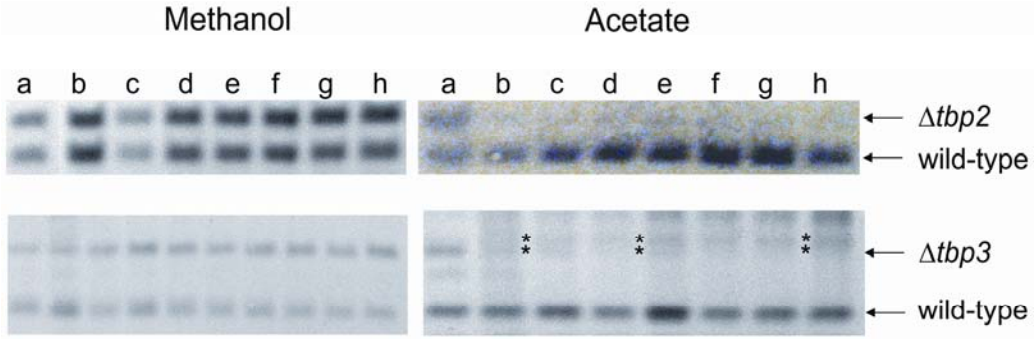


**Figure 3-11. Competition between methanol-grown wild-type and Δ*tbp2* or Δ*tbp3* strains of *M. acetivorans* cultured with methanol or acetate.** (A) Growth with either 250 mM methanol or acetate maintained between 75-100 mM inoculated with equal amounts of wild-type and Δ*tbp2* (open symbols) or wild-type and Δ*tbp3* (filled symbols) cells previously cultured with 250 mM methanol. (B) Genomic DNA isolated from cells collected at the time points denoted with arrows in panel A was subjected to Southern blot analysis for DNA specific to wild-type and Δ*tbp2* or Δ*tbp3*. Probe 1 (from Fig. 3-8) was used to distinguish wild-type from Δ*tbp2*. Probe 2 used to distinguish wild-type from Δ*tbp3* (from Fig. 3-8). Asterisks in lanes c, e and h (bottom right image) mark a doublet band in the vicinity of the Δ*tbp3* band. The top band is an unknown band resulting form incomplete restriction digestion non-specific hybridization of probe 2 with *M. acetivorans* genomic DNA. The bottom band represents the Δ*tbp3* specific genomic DNA band.

throughout growth. Because the inserted a *pac* cassette in place of *tbp2* or *tbp3* increased the genome size of the mutants by ~one kb, the proportion of mutant DNA and wild-type DNA in the total DNA population could be readily distinguished by Southern blot

analysis using a single probe that targets the unaltered genomic region adjacent mutated TBP gene. Both mutants proliferated comparable to the wild-type when cultured with methanol. However, a competitive defect was revealed for both the Δ*tbp2* and Δ*tbp3* strains growing with 75-100 mM acetate, suggesting that TBP2 and TBP3 provide added fitness during adaptation from methanol to 75-100 mM acetate.

The competitive fitness of the Δ*tbp2* and Δ*tbp3* strains was evaluated further in media containing 20 mM acetate, 50 mM acetate or 250 mM methanol that was inoculated with equal mixtures of the mutant and wild-type strains fully adapted to growth with 75-100 mM acetate. The Δ*tbp2* strain was competitive with wild-type when growing with 250 mM methanol and either concentration of acetate (Fig. 3-12B). Further, the populations of wild-type and Δ*tbp2* cells remained approximately equal after four subsequent sub-cultures grown with 50 or 20 mM acetate (Fig. 3-12B). These data suggest that TBP2 has no discernable role in providing a competitive advantage after cells fully adapted to growth on acetate. In contrast, the Δ*tbp3* strain showed a competitive disadvantage when cultured with growth-limiting acetate concentrations but proliferated comparable to wild-type when cultured with methanol (Fig. 3-12). This competitive defect was more apparent at during growth with 20 mM acetate than with 50 mM acetate (Fig. 3-12B) although a defect for the Δ*tbp3* strain during growth with 50 mM acetate was clearly apparent at the completion of a second passage of the mixed culture into fresh media (Fig. 3-12B). These results further illustrate that TBP3 is important for growth when acetate concentrations are limited as in the native environment.

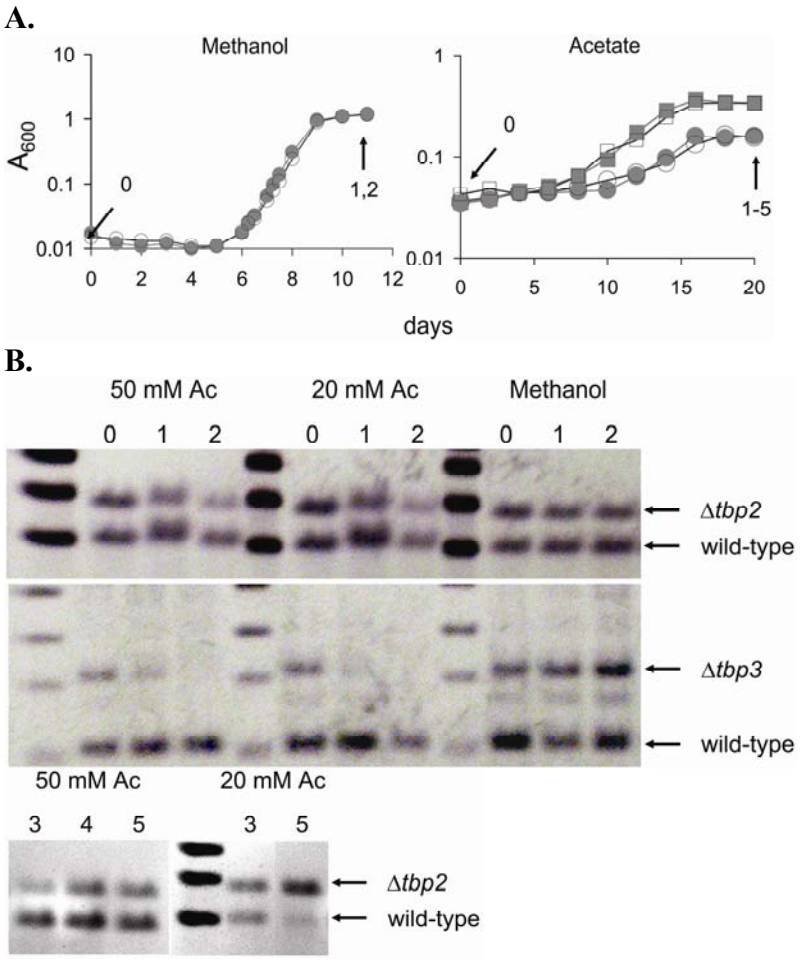


**Figure 3-12. Competition between acetate-grown wild-type and Δ*tbp2* or Δ*tbp3* strains of *M. acetivorans* cultured with methanol or growth-limiting concentrations of acetate.** (A) First passage of growth with 250 mM methanol *versus* 20 mM acetate (squares) or 50 mM acetate (circles) for mixed cultures inoculated with equal amounts of wild-type and Δ*tbp2* (open symbols) or wild-type and Δ*tbp3* (filled symbols) cells previously cultured with acetate maintained between 75-100 mM. Arrows denote time points at which samples were collected for DNA isolation. The original inocula represent time point 0; all other samples were collected at stationary phase. Time point 1 denotes the sample collected at stationary phase from the first passage of growth. Time points 2-5 represent samples collected at stationary phase from the 2$^{nd}$ to 5$^{th}$ passages respectively. (B) Genomic DNA isolated from cells collected at the time points denoted with arrows in panel A was subjected to Southern blot analysis for DNA specific to wild-type and Δ*tbp2* or Δ*tbp3*. Probe 1 (from Fig. 3-8) was used to distinguish wild-type from Δ*tbp2*. Probe 2 (from Fig. 3-8) used to distinguish wild-type from Δ*tbp3*. The wild-type and Δ*tbp3* mixed cultures were not carried out further than the 2$^{nd}$ passage of growth due to lack of detectible Δ*tbp3* DNA. Passage 4 from the wild-type and Δ*tbp2* mixed culture on 20 mM acetate DNA yield was poor and could not be visualized on the blot.

**Involvement of TBP2 and TBP3 in gene regulation**

It was anticipated that the defects in growth for the two mutant strains *versus* the wild-type might be reflected in the gene expression profiles. Indeed, there were 92 and 77 genes identified for Δ*tbp2* and Δ*tbp3* respectively which exhibited a ≥2-fold change in transcript abundance *versus* wild-type, several of which were common to both strains (Fig 3-13; Supplementary files 2-3) consistent with a role for TBP2 and TBP3 in the regulation of gene expression. Interestingly, a substantial proportion of the genes in Δ*tbp3* and the majority of the genes in Δ*tbp2* exhibited increased transcript abundance *versus* the wild-type (Fig 3-13; Supplementary files 2-3) suggesting a possible involvement for TBP2 and TBP3 in the negative regulation of numerous genes. Among the genes with increased transcript abundance in Δ*tbp2 versus* wild-type, those encoding proteins in the functional categories amino acid transport and metabolism and inorganic ion transport and metabolism were highly over represented (*P*-value = $1.57 \times 10^{-13}$ and $8.70 \times 10^{-4}$ respectively) (Appendix ?-?). However, the biological significance of this trend is not known. Numerous other genes were identified that exhibited decreased transcript abundance *versus* the wild-type in either the Δ*tbp2* or Δ*tbp3* strains. Although none had functional annotations clearly linked to acetate metabolism (Supplementary files 2-3), genes were identified that may function to provide added fitness under conditions of low nutrient availability. Of note were two genes encoding putative Hsp60 proteins (MA0857 and MA4386) both of which exhibited greatly decreased transcript abundance in both the Δ*tbp2* and Δ*tbp3* strains *versus* the wild-type with a larger decrease

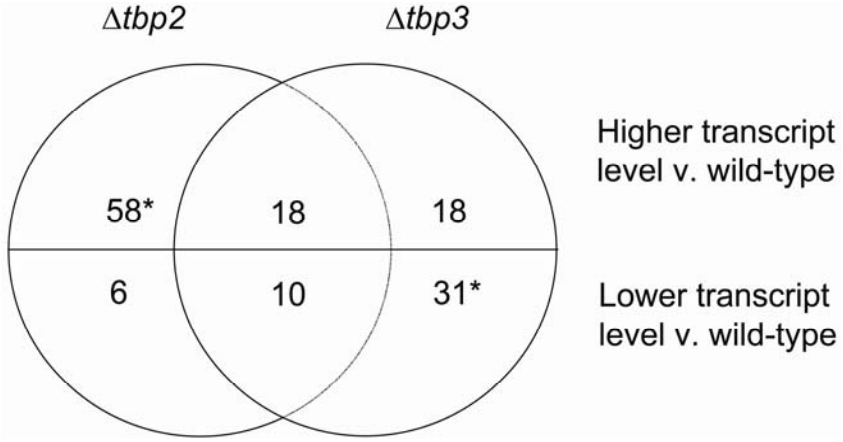


**Figure 3-13. Distribution of genes which exhibited a ≥2-fold change in transcript abundance in wild-type *M. acetivorans versus* mutant strains.** The left and right sides of the Venn diagram show the number of genes with a change in transcript abundance in the Δ*tbp2* and the Δ*tbp3* strains respectively. The middle shows the number with a change in transcript abundance in both strains. The top and bottom halves show the number with either a higher or lower transcript abundance *versus* wild-type *M. acetivorans*. Asterisks indicate that 4 of the genes with higher transcript abundance in Δ*tbp2 versus* wild-type had lower transcript abundance in Δ*tbp3 versus* wild-type.

observed in the Δ*tbp3* strain (Supplementary files 2-3) consistent with roles for TBP2 and TBP3 in the regulation of their transcription.

## TBP1, TBP2 and TBP3 sequence analysis

The three *M. acetivorans* TBPs differ in overall amino acid identity consistent with multiple functional roles in transcription. This hypothesis is supported by experimental data showing differing phenotypic effects for deletion or altered expression for each of the three TBP orthologs and different sets of genes with altered transcription in the Δ*tbp2 versus* the Δ*tbp3* strain. To explore the possibility that TBP1, TBP2 and

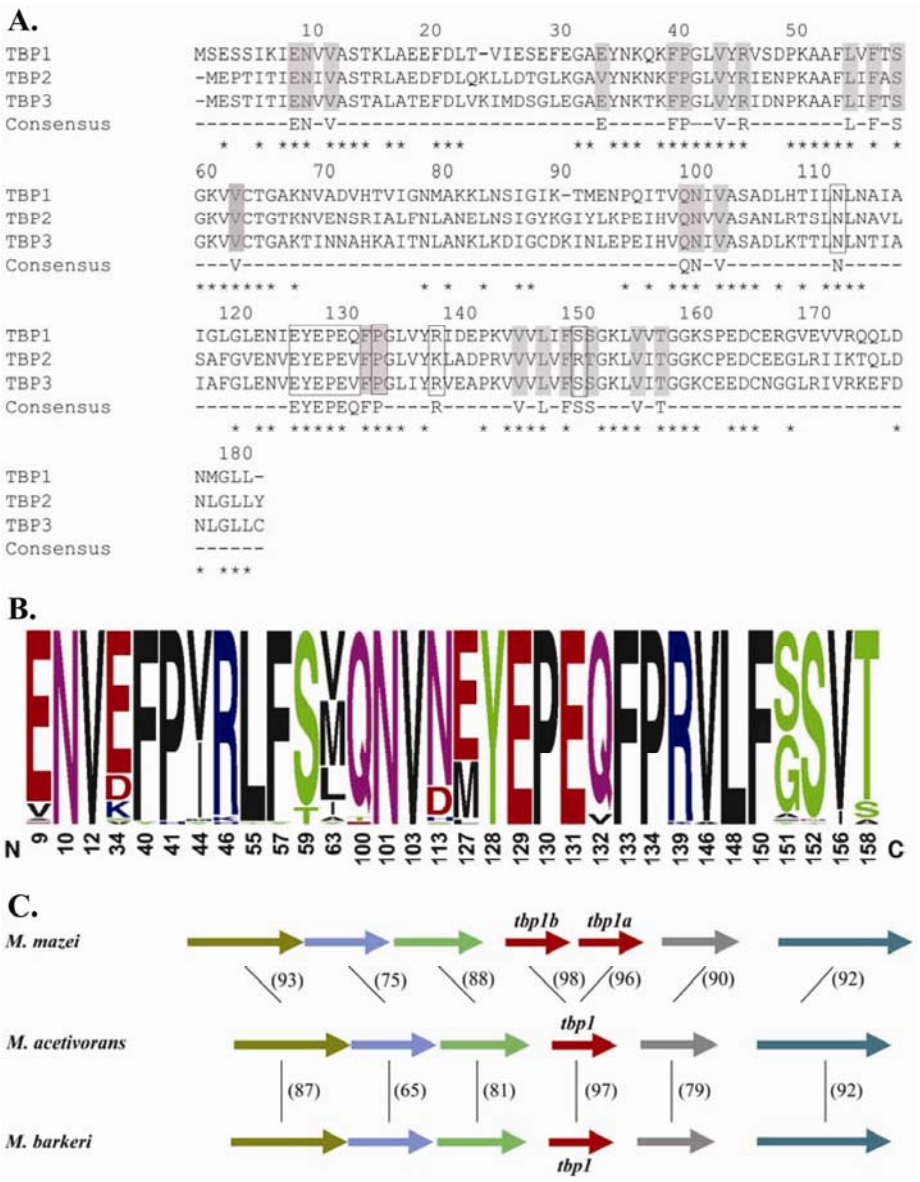


**Figure 3-14. Comparison of TBP1, TBP2 and TBP3 sequence and gene organization.** (A) TBP1, 2 and 3 sequence alignment. Conserved residues are indicated with an asterisk. Residues predicted to contact DNA and/or TFB in the tertiary complex are shaded in gray and the sequence consensus archaeal TFB- and DNA-binding residues is shown in the line labeled consensus. (B) The graphical representation of the consensus sequence for the archaeal TBP DNA- and TFB-binding residues was generated with WebLogo (12). The DNA- and TFB-binding residues 68 archaeal TBPs available in the public database were aligned with ClustalW. Predictions of DNA and TFB binding are based on alignments against the crystal structure of the *Pyrococcus woesei* TBP-TFB-DNA tertiary structure. Numbers represent the equivalent residues on TBP1. (C) Comparison of the *M. acetivorans tbp1* gene cluster (MA4334-4329) with the *M. mazei* (MM1031-1025) and *M. barkeri* (MbarA0598-0593) *tbp1* gene clusters (19). The numbers in parentheses are percent identities between the proteins encoded by the genes as indicated by the arrows.

TBP3 differ intrinsically in their ability to bind DNA or TFB, further analysis was carried out on the functionally important DNA- and TFB-binding surfaces. In the crystal structure of the *Pyrococcus woesei* TBP-TFB-DNA tertiary complex, 32 amino acids were identified on TBP that make direct contact with either DNA or TFB (29, 37). A consensus sequence for these 32 functionally important residues was generated based on an alignment of 68 annotated archaeal TBPs in the public database (Fig. 3-14A,B). An examination of the equivalent residues on the *M. acetivorans* proteins showed that all 32 are conserved in TBP1, 31 are conserved in TBP3 and 27 are conserved in TBP2 (Fig. 3-14A). TBP2 and TBP3 each contain a Val at position 133 (equivalent to TBP1) in place of an otherwise perfectly conserved Gln on the putative TFB-binding surface of all other archaeal TBPs potentially reflective of a difference in TFB-binding for TBP2 and TBP3 compared to TBP1.

All other putative DNA- and TFB-binding residues were identical between TBP1 and TBP3. However, four additional residues were identified in TBP2 that differed from TBP1, TBP3 and the archaeal consensus. Two of these residues are present on the DNA-binding surface, Val and Lys in place of the Glu and Arg at positions 34 and 140, respectively. The other two are present on the TFB-binding surface, Arg and Thr in the place of the Ser at positions 152 and 153, respectively (Fig. 3-14A). These residues are unique to TBP2 when compared to all other archaeal TBPs consistent with the possibility that TBP2 is functionally unique.

Multiple TBP homologs were also identified in the genomes of *Methanosarcina mazei* Gö1 which has three (13) and *Methanosarcina barkeri* Fusaro which has two (www.tigr.org). Both species possess homologs to TBP1 with >96% overall sequence

identity (Fig. 3-14C; Table 3-1). The genomic positioning of all *tbp1* orthologs is conserved, and the nucleotide sequences immediately upstream of all *tbp1* is highly conserved (84% identical in all three species) (Fig 3-15) consistent with similar promoter architecture and expression level for *tbp1* in all three species. Furthermore, the TSS identified 56 nucleotides upstream of *tbp1* was also identified in *M. mazei* (26). Interestingly, *M. mazei* carries two copies of *tbp1* with 97% amino acid sequence identity (MM1027 and MM1028) located adjacent to one another on the chromosome. The genes were annotated as *tbp1* and *tbp2*. However, in the interest of keeping a uniform nomenclature, I suggest here that these be renamed TBP1a (MM1027) and TBP1b (MM1028). All 32 putative DNA- and TFB-binding residues from TBP1 are conserved in *M. mazei* TBP1b and *M. barkeri* TBP1, and all but one are conserved in *M. mazei* TBP1a. The strict conservation of TBP1 orthologs in *Methanosarcina* is consistent with a TBP1 functional conservation in all three species.

*M. mazei* and *M. barkeri* also have an additional TBP (MM2185 and MbarA1062) that is orthologous to TBP3 (85 and 76% amino acid sequence identity respectively) (Table 3-1). The genomic positioning of the *tbp3* orthologs is not conserved between the three species. However the nucleotide sequence immediately upstream of *tbp3* is conserved (Fig. 3-15), although less than that for *tbp1*. All 32 putative DNA- and TFB-binding residues are identical in the TBP3 orthologs including the Val at position 133 on the putative TFB-binding surface. The retention of *tbp3* on the genomes of three different *Methanosarcina* species is consistent with a functional role for TBP3 in all three species distinct from that of TBP1. No TBP2 orthologs are present in *M. mazei* or *M. barkeri* consistent with the possibility for a unique role for TBP2 in *M. acetivorans*.

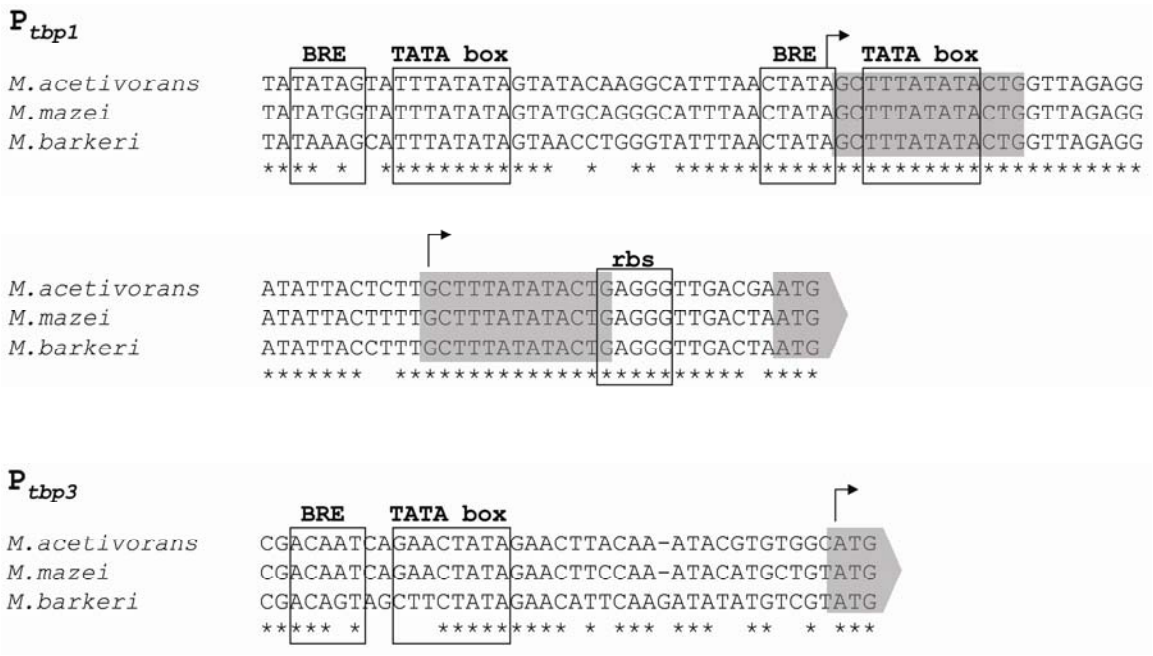


**Figure 3-15. Promoter alignment for *tbp1* and *tbp3* from *M. acetivorans, M. mazei* and *M. barkeri*.** Alignments were performed using ClustalW. Nucleotides that are conserved are denoted with asterisks. The TSSs for *M. acetivorans tbp1* and *tbp3* are denoted with hooked arrows above the corresponding nucleotide. The putative start codon for each corresponding protein is denoted with a boxed arrow. Putative TATA-boxes, BREs and the ribosome binding site for *tbp1* are boxed. Repeated sequence motifs in the *tbp1* transcripts are shaded in gray.

## Discussion

This study, the first genetic analysis of general transcription factors for a methane-producing archaeon, has revealed initial insight into roles for the three TBP orthologs in *M. acetivorans*.

### TBP1 in *M. acetivorans* has a more universal role than TBP2 or TBP3

The data obtained in this investigation reveal that TPB1 plays a greater role in gene expression for *M. acetivorans* compared to TBP2 and TBP3. This prediction is supported by the following observations: (i) transcripts of *tbp1* were found to be substantially more abundant than for *tbp2* and *tbp3* in cells cultured on methanol, acetate or TMA; (ii) the genes encoding either TBP2 or TBP3 could be knocked-out by homologous recombination and these mutants obtained could be cultured with acetate and methylotrophic substrates; (iii) the Δ*tbp1* strain could not be obtained by homologous recombination-mediated gene replacement; (iv) the ΔP*tbp1*::P*mcrB*(tetO1)-*tbp1* was unable to grow in the absence of tetracycline during which expression of *tbp1* is inhibited. Accordingly, genes encoding TBP1 orthologs are strictly conserved among *Methanosarcina* species (Fig. 3-14C, Table 3-1). Furthermore, the TBP1 from *M. acetivorans* has 88 and 80% identity with the only TBPs annotated for phylogenetically related *Methanococcoides burtonii* and *Methanosaeta thermophila* (Table 3-1).

For organisms with multiple TBP orthologs, the concept of one TBP serving as the primary TBP for gene expression is not unique. It has been suggested that TBPe

plays a dominant role among the TBP homologs of *Halobacterium* sp. NRC-1 based on proteomic analyses in which TBPe was the sole TBP detected in *Halobacterium* sp. NRC-1 cell lysates (15, 20). Furthermore, like TBP1 in the *Methanosarcinaceae,* TBPe is the most phylogenetically conserved among TBP homologs in the haloarchaea and is the only TBP annotated for the genomes of several species (15).

Although acquisition of the Δ*tbp2* and Δ*tbp3* mutants established that TBP2 and TBP3 are not essential, it is yet to be determined if either is essential under any particular conditions. No phenotypic effects were observed for the mutants cultured with methylotrophic substrates which could indicate that either TBP2 and TBP3 are both unimportant during growth on these substrates or that TBP2 can replace TBP3 and *vice versa*. Nonetheless, the finding that not all TBP orthologs are essential for growth of *M. acetivorans* is consistent with the archaeon *Halobacterium* sp. NRC-1 for which four of the six *tbp* homologs were successfully deleted (10, 15). The results for *Halobacterium* sp. NRC-1 do not rule out a role for the non-essential TBP orthologs to provide added fitness under various growth conditions. Indeed, the results presented here suggest that TBP2 and TBP3 of *M. acetivorans* play this role.

**TBP2 and TBP3 are important for growth with limiting concentrations of acetate**

Previous results (32, 34, 35) show that all TBP proteins are present in *M. acetivorans* cells during growth. The >20-fold excess of *tbp1* transcripts relative to *tbp2* and *tbp3* transcripts argues against the idea that TBP2 and TBP3 are needed simply to

increase intracellular TBP concentrations. Instead, the results presented here indicate that TBP2 and TBP3 are important for optimal growth with limiting acetate concentrations. Interestingly, although required for optimal yields when growing with limiting concentrations of acetate, TBP2 has no discernable role in providing a competitive advantage under these conditions. The simplest explanation for these apparently contradictory results is that during growth in a mixed culture and assuming neither strain has a competitive advantage, individual strains will achieve a final yield which is half of that achieved under pure culture conditions. The results also indicate that TBP3 plays a larger role than TBP2. Consistent with this idea, the genomes of both *M. mazei* and *M. barkeri* only have TBP1 and TBP3 orthologs, but no TBP2 orthologs (Table 3-1). Contrary to growth phenotypes of the Δ*tbp2* and Δ*tbp3* strains reported here, *tbp2* transcripts were more abundant than *tbp3* transcripts during growth on acetate (Table 3-2) consistent with a more prominent role for *tbp2* than for *tbp3* during growth on acetate, an anomaly that is unexplained at this juncture.

In marine environments, acetotrophic sulfate-reducing species have a competitive advantage over methanogens for acetate (41, 46) which suggests that TBP3 may be essential for *M. acetivorans* to utilize this substrate in its native habitat. The 20 mM acetate used in growth-limiting experiments reported here was the minimum concentration that allowed determination of reliable growth parameters, although levels of acetate reported in various marine sediments (~1-2 mM) are well below this value (27, 47). Thus, growth defects of this mutant are expected to be even more severe in the native habitat. Conversely, it is reported that methanogens compete very well with

sulfate reducers for methylotrophic substrates (41) due in part to the greater energy available by conversion to methane *versus* conversion of acetate to methane (50).

## Potential involvement of TBP2 and TBP3 gene regulation

The *Methanosarcina* are the most metabolically diverse within the methane-producing Archaea (16, 17), and global gene expression profiles for various *Methanosarcina* species differ substantially during growth with different substrates (14, 23, 32-36). However, it is largely unknown how these pathways are regulated. The growth defects of the Δ*tbp2* and Δ*tbp3* strains suggest the possibility that TBP2 and TBP3 may be necessary for the regulation of genes when *M. acetivorans* encounters growth-limiting concentrations of acetate or when switching from growth on methylotrophic substrates to growth on acetate. If TBP2 and TBP3 have roles in the regulation of genes specific for diverse metabolic pathways, methanogenic species with less metabolic diversity than *Methanosarcina* species might be expected to have fewer TBP homologs. Consistent with this idea, most methanogenic species that only obtain energy for growth by reducing carbon dioxide to methane have genomic annotations for only one *tbp* gene (www.tigr.org). The only exceptions are the genomes of *Candidatus methanoregula boonei* 6A8 which has three, *Methanococcus maripaludis* C5 which has two (the C7 and S2 strains each have one), *Methanocorpusculum labreanum* Z which has two, *Methanoculleus marisnigri* JR1 which has two, and *Methanospirillum hungatei* JF-1 which also has two. Furthermore, *M. burtonii* that only utilizes methylotrophic substrates

and *M. thermophila* that only utilizes acetate have genomes annotated with only one TBP (www.tigr.org). Therefore, it is tempting to speculate that during the acquirement of metabolic diversity in *Methanosarcina* species, multiple TBPs evolved in response to play a key role in optimizing gene expression. Indeed, DNA microarray analyses suggest TBP2 and TBP3 are involved in the regulation of gene expression. The results presented here suggest that TBP3 is important for adaptation to growth on acetate from growth on methylotrophic substrates and that TBP2 and TBP3 are important for optimal growth during culturing with growth-limiting acetate concentrations. Increases in transcription of numerous genes in the Δ*tbp2* or Δ*tbp3* strains *versus* wild-type *M. acetivorans* could potentially cause protein imbalances which place further energetic burdens on cells during these conditions of poor nutrient availability. Conversely, decreases in transcription of other genes could compromise functions necessary for efficient growth under these conditions. Although none of the annotations for genes with decreased transcript abundance identified functions that could be linked specifically to acetate metabolism, it is plausible that some differentially regulated genes have roles necessary for efficient growth on acetate. For example, the proteins encoded by MA0857 and MA4386 which are homologous to group II chaperonins present in the *Archaea* and *Eukarya* domains (22, 28) could presumably function in proper folding of nascent peptides or denatured proteins to facilitate the metabolic transition from methanol to acetate. These changes in transcription are consistent with roles for TBP2 and TBP3 in the optimization of gene expression necessary for efficient transition from one-carbon substrates such as methanol to the least energetically favorable substrate, acetate,

particularly when the acetate concentration is growth-limiting as in the native environment.

Alternative residues found on the TFB- and DNA-binding surfaces of TBP2 and TBP3 might be reflective of differences in TBP-TFB interaction and promoter recognition. This is certainly plausible in the case of the Val in place of Gln at position 133 in TBP2 and TBP3 and the TBP3 orthologs in *M. mazei* and *M. barkeri* (Fig. 3-2A). The equivalent residue in the yeast TBP has been shown to be important for optimal TFIIB binding (31). Although this position is occupied by a Leu in eukaryal TBPs, it could simply be a reflection of the differences between TFB and TFIIB. Nonetheless, it is indeed an interesting candidate for future mutagenic studies to investigate TBP-TFB interactions *in vitro* as are other alternative amino acid residues specific to TBP2 (Fig. 3-2A). The Val at position 34 is occupied by a negatively charged residue (Glu or a Asp) in most other archaeal TBPs, and previous biochemical analysis has implicated these negatively charged residues in DNA-binding through cation uptake (7). Residues Lys 140 and Thr 153 on the TFB-binding surface of TBP2 are also significant. Although both residues are similar to the consensus Arg and Ser at these positions, they are otherwise perfectly conserved across all TBPs both archaeal and eukaryal suggesting that strict conservation of these residues is important and the subtle changes in TBP2 may possibly influence the ability of TBP2 and TFB to interact.

## Conclusions

In this study, the physiological roles of the three TBP homologs in *M. acetivorans* were investigated. TBP1 is an essential gene and has a more universal role than TBP2 or TBP3. Although not essential for cell growth, TBP3 is important for optimal growth when adapting to growth on acetate from methylotrophic substrates, and both TBP2 and TBP3 are important for optimal growth with ecologically relevant growth-limiting acetate concentrations. Alternative TBPs, TBP2 and TBP3 may have a role in optimization of gene expression which helps *M. acetivorans* in the metabolic transition to growth on acetate and for efficient utilization of ecologically relevant concentrations of acetate.

## Materials and Methods

*Cell Growth.* Growth and harvesting of *M. acetivorans* C2A (DSM 800) in single cell morphology (49) cultured on high-salt (HS) broth medium with acetate, methanol, TMA, DMA, MMA and CO was as previously described (32). Growth was monitored by measuring the optical density at 600 nm. The acetate concentration was maintained at 75-100 mM by periodically supplementing cultures with 10 M glacial acetic acid added from sterile anaerobic stock solution. Acetic acid was added in 1:1 molar ratio to the amount of methane produced which was calculated based on the volume of gas over pressure released from the culture vessel headspace. The pH for cultures grown on acetate fluctuated from 6.5-7.5 during growth. Cultures with initial concentrations of 20

and 50 mM sodium acetate were not supplemented with acetic acid throughout growth and the pH at the end of growth did not exceed 7.5.

*RNA Isolation.* All *M. acetivorans* RNA samples were isolated from using an RNeasy Total RNA Mini kit (QIAGEN). Purified RNA was treated twice with RNase-free DNase I (QIAGEN) and once with RQ1 DNase (Promega) to remove contaminating DNA.

*RT-PCR.* RT-PCR was carried out with an Access RT-PCR kit (Promega) using 50 ng of purified total RNA (primer sequences and primer pairs used are listed in Table A1-3). Positive control PCRs were performed using *M. acetivorans* genomic DNA as a template to confirm the quality of the primer pairs. Negative control PCRs were performed without the addition of RT to ensure complete removal of DNA.

*RLM-RT-PCR.* RNA ligation-mediated (RLM) RT-PCR was performed as described with modifications (6). 10 μg purified total RNA added to 5 μL 10x Tobacco Acid Pyrophosphatase (TAP) buffer (Epicentre) and 40 U (1 μL) RNasin RNase inhibitor (Promega). The mixture was brought to a volume of 49 μL using nuclease-free $H_2O$ and was divided into two equal fractions. 5 U (0.5 μL) TAP was added to the first fraction (TAP-treated sample), and 0.5 μL nuclease-free $H_2O$ was added to the second (untreated sample). Both RNA samples were incubated 1 hr at 37$^{o}$C and then phenol/chloroform extracted, ethanol precipitated and resuspended in 38 μL nuclease-free $H_2O$. 150 ng (I μL) TAP-RNA oligonucleotide (Table A1-3), 5 μL 10x T4 RNA ligase buffer and 120 U (6 μL) T4 RNA ligase were added to each RNA sample. Both samples were incubated 1 hr at 37$^{o}$C and then phenol/chloroform extracted, ethanol precipitated and resuspended in

50 μL nuclease-free $H_2O$. Resuspended RNA was then used as a template for RT-PCR using reverse primers listed in Table C-1 and TAP-DNA primer (Table C-1).

*Primer extension.* Primer extension reactions were performed with a Primer extension system-AMV reverse transcriptase (Promega) according to the manufacturer's recommendations using 10 μg of total RNA from methanol-grown cells, and ATP [$\gamma^{32}$P]-end-labeled primers. DNA sequencing reactions were carried out using a Sequenase version 2.0 DNA sequencing kit (USB) according to the manufacturer's recommendations using dATP [$\alpha^{33}$P]. Primers and sequencing templates used are listed in Table C-1.

*Taqman quantitative RT-PCR.* *Taq*man assays were performed using total RNA isolated from at mid-exponential phase ($A_{600}$ ~ 0.6-0.7, 0.4-0.5, 0.6-0.7 and 0.15-0.2 for methanol-, acetate-, TMA- and CO-grown cells respectively). *Taq*man primers and probes were designed using Primer Express 1.0 (Applied Biosystems, Foster City, CA). Primers were synthesized on the Bioautomation MerMade 12 (Plano, TX) at the Nucleic Acid Facility of the Pennsylvania State University. Probes were synthesized by Biosearch Technologies (Novato, CA) and were labeled with the reporter dye 6-carboxyfluorescein (6'-FAM) at the 5' end and with the quencher dye Black Hole Quencher at the 3' end. Primers and probes are summarized in Table C-1. cDNA was prepared using the ABI High Capacity RT kit (Applied Biosystems) and was amplified and quantified on the ABI 7300 Real-Time PCR System (Applied Biosystems). Thermal cycling conditions were as follows: 2 min at 50°C, 10 min at 95°C followed by 40 cycles of 15 s at 95°C and 1 min at 60°C. Relative abundances of each gene were determined using the $\Delta\Delta C_t$ method (Applied Biosystems) using the 16s rRNA gene as the invariant

control. *Taq*man primers and probes are listed in Table C-1. To determine transcript copy numbers of *tbp1, tbp2* and *tbp3* for wild-type *M. acetivorans*, *in vitro*-transcribed *tbp1, tbp2* and *tbp3* RNA standards were generated using the MEGAscript T7 kit (Ambion, Austin, TX) following manufacturer's instructions. Linearized plasmids containing *tbp1, tbp2* or *tbp3* cloned into the pET21a vector under the control of the T7 promoter were used as templates for the *in vitro*-transcription reaction. Completed reactions were treated with TURBO DNA-*free* DNase to remove template DNA and were further purified using the RNeasy Mini kit (QIAGEN, Valencia, CA) following manufacturer's instructions. Product size and purity was checked by agarose gel electrophoresis. The RNA standards were diluted to 1 X $10^{-11}$ copies $\mu L^{-1}$. A standard curve was generated using the average of triplicate measurements of 10-fold serial dilutions of the RNA standards. The $C_t$ values of triplicate measurements of serially diluted total RNA from methanol-grown cells plotted against the standard curve were used to calculate the transcript copy number $ng^{-1}$ for *tbp1, tbp2* and *tbp3*.

*Overexpression and Purification of recombinant TBP1, TBP2 and TBP3***.** The over expression and purification of recombinant TBP1, TBP2 and TBP3 was carried out by Dr. KS Murakami. The genes encoding *M. acetivorans* TBP1, TBP2 and TBP3 were cloned from genomic DNA by PCR, and the protein expression vector was constructed using a pET15b (Novagen) with N-terminal $His_6$-tag. Proteins were over-expressed in BL21(DE3)-CodonPlus RIPL (Stratagene) in LB media at 25 °C. After the cells were lysed by sonication, soluble proteins were isolated by centrifugation (17,000 x g, 15 min). Only TBP1 and TBP3 were recovered in soluble fraction and these proteins were further purified by Ni-affinity column (GE Healthcare) followed by Superdex-75 gel filtration

column chromatography (GE Healthcare). The recombinant TBP2 was purified from insoluble fraction: inclusion bodies were denatured by 6 M Urea and the proteins were purified by Ni-affinity column, and the proteins were renatured by removing Urea by dialysis.

*Western blot analysis***.** Polyclonal antibodies directed against *M. acetivorans* TBP1 and TBP3 were raised in rabbits (Covance). To prepare *M. acetivorans* cell lysate, cells were collected at mid-log phase by centrifugation, resuspended in SDS denaturing buffer (62.5 mM Tris-HCl [pH = 6.8], 2% SDS, 10% glycerol, 1% β-ME, 0.005% Bromophenol Blue) and lysed by incubation at 95$^{o}$C for 5 min.

*M. acetivorans* cell extract proteins were separated by SDS-PAGE on 12% gels and electrotransferred to a polyvinylidene difluoride membrane (Sequi-Blot™ PVDF Membrane; Bio-Rad) following manufacturer's guidelines. Additional protein binding sites were blocked by incubating the membrane one hour at room temperature under constant agitation in TBS-T buffer (10 mM Tris-HCl [pH 8.0], 150 mM NaCl and 0.1% Tween 20) with the addition of 3-10% BSA. A 1:500 dilution of anti-TBP1 and anti-TBP3 antisera and 1:20,000 dilution of anti-rabbit immunoglobulin G-alkaline phosphatase-linked antibody containing sodium azide in TBS-T were used. The specificity of anit-TBP1 antisera to TBP1 was increased by incubating the diluted anitsera overnight at room temperature under constant agitation in the presence of 100 μg of recombinant TBP2 and recombinant TBP3. The specificity of anit-TBP3 antisera to TBP2 and TBP3 was increased by incubating the diluted anitsera overnight at room temperature under constant agitation in the presence of 100 μg of recombinant TBP1.

The antibody/antigen complexes were detected using ECF Western Blotting Reagent Packs (Amersham Biosciences) following manufacturer's guidelines.

*Construction of M. acetivorans deletion mutant strains*. Liposome-mediated transformation and homologous recombination-mediated gene replacement were used as described (8, 39) to generate *M. acetivorans* Δ*tbp2::pac*, Δ*tbp3::pac*, and P*mcrB*(tetO1)*::tbp1* (hereafter designated Δ*tbp2*, Δ*tbp3* and ΔP*tbp1*::P*mcrB*(tetO1)-*tbp1* respectively). The Δ*tbp2* and Δ*tbp3* strains were generated in a *M. acetivorans* C2A background, and the ΔP*tbp1*::P*mcrB*(tetO1)-*tbp1* strain was generated in a *M. acetivorans* WWM75 background. Cells were transformed with 2 μg pMR18, pMR19 or pMR58 linearized by restriction digestion, and transformants were selected on HS agar media with 0.8% (w/v) agar, with either 250 mM methanol or 50 mM TMA, and 2 μg $mL^{-1}$ puromycin (Sigma, St Louis, MO) added from sterile, anaerobic 100X stock solution. For generation of the ΔP*tbp1*::P*mcrB*(tetO1)-*tbp1* strain, 100 μg $mL^{-1}$ tetracycline (Sigma, St Louis, MO) was added to HS agar in addition to the other components.

*Genomic DNA isolation.* Cells were pelleted by centrifugation for 3 min at 10,000 x g and lysed by incubation for 30 min at 37°C in TE salts buffer (10 mM Tris-Cl, pH = 7.6; 1 mM EDTA, pH = 8.0; 400 mM NaCl; 50 mM $MgCl_2$) with 0.3% (w/v) SDS and 3 μg $mL^{-1}$ RNaseA (Roche, Madison, WI). DNA was purified from the cell lysate using the PureGene genomic DNA isolation kit following manufacturer's instructions.

*Southern Blot analysis.* DIG-labeled probes were generated using the DIG High Prime DNA Labeling and Detection Starter Kit I (Roche) following manufacturer's guidelines. Probes 1, 2 and 3 were PCR amplified from *M. acetivorans* genomic DNA using primers TBP2up-F plus TBP2up-R, TBP3up-F plus TBP3up-R and TBP1in-F plus

TBP1in-R respectively (Table C-1). Positions of these probes on the *M. acetivorans* chromosome are indicated in Fig. 3-8A. Aliquots of genomic DNA (1-5µg) from wild-type C2A, WWM75, Δ*tbp2*, Δ*tbp3* and ΔP*tbp1 M. acetivorans* strains were digested overnight with either NdeI, PvuII or EcoRI and fragments were separated on 0.3% (w/v) agarose gels, denatured, neutralized and transferred to positively charged nylon membranes (Boehringer Mannheim). Membranes were hybridized with DIG-labeled probes following manufacturer's guidelines.

*Adaptation to different methanogenic substrates*. 10 mL early stationary phase wild-type and Δ*tbp2* or Δ*tbp3* cells ($A_{600}$ ~ 1.2, 0.9 and 1.3 for methanol-, acetate- and TMA-grown cells respectively) were pelleted by centrifugation anaerobically for 10 min at 5000 x g. Cells were washed once with 10 mL media without substrate, resuspended in 10 mL media without substrate and inoculated 1 mL into 100 mL media containing the new methanogenic substrate.

*Mixed culture growth competition experiments*. 5 mL of early stationary phase wild-type and 5 mL early stationary phase Δ*tbp2* or Δ*tbp3* cells ($A_{600}$ ~ 1.2, 0.9 and 1.3 for methanol-, acetate- and TMA-grown cells respectively) were pooled together, pelleted and washed as described for adaptation to different methanogenic substrates and inoculated 1 mL into 100 mL media containing the appropriate methanogenic substrate. Genomic DNA extracted from mixed cell suspensions was subjected to Southern blot analysis to ensure that the cell suspension consisted of an equal population of wild-type and Δ*tbp2* or Δ*tbp3* cells.

*DNA microarray analysis*. RNA was collected from four replicate cultures each for wild-type, Δ*tbp2* and Δ*tbp3* grown on methanol at mid-exponential phase ($A_{600}$ ~ 0.6).

RNA samples were checked for purity and concentration using a NanoDrop spectrophotometer and RNA quality was assessed using an Agilent Bioanalyzer RNA 6000 Nano assay. RNA samples were labeled with the Message Amp II - Bacteria kit (Ambion Inc., Austin, TX) according to the manufacturer's instruction with the use of amino allyl UTP in place of biotin modified nucleotides. Briefly, 500 ng of total RNA was polyadenylated and subsequently reverse transcribed with T7oligo(dT)VN primer. Second strand cDNA synthesis was performed and the resulting dsDNA was used as a template for in vitro transcription. Amino allyl modified UTP was incorporated into the resulting cRNA. 20 µg of this modified aRNA was coupled with Cy3 or Cy5 using the CyDye Post Labeling Reactive Dye Pack (GE Healthcare, Buckinghamshire, England) according to the Amino Allyl Message Amp II kit instructions (Ambion, Austin, TX). Samples were hybridized to NimbleGen 4-plex arrays (Catalog number: A7240-00-01; Design Name: 080303 MacetC2A EXP X4). Two color hybridizations were performed and 2 µg of each sample was hybridized to an array. Array hybridization, washing, scanning and data acquisition were performed according to the manufacturer's instruction (Roche NimbleGen Inc., Madison, WI). All data analysis was carried out using the ArrayStar (v3) software package (DNA Star, Madison, WI). Robust Multichip Averaging (RMA) and quantile normalization (9, 24, 25) were applied to the entire data set which consisted of four biological replicates and two technical replicates (dye swap) of each strain. Statistical analyses were carried out on the normalized data using a moderated *t*-test with FDR multiple testing correction (Benjamini-Hochberg) to determine differential transcript abundance. Changes in transcript abundance were considered significant if they met the following criteria: ≥2-fold change in abundance; *P*-

values < 0.05; $Log_2$ transcript abundance >11.0 in the condition with greater abundance. The *Z*-test with FDR multiple testing correction (Benjamini-Hochberg) was used to assess the statistical significance of the sampling distribution of genes according to their COG functional categories.

## Acknowledgements

I thank W.W. Metcalf (University of Illinois, Urbana, IL) for the donation of all plasmids and strains used for the genetic manipulation of *M. acetivorans*, D. Grove (Penn State Genomics Core Facility – University Park, PA) for optimization of *Taq*man assays, and C. Praul and H. Xiang (Penn State Genomics Core Facility – University Park, PA) for DNA microarray labeling, hybridization and scanning. This work was funded by the Pew Scholar's Program in the Biomedical Sciences to KSM and by grants from the National Science Foundation and Department of Energy to JGF.

## References

1. **Baliga, N. S., Y. A. Goo, W. V. Ng, L. Hood, C. J. Daniels, and S. DasSarma.** 2000. Is gene expression in Halobacterium NRC-1 regulated by multiple TBP and TFB transcription factors? Mol Microbiol **36:**1184-5.
2. **Bartlett, M. S., M. Thomm, and E. P. Geiduschek.** 2004. Topography of the euryarchaeal transcription initiation complex. J Biol Chem **279:**5894-903.

3. **Baumann, P., S. A. Qureshi, and S. P. Jackson.** 1995. Transcription: new insights from studies on Archaea. Trends Genet **11:**279-83.

4. **Bell, S. D., and S. P. Jackson.** 1998. Transcription and translation in Archaea: a mosaic of eukaryal and bacterial features. Trends Microbiol **6:**222-8.

5. **Bell, S. D., C. P. Magill, and S. P. Jackson.** 2001. Basal and regulated transcription in Archaea. Biochem Soc Trans **29:**392-5.

6. **Bensing, B. A., B. J. Meyer, and G. M. Dunny.** 1996. Sensitive detection of bacterial transcription initiation sites and differentiation from RNA processing sites in the pheromone-induced plasmid transfer system of Enterococcus faecalis. Proc Natl Acad Sci U S A **93:**7794-9.

7. **Bergqvist, S., M. A. Williams, R. O'Brien, and J. E. Ladbury.** 2002. Reversal of halophilicity in a protein-DNA interaction by limited mutation strategy. Structure **10:**629-37.

8. **Boccazzi, P., J. K. Zhang, and W. W. Metcalf.** 2000. Generation of dominant selectable markers for resistance to pseudomonic acid by cloning and mutagenesis of the ileS gene from the archaeon Methanosarcina barkeri fusaro. J Bacteriol **182:**2611-8.

9. **Bolstad, B. M., R. A. Irizarry, M. Astrand, and T. P. Speed.** 2003. A comparison of normalization methods for high density oligonucleotide array data based on variance and bias. Bioinformatics **19:**185-93.

10. **Coker, J. A., P. Dassarma, J. Kumar, J. A. Muller, and S. Dassarma.** 2007. Transcriptional profiling of the model Archaeon Halobacterium sp. NRC-1: responses to changes in salinity and temperature. Saline Systems **3:**6.

11. **Coker, J. A., and S. DasSarma.** 2007. Genetic and transcriptomic analysis of transcription factor genes in the model halophilic Archaeon: coordinate action of TbpD and TfbA. BMC Genet **8:**61.

12. **Crooks, G. E., G. Hon, J. M. Chandonia, and S. E. Brenner.** 2004. WebLogo: a sequence logo generator. Genome Res **14:**1188-90.

13. **Deppenmeier, U., A. Johann, T. Hartsch, R. Merkl, R. A. Schmitz, R. Martinez-Arias, A. Henne, A. Wiezer, S. Baumer, C. Jacobi, H. Bruggemann, T. Lienard, A. Christmann, M. Bomeke, S. Steckel, A. Bhattacharyya, A. Lykidis, R. Overbeek, H. P. Klenk, R. P. Gunsalus, H. J. Fritz, and G. Gottschalk.** 2002. The genome of Methanosarcina mazei: evidence for lateral gene transfer between bacteria and archaea. J Mol Microbiol Biotechnol **4:**453-61.

14. **Ding, Y. H., S. P. Zhang, J. F. Tomb, and J. G. Ferry.** 2002. Genomic and proteomic analyses reveal multiple homologs of genes encoding enzymes of the methanol:coenzyme M methyltransferase system that are differentially expressed in methanol- and acetate-grown Methanosarcina thermophila. FEMS Microbiol Lett **215:**127-32.

15. **Facciotti, M. T., D. J. Reiss, M. Pan, A. Kaur, M. Vuthoori, R. Bonneau, P. Shannon, A. Srivastava, S. M. Donohoe, L. E. Hood, and N. S. Baliga.** 2007. General transcription factor specified global gene regulation in archaea. Proc Natl Acad Sci U S A **104:**4630-5.

16. **Ferry, J. G. (ed.).** 1993. Methanogenesis: Ecology, Physiology, Biochemistry and Genetics, vol. I. Chapman and Hall, New York, NY.

17. **Ferry, J. G., and K. A. Kastead.** 2007. Methanogenesis, p. 288-314. *In* R. Cavicchioli (ed.), Archaea: Molecular and Cellular Biology. ASM Press, Washington, DC.

18. **Galagan, J. E., C. Nusbaum, A. Roy, M. G. Endrizzi, P. Macdonald, W. FitzHugh, S. Calvo, R. Engels, S. Smirnov, D. Atnoor, A. Brown, N. Allen, J. Naylor, N. Stange-Thomann, K. DeArellano, R. Johnson, L. Linton, P. McEwan, K. McKernan, J. Talamas, A. Tirrell, W. Ye, A. Zimmer, R. D. Barber, I. Cann, D. E. Graham, D. A. Grahame, A. M. Guss, R. Hedderich, C. Ingram-Smith, H. C. Kuettner, J. A. Krzycki, J. A. Leigh, W. Li, J. Liu, B. Mukhopadhyay, J. N. Reeve, K. Smith, T. A. Springer, L. A. Umayam, O. White, R. H. White, E. Conway de Macario, J. G. Ferry, K. F. Jarrell, H. Jing, A. J. Macario, I. Paulsen, M. Pritchett, K. R. Sowers, R. V. Swanson, S. H. Zinder, E. Lander, W. W. Metcalf, and B. Birren.** 2002. The genome of M. acetivorans reveals extensive metabolic and physiological diversity. Genome Res **12:**532-42.

19. **Geiduschek, E. P., and M. Ouhammouch.** 2005. Archaeal transcription and its regulators. Mol Microbiol **56:**1397-407.

20. **Goo, Y. A., E. C. Yi, N. S. Baliga, W. A. Tao, M. Pan, R. Aebersold, D. R. Goodlett, L. Hood, and W. V. Ng.** 2003. Proteomic analysis of an extreme halophilic archaeon, Halobacterium sp. NRC-1. Mol Cell Proteomics **2:**506-24.

21. **Guss, A. M., M. Rother, J. K. Zhang, G. Kulkarni, and W. W. Metcalf.** 2008. New methods for tightly regulated gene expression and highly efficient

chromosomal integration of cloned genes for Methanosarcina species. Archaea **2:**193-203.

22. **Hirtreiter, A. M., G. Calloni, F. Forner, B. Scheibe, M. Puype, J. Vandekerckhove, M. Mann, F. U. Hartl, and M. Hayer-Hartl.** 2009. Differential substrate specificity of group I and group II chaperonins in the archaeon Methanosarcina mazei. Mol Microbiol **74:**1152-68.

23. **Hovey, R., S. Lentes, A. Ehrenreich, K. Salmon, K. Saba, G. Gottschalk, R. P. Gunsalus, and U. Deppenmeier.** 2005. DNA microarray analysis of Methanosarcina mazei Go1 reveals adaptation to different methanogenic substrates. Mol Genet Genomics **273:**225-39.

24. **Irizarry, R. A., B. M. Bolstad, F. Collin, L. M. Cope, B. Hobbs, and T. P. Speed.** 2003. Summaries of Affymetrix GeneChip probe level data. Nucleic Acids Res **31:**e15.

25. **Irizarry, R. A., B. Hobbs, F. Collin, Y. D. Beazer-Barclay, K. J. Antonellis, U. Scherf, and T. P. Speed.** 2003. Exploration, normalization, and summaries of high density oligonucleotide array probe level data. Biostatistics **4:**249-64.

26. **Jager, D., C. M. Sharma, J. Thomsen, C. Ehlers, J. Vogel, and R. A. Schmitz.** 2009. Deep sequencing analysis of the Methanosarcina mazei Go1 transcriptome in response to nitrogen availability. Proc Natl Acad Sci U S A.

27. **King, G. M., M. J. Klug, and D. R. Lovley.** 1983. Metabolism of Acetate, Methanol, and Methylated Amines in Intertidal Sediments of Lowes Cove, Maine. Appl Environ Microbiol **45:**1848-1853.

28. **Klunker, D., B. Haas, A. Hirtreiter, L. Figueiredo, D. J. Naylor, G. Pfeifer, V. Muller, U. Deppenmeier, G. Gottschalk, F. U. Hartl, and M. Hayer-Hartl.** 2003. Coexistence of group I and group II chaperonins in the archaeon Methanosarcina mazei. J Biol Chem **278:**33256-67.

29. **Kosa, P. F., G. Ghosh, B. S. DeDecker, and P. B. Sigler.** 1997. The 2.1-A crystal structure of an archaeal preinitiation complex: TATA-box-binding protein/transcription factor (II)B core/TATA-box. Proc Natl Acad Sci U S A **94:**6042-7.

30. **Kyrpides, N. C., and C. A. Ouzounis.** 1999. Transcription in archaea. Proc Natl Acad Sci U S A **96:**8545-50.

31. **Lee, M., and K. Struhl.** 1997. A severely defective TATA-binding protein-TFIIB interaction does not preclude transcriptional activation in vivo. Mol Cell Biol **17:**1336-45.

32. **Lessner, D. J., L. Li, Q. Li, T. Rejtar, V. P. Andreev, M. Reichlen, K. Hill, J. J. Moran, B. L. Karger, and J. G. Ferry.** 2006. An unconventional pathway for reduction of CO2 to methane in CO-grown Methanosarcina acetivorans revealed by proteomics. Proc Natl Acad Sci U S A **103:**17921-6.

33. **Li, L., Q. Li, L. Rohlin, U. Kim, K. Salmon, T. Rejtar, R. P. Gunsalus, B. L. Karger, and J. G. Ferry.** 2007. Quantitative proteomic and microarray analysis of the archaeon Methanosarcina acetivorans grown with acetate versus methanol. J Proteome Res **6:**759-71.

34. **Li, Q., L. Li, T. Rejtar, B. L. Karger, and J. G. Ferry.** 2005. Proteome of Methanosarcina acetivorans Part I: an expanded view of the biology of the cell. J Proteome Res **4:**112-28.

35. **Li, Q., L. Li, T. Rejtar, B. L. Karger, and J. G. Ferry.** 2005. Proteome of Methanosarcina acetivorans Part II: comparison of protein levels in acetate- and methanol-grown cells. J Proteome Res **4:**129-35.

36. **Li, Q., L. Li, T. Rejtar, D. J. Lessner, B. L. Karger, and J. G. Ferry.** 2006. Electron transport in the pathway of acetate conversion to methane in the marine archaeon Methanosarcina acetivorans. J Bacteriol **188:**702-10.

37. **Littlefield, O., Y. Korkhin, and P. B. Sigler.** 1999. The structural basis for the oriented assembly of a TBP/TFB/promoter complex. Proc Natl Acad Sci U S A **96:**13668-73.

38. **Lu, Q., J. Han, L. Zhou, J. A. Coker, P. DasSarma, S. DasSarma, and H. Xiang.** 2008. Dissection of the regulatory mechanism of a heat-shock responsive promoter in Haloarchaea: a new paradigm for general transcription factor directed archaeal gene regulation. Nucleic Acids Res **36:**3031-42.

39. **Metcalf, W. W., J. K. Zhang, E. Apolinario, K. R. Sowers, and R. S. Wolfe.** 1997. A genetic system for Archaea of the genus Methanosarcina: liposome-mediated transformation and construction of shuttle vectors. Proc Natl Acad Sci U S A **94:**2626-31.

40. **Micorescu, M., S. Grunberg, A. Franke, P. Cramer, M. Thomm, and M. Bartlett.** 2008. Archaeal transcription: function of an alternative transcription factor B from Pyrococcus furiosus. J Bacteriol **190:**157-67.

41. **Oremland, R. S., and S. Polcin.** 1982. Methanogenesis and Sulfate Reduction: Competitive and Noncompetitive Substrates in Estuarine Sediments. Appl Environ Microbiol **44:**1270-1276.

42. **Paytubi, S., and M. F. White.** 2009. The crenarchaeal DNA damage-inducible transcription factor B paralogue TFB3 is a general activator of transcription. Mol Microbiol **72:**1487-99.

43. **Rother, M., and W. W. Metcalf.** 2004. Anaerobic growth of Methanosarcina acetivorans C2A on carbon monoxide: an unusual way of life for a methanogenic archaeon. Proc Natl Acad Sci U S A **101:**16929-34.

44. **Rother, M., E. Oelgeschlager, and W. M. Metcalf.** 2007. Genetic and proteomic analyses of CO utilization by Methanosarcina acetivorans. Arch Microbiol **188:**463-72.

45. **Santangelo, T. J., L. Cubonova, C. L. James, and J. N. Reeve.** 2007. TFB1 or TFB2 Is Sufficient for Thermococcus kodakaraensis Viability and for Basal Transcription in Vitro. J Mol Biol **367:**344-57.

46. **Schönheit, P., Kristjansson, J.K., and R.K. Thauer.** 1982. Kinetic mechanism for the ability of sulfate reducers to out-compete methanogens for acetate. Archives of Microbiology **132:**285.

47. **Sørensen, J., Christensen D., and B. B. Jørgensen.** 1981. Volatile Fatty Acids and Hydrogen as Substrates for Sulfate-Reducing Bacteria in Anaerobic Marine Sediment. Appl. Envir. Microbiol. **42:**5-11.

48. **Sowers, K. R., S. F. Baron, and J. G. Ferry.** 1984. Methanosarcina acetivorans sp. nov., an Acetotrophic Methane-Producing Bacterium Isolated from Marine Sediments. Appl Environ Microbiol **47:**971-978.

49. **Sowers, K. R., J. E. Boone, and R. P. Gunsalus.** 1993. Disaggregation of Methanosarcina spp. and Growth as Single Cells at Elevated Osmolarity. Appl Environ Microbiol **59:**3832-3839.

50. **Sowers, K. R., and J. G. Ferry.** 2002. Methanogenesis in the marine environment, p. 1913-1923. *In* G. Bitton (ed.), The Encyclopedia of Environmental Microbiology. John Wiley & Sons, Inc.

51. **Thomm, M.** 1996. Archaeal transcription factors and their role in transcription initiation. FEMS Microbiol Rev **18:**159-71.

52. **Thomm, M.** 2007. Transcription: Mechanism and Regulation, p. 139-157. *In* R. Cavicchioli (ed.), Archaea: Molecular and Cellular Biology. ASM Press, Washington, DC.

JOURNAL OF BACTERIOLOGY, Mar. 2010, p. 1511–1517 Vol. 192, No. 6
0021-9193/10/$12.00 doi:10.1128/JB.01165-09
Copyright © 2010, American Society for Microbiology. All Rights Reserved.

# Functional Analysis of the Three TATA Binding Protein Homologs in *Methanosarcina acetivorans*▽†

Matthew J. Reichlen, Katsuhiko S. Murakami,* and James G. Ferry*

*Department of Biochemistry and Molecular Biology and Center for Microbial Structural Biology, 205 South Frear Laboratory, The Pennsylvania State University, University Park, Pennsylvania 16802*

Received 29 August 2009/Accepted 19 December 2009

**The roles of three TATA binding protein (TBP) homologs (TBP1, TBP2, and TBP3) in the archaeon *Methanosarcina acetivorans* were investigated by using genetic and molecular approaches. Although *tbp2* and *tbp3* deletion mutants were readily obtained, a *tbp1* mutant was not obtained, and the growth of a conditional *tbp1* expression strain was tetracycline dependent, indicating that TBP1 is essential. Transcripts of *tbp1* were 20-fold more abundant than transcripts of *tbp2* and 100- to 200-fold more abundant than transcripts of *tbp3*, suggesting that TBP1 is the primary TBP utilized during growth. Accordingly, *tbp1* is strictly conserved in the genomes of *Methanosarcina* species. Δ*tbp3* and Δ*tbp2* strains exhibited an extended lag phase compared with the wild type, although the lag phase for the Δ*tbp2* strain was less pronounced when this strain was transitioning from growth on methylotrophic substrates to growth on acetate. Acetate-adapted Δ*tbp3* cells exhibited growth rates, final growth yields, and lag times that were significantly reduced compared with those of the wild type when the organisms were cultured with growth-limiting concentrations of acetate, and the acetate-adapted Δ*tbp2* strain exhibited a final growth yield that was reduced compared with that of the wild type when the organisms were cultured with growth-limiting acetate concentrations. DNA microarray analyses identified 92 and 77 genes with altered transcription in the Δ*tbp2* and Δ*tbp3* strains, respectively, which is consistent with a role for TBP2 and TBP3 in optimizing gene expression. Together, the results suggest that TBP2 and TBP3 are required for efficient growth under conditions similar to the conditions in the native environment of *M. acetivorans*.**

The basal transcription machinery of the *Archaea* resembles that of the RNA polymerase II system in the *Eukarya* domain that includes two essential general transcription factors, TATA binding protein (TBP) and transcription factor B (TFB) (3–5, 16, 25, 42). In order to establish promoter-directed transcription, TBP binds a TATA box located ~25 bp upstream of the transcription start site. The binding of TBP to the promoter allows TFB to bind at sites both upstream and downstream of the TATA box. TFB then recruits RNA polymerase to the promoter to establish the preinitiation complex, which is followed by transcription (2).

Genes encoding multiple homologs of TBP and/or TFB have been identified in the genomes of several species in the domain *Archaea*. It has been proposed that the function of the homologs is to direct gene-specific transcription, analogous to the function of alternative σ factors specific to the domain *Bacteria* (1). Experimental evidence that supports this hypothesis has been reported for the archaeon *Halobacterium* sp. NRC-1, which contains six *tbp* genes and seven *tfb* genes (9, 12). A comprehensive systems approach provided evidence suggesting that there is global gene regulation by specific TFB-TBP pairs (12). In another study, two different mutants in which there was deletion of either the *tbpD* or *tfbA* homolog exhibited coordinated downregulation of 363 genes compared with the parental strain, further supporting the hypothesis that there is global gene regulation by specific TFB-TBP pairs (9). Many of the regulated genes are involved in the heat shock response, and one of the TFB homologs binds specifically to the promoter of the heat shock protein gene *hsp5* (31). The functional roles of multiple TFB homologs in various hyperthermophilic archaeal species have been investigated as well (33, 35, 36). In contrast to the reports for *Halobacterium*, none of these reports presented direct evidence that there is differentially gene regulation *in vivo* by the different TFB homologs. One factor complicating the study of *Halobacterium* sp. NRC-1 is the presence of multiple homologs of both TBP and TFB, which gives this organism the opportunity to exploit as many as 42 different TBP-TFB combinations for recruitment of RNA polymerase to specific promoters. However, this is not the case for *Methanosarcina acetivorans* C2A, a genetically tractable methanogen with genome annotations for three homologs of TBP and only a single TFB (32, 39, 40), which provides an opportunity to study the role of multiple TBPs in the context of a single TFB. *M. acetivorans* is the only acetotrophic methanogen that has been isolated from a marine environment where it must compete for acetate with acetotrophic sulfate-reducing bacteria (23, 34, 37–39). Here we report the results obtained using molecular and genetic approaches to examine the roles of the three TBP homologs in *M. acetivorans*. These results show that TBP1 is essential and that TBP2 and TBP3 are not

* Corresponding author. Mailing address: Department of Biochemistry and Molecular Biology and Center for Microbial Structural Biology, 205 South Frear Laboratory, The Pennsylvania State University, University Park, PA 16802. Phone for James G. Ferry: (814) 863-5721. Fax: (814) 863-6217. E-mail: jgf3@psu.edu. Phone for Katsuhiko S. Murakami: (814) 865-2758. Fax: (814) 865-2759. E-mail: kum14@psu.edu.

† Supplemental material for this article may be found at http://jb.asm.org/.

▽ Published ahead of print on 14 January 2010.



Downloaded from jb.asm.org at PENN STATE UNIV on March 29, 2010

essential, although they have specialized roles during adaptation to acetate and during growth with growth-limiting acetate concentrations.

## MATERIALS AND METHODS

**Cell growth.** The methods used for growth and harvesting of *M. acetivorans* C2A (= DSM 800) as single cells (40) in high-salt (HS) broth with acetate, methanol, and trimethylamine (TMA) have been described previously (26). Growth was monitored by measuring the optical density at 600 nm. The acetate concentration was maintained at 75 to 100 mM by periodically supplementing cultures with 10 M glacial acetic acid from a sterile anaerobic stock solution. Acetic acid was added at a molar ratio of acetic acid to the methane produced of 1:1; the amount of methane produced was calculated based on the volume of gas overpressure released from the culture vessel headspace. The pH of cultures grown on acetate fluctuated from 6.5 to 7.5 during growth. Cultures with initial concentrations of sodium acetate of 20 and 50 mM were not supplemented with acetic acid during growth, and the pH at the end of growth did not exceed 7.5.

**TaqMan quantitative reverse transcription-PCR (qRT-PCR).** TaqMan assays were performed essentially as described previously (26), using total RNA isolated at mid-exponential phase ($A_{600}$, approximately 0.6 to 0.7, 0.4 to 0.5, and 0.6 to 0.7 for methanol-, acetate-, and TMA-grown cells, respectively). The TaqMan primers and probes used are listed in Table S2 in the supplemental material. The primers and probes used for 16S rRNA have been described previously (26). To determine the numbers of transcripts of *tbp1*, *tbp2*, and *tbp3* for wild-type *M. acetivorans*, *in vitro*-transcribed *tbp1*, *tbp2*, and *tbp3* RNA standards were generated using a MEGAscript T7 kit (Ambion, Austin, TX) according to the manufacturer's instructions. Linearized plasmids containing *tbp1*, *tbp2*, or *tbp3* cloned into the pET21a vector under control of the T7 promoter were used as templates for the *in vitro* transcription reaction. Completed-reaction mixtures were treated with TURBO DNA-*free* DNase to remove template DNA and were then purified using an RNeasy mini kit (Qiagen, Valencia, CA) according to the manufacturer's instructions. Product size and purity were checked by agarose gel electrophoresis. The RNA standards were diluted to obtain $1 \times 10^{-11}$ copies $\mu l^{-1}$. A standard curve was generated using the averages of triplicate measurements for 10-fold serial dilutions of the RNA standards. The cycle threshold ($C_T$) values for triplicate measurements for serially diluted total RNA from methanol-grown cells plotted against the standard curve were used to calculate the number of transcript copies per nanogram for *tbp1*, *tbp2*, and *tbp3*.

**Construction of *M. acetivorans* deletion mutant strains.** Liposome-mediated transformation and homologous recombination-mediated gene replacement were performed as described previously (6, 32) to generate *M. acetivorans* Δ*tbp2*::*pac*, Δ*tbp3*::*pac*, and P*mcrB*(tetO1)::*tbp1* strains [designated the Δ*tbp2*, Δ*tbp3*, and ΔP*tbp1*::P*mcrB*(tetO1)-*tbp1* strains, respectively]. The Δ*tbp2* and Δ*tbp3* strains were generated in an *M. acetivorans* C2A background, and the ΔP*tbp1*::P*mcrB*(tetO1)-*tbp1* strain was generated in an *M. acetivorans* WWM75 background. Cells were transformed with 2 μg pMR18, pMR19, or pMR58 linearized by restriction digestion, and transformants were selected on HS agar media with 0.8% (wt/vol) agar, with either 250 mM methanol or 50 mM TMA, and with 2 $\mu g\ ml^{-1}$ puromycin (Sigma, St. Louis, MO) from a sterile, anaerobic 100× stock solution. For generation of the ΔP*tbp1*::P*mcrB*(tetO1)-*tbp1* strain, 100 $\mu g\ ml^{-1}$ tetracycline (Sigma, St, Louis, MO) was added to HS agar in addition to the other components.

**Southern blot analysis.** Digoxigenin (DIG)-labeled probes were generated using a DIG High Prime I DNA labeling and detection starter kit (Roche) according to the manufacturer's guidelines. Probes 1, 2, and 3 were PCR amplified from *M. acetivorans* genomic DNA using primers TBP2up-F and TBP2up-R, primers TBP3up-F and TBP3up-R, and primers TBP1in-F and TBP1in-R, respectively (see Table S2 in the supplemental material). The positions of these probes on the *M. acetivorans* chromosome are indicated in Fig. S1A in the supplemental material. Aliquots of genomic DNA (1 to 5 μg) from the wild-type C2A, WWM75, Δ*tbp2*, Δ*tbp3*, and ΔP*tbp1*::P*mcrB*(tetO1)-*tbp1 M. acetivorans* strains were digested overnight with either NdeI, PvuII, or EcoRI, and fragments were separated on 0.6% (wt/vol) agarose gels, denatured, neutralized, and transferred to positively charged nylon membranes (Boehringer Mannheim). Membranes were hybridized with DIG-labeled probes by following the manufacturer's guidelines.

**Adaptation to different methanogenic substrates.** Portions (10 ml) of early-stationary-phase wild-type and Δ*tbp2* or Δ*tbp3* cell cultures ($A_{600}$, approximately 1.2, 0.9, and 1.3 for methanol-, acetate-, and TMA-grown cells, respectively) were pelleted by centrifugation anaerobically for 10 min at 5,000 × *g*. Cells were washed once with 10 ml medium without substrate and resuspended in 10 ml medium without substrate, and 1-ml portions were inoculated into 100 ml medium containing the new methanogenic substrate.

**DNA microarray analysis.** RNA was collected from four replicate cultures each of the wild-type, Δ*tbp2*, and Δ*tbp3* strains grown on methanol at mid-exponential phase ($A_{600}$, ~0.6). The purity and concentration of RNA samples were checked using a NanoDrop spectrophotometer (Fisher Scientific, Pittsburg, PA), and RNA quality was assessed using an Agilent 6000 bioanalyzer nano RNA assay. RNA samples were labeled with a Message Amp II bacterial kit (Ambion Inc., Austin, TX) used according to the manufacturer's instructions, using aminoallyl UTP in place of biotin-modified nucleotides. Briefly, 500 ng of total RNA was polyadenylated and subsequently reverse transcribed with primer T7oligo(dT)VN. Second-strand cDNA synthesis was performed, and the resulting double-stranded DNA was used as a template for *in vitro* transcription. Aminoallyl-modified UTP was incorporated into the resulting complementary RNA. Twenty micrograms of this modified aminoallyl RNA was coupled with Cy3 or Cy5 using a CyDye postlabeling reactive dye pack (GE Healthcare, Buckinghamshire, England) according to the aminoallyl message Amp II kit instructions (Ambion, Austin, TX). Samples were hybridized to NimbleGen 4-plex arrays (catalog number A7240-00-01; design name 080303 MacetC2A EXP X4). Two-color hybridizations were performed, and 2 μg of each sample was hybridized to an array. Array hybridization, washing, scanning, and data acquisition were performed according to the manufacturer's instructions (Roche NimbleGen Inc., Madison, WI). All data analysis was carried out using the ArrayStar (v3) software package (DNAStar, Madison, WI). Robust multichip averaging (RMA) and quantile normalization (7, 21, 22) were applied to the entire data set, which consisted of four biological replicates and two technical replicates (dye swap) for each strain. Statistical analyses were carried out with the normalized data using a moderated *t* test with false discovery rate (FDR) multiple-test correction (Benjamini-Hochberg) to determine differential transcript abundance. Changes in transcript abundance were considered significant if they met the following criteria: ≥2-fold change in abundance, *P* value of <0.05, and $\log_2$ transcript abundance of >11.0 under the conditions with greater abundance. The *Z* test with FDR multiple-test correction (Benjamini-Hochberg) was used to assess the statistical significance of the sampling distribution of genes according to their COG functional categories.

## RESULTS

**Transcription of *tbp1*, *tbp2*, and *tbp3*.** The genome of *M. acetivorans* is annotated with genes encoding three TBP homologs (15) distinguished by sequence identity (see Table S1 in the supplemental material). In previous proteomics studies, peptides specific to TBP1, TBP2, and TBP3 were detected in cell lysates of methanol-, acetate-, and CO-grown *M. acetivorans* (26, 30). Transcript abundance was determined for each TBP gene by real-time quantitative reverse transcription-PCR (qRT-PCR) at mid-exponential phase during growth with methanol, acetate, or trimethylamine (TMA). The transcript abundance for *tbp1* was ~20-fold greater than the transcript abundance for *tbp2* in cells cultured with any of the three growth substrates, ~100-fold greater than the transcript abundance for *tbp3* during growth on methanol or TMA, and ~200-fold greater than the transcript abundance for *tbp3* during growth on acetate (Table 1). The transcript abundance for *tbp2* was ~3-, 5-, and 10-fold greater than the transcript abundance for *tbp3* during growth on methanol, TMA, and acetate, respectively (Table 1). The transcript abundance values for *tbp1*, *tbp2*, and *tbp3* were also determined in early log phase and late log phase during growth on methanol. In each case, the ratio of *tbp2* and *tbp3* transcript abundance to *tbp1* abundance remained the same (data not shown). Together, these results are consistent with undetermined physiological functions for each of the three TBPs.

**Analysis of *tbp* mutant strains.** To assess the biological significance of each TBP homolog in *M. acetivorans*, we attempted to delete the three encoding genes individually by

Downloaded from jb.asm.org at PENN STATE UNIV on March 29, 2010

TABLE 1. Abundance of *tbp1*, *tbp2*, and *tbp3* transcripts in *M. acetivorans* cultured with various substrates

| Gene | No. of transcript copies ($10^{-3}$)/ng with the following growth substrates[a]: | | |
|---|---|---|---|
| | Methanol | Acetate | TMA |
| *tbp1* | 393 ± 49 | 376 ± 113 | 369 ± 21 |
| *tbp2* | 13.3 ± 4.9 | 16.5 ± 4.5 | 20.8 ± 1.2 |
| *tbp3* | 4.9 ± 0.8 | 1.7 ± 0.4 | 3.9 ± 0.4 |

[a] The values are the numbers of transcript copies per nanogram of total cellular RNA and are the averages ± standard deviations of triplicate measurements. Absolute copy numbers were determined as described in Materials and Methods using RNA from methanol-grown cells. Copy numbers for acetate- and TMA-grown cells were inferred based on the relative abundance compared with the numbers in methanol-grown cells calculated using the $\Delta\Delta C_T$ method with the 16S rRNA gene used as an invariant control. The $\Delta C_T$ values for methanol-grown cells were used as the calibrator.

homologous recombination and selection for puromycin resistance in the presence of methanol in the growth medium. Mutant strains with either *tbp2* or *tbp3* deleted (the Δ*tbp2* and Δ*tbp3* strains) were obtained and confirmed by Southern hybridization (see Fig. S1 in the supplemental material), indicating that TBP2 and TBP3 are not essential for growth on methanol. The levels of the *tbp2* and *tbp3* transcripts in the Δ*tbp2* and Δ*tbp3* strains, respectively, were below the limits of detection by qRT-PCR, and the transcription of both of the remaining TBP genes in these strains was not affected (data not shown). Attempts to delete *tbp1* by double crossover were unsuccessful. Therefore, a conditional *tbp1* expression strain was constructed using a previously described approach (18). Instead of deleting the *tbp1* coding sequence, we modified the promoter for *tbp1* by replacing the native promoter (P*tbp1*) with a chimeric version of the *mcrB* promoter that contains an operator sequence for the Tn*10* TetR protein [P*mcrB*(tetO1)]. The Tn*10* TetR protein gene is constitutively expressed from two remote sites on the chromosome. Transcription of P*mcrB*(tetO1) is repressed by the Tn*10* TetR protein in the absence of tetracycline. Thus, in the strain obtained [ΔP*tbp1*::P*mcrB*(tetO1)-*tbp1*], *tbp1* can be expressed only in the presence of tetracycline, and its growth was comparable to that of the parental strain in the presence of 100 μg ml$^{-1}$ of tetracycline (Fig. 1). However, no growth was observed in the absence of tetracycline, indicating that *tbp1* is essential for growth (Fig. 1).

To identify growth phenotypes associated with deletion of either *tbp2* or *tbp3*, substrate-dependent cell growth was investigated by comparing the initial growth rates, the maximum $A_{600}$ values, and the lag times needed to reach mid-log phase for the Δ*tbp2* and Δ*tbp3* strains with those of the wild type when the organisms were cultured with a substrate at initial concentrations of 250 mM for methanol, 100 mM for TMA, and 100 mM for acetate. The acetate concentration was then maintained in the range from 75 to 100 mM by periodic addition of acetic acid. The growth parameters of the Δ*tbp2* and Δ*tbp3* strains were indistinguishable from those of the wild-type strain when the organisms were cultured with the methylotrophic substrates methanol and TMA (data not shown). However, on average, the lag time until mid-log phase was reached for acetate-grown cultures of the Δ*tbp3* strain (25.7 ± 6.1 days; $n = 30$) inoculated with methanol-grown cells was 12 days longer than that for the wild-type strain (13.2 ± 3.7 days; $n = 30$) (Fig. 2A). The Δ*tbp3* strain also exhibited a comparably longer lag time when it was transitioning from growth on TMA to growth on acetate (data not shown). Once the mutant strains were fully adapted to growth on acetate (after ≥30 generations of growth on acetate), the growth parameters were indistinguishable from those of the wild-type strain during culture with acetate maintained at a concentration of 75 to 100 mM (data not shown). These results suggest that TBP3 has a role in the transition from growth on methylotrophic substrates to growth on acetate maintained at concentrations between 75 and 100 mM. Although its phenotype was not as robust as the phenotype observed for the Δ*tbp3* strain, the Δ*tbp2* strain also showed a trend toward a lag phase longer than that of the wild-type strain (18.4 ± 4.2 days; $n = 30$) when it was transitioning from growth on methanol to growth on acetate (Fig. 2A).

To examine the roles of TBPs under more ecologically relevant growth conditions, growth parameters of the Δ*tbp2* and Δ*tbp3* strains (Table 2) were determined with 20 and 50 mM acetate, concentrations that are nearer the acetate concentrations (~1 to 2 mM) in the native environment of *M. acetivorans* (23, 38, 39). In this experiment, the inocula were fully adapted to growth on acetate, and the cultures were not supplemented with acetic acid during growth. The growth rates and lag times for the Δ*tbp2* strain were comparable to those for the wild-type strain. However, the maximum $A_{600}$ for the Δ*tbp2* strain was ~20% less than the maximum $A_{600}$ for the wild-type strain

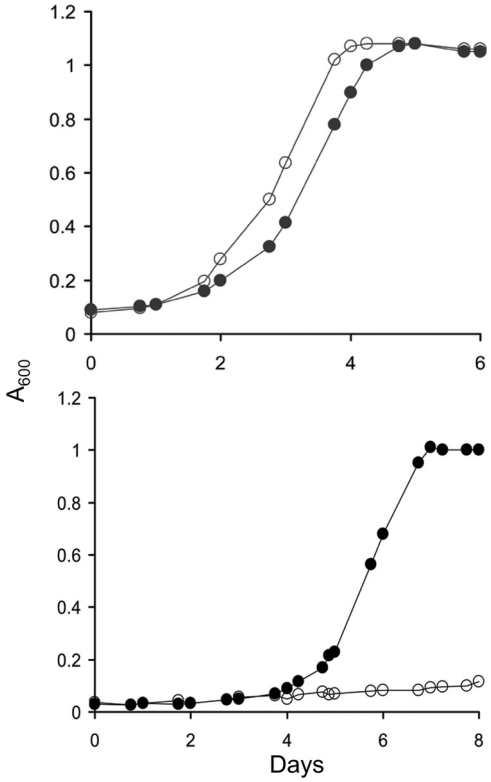


FIG. 1. Growth of the ΔP*tbp1*::P*mcrB*(tetO1)-*tbp1* strain (bottom panel) and its parental strain, WWM75 (top panel). Strains were cultured with 50 mM TMA in the presence (filled circles) or absence (open circles) of 100 μg ml$^{-1}$ of tetracycline.

Downloaded from jb.asm.org at PENN STATE UNIV on March 29, 2010

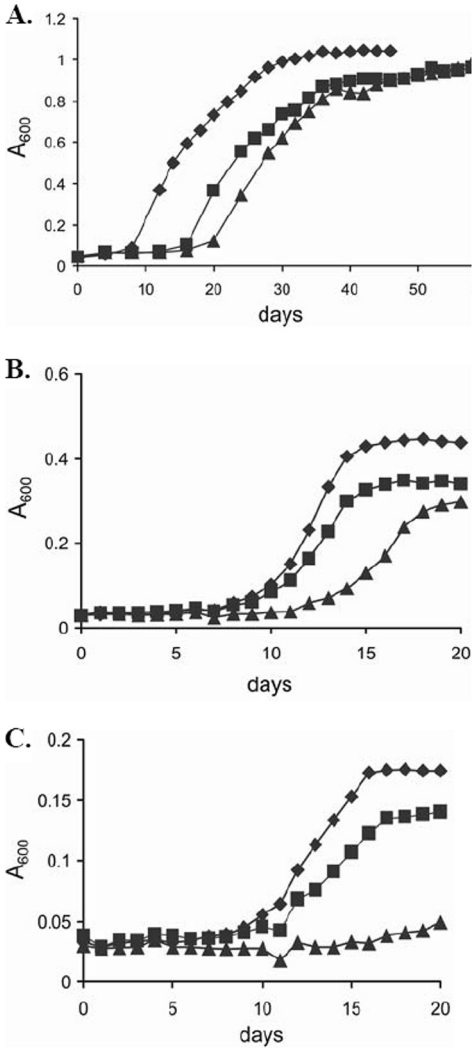


FIG. 2. Representative growth curves for the wild-type, Δ*tbp2*, and Δ*tbp3* strains of *M. acetivorans* cultured with acetate (single replicates). (A) Growth with the acetate concentration maintained between 75 and 100 mM. The inocula were cultured with 250 mM methanol. (B) Growth with 50 mM acetate. The inocula were cultured with the acetate concentration maintained between 75 and 100 mM. (C) Growth with 20 mM acetate. The inocula were cultured with the acetate concentration maintained between 75 and 100 mM. Symbols: triangles, Δ*tbp3* strain; squares, Δ*tbp2* strain; diamonds, wild-type strain.

during growth with 50 mM acetate, which is consistent with a role for TBP2 in efficient growth with growth-limiting acetate concentrations (Table 2 and Fig. 2B and C). For the Δ*tbp3* strain cultured with 50 mM acetate, the growth rates and yields

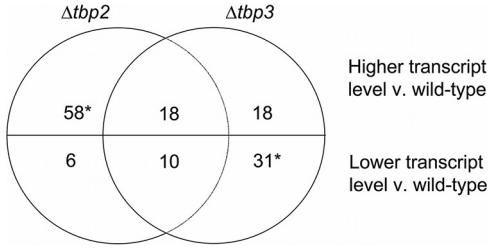


FIG. 3. Distribution of genes for which there was a difference in transcript abundance between wild-type *M. acetivorans* and mutant strains. The left side and right sides of the Venn diagram show the numbers of genes whose transcript abundance changed only in the Δ*tbp2* and Δ*tbp3* strains, respectively. The middle shows the number of genes whose transcript abundance changed in both strains. The top and bottom halves show the numbers of genes with higher and lower transcript abundance than that in wild-type *M. acetivorans*. For four of the genes whose transcript abundance was higher in the Δ*tbp2* strain than in the wild type the transcript abundance was lower in the Δ*tbp3* strain than in the wild type (indicated by asterisks).

were ~40% and ~30% less, respectively, than those for the wild-type strain, and the lag time was 6 days longer than the lag time for the wild-type strain (Table 2 and Fig. 2B). The growth defects of the Δ*tbp3* strain were more profound when it was cultured with 20 mM acetate. Seven replicate cultures of the Δ*tbp3* strain were prepared, all of which showed little detectable growth over the first 3 weeks of incubation (Fig. 2C). However, 4 of these cultures eventually began to grow after this period. The growth rates and yields of these 4 cultures were significantly lower than the growth rates and yields of the wild-type cultures, and the lag time was 17 days longer than the lag time of the wild-type cultures (Table 2). There were no differences in any of the growth parameters between either mutant strain and the wild type when the organisms were cultured with limiting methanol concentrations (25 and 50 mM) (data not shown). These results indicate that TBP3 is important for optimal growth with limiting concentrations of acetate.

**Involvement of TBP2 and TBP3 in gene regulation.** It was anticipated that the defects in the growth of the two mutant strains compared with the wild type might be reflected in the gene expression profiles. Indeed, for the Δ*tbp2* and Δ*tbp3* strains we identified 92 and 77 genes, respectively, which exhibited a ≥2-fold change in transcript abundance compared with the wild type; several of these genes were present in both strains (Fig. 3; see Tables S3 and S4 in the supplemental material), which is consistent with a role for TBP2 and TBP3 in the regulation of gene expression. Interestingly, a substantial proportion of the genes in the Δ*tbp3* strain and the majority of

TABLE 2. Growth parameters of *M. acetivorans* wild-type and mutant strains

| Acetate concn (mM) | Wild type[a] | | | Δ*tbp2* strain[a] | | | Δ*tbp3* strain[a] | | |
|---|---|---|---|---|---|---|---|---|---|
| | Generation time (h) | Maximum $A_{600}$ | Lag time (days)[b] | Generation time (h) | Maximum $A_{600}$ | Lag time (days)[b] | Generation time (h) | Maximum $A_{600}$ | Lag time (days)[b] |
| 50 | 45.4 ± 3.9 | 0.45 ± 0.02 | 10.9 ± 1.5 | 51.8 ± 5.9 | 0.36 ± 0.02 | 12.9 ± 1.4 | 63.0 ± 8.8 | 0.30 ± 0.02 | 16.9 ± 1.6 |
| 20 | 69.9 ± 5.1 | 0.18 ± 0.02 | 13.5 ± 2.9 | 73.8 ± 11.1 | 0.15 ± 0.02 | 14.4 ± 1.2 | 121 ± 37 | 0.13 ± 0.02 | 30.1 ± 2.9 |

[a] Cultures were fully adapted to growth on acetate. All values are the means ± standard deviations of 7 replicate cultures.
[b] Time required to reach mid-exponential phase of growth.

Downloaded from jb.asm.org at PENN STATE UNIV on March 29, 2010

the genes in the Δ*tbp2* strain exhibited increased transcript abundance compared with the transcript abundance in the wild type (Fig. 3; see Tables S3 and S4 in the supplemental material), suggesting that TBP2 and TBP3 may be involved in the negative regulation of numerous genes. Among the genes with increased transcript abundance in the Δ*tbp2* strain compared with the wild type, the genes encoding proteins in the amino acid transport and metabolism and inorganic ion transport and metabolism functional categories were highly overrepresented ($P = 1.57 \times 10^{-13}$ and $P = 8.70 \times 10^{-4}$, respectively) (see Tables S3 and S4 in the supplemental material). However, the biological significance of this trend is not known. Numerous other genes were identified that exhibited decreased transcript abundance in either the Δ*tbp2* or Δ*tbp3* strain compared with the wild type. Although none of these genes had functional annotations clearly linked to acetate metabolism (see Tables S3 and S4 in the supplemental material), genes that may provide added fitness under low-nutrient-availability conditions were identified. Of note were two genes encoding putative Hsp60 proteins (MA0857 and MA4386), both of which exhibited greatly decreased transcript abundance in both the Δ*tbp2* and Δ*tbp3* strains compared with the wild type and for which a larger decrease was observed for the Δ*tbp3* strain (see Tables S3 and S4 in the supplemental material), which is consistent with roles for TBP2 and TBP3 in the regulation of their transcription.

## DISCUSSION

This study, the first genetic analysis of general transcription factors for a methane-producing archaeon, provided initial insight into the roles of the three TBP homologs in *M. acetivorans*.

**TBP1 has a greater role than TBP2 or TBP3 in *M. acetivorans*.** We propose that in *M. acetivorans* TPB1 plays a greater role in gene expression than TBP2 and TBP3. This proposal is supported by the following observations: (i) transcripts of *tbp1* were found to be substantially more abundant than transcripts of *tbp2* and *tbp3* in cells cultured on methanol, acetate, or TMA; (ii) the genes encoding either TBP2 or TBP3 could be knocked out by homologous recombination, and the strains obtained could be cultured with acetate and methylotrophic substrates; (iii) a Δ*tbp1* strain could not be obtained by homologous recombination-mediated gene replacement; and (iv) the ΔP*tbp1*::P*mcrB*(tetO1)-*tbp1* strain was unable to grow in the absence of tetracycline, which inhibits the expression of *tbp1*. Accordingly, genes encoding TBP1 orthologs are strictly conserved among *Methanosarcina* species (see Table S1 in the supplemental material). The genome of *Methanosarcina mazei* Gö1 (10) contains two orthologs of *tbp1* (MM1028 and MM1027), and the gene products exhibit ≥96% amino acid sequence identity to TBP1 of *M. acetivorans*. Despite this high level of identity to TBP1, the annotations for the proteins encoded by these genes are TBP1 (MM1028) and TBP2 (MM1027). In the interest of keeping a uniform nomenclature, we suggest here that these proteins be renamed TBP1a (MM1027) and TBP1b (MM1028). The genome of *Methanosarcina barkeri* Fusaro (available at www.tigr.org) also contains a *tbp1* gene, whose product exhibits 97% amino acid sequence identity to TBP1 of *M. acetivorans*. The TBP1 protein from *M. acetivorans* exhibits 88 and 80% identity with the only TBPs annotated for the phylogenetically and metabolically related organisms *Methanococcoides burtonii* and *Methanosaeta thermophila* (see Table S1 in the supplemental material).

For organisms with multiple TBP homologs, the concept that one TBP is the primary TBP for gene expression is not unique. It has been suggested that TBPe plays a dominant role among the TBP homologs of *Halobacterium* sp. NRC-1 based on proteomic analyses in which TBPe was the sole TBP detected in *Halobacterium* sp. NRC-1 cell lysates (12, 17). Furthermore, like TBP1 in the *Methanosarcinaceae*, TBPe is the most phylogenetically conserved of the TBP homologs in the haloarchaea and is the only TBP annotated for the genomes of several species (12).

Although construction of the Δ*tbp2* and Δ*tbp3* strains established that TBP2 and TBP3 are not essential, it is yet to be determined if either gene is essential under any conditions. No phenotypic effects were observed for these strains cultured with methylotrophic substrates, which could indicate either that neither TBP2 nor TBP3 is important during growth on these substrates or that TBP2 can replace TBP3 and *vice versa*. Nonetheless, the finding that not all TBP homologs are essential for growth of *M. acetivorans* is consistent with findings for the archaeon *Halobacterium* sp. NRC-1, from which four of the six *tbp* homologs were successfully deleted (8, 12). The results for *Halobacterium* sp. NRC-1 do not rule out the possibility that the nonessential TBP homologs provide added fitness under various growth conditions. Alternatively, the results presented here suggest that TBP2 and TBP3 of *M. acetivorans* do this.

**TBP2 and TBP3 are important for growth with limiting concentrations of acetate.** Previous results (26, 28, 29) showed that all three TBP proteins are present in *M. acetivorans* during growth. The >20-fold excess of *tbp1* transcripts compared to *tbp2* and *tbp3* transcripts argues against the idea that TBP2 and TBP3 are needed simply to increase intracellular TBP concentrations. Instead, the results presented here indicate that TBP2 and TBP3 are important for optimal growth with limiting acetate concentrations. The results also indicate that TBP3 plays a larger role than TBP2. Consistent with this idea, the genomes of both *M. mazei* and *M. barkeri* are annotated with only one additional gene encoding a TBP (MM2184 and MbarA1062), which has the highest level of identity to TBP3 of *M. acetivorans* (see Table S2 in the supplemental material). In contrast to the growth phenotypes of the Δ*tbp2* and Δ*tbp3* strains reported here, *tbp2* transcripts were more abundant than *tbp3* transcripts during growth on acetate (Table 1), which is consistent with a more prominent role for *tbp2* than for *tbp3* during growth on acetate, an anomaly that has not been explained at this juncture.

In marine environments, acetotrophic sulfate-reducing species have a competitive advantage over methanogens for acetate (34, 37), which suggests that TBP3 may be necessary for *M. acetivorans* to utilize this substrate in its native habitat. The 20 mM acetate used in growth-limiting experiments reported here was the minimum concentration that allowed determination of reliable growth parameters, although the levels of acetate reported for various marine sediments (~1 to 2 mM) are well below this value (23, 38). Thus, growth defects of the mutants are expected to be even more severe in the native habitat of *M.*

Downloaded from jb.asm.org at PENN STATE UNIV on March 29, 2010

*acetivorans*. Conversely, it has been reported that methanogens compete very well with sulfate reducers for methylotrophic substrates (34) due in part to the greater energy available from conversion of these substrates to methane than from conversion of acetate to methane (41).

**Potential involvement of TBP2 and TBP3 in gene regulation.** The *Methanosarcina* species are the most metabolically diverse species in the methane-producing *Archaea* (13, 14), and the global gene expression profiles for various *Methanosarcina* species differ substantially during growth with different substrates (11, 20, 26–30). However, how the pathways are regulated is largely unknown. The growth defects of the Δ*tbp2* and Δ*tbp3* strains suggest that TBP2 and TBP3 may be necessary for the regulation of genes when *M. acetivorans* encounters growth-limiting concentrations of acetate or when it is switching from growth on methylotrophic substrates to growth on acetate. If TBP2 and TBP3 have roles in the regulation of genes specific for diverse metabolic pathways, methanogenic species with less metabolic diversity than *Methanosarcina* species might be expected to have fewer TBP homologs. Consistent with this idea, most methanogenic species that obtain energy for growth only by reducing carbon dioxide to methane have genomic annotations for only one *tbp* gene (www.tigr.org). The only exceptions are the genomes of "*Candidatus* Methanoregula boonei 6A8," which has three *tbp* genes, *Methanococcus maripaludis* C5, which has two *tbp* genes (the C7 and S2 strains each have one *tbp* gene), *Methanocorpusculum labreanum* Z, which has two *tbp* genes, *Methanoculleus marisnigri* JR1s which has two *tbp* genes, and *Methanospirillum hungatei* JF-1s, which also has two *tbp* genes. Furthermore, *M. burtonii*, which utilizes only methylotrophic substrates, and *M. thermophila*, which utilizes only acetate, have genomes annotated with only one TBP gene (www.tigr.org). Therefore, it is tempting to speculate that during the acquisition of metabolic diversity in *Methanosarcina* species, multiple TBPs evolved to play key roles in optimizing gene expression. Indeed, DNA microarray analyses have suggested that TBP2 and TBP3 are involved in the regulation of gene expression. The results presented here suggest that TBP3 is important for adaptation to growth on acetate from growth on methylotrophic substrates and that TBP2 and TBP3 are important for optimal growth during culture with growth-limiting acetate concentrations. Increases in transcription of numerous genes in the Δ*tbp2* and Δ*tbp3* strains compared with wild-type *M. acetivorans* could potentially cause protein imbalances that place further energetic burdens on cells when nutrient availability is poor. Conversely, decreases in transcription of other genes could compromise functions necessary for efficient growth under these conditions. Although none of the annotations for genes with decreased transcript abundance identified functions that could be linked specifically to acetate metabolism, it is plausible that some differentially regulated genes have roles necessary for efficient growth on acetate. For example, the proteins encoded by MA0857 and MA4386, which are homologous to group II chaperonins present in the *Archaea* and *Eukarya* domains (19, 24), could presumably function in proper folding of nascent peptides or denatured proteins to facilitate the metabolic transition from methanol to acetate. These changes in transcription are consistent with roles for TBP2 and TBP3 in the optimization of gene expression necessary for efficient transition from one-carbon substrates, such as methanol, to the least energetically favorable substrate, acetate, particularly when the acetate concentration is growth limiting, as it is in the native environment.

**Conclusion.** In this study, the physiological roles of the three TBP homologs in *M. acetivorans* were investigated. TBP1 is essential and has a greater role than TBP2 or TBP3. Although not essential for cell growth, TBP3 is important for optimal growth when cells are adapting to growth on acetate from growth on methylotrophic substrates, and both TBP2 and TBP3 are important for optimal growth with ecologically relevant growth-limiting acetate concentrations. The alternative TBPs TBP2 and TBP3 may have a role in optimization of gene expression which helps *M. acetivorans* in the metabolic transition to growth on acetate and a role in efficient utilization of ecologically relevant concentrations of acetate.

## ACKNOWLEDGMENTS

We thank W. W. Metcalf (University of Illinois, Urbana, IL) for donation of all plasmids and strains used for the genetic manipulation of *M. acetivorans*, D. Grove (Penn State Genomics Core Facility, University Park, PA) for optimization of TaqMan assays, and C. Praul and H. Xiang (Penn State Genomics Core Facility, University Park, PA) for DNA microarray labeling, hybridization, and scanning.

This work was funded by grants from the Pew Scholar's Program in the Biomedical Sciences and the National Institutes of Health (GM071897) to K.S.M. and by grants from the National Science Foundation and Department of Energy to J.G.F.

## REFERENCES

1. **Baliga, N. S., Y. A. Goo, W. V. Ng, L. Hood, C. J. Daniels, and S. DasSarma.** 2000. Is gene expression in Halobacterium NRC-1 regulated by multiple TBP and TFB transcription factors? Mol. Microbiol. **36:**1184–1185.
2. **Bartlett, M. S., M. Thomm, and E. P. Geiduschek.** 2004. Topography of the euryarchaeal transcription initiation complex. J. Biol. Chem. **279:**5894–5903.
3. **Baumann, P., S. A. Qureshi, and S. P. Jackson.** 1995. Transcription: new insights from studies on Archaea. Trends Genet. **11:**279–283.
4. **Bell, S. D., and S. P. Jackson.** 1998. Transcription and translation in Archaea: a mosaic of eukaryal and bacterial features. Trends Microbiol. **6:**222–228.
5. **Bell, S. D., C. P. Magill, and S. P. Jackson.** 2001. Basal and regulated transcription in Archaea. Biochem. Soc. Trans. **29:**392–395.
6. **Boccazzi, P., J. K. Zhang, and W. W. Metcalf.** 2000. Generation of dominant selectable markers for resistance to pseudomonic acid by cloning and mutagenesis of the ileS gene from the archaeon Methanosarcina barkeri fusaro. J. Bacteriol. **182:**2611–2618.
7. **Bolstad, B. M., R. A. Irizarry, M. Astrand, and T. P. Speed.** 2003. A comparison of normalization methods for high density oligonucleotide array data based on variance and bias. Bioinformatics **19:**185–193.
8. **Coker, J. A., P. Dassarma, J. Kumar, J. A. Muller, and S. Dassarma.** 2007. Transcriptional profiling of the model archaeon Halobacterium sp. NRC-1: responses to changes in salinity and temperature. Saline Syst. **3:**6.
9. **Coker, J. A., and S. DasSarma.** 2007. Genetic and transcriptomic analysis of transcription factor genes in the model halophilic archaeon: coordinate action of TbpD and TfbA. BMC Genet. **8:**61.
10. **Deppenmeier, U., A. Johann, T. Hartsch, R. Merkl, R. A. Schmitz, R. Martinez-Arias, A. Henne, A. Wiezer, S. Baumer, C. Jacobi, H. Bruggemann, T. Lienard, A. Christmann, M. Bomeke, S. Steckel, A. Bhattacharyya, A. Lykidis, R. Overbeek, H. P. Klenk, R. P. Gunsalus, H. J. Fritz, and G. Gottschalk.** 2002. The genome of Methanosarcina mazei: evidence for lateral gene transfer between bacteria and archaea. J. Mol. Microbiol. Biotechnol. **4:**453–461.
11. **Ding, Y. H., S. P. Zhang, J. F. Tomb, and J. G. Ferry.** 2002. Genomic and proteomic analyses reveal multiple homologs of genes encoding enzymes of the methanol:coenzyme M methyltransferase system that are differentially expressed in methanol- and acetate-grown Methanosarcina thermophila. FEMS Microbiol. Lett. **215:**127–132.
12. **Facciotti, M. T., D. J. Reiss, M. Pan, A. Kaur, M. Vuthoori, R. Bonneau, P. Shannon, A. Srivastava, S. M. Donohoe, L. E. Hood, and N. S. Baliga.** 2007. General transcription factor specified global gene regulation in archaea. Proc. Natl. Acad. Sci. U. S. A. **104:**4630–4635.
13. **Ferry, J. G. (ed.).** 1993. Methanogenesis: ecology, physiology, biochemistry and genetics, vol. I. Chapman and Hall, New York, NY.
14. **Ferry, J. G., and K. A. Kastead.** 2007. Methanogenesis, p. 288–314. *In* R. Cavicchioli (ed.), Archaea: molecular and cellular biology. ASM Press, Washington, DC.

Downloaded from jb.asm.org at PENN STATE UNIV on March 29, 2010

15. **Galagan, J. E., C. Nusbaum, A. Roy, M. G. Endrizzi, P. Macdonald, W. FitzHugh, S. Calvo, R. Engels, S. Smirnov, D. Atnoor, A. Brown, N. Allen, J. Naylor, N. Stange-Thomann, K. DeArellano, R. Johnson, L. Linton, P. McEwan, K. McKernan, J. Talamas, A. Tirrell, W. Ye, A. Zimmer, R. D. Barber, I. Cann, D. E. Graham, D. A. Grahame, A. M. Guss, R. Hedderich, C. Ingram-Smith, H. C. Kuettner, J. A. Krzycki, J. A. Leigh, W. Li, J. Liu, B. Mukhopadhyay, J. N. Reeve, K. Smith, T. A. Springer, L. A. Umayam, O. White, R. H. White, E. Conway de Macario, J. G. Ferry, K. F. Jarrell, H. Jing, A. J. Macario, I. Paulsen, M. Pritchett, K. R. Sowers, R. V. Swanson, S. H. Zinder, E. Lander, W. W. Metcalf, and B. Birren.** 2002. The genome of M. acetivorans reveals extensive metabolic and physiological diversity. Genome Res. **12:**532–542.
16. **Geiduschek, E. P., and M. Ouhammouch.** 2005. Archaeal transcription and its regulators. Mol. Microbiol. **56:**1397–1407.
17. **Goo, Y. A., E. C. Yi, N. S. Baliga, W. A. Tao, M. Pan, R. Aebersold, D. R. Goodlett, L. Hood, and W. V. Ng.** 2003. Proteomic analysis of an extreme halophilic archaeon, Halobacterium sp. NRC-1. Mol. Cell Proteomics **2:**506–524.
18. **Guss, A. M., M. Rother, J. K. Zhang, G. Kulkarni, and W. W. Metcalf.** 2008. New methods for tightly regulated gene expression and highly efficient chromosomal integration of cloned genes for Methanosarcina species. Archaea **2:**193–203.
19. **Hirtreiter, A. M., G. Calloni, F. Forner, B. Scheibe, M. Puype, J. Vandekerckhove, M. Mann, F. U. Hartl, and M. Hayer-Hartl.** 2009. Differential substrate specificity of group I and group II chaperonins in the archaeon Methanosarcina mazei. Mol. Microbiol. **74:**1152–1168.
20. **Hovey, R., S. Lentes, A. Ehrenreich, K. Salmon, K. Saba, G. Gottschalk, R. P. Gunsalus, and U. Deppenmeier.** 2005. DNA microarray analysis of Methanosarcina mazei Go1 reveals adaptation to different methanogenic substrates. Mol. Genet Genomics **273:**225–239.
21. **Irizarry, R. A., B. M. Bolstad, F. Collin, L. M. Cope, B. Hobbs, and T. P. Speed.** 2003. Summaries of Affymetrix GeneChip probe level data. Nucleic Acids Res. **31:**e15.
22. **Irizarry, R. A., B. Hobbs, F. Collin, Y. D. Beazer-Barclay, K. J. Antonellis, U. Scherf, and T. P. Speed.** 2003. Exploration, normalization, and summaries of high density oligonucleotide array probe level data. Biostatistics **4:**249–264.
23. **King, G. M., M. J. Klug, and D. R. Lovley.** 1983. Metabolism of acetate, methanol, and methylated amines in intertidal sediments of Lowes Cove, Maine. Appl. Environ. Microbiol. **45:**1848–1853.
24. **Klunker, D., B. Haas, A. Hirtreiter, L. Figueiredo, D. J. Naylor, G. Pfeifer, V. Muller, U. Deppenmeier, G. Gottschalk, F. U. Hartl, and M. Hayer-Hartl.** 2003. Coexistence of group I and group II chaperonins in the archaeon Methanosarcina mazei. J. Biol. Chem. **278:**33256–33267.
25. **Kyrpides, N. C., and C. A. Ouzounis.** 1999. Transcription in archaea. Proc. Natl. Acad. Sci. U. S. A. **96:**8545–8550.
26. **Lessner, D. J., L. Li, Q. Li, T. Rejtar, V. P. Andreev, M. Reichlen, K. Hill, J. J. Moran, B. L. Karger, and J. G. Ferry.** 2006. An unconventional pathway for reduction of $CO_2$ to methane in CO-grown Methanosarcina acetivorans revealed by proteomics. Proc. Natl. Acad. Sci. U. S. A. **103:**17921–17926.
27. **Li, L., Q. Li, L. Rohlin, U. Kim, K. Salmon, T. Rejtar, R. P. Gunsalus, B. L. Karger, and J. G. Ferry.** 2007. Quantitative proteomic and microarray analysis of the archaeon Methanosarcina acetivorans grown with acetate versus methanol. J. Proteome Res. **6:**759–771.
28. **Li, Q., L. Li, T. Rejtar, B. L. Karger, and J. G. Ferry.** 2005. Proteome of Methanosarcina acetivorans. Part I. An expanded view of the biology of the cell. J. Proteome Res. **4:**112–128.
29. **Li, Q., L. Li, T. Rejtar, B. L. Karger, and J. G. Ferry.** 2005. Proteome of Methanosarcina acetivorans. Part II. Comparison of protein levels in acetate- and methanol-grown cells. J. Proteome Res. **4:**129–135.
30. **Li, Q., L. Li, T. Rejtar, D. J. Lessner, B. L. Karger, and J. G. Ferry.** 2006. Electron transport in the pathway of acetate conversion to methane in the marine archaeon Methanosarcina acetivorans. J. Bacteriol. **188:**702–710.
31. **Lu, Q., J. Han, L. Zhou, J. A. Coker, P. DasSarma, S. DasSarma, and H. Xiang.** 2008. Dissection of the regulatory mechanism of a heat-shock responsive promoter in Haloarchaea: a new paradigm for general transcription factor directed archaeal gene regulation. Nucleic Acids Res. **36:**3031–3042.
32. **Metcalf, W. W., J. K. Zhang, E. Apolinario, K. R. Sowers, and R. S. Wolfe.** 1997. A genetic system for Archaea of the genus Methanosarcina: liposome-mediated transformation and construction of shuttle vectors. Proc. Natl. Acad. Sci. U. S. A. **94:**2626–2631.
33. **Micorescu, M., S. Grunberg, A. Franke, P. Cramer, M. Thomm, and M. Bartlett.** 2008. Archaeal transcription: function of an alternative transcription factor B from Pyrococcus furiosus. J. Bacteriol. **190:**157–167.
34. **Oremland, R. S., and S. Polcin.** 1982. Methanogenesis and sulfate reduction: competitive and noncompetitive substrates in estuarine sediments. Appl. Environ. Microbiol. **44:**1270–1276.
35. **Paytubi, S., and M. F. White.** 2009. The crenarchaeal DNA damage-inducible transcription factor B paralogue TFB3 is a general activator of transcription. Mol. Microbiol. **72:**1487–1499.
36. **Santangelo, T. J., L. Cubonova, C. L. James, and J. N. Reeve.** 2007. TFB1 or TFB2 is sufficient for Thermococcus kodakaraensis viability and for basal transcription in vitro. J. Mol. Biol. **367:**344–357.
37. **Schönheit, P., J. K. Kristjansson, and R. K. Thauer.** 1982. Kinetic mechanism for the ability of sulfate reducers to out-compete methanogens for acetate. Arch. Microbiol. **132:**285.
38. **Sørensen, J., D. Christensen, and B. B. Jørgensen.** 1981. Volatile fatty acids and hydrogen as substrates for sulfate-reducing bacteria in anaerobic marine sediment. Appl. Environ. Microbiol. **42:**5–11.
39. **Sowers, K. R., S. F. Baron, and J. G. Ferry.** 1984. Methanosarcina acetivorans sp. nov., an acetotrophic methane-producing bacterium isolated from marine sediments. Appl. Environ. Microbiol. **47:**971–978.
40. **Sowers, K. R., J. E. Boone, and R. P. Gunsalus.** 1993. Disaggregation of Methanosarcina spp. and growth as single cells at elevated osmolarity. Appl. Environ. Microbiol. **59:**3832–3839.
41. **Sowers, K. R., and J. G. Ferry.** 2002. Methanogenesis in the marine environment, p. 1913–1923. *In* G. Bitton (ed.), The encyclopedia of environmental microbiology. John Wiley & Sons, Inc., New York, NY.
42. **Thomm, M.** 2007. Transcription: mechanism and regulation, p. 139–157. *In* R. Cavicchioli (ed.), Archaea: molecular and cellular biology. ASM Press, Washington, DC.

Downloaded from jb.asm.org at PENN STATE UNIV on March 29, 2010

# Chapter 4

# Genome-wide transcription profiling of *Methanosarcina acetivorans* diauxic growth on methanol and acetate


## Summary

Transcriptional profiling was carried out on the marine methanogen *M. acetivorans* during diauxic growth to investigate differences in gene expression during transition from methanol to acetate. The expression profiles for the methanol and acetate growth phases closely resembled those for cells grown exclusively on either substrate. The transition between methanol and acetate growth phases was characterized by a prolonged growth arrest and methanogenesis accompanied by decreased transcript abundance of genes involved in housekeeping functions and increased abundance for stress response genes. Also in the transition phase, the transcript abundance increased for several genes encoding components of the archaeal flagellum although cell motility was not observed. During substrate-limited growth in the late methanol phase, the transcript abundance for the *cdh/acs* and *pta/ack* operons essential for acetate metabolism significantly increased *versus* the mid methanol phase. There was also a greater abundance of transcripts during the late methanol phase for genes encoding novel MT2 methyltransferases fused to corrinoid binding domain proteins. These analyses also uncovered novel insights into the methanol and acetate pathways including the

identification of candidate genes for acetate transport and transcription regulation of methanol and acetate metabolism. Lastly, comparisons between the genes with differential transcript abundance in the mid methanol *versus* mid acetate phases to those with altered transcription in the Δ*tbp2* and Δ*tbp3* mutants *versus* wild-type *M. acetivorans* described in chapter 3. These comparisons revealed significant correlations in expression indicative of misregulated sets of genes in the Δ*tbp2* and Δ*tbp3* mutants. This suggests that the perturbations in transcription of these genes may contribute to the observed growth defects in these mutant strains.

## Introduction

The conversion of organic material to methane by consortia of anaerobic microbes is an essential component of the global carbon cycle, producing approximately 1 billion metric tons annually (51). Methanogens are terminal organisms of the consortia, of which the genus *Methanosarcina* is the most metabolically diverse utilizing several substrates for growth and methanogenesis (21, 58). Not unexpected, the *Methanosarcina* regulate their energy-yielding metabolism in response to the most energetically favorable substrate. For example, faced with both methanol and acetate, cultures utilize methanol first then transition to the less energetically rich acetate (21, 58). This aspect makes these organisms ideal candidates for the study of gene regulation in the *Archaea* domain. Indeed, previous analyses have revealed large scale differences in gene expression profiles in *Methanosarcina* species grown on methanol *versus* acetate (18, 25, 35-39).

However, to date, there have been only a handful of investigations into the mechanisms of gene regulation in *Methanosarcina* species (4, 5, 10-12, 49). Furthermore, the majority of these studies were carried out with cells metabolizing a single growth substrate which fails to adequately address the physiology of these organisms in their native environment where the availability of a particular energy source is transient and cells are forced to constantly adjust the metabolic machinery accordingly.

It was shown that the *M. acetivorans* Δ*tbp2* and Δ*tbp3* strains described in chapter 3 exhibited defective growth *versus* wild-type cells during adaptation from use of methanol to acetate. However, a better understanding of the implications of this phenotype is precluded by a dearth of information pertaining to the cellular response to this metabolic transition.

When *Methanosarcina* species are grown in the presence of both substrates, a prolonged period of transient growth arrest ensues following depletion of methanol prior to the initiation of growth with acetate (30, 47, 59). Such metabolic transitions for species in the *Bacteria* domain have been characterized by large scale changes in gene expression as cells adjust metabolic machinery and cope with the stresses brought on by transient growth arrest (15). Similar investigations of diauxic growth by methanogenic species have not been reported. Presented here are growth parameters and transcriptional profiles throughout the course of diauxic growth of *M. acetivorans*, a marine species, in the presence of both methanol and acetate. The results have revealed for the first time gene expression patterns in response to the transition between growth substrates for any methanogen that provides insight to diauxic growth as well as advancing an understanding of independent growth on either substrate.

## Results and Discussion

### Data set overview

Growth of *M. acetivorans* in the presence of methanol (25 mM) and acetate (100 mM) was bi-phasic (Fig. 4-1). Significant consumption of acetate was not detectible in the first growth phase (Fig. 4-2) consistent with a diauxic shift from the more energetically favorable substrate methanol to less favorable acetate, as is the case for the fresh water isolates *Methanosarcina barkeri* (6) and *Methanosarcina thermophila* (59). In addition to transient growth arrest, no increase in gas over pressure from the culture headspace was detected between growth phases consistent with a cessation of methanogenesis as well (data not shown).

Transcriptional profiling was carried out on *M. acetivorans* during diauxic growth to investigate the global response to transitioning between growth substrates, the first for any methanogen. RNA was collected during the mid (MM) and late (LM) methanol phases, the transition period (T) and mid acetate growth phase (MA) (Fig. 4-1, Fig. 4-3). Each data set represents the mean of four replicate cultures.

Comparison of the MM and MA profiles identified a total of 760 transcripts with a significant change in abundance of at least 2.5-fold (Supplementary file 3) of which 386 were greater at MM and 374 greater at MA. Included in these data sets were nearly all the genes with known roles specific to either the methanol or acetate pathway of methanogenesis up regulated in the appropriate growth phase (Supplementary file 3).

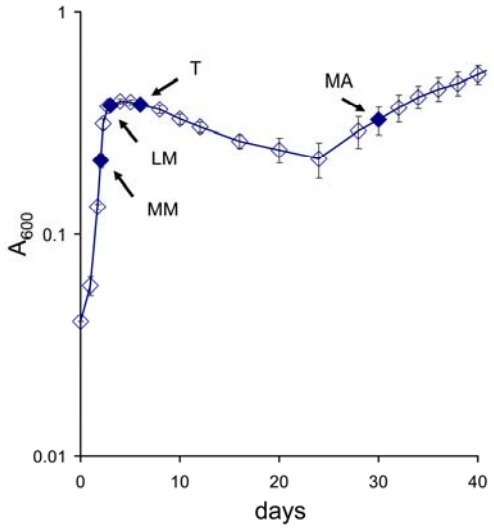


**Figure 4-1. Diauxic growth of *M. acetivorans* on methanol (25 mM) and acetate (100 mM).** Error bars represent the standard deviation of four replicate cultures. Filled data points indicate times when cells were harvested for RNA isolation. Data points are labeled to indicate the mid (MM) and late (LM) methanol phases, the transition period (T) and the mid acetate phase (MA).

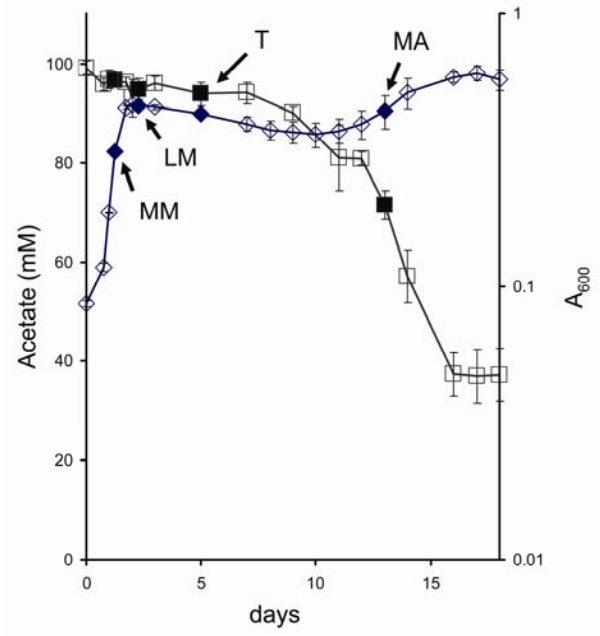


**Figure 4-2. Growth and depletion of acetate during culturing of *M. acetivorans* with methanol (25 mM) and acetate (100 mM).** Blue diamonds indicate growth. Values represent the average and standard deviation of duplicate cultures. Black squares indicate acetate concentration. Values represent the average and standard deviation of replicate cultures assayed in triplicate. Data points are labeled to indicate the mid (MM) and late (LM) methanol phases, the transition period (T) and the mid acetate phase (MA).

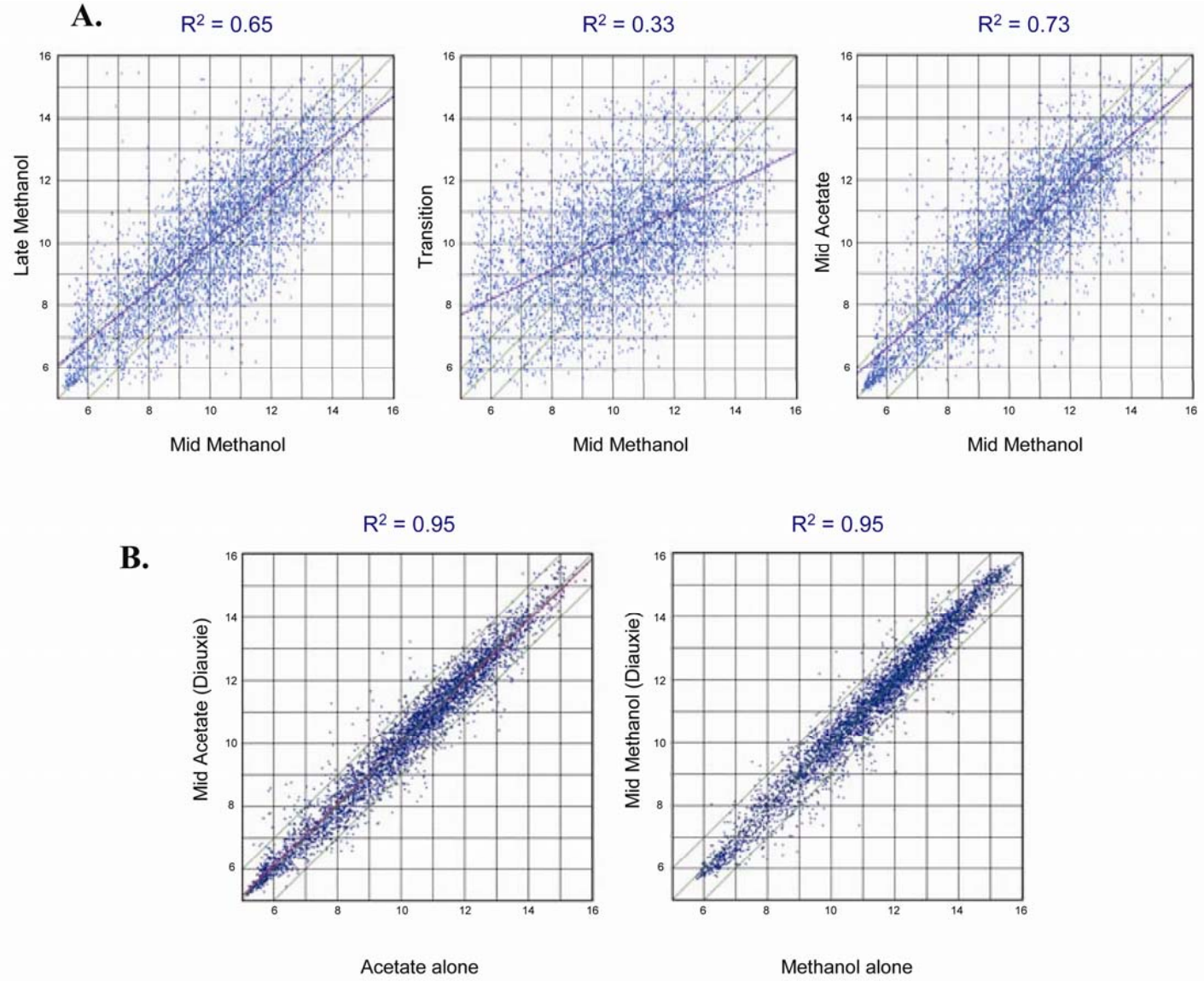
A.
R2 = 0.65
R2 = 0.33
R2 = 0.73
Late Methanol
Transition
Mid Acetate
Mid Methanol
Mid Methanol
Mid Methanol
B.
R2 = 0.95
R2 = 0.95
Mid Acetate (Diauxie)
Mid Methanol (Diauxie)
Acetate alone
Methanol alone

**Figure 4-3. Scatter plots depicting differences in expression profiles across different phases of growth.** (A) Depicts mid methanol *versus* late methanol, transition and mid acetate phases respectively. (B) Depicts the mid methanol or mid acetate phase from Diauxic growth *versus* mid log from cells grown on methanol or acetate alone. Values on the X-axis and Y-axis represent normalized $Log_2$ transcript abundances for the growth phase depicted. The coefficient of correlation between the different phases is indicated above each scatter plot.

Furthermore, expression profiles from MM and MA showed good correlation with those from *M. acetivorans* cells fully adapted to methanol and acetate respectively (Fig. 4-3). No significant difference in transcript abundance in MM *versus* MA was detected for genes encoding the two enzyme complexes common both the methanol and acetate pathways, methyl-CoM reductase (Mcr), tetrahydromethanopterin S-methyltransferase (Mtr) or for the $A_1A_0$ ATPase, which is speculated to function as the primary ATPase in both pathways (Table 4-1) consistent with essential functions for these enzymes.

A total of 921 genes were identified with a significant change in transcript abundance between MM and LM of which 531 were greater at MM and 390 greater at LM (Tables 4-1 and Supplementary file 4). A total of 1531 transcripts exhibited a significant change in abundance between MM and T of which 929 were greater at MM and 604 greater at T (Tables 4-1 and Supplementary file 5). These large numbers of affected genes in LM and T *versus* MM suggest a robust transcriptional response to the metabolic transition.

A combined total of 402 genes were less abundant in both LM and T compared to M the majority of which were involved in housekeeping functions (Table 4-2). The functional categories with the highest representation included: translation, transcription (including RNA polymerase and all of the general transcription factors), amino acid transport and

**Table 4-1. Genes with at least 2.5-fold difference in transcript abundance in mid methanol phase *versus* late methanol phase, transition period or mid acetate phase.**

| loci | annotation [a] | Fold change LM/MM[b] | T/MM | MA/MM |
|---|---|---|---|---|
| **Enzymes essential to both methanol and acetate methanogenesis** | | | | |
| MA4546 | methyl coenzyme M reductase, subunit alpha | 0.87 | 0.25 | 1.09 |
| MA4550 | methyl coenzyme M reductase, subunit beta | 0.75 | 0.38 | 1.12 |
| MA4155 | V-type ATP synthase subunit E | 1.14 | 0.05 | 1.49 |
| MA4160 | V-type ATP synthase subunit D | 0.99 | 0.12 | 1.61 |
| MA0269 | tetrahydromethanopterin S-methyltransferase subunit H | 0.48 | 0.10 | 0.84 |
| MA0276 | tetrahydromethanopterin S-methyltransferase subunit E | 0.36 | 0.20 | 1.08 |
| **Energy utilization during transition phase** | | | | |
| MA0975 | coenzyme F420 hydrogenase, subunit alpha | 4.99 | 11.62 | 0.30 |
| MA0976 | hydrogenase maturation protease | 3.68 | 6.23 | 0.19 |
| MA0977 | coenzyme F420 hydrogenase, subunit gamma | 3.62 | 4.02 | 0.27 |
| MA3895 | nitrogenase (iron protein) | 8.54 | 6.97 | 0.95 |
| MA3897 | P-II family nitrogen regulatory protein | 7.74 | 3.35 | 0.59 |
| MA3898 | nitrogenase, subunit alpha | 4.73 | 5.47 | 0.57 |
| MA3900 | nitrogenase associated protein E | 5.01 | 4.14 | 0.65 |
| MA3901 | nitrogenase associated protein N | 4.64 | 3.31 | 0.53 |
| **General stress response** | | | | |
| MA1462 | universal stress protein | 5.66 | 12.59 | 1.47 |
| MA2866 | universal stress protein | 5.89 | 8.09 | 5.36 |
| MA3284 | universal stress protein | 4.14 | 7.03 | 3.87 |
| MA3589 | small heat shock protein, class I | 4.70 | 7.00 | 0.24 |
| MA3944 | universal stress protein | 3.76 | 2.98 | 1.09 |
| **Acetate catabolite repression** | | | | |
| MA1012 | acetyl-CoA decarbonylase/synthase complex subunit delta | 3.85 | 1.01 | 2.52 |
| MA1015 | acetyl-CoA decarbonylase/synthase complex subunit epsilon | 6.36 | 0.86 | 3.49 |
| MA1016 | acetyl-CoA decarbonylase/synthase complex subunit alpha | 5.74 | 1.03 | 5.69 |
| MA3860 | acetyl-CoA decarbonylase/synthase complex subunit alpha | 2.85 | 1.57 | 2.92 |
| MA3863 | carbon-monoxide dehydrogenase accessory protein | 2.56 | 0.61 | 2.63 |
| MA3606 | acetate kinase | 3.06 | 0.90 | 4.12 |
| MA3607 | phosphate acetyltransferase | 4.46 | 0.51 | 6.43 |
| MA1616 | methanol-5-hydroxybenzimidazolylcobamide co-methyltransferase, isozyme 3 | 4.49 | 1.06 | 8.90 |
| MA1617 | methanol-5-hydroxybenzimidazolylcobamide co-methyltransferase, isozyme 3 | 6.62 | 3.43 | 10.85 |
| MA2536 | carbonate dehydratase | 1.62 | 1.13 | 8.69 |
| MA4569 | multiple resistance/pH regulation related protein D (Na+/H+ antiporter) | 0.88 | 0.52 | 2.88 |
| MA4570 | multiple resistance/pH regulation related protein C (Na+/H+ antiporter) | 1.31 | 1.00 | 2.64 |
| MA4665 | multiple resistance/pH regulation related protein B (Na+/H+ antiporter) | 1.12 | 0.98 | 2.70 |
| MA4572 | multiple resistance/pH regulation related protein A (Na+/H+ antiporter) | 0.89 | 1.06 | 2.57 |
| **Putative methyltransferease genes** | | | | |
| MA0859 | hypothetical protein (multi-domain) | 335.81 | 9.49 | 1.10 |
| MA4164 | corrinoid protein | 47.94 | 10.74 | 1.43 |
| MA4165 | methylcobalamin:CoM methyltransferase isozyme A | 45.34 | 6.27 | 1.35 |
| MA4558 | hypothetical protein (multi-domain) | 231.96 | 7.59 | 0.52 |
| MA0144 | monomethylamine methyltransferase | 5.48 | 0.85 | 1.49 |
| MA0528 | trimethylamine methyltransferase | 4.60 | 4.77 | 6.08 |
| MA0934 | dimethylamine corrinoid protein | 3.84 | 5.08 | 0.30 |

| | | | | |
|---|---|---|---|---|
| MA2425 | dimethylamine methyltransferase | 7.71 | 34.57 | 1.56 |
| MA2972 | monomethylamine methyltransferase | 1.28 | 2.74 | 0.14 |
| **Cell motility** | | | | |
| MA0015 | chemotaxis protein-glutamate methylesterase | 2.95 | 4.79 | 1.01 |
| MA0234 | type IV secretion system protein | 1.94 | 4.94 | 4.64 |
| MA3055 | flagellar accessory protein FlaJ | 1.20 | 5.05 | 0.48 |
| MA3066 | chemotaxis sensor histidine kinase | 1.10 | 3.94 | 0.87 |
| MA3077 | flagellin | 5.06 | 39.04 | 2.11 |
| MA3096 | type IV secretion system protein | 1.86 | 10.02 | 0.89 |
| **Acetate transport** | | | | |
| MA0103 | GPR1/FUN34/yaaH family protein | 6.52 | 12.46 | 0.87 |
| MA4008 | Fun34 related protein | 35.13 | 20.77 | 39.28 |
| MA4393 | GPR1/FUN34/yaaH family protein | 0.64 | 0.21 | 0.24 |
| **Iron transport** | | | | |
| MA0161 | ferritin | 4.67 | 5.13 | 0.73 |
| MA1005 | ferric uptake regulation protein | 5.26 | 31.79 | 1.15 |
| MA1198 | iron ABC transporter, ATP-binding protein | 1.84 | 17.35 | 0.91 |
| MA1850 | iron(III) ABC transporter, solute-binding protein | 4.51 | 38.20 | 1.36 |
| MA2776 | iron(III) ABC transporter, ATP-binding protein | 4.79 | 42.23 | 1.87 |
| MA3453 | iron ABC transporter, ATP-binding protein | 1.24 | 4.93 | 0.29 |
| MA4532 | iron compounds ABC transporter, ATP-binding protein | 0.95 | 3.85 | 0.88 |
| MA4533 | iron compounds ABC transporter, permease protein | 1.64 | 5.87 | 0.69 |
| MA4604 | iron(III) ABC transporter, solute-binding protein HemV2 | 3.69 | 3.97 | 1.13 |
| MA4605 | iron(III) ABC transporter, permease protein | 7.46 | 31.10 | 3.25 |
| **Regulation – methanol or acetate metabolism** | | | | |
| MA0459 | hypothetical protein | 0.19 | 0.17 | 0.06 |
| MA0460 | hypothetical protein | 0.15 | 0.53 | 0.07 |
| MA4383 | hypothetical protein | 1.47 | 0.59 | 0.10 |
| MA4397 | hypothetical protein | 0.26 | 0.17 | 0.37 |
| MA1671 | hypothetical protein | 1.43 | 2.41 | 0.18 |
| MA3130 | hypothetical protein | 1.86 | 0.43 | 0.011 |
| MA2013 | sensory transduction histidine kinase | 4.45 | 4.01 | 25.45 |
| MA2256 | sensory transduction histidine kinase | 2.07 | 8.98 | 43.13 |
| MA4671 | Response regulator receiver | 9.73 | 12.69 | 36.88 |
| MA2211 | transcription repressor | 1.14 | 0.48 | 10.84 |
| MA2212 | hypothetical protein | 0.60 | 0.52 | 7.10 |
| MA3302 | hypothetical protein | 5.11 | 2.85 | 5.56 |
| **Regulation – transition phase** | | | | |
| MA1862 | endopeptidase La | 4.33 | 3.30 | 0.65 |
| MA1863 | transcriptional regulator, MarR family | 6.28 | 7.34 | 0.92 |
| MA4575 | cell division control protein 48 | 2.68 | 3.30 | 0.67 |
| MA4576 | Hth5 family protein | 4.55 | 6.42 | 1.01 |

[a] Annotations are those listed at http://www.tigr.org

[b] MM, mid methanol phase; LM, late methanol phase; T, transition period; MA, mid acetate phase

**Table 4-2. Genes with differential transcript abundance both late methanol and transition phase *versus* methanol phase divided into functional categories.**

| Functional Group | total in category [b] | Decreased [c] | | Increased [d] | |
|---|---|---|---|---|---|
| | | No [e] | % [f] | No | % |
| Amino acid transport and metabolism | 299 | 38 | 12.71 | 7 | 2.34 |
| Carbohydrate transport and metabolism | 99 | 19 | 19.19 | 5 | 5.05 |
| Cell cycle control, mitosis and meiosis | 31 | 2 | 6.45 | 0 | 0 |
| Cell motility | 43 | 2 | 4.65 | 3 | 6.98 |
| Cell wall/membrane biogenesis | 109 | 18 | 16.51 | 5 | 4.59 |
| Chromatin structure and dynamics | 3 | 0 | 0.00 | 0 | 0 |
| Coenzyme transport and metabolism | 166 | 25 | 15.06 | 8 | 4.82 |
| Cytoskeleton | 1 | 0 | 0 | 0 | 0.00 |
| Defense mechanisms | 84 | 3 | 3.57 | 2 | 2.38 |
| Extracellular structures | 1 | 0 | 0 | 0 | 0 |
| Energy production and conversion | 280 | 20 | 7.14 | 23 | 8.21 |
| General function prediction only | 601 | 48 | 7.99 | 37 | 6.16 |
| Inorganic ion transport and metabolism | 198 | 20 | 10.10 | 10 | 5.05 |
| Intracellular trafficking and secretion | 26 | 1 | 3.85 | 0 | 0 |
| Lipid transport and metabolism | 37 | 5 | 13.51 | 1 | 2.70 |
| Nucleotide transport and metabolism | 60 | 14 | 23.33 | 2 | 3.33 |
| Posttranslational modification, protein turnover, chaperones | 112 | 8 | 7.14 | 10 | 8.93 |
| Replication, recombination and repair | 243 | 23 | 9.47 | 5 | 2.06 |
| RNA processing and modification | 2 | 0 | 0 | 0 | 0 |
| Secondary metabolites biosynthesis, transport and catabolism | 24 | 2 | 8.33 | 0 | 0 |
| Signal transduction mechanisms | 104 | 8 | 7.69 | 9 | 8.65 |
| Transcription | 157 | 23 | 14.65 | 8 | 5.10 |
| Translation | 159 | 43 | 27.04 | 1 | 0.63 |
| Uncharacterized | 1594 | 79 | 4.96 | 83 | 5.21 |
| Total [a] | 4433 | 402 | 9.07 | 219 | 4.94 |

[a] Total number of genes represented on the Nimblegen microarray slide.

[b] Total number of genome annotations for each functional group.

[c] Decreased transcript abundance *versus* the mid methanol phase.

[d] Increased transcript abundance *versus* the mid methanol phase.

[e] Number of genes with significantly increased or decreased transcript abundance in both the late methanol and transition phases *versus* the methanol phase for each functional group.

[f] Percentage of gene with significant change in transcript abundance against the total number of genes in that functional category.

metabolism, coenzyme transport and metabolism, nucleotide transport and metabolism, carbohydrate transport and metabolism and cell wall/membrane biogenesis. A similar decrease in transcript abundance for housekeeping genes was observed in *Methanosarcina barkeri* following exposure to oxygen which also leads to transient growth arrest (56). During transient growth arrest which occurs during diauxic shifts, bacteria elicit a stringent response wherein rRNA transcription is repressed. Presently, it is unclear whether *Methanosarcina* species exhibit stringent control of rRNA synthesis or if they exhibit the relaxed phenotype as both phenotypes have been observed in the different species of *Archaea* (8, 14, 16). Additionally, it is unclear how *M. acetivorans* might coordinate a stringent response since guanosine tetra- (ppGpp) and pentaphosphate (pppGpp) accumulation during stringent response has not been observed in *Archaea*, and *relA* and *spoT* homologues are absent from the *M. acetivorans* genome. Thus, the mechanism underlying the global changes during the transition phase is unknown.

There were an additional 219 genes in greater abundance at both LM and T *versus* MM of which the functional category of energy production and conversion was most represented. Interestingly, several genes from this category with greater transcript abundance at T were not annotated for proteins previously implicated in either the acetate or methanol pathway of methanogenesis for *M. acetivorans*. For instance, transcripts for three of the four genes encoding the $F_{420}$-reducing hydrogenase (Frh) were in greater abundance at LM and T *versus* MM (Table 4-1). This finding was surprising in light of previous findings in which little hydrogenase activity is reported for *M. acetivorans* (41) and that the promoter for the *frh* operon is apparently inactive during growth with either methanol or acetate (24). It is unclear what role Frh might play in the transition.

However, it is unlikely that this hydrogenase could serve as a functional replacement of the $F_{420}$ dehydrogenase (Fpo) in an analogous fashion to the $H_2$ cycling mechanism described for *Methanosarcina barkeri* (31) in that neither of the putative $F_{420}$-nonreducing hydrogenase (Vht/Vhx) operons nor the genes encoding the putative hydrogenase maturation proteins showed an increase in transcript abundance at LM or T *versus* MM. Additionally, any evolved $H_2$ produced by Frh is likely to be quickly consumed by sulfate-reducing bacteria in the native marine environment of *M. acetivorans*.

Several genes with annotated functions for stress response were also represented among those with greater transcript abundance at the LM and T stages *versus* the MM stage consistent with a need for the cell to respond to the general stress of energy starvation. Among these genes were four annotated as universal stress proteins (MA1462, MA2866, MA3284 and MA3944) and one (MA3589) annotated as a small heat shock protein (Table 4-1). The transcript abundance for two of these genes (MA2866 and MA3284) were in greater abundance at the MA stage *versus* the MM stage consistent with previous reports describing acetate growth as a general stress due to the lower available free energy (36). Universal stress proteins are among the most highly expressed in *E. coli* during growth arrest, and are thought to provide the cell with added "stress endurance" (32) thus, it is plausible that stress proteins perform a similar role in growth arrested *M. acetivorans.*

Another set of genes with greater transcript abundance at stages LM and T relative to MM and MA was the *nif* operon (Table 4-1). These genes encode for the nitrogenase enzyme complex which catalyzes nitrogen fixation. In *Methanosarcina*

*mazei,* homologs to these genes have been shown to be up regulated during growth in the absence of fixed nitrogen (53). However, in this experiment, growth was carried out in media with an adequate supply of fixed nitrogen (19 mM ammonium). Thus, it is unclear how the energetically expensive process of nitrogen fixation would benefit the cell particularly when it is experiencing the high stress of a metabolic transition.

**Methanol repression of acetate metabolism**

Although both methanol and acetate were present at the onset of growth, a significant depletion of acetate was not detected prior to the acetate phase of growth (Fig. 4-2) indicating that methanol is the preferred substrates for growth. This is consistent with previous reports for growth of fresh water *Methanosarcina* strains with methanol and acetate (30, 47, 54, 59). Numerous genes reported upregulated in response to growth with acetate showed greater transcript abundance at the LM stage *versus* the MM stage. This was followed by a return to MM abundance levels at the T stage followed once again by an increase in abundance at MA (Table 4-1). This expression pattern is consistent with a model in which methanol represses the expression of genes required for acetate metabolism. As the concentration of methanol diminishes at the LM stage, genes essential for acetate metabolism are released from repression. The activation of these genes is apparently overridden during transition for unknown reasons. Perhaps there is insufficient energy to synthesize the cognate proteins for these genes, or their transcription may be repressed as part of a global stress response.

Genes exhibiting this expression pattern include the two *cdh/acs* operons (49) encoding CO dehydrogenase/acetyl-CoA synthase enzyme complexes, the *ack/pta* operon (1) encoding acetate kinase and phosphotransactylase and the *mtaCB3* operon which encodes the methanol-specific MT1 isozyme 3 enzyme complex shown previously to be up regulated in response to growth with acetate (Table 4-1) (11, 12, 18, 38). Oddly, this expression pattern did not apply to other genes with proposed functions specific to acetate metabolism. Genes encoding a carbonic anhydrase (Cam) (2) and a putative $Na^+$/proton antiporter complex (Mrp), (39) while higher at the MA stage *versus* MM, did not exhibit an increase in transcript abundance at either the LM or T stages (Table 4-1). Unlike *cdh/acs, pta* and *ack* which are required for the activation of acetate to acetyl-CoA (20), the genes for Cam (57) and Mrp (Chavez and Ferry unpublished data), while important for optimal growth on acetate, are not essential consistent with alternative regulatory mechanisms for genes of varying importance. Alternatively, *cdh/acs* and *ack/pta* may be induced for acetate for incorporation into biomass sparing methanol as an energy source when the concentration decreases.

**Putative methyltransferase genes**

In the methylotrophic pathway of methanogenesis, transfer of the methyl moiety of various C-1 compounds to HS-CoM proceeds *via* two distinct methyl-transfer reactions catalyzed by methyltransferases MT1 and MT2. MT1 consists of two polypeptides. The first is methyltransferase, catalyzing transfer of the methyl group of

the C-1 compound to a corrinoid cofactor in the second polypeptide. MT2 transfers the methyl group of the corrinoid cofactor to HS-CoM generating $CH_3$-S-CoM. The *M. acetivorans* genome contains three peculiar genes (MA0859, MA4384 and MA4558) not found elsewhere in nature which encode fused proteins containing both an MT2 domain and the corrinoid-binding domain of MT1. Genes encoding two of these fused proteins (MA0859 and MA4558) exhibited large increases in transcript abundance at LM *versus* MM. Two additional genes encoding a putative corrinoid protein (MA4164) and a putative MT2 methyltransferase (MA4165) also exhibited a large increase in transcript abundance at LM *versus* MM. The MA4164 gene product is homologous to the corrinoid-binding domain of the fused proteins encoded by MA0859, MA4384 and MA4558 (Fig. 4-4A) and the protein encoded by MA4165 is homologous to the MT2 methyltransferase domain of the three fused proteins (Fig. 4-4B). Therefore, the proteins encoded by MA4164 and MA4165 could conceivably carry out a similar function to the fused methyltransferase/corrinoid proteins.

The robust increase in transcription of MA0859, MA4558, MA4164 and MA4165 is consistent with a role in facilitating the metabolic transition from methanol to acetate utilization. Although previous reports have implicated the fused proteins in CO (35, 45), dimethylsulfide (DMS) (10, 42) and methanol metabolism (13), precise physiological roles are unclear. Presently, two different models have been proposed. The Mtr bypass model proposes a functional replacement of the eight subunit $Na^+$ translocating Mtr complex in the transfer of the methyl moiety of $CH_3$-THMPT to HS-CoM (35). This model is supported by increased expression of MA0859 and MA4384 coupled with decreased expression of Mtr in CO- *versus* acetate-grown *M. acetivorans* and through

**A.**

```
4164          MDDLPEEVQELIEELDEAAEDEDEDAIKDLTQKLLATGVDVEAITLKKLALLVMDGEEEM    60
859           ---------------------------------MLEAFFMAADILNQLAEAVVDGDDDL    26
4384          -------------------------------------MAKEDILNTLADAVVDGDDEL    21
4558          --------------------------MAIENENQGADAISEEELFRQMAEAVVDGDDEI    33
                                                    :. :*  *:**::::

4164          TQGWTQVAIQIGTDPFKTLIEGLAAGMSLIGKKYEEGEAFVPQLLIASAAMYGGMDLLAP   120
859           AEELAYKALEEGVDPYDAIVNGLARGMAIVSDQYEKGEAFVPHLLLASGAMYAGMDILSP    86
4384          AEEFAQKALDEELDAYEAIVDGLARGMKIISDMYERGEAFVPSLLLAADAMYAGMDILTP    81
4558          IEELANRVLELNIDPYTAIVEGLTKGMSIVSDMYENGKAFVPNLMVSAGAMYEGLDILSP    93
               :  :  .::   *.: ::::**: ** ::.. **.*:**** *:::: *** *:*:*:*

4164          YMKQDENSGSKAATVVIGTVEGDVHDIGKSLVKTLLSANGFNCVDLGNDVPASRFIEAAR   180
859           EMIKE--GEAMQAVGVIGTIEGDVHDIGKNLVKTMLSAGGFEMIDLGADVPIEKFVETAK   144
4384          YMKVD--GTAAPKNVIIGTVEGDVHDIGKNLVKTMMTAAGFNMIDLGCDVPLDKFAETAK   139
4558          YLKSD--STNKPSKIIIGTVEGDVHDIGKNLVKTMMTAAGFDMIDLGSDVPLSSFVSSAR   151
               :  :  .       :***:*********.****::** **: :*** *** . * .:*:

4164          ENKATAVSMSTLMTTTMAEMPKVVKMLENEGIRDKLLVMVGGAPITAEYASQIGADVSPH   240
859           ERKADIISMSALMTTTMTNMEKVIEILQEEGIRDSMKVMIGGAPVSEEYASGIGADSTHP   204
4384          EKKAAAISMSTLMTTTMGGMETVIEQLQEEGIRDSLIVMVGGAPISQTFADSVGADGTAL   199
4558          DQKADAISMSTLMTTTMPGMEKVIEQLKEEGLRDSLLVMVGGAPINADYAAKIGADATRD   211
              :.**  :***:******  * .*:: *::**:**.: **:****:.  :*  :*** :

4164          DAASAASWLKGAVFDFPSESVRWS   264
859           DAMHASAWASEAVKELEPKAARWS   228
4384          DASAAVETLTSLVSELP--SDSWS   221
4558          DASAATEWLKGAIVELPDADLRWS   235
              **  *    .  : ::      **
```

**B.**

```
4165          ------------------------------------MVSEMTSKERVFAMLNRKPVD    21
859           LGKIKYREILAKKTVSDKVDVGLETANKIKEEFESIGVKSKEEMTHIDRTISAMSDKKVD   293
4384          ASKMKYKEVLAQKSGKEKVDIGRITAEKIIAEFDSVVPKFNETMTKAERFGAAFQDKKVD   286
4558          LNKVKYKEELAKKGTVEAVDIGLETAKAIIEEFESVGVKTKESMTHADRTVSAMSDKKVD   300
                                                  . **  :*  : :. * **

4165          RVPVITGSVMVKEYIEKSGSSWPDYHSNAEMMVNTVSLMHTDAGLDNIVMPFGMFIESMA    81
859           HLPVYPLACGVLRKFVP--VTYKEYATNEDAFVQSAYLGSKYLDLDMFVGLIDLSATSAD   351
4384          RLPVAPLACGVSRKFVP--CSYVDYSTKAEKYADCVEAGIKYFNMDTFVGLTDLCVDAAD   344
4558          RLPVYPLACGVLRKFAP--VTYKEYATNEDAFVQSAYLGSKYLDLDMFVGLIDLSITSAD   358
              ::** . :  * . :     :: :* :: :  .: .    .  .:* :*   .:   :

4165          LGLEVKMGRIDIQPSVRSFFNKPEEVKYDNFLEDKYVQTTLDAIKLAKEKYP---DAAVT   138
859           FGCKIKYP-EDDTPSSEGHIKDYEKIEVPELKEGTRGYELVMASKKAKEKLNKELNTPFV   410
4384          FGATIRYP-EEDTPAATGHLEDYEKLEVPELKEGTRAYNLIQGNKLATEKA-HALDAPMT   401
4558          LGCGVKFP-EEDTPSSEGHLEDYEKIEVPEVKEGTRAYELIKATKLAKAKLNSELATPMV   417
              :*  ::    :  *:  ..::. *:::  :. *..     : . * *. *      :...

4165          AFLVAPITLAGDLMGAENLSMLSIKCLQKEKQMQKMKDWISIALEINKIYAEACVEAGAD   198
859           GFHEGPLLTLTQLMGADRVLMDMKTQPDVVLEAVQKCTDYVCQLSELFFNEDACDALCID   470
4384          ALIEGPMVALTQIMGATRVLSDLRTNPDVVLKALDKTTVYVEEIMKGMFEEAQPDNLCMV   462
4558          GFHEGPLLTLTQLMGASRVLGDMNTNPDVVLKAVDKCADYVAEVSRAFFEEDACDALCID   477
              .:  .*:    ::*** .:     .  :   :  .        :    :

4165          ILYYSDASASPNLVMP---EFYYQVAVPAEKEIGDFVH-HLGCPWELHICGDTVPIIEGM   254
859           NLWSNNVIMSEQDYWKFDGKFVYDQQIPIFKQYNQPYIIH-NCADAVHFETQIRKFGTAL   529
4384          NLWTNNVILSADEYMKSEGQVMQNRIAPLYKKYNKPVVIH-NCADAPHWELIN-KWNTEY   520
4558          NLWSNNVIMGQDDYWKFDGQFVYNKHVPVFKEYNQPYIIH-NCADAVHYDIQISKFGTAL   536
               *: .:.  . :       :.  :   *  *: ..    * .*.   *

4165          ASTGADCLSVEQAVN--MEEATKIAGDVPVVGNVTPLLMVEG--------------TEAQ   298
859           YSYAYYEKSRDKGSQNYADLIPKYGDMCCMMGEVNPVEFMDGSAAGVQKVKDDTKNLLEN   589
4384          YSYTFYPDEAGKGSKDHKYLINNYGKETMFGGEVSPIVFLDNSPEGLQKMKADTIALQES   580
4558          YSYAYYPSGKGKGSYSYDELIPKYGKTCCMMGEVDPIQFLDNSPEGIQKIRNDTESNLRG   596
               *         :.         : .    . *:* *: :::.

4165          IIEETRKGLDGGAKASMLGCGTPPLSSSDKLKTWVKAAADWSADKL-----   344
859           VLPVLKENGLQSKYILSSGCEIPPGGPLTTVQAMVNVVKELGPELQKNIMG   640
4384          VLNTLKENGMQSKYMISTGCEVPPGAPCDSITAQTYTVAEKGPELYKKIIG   631
4558          AIQALKENGFQSKYVMSTGCEIPPGAPLDTSKAMVDVVKELGPELQKMIG-   646
               :   ::.   .      *:  ** ..  .  : . .. : ..:
```

**Figure 4-4. Alignments of MA4164 (A) and MA4165 (B) with the fused proteins encoded by MA0859, MA4384 and MA4558.** Alignments were performed using ClustalW followed by manual changes. Conserved amino acids are denoted with asterisks. Similar residues are denoted with dots. The residues important for corrinoid binding in MA4164 and the corrinoid binding domains of MA0859, MA4384 and MA4558 are shaded in gray and the Histidine residue required for Cobalt binding is denoted with an arrow. Residues involved in zinc coordination in MA4165 and the MT2 domains of MA0859, MA4384 and MA4558 are shaded in gray.

biochemical analyses with recombinant MA4384 (Vepachedu and Ferry unpublished data). The methylsulfide methyltransferase model proposes a role for the fused proteins in the reversible transfer of methyl groups between $CH_3$-S-CoM and dimethylsulfide as a means to prevent accumulation of excess of $CH_3$-S-CoM and for the utilization of dimethylsulfide as a methanogenic substrate (10, 13, 40, 42). This model is supported by observed increases in the presence of DMS for transcription of the genes encoding the fused proteins, in a mutant deleted of the *hdrA1B1C1* operon (10), and by impaired growth with DMS and production of DMS in a triple mutant deleted for all three fused proteins (42). Presently, it is unclear what role the fused proteins might play at the LM stage since either model can provide rationale for their elevated transcription. One possibility is that the cell casts a wide net readying metabolic capacity for all potential substrates including CO.

Several genes encoding putative MT1 and MT2 methyltransferases specific to metabolism of methylamines showed greater transcript abundance at either LM or T *versus* MM (Table 4-1). This result was unexpected since methylamines were not present in the growth media. However, it is conceivable that the genes are being induced in anticipation of arrival of these substrates consistent with the proposed rationale for increases of the fused proteins.

## Cell Motility

Cell motility has not been observed in *Methanosarcina* species. Nonetheless, genes encoding for chemotaxis and flagellar machinery are present on the genomes of *M. acetivorans, M. mazei* and *M. barkeri* (17, 22) (www.tigr.org). Interestingly, genes in this functional category had the highest representation of genes with greater transcript abundance at T *versus* MM suggesting *M. acetivorans* evolved a mechanism for regulation of these genes consistent with a physiological function. Included were genes encoding a flagellin (MA3077), type IV secretion system proteins (MA0234 and MA3096), a flagellar accessory protein, FlaJ (MA3055), a chemotaxis sensor histidine kinase (MA3066) and a chemotaxis protein-glutamate methylesterase (MA0015) (Table 4-1) (28). However, cell motility was not observed during the transition period suggesting functions other than motility. An alternative possibility is loss of other genes required for motility such as the gene encoding the preflagellin peptidase consistent with a previous report in which this activity was not detected in *M. acetivorans* (22).

## Acetate transport

The mechanism for acetate uptake by *Methanosarcina* species is not understood, and previous analyses failed to identify candidate genes for this process (35-39). It was once assumed that acetate uptake in acetotrophic microbes was by simple diffusion of un-dissociated acetic acid across the cytoplasmic membrane (7, 29). However, it has been

shown that for *Corynebacterium glutamicum* that acetate uptake is facilitated by an un-characterized acetate/proton symport mechanism with little contribution by simple diffusion (19, 23). More recently, genes from the family *GPR1/Fun34/yaaH* were implicated in active transport of acetate for two species of yeast. For the dimorphic non-acetate utilizing yeast, *Yarrowia lipolytica*, *trans*-dominant mutations in the *GPR1* gene caused a sensitivity to acetic acid at low pH suggesting that *GPR1* may play a role in transport of toxic acetic acid out of the cell (52). Deletion of the *ADY2* gene, another member of the *GPR1/Fun34/yaaH* family, abolished active acetate transport in the acetate utilizing yeast *Saccharomyces cerevisiae* (43).

The genome of *M. acetivorans* contains three homologs of the *GPR1/Fun34/yaaH* family (MA0103, MA4008 and MA4393). One of these genes (MA4008) was previously shown to be one the most highly up-regulated genes in *M. acetivorans* during growth on acetate (44). The involvement of this gene family in acetate transport has also been speculated for the obligate acetotrophic methanogen *Methanosaeta thermophila* (46). Consistent with these reports, MA4008 showed a substantial increase in transcript abundance at LM and T *versus* MM further supporting a role in acetate metabolism. The transcript abundance for MA0103 was greater at LM and T but not MA *versus* MM (Table 4-1). In contrast, MA4393 which is co-transcribed with *mtaCB2* encoding a methanol-specific MT1 methyltransferase is highly up-regulated when cultured with methanol (12, 18, 38). Based on the gene context and expression pattern, it is unlikely that MA4393 is involved in acetate uptake for growth with methanol, although a role for acetate uptake for cell carbon synthesis cannot be ruled out. Homologs of MA4008 are found in other *Methanosarcina* species as well as in the only other known acetotrophic

methanogen, *Methanosaeta thermophila* (44), consistent with a conserved role in all of these species. On the other hand, MA0103 and MA4393 homologs are only found in *Methanosarcina* species (44). Therefore, if a member of the *GPR1/Fun34/yaaH* family does facilitate acetate uptake in *M. acetivorans*, it is most likely that MA4008 carries out this function during growth with acetate.

## Iron transport

It has been speculated that during growth of *Methanosarcina* species on acetate, there is an increased demand for iron uptake in order to support synthesis of the five-subunit CO dehydrogenase/acetyl CoA synthase complex which has several iron-sulfur clusters and accounts for approximately 10% of the total cell protein in acetate-grown cells (25, 50). Consistent with this idea, several genes encoding ferric iron transporters (MA1198, MA1850, MA2776, MA3453, MA4532, MA4533, MA4604 and MA4605) exhibited greater transcript abundance at T *versus* MM (Table 4-1). In addition genes encoding a ferritin (MA0161) potentially involved in iron storage and sequestration and a homolog of the ferric uptake regulation (Fur) protein (MA1005) potentially involved in the regulation of iron uptake also showed greater transcript abundances at T *versus* MM (Table 4-1). Increases in transcript abundance for MA0161, MA1005, MA4604 and MA4605 were also observed at LM *versus* MM (Table 4-1). These results are consistent with a function for these genes in iron uptake to facilitate the metabolic transition from growth with methanol to growth with acetate.

## Regulation

Although not reported in previous proteomic and transcriptomic analyses, genes encoding two methanol-specific regulatory (Msr) proteins (MA459 and MA460) (11) displayed higher transcript abundance at MM *versus* MA (Table 4-1). Genes (MA4383 and MA4397) (11) encoding two other Msr proteins reported present in methanol- but not acetate-grown cells by proteomic analyses (35) also exhibited higher transcript abundance in MM *versus* MA (Table 4-1). These data are consistent with a previous report demonstrating the importance of these genes in methanol metabolism (11). Interestingly, it was another gene (MA3130) whose product was not identified in previous proteomic or transcriptomic analyses (35-39) that had the greatest increase in transcript abundance at MM *versus* MA (Table 4-1). A homolog to MA3130 (MA1671) also exhibited significantly elevated transcript abundance in the mid methanol *versus* mid acetate phase (Table 4-1). The proteins encoded by MA3130 and MA1671 are homologous to the TrmB family of transcription factors which regulate the metabolism of various sugars in several species of *Archaea* (34). Homologs of MA3130 and MA1671 are present in *M. mazei* (17), *M. barkeri* (www.tigr.org) and in the closely related methanogen, *Methanococcoides burtonii* (3) consistent with a conserved role in all of these methanol-utilizing species. These results suggest roles for MA3130 and MA1671 in the regulation of methanol metabolism.

In contrast to methanol, nothing is known about the regulatory proteins involved in acetate metabolism or transition between substrates. In a previous study (36), numerous genes encoding for putative sensory transduction histidine kinases or response

regulator receivers were shown to have increased transcript abundance in acetate- *versus* methanol-grown cells suggesting a potential role in regulation of acetate metabolism. Three of those genes (MA2013, MA2256 and MA4671) showed 25-fold greater transcript abundance at MA *versus* MM consistent with this hypothesis. Also consistent with a previous report (36), transcripts of a putative transcription factor (MA3302) were significantly more abundant in the acetate *versus* methanol phase (Table 4-1). The MA3302 protein is homologous to MA1671 and MA3130 which were up regulated in the mid methanol phase consistent with diverse roles for this protein family gene regulation. Numerous other genes encoding putative transcriptional regulators exhibited an increase in transcript abundance in the acetate phase relative to the methanol phase which were not identified in previous proteomics or transcriptomic analyses (35-39). For example, the co-transcribed genes (data not shown), MA2211 and MA2212 were considerably more abundant in the acetate *versus* methanol phase (Table 4-1). The protein encoded by MA2211 is homologous to MarR-family transcription factors of the *Bacteria* domain involved in resistance to antibiotics (55). The protein encoded by MA2212 is homologous to TrmB-family transcription factors. Homologs of MA2211, MA2212 and MA3302 are found in both *M. mazei* and *M. barkeri* consistent with conserved function across all three acetotrophic species (17) (www.tigr.org). These results suggest a role for MA2211, MA2212 and MA3302 in the regulation of acetate metabolism.

Other genes annotated as transcription factors exhibited an increase in transcript abundance specifically at LM and T *versus* MM. The genes with the largest change were MA1863 and MA4576 (Table 4-1), neither of which changed in abundance in the mid methanol *versus* the mid acetate phase. The annotation for MA1863 is a MarR-family

transcription factor and MA4576 an Hth5-family protein. Both are members of the ArsR super family of metal-binding transcription regulators. Both of these genes are positioned immediately upstream of genes encoding putative AAA+ ATPase (MA1862 and MA4575) which also showed greater transcript abundance at both LM and T *versus* MM (Table 4-1) consistent with a role for these genes in the regulation of MA1862 and MA4575 respectively. Homologs of these genes with >80% identity are found in both *M. mazei* and *M. barkeri* which are also positioned immediately upstream of homologs of the same putative AAA+ ATPase genes. AAA+ ATPase proteins commonly function as proteases. Thus, it is conceivable that these enzymes are involved in protein recycling during the transition phase.

## Involvement of alternative TBP homologs, TBP2 and TBP3 in regulating the diauxic shift

The transcriptional profiling of *M. acetivorans* diauxic growth was undertaken, in part to assess the potential involvement of the alternative TBPs, TBP2 and TBP3 and to potentially provide a better understanding of why the Δ*tbp2* and Δ*tbp3* strains are defective in adjusting from metabolism of C-1 substrates to acetate. Although the analyses described in this chapter provide substantial insight into overall *M. acetivorans* physiology, the basic question of how TBP2 and TBP3 are involved remains elusive. One hypothetical model for the function of the multiple *M. acetivorans* TBP homologs proposed that each isomer functioned analogously to multiple sigma factors in bacterial

systems in order to direct RNAP to different promoters specific to each TBP. Previous investigations into the roles of the multiple GTF isomers of *Halobacterium* sp. NRC-1 found that while this model could explain that patterns of expression for a limited number of genes, as a general rule, it appears to be overly simplified. An examination of the promoter occupancies of the seven TFBs found only approximately one third of the functionally expressed promoters to be bound by a single TFB whereas the remaining two thirds were bound and presumably regulated by two or more TFBs (21) suggesting at least partial functional overlap in the roles for these TFBs. Evidence for such a scenario in *M. acetivorans* among the different TBP isomers can inferred from the 32 genes which exhibited ≥2-fold change in transcript abundance *versus* the wild-type strain in both the Δ*tbp2* and the Δ*tbp3* strain (see Fig. 3-13).

It was postulated that the growth defects observed in the Δ*tbp2* and Δ*tbp3* strains when switching to acetate metabolism were the result of protein imbalances which place unnecessary energetic burdens on the cell that already under the stress of nutrient starvation. To extend this idea further, an examination was undertaken to look for correlations in the genes with altered transcription in the Δ*tbp2* and Δ*tbp3* strains *versus* wild-type *M. acetivorans* and the 760 genes which exhibited differential transcript abundance in the mid methanol *versus* the mid acetate phase. Using the rationale that many genes are likely to be regulated by more than one TBP, the gene sets used in this analysis for the Δ*tbp2* and Δ*tbp3* strains were modified to take into account genes with subtle alternations in transcription that were < 2-fold but highly significant (*P*-value ≤ 0.001). It can be argued that TBP2 and/or TBP3 contribute to the regulation of these genes, but are not absolutely required for their expression.

Using these new criteria, the number of genes with altered transcription *versus* wild-type *M. acetivorans* in Δ*tbp2* and Δ*tbp3* strains expanded to 257 and 337 genes respectively (Fig. 4-5) (Supplementary files 6-7). These genes sets were then filtered against the 760 genes with differential transcript abundance between the mid methanol and mid acetate phases. It was determined that highly significant fractions of the genes with altered transcription in either the Δ*tbp2* or Δ*tbp3* strain were common to both sets consistent with functionally overlapping roles for TBP2 and TBP3 in the regulation of these genes. Additionally, a disproportionate fraction of genes exhibiting decreased transcript abundance in the Δ*tbp2* and Δ*tbp3* strains exhibited increased abundance in the mid acetate *versus* mid methanol phase (Fig. 4-5A) and a disproportionate fraction of the genes exhibiting increased abundance in the Δ*tbp2* and Δ*tbp3* strains exhibited increased abundance in the mid methanol *versus* mid acetate phase (Fig. 4-5B). This strong correlation between acetate-responsive and TBP2 and/or TBP3 responsive genes is consistent with the observed growth defects with acetate in the Δ*tbp2* and Δ*tbp3* strains. Rather interestingly, this analysis seems to suggest that in the absence of TBP2 or TBP3, acetate responsive genes exhibit a tendency to be mis-regulated: i.e. they tend to be down- or up-regulated in excess of their wild-type levels. Mechanistically, it is unclear exactly how TBP2 and TBP3 would carry out this type of regulation. However, one could envision several possibilities. For instance, there may be competition for promoter occupancy among the different TBP isomers at these genes or interactions away from the promoter such as formation of different combination TBP heterodimers, both of which could explain the roles for TBP2 and TBP3 in negative regulation of genes.

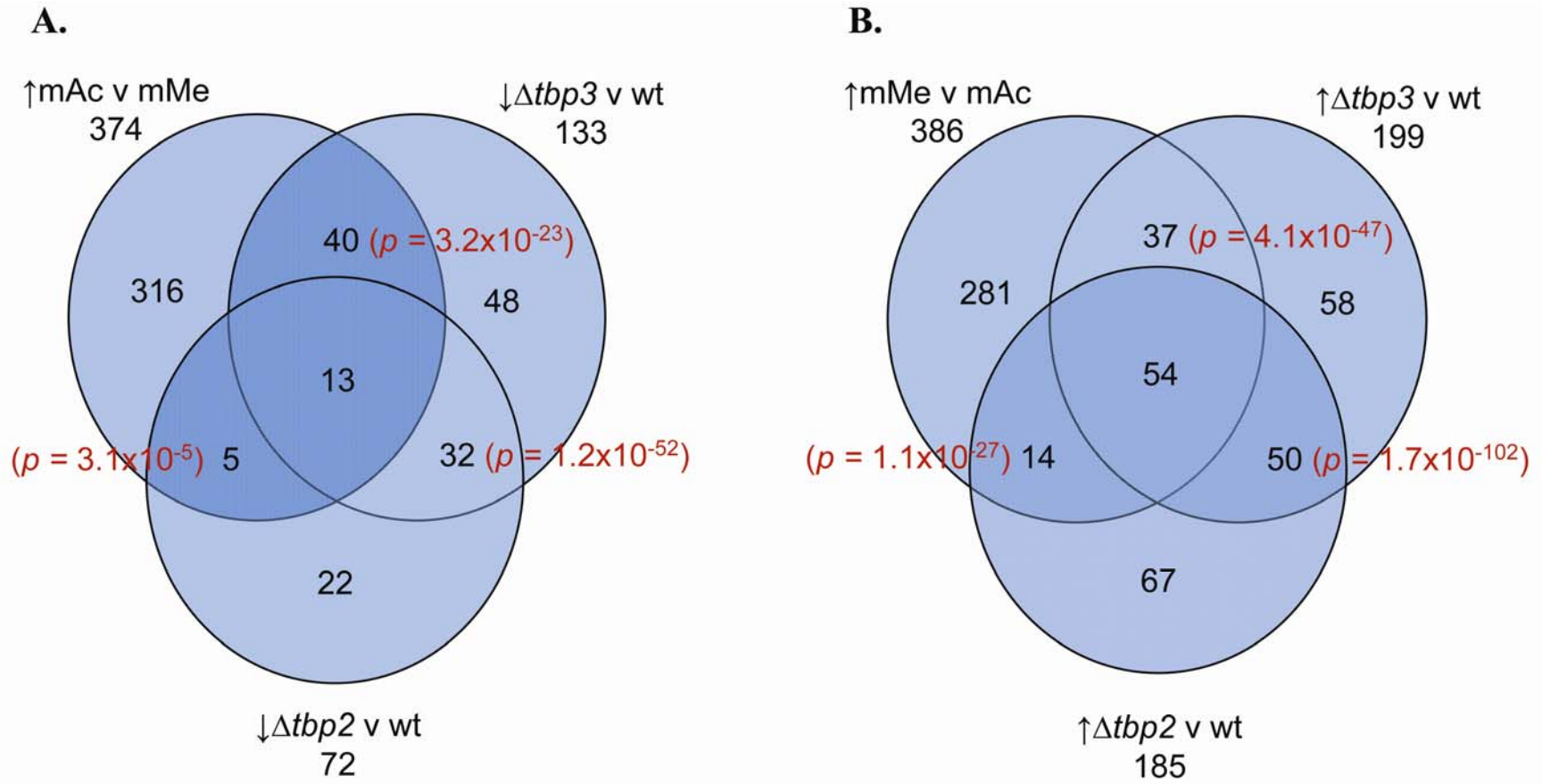


**Figure 4-5: Venn diagrams depicting correlations in expression for genes with altered transcription in the MA *versus* MM phases, the Δ*tbp2* strain *versus* wild-type and the Δ*tbp3* strain *versus* wild-type.** (A) Compares the 374 genes with increased abundance in the MA *versus* MM phase with 72 and 133 genes with decreased abundance in the Δ*tbp2* and Δ*tbp3* strains respectively. (B) Compares the 386 genes with increased abundance in the MM *versus* MA phase with 185 and 199 genes with increased abundance in the Δ*tbp2* and Δ*tbp3* strains respectively. Significance values for overlapping sets of genes are shown in red.

Alternatively, TBP2 and TBP3 could supplement TBP1-directed transcription at other promoters as the intracellular concentrations of TBP1 fluctuate. Ultimately, additional work will be required to fully understand these interesting phenomena.

## Conclusions

This analysis has, for the first time, revealed insights into the metabolic transition between growth substrates for any methanogen. Differences in transcript abundance for numerous genes of *M. acetivorans* were attributed to the transition, many not previously reported to be regulated. These included genes annotated for iron transport and storage, novel methyltransferases and motility. The transition was also characterized by reduced transcription of housekeeping genes and increased transcription of stress response genes. The results support a mechanism in which methanol suppresses transcription of genes essential for acetate metabolism. These analyses revealed numerous insights into methanol and acetate metabolism including the identification of potential acetate transporters and transcriptional regulators of the methanol and acetate pathways and for the metabolic transition period. Additionally, correlations in expression between MM- and MA-activated genes to those with perturbed expression in the Δ*tbp2* and Δ*tbp3* mutant strains shed light on the roles of the minor TBPs in global regulation.

## Materials and Methods

*Cell Growth.* Growth and harvesting of *M. acetivorans* C2A (DSM 800) in single cell morphology cultured on high-salt (HS) broth medium (48) was as previously described (35). Culturing was carried out in 160 mL anaerobic serum bottles containing 100 mL culture media. Bottles were sealed with a butyl rubber stopper secured with an Al crimp collar. For transcription profiling of methanol plus acetate diauxic growth, four independent cultures were prepared using *M. acetivorans* cells previously cultured on methanol (for >50 generations) inoculated into HS media containing 25 mM methanol and 100 mM acetate. Cells were harvested for RNA isolation at time points indicated in Figure 1. For transcription profiling of growth on either methanol or acetate exclusively, two replicate cultures were prepared using *M. acetivorans* cells previously grown on methanol (for >50 generations) inoculated into HS media containing 125 mM methanol and two replicate cultures previously grown acetate (for >50 generations) were inoculated into HS media containing 100 mM acetate. Cells were harvested for RNA isolation at mid-logarithmic phase ($A_{600}$ ~ 0.5).

*Acetate concentration determination.* The measurement of acetate concentration in the culture media was carried out using the acetate kinase hydroxamate assay (1, 33). Recombinant acetate kinase (Ack) from *Methanosarcina thermophila* was purified by Dr. Suharti in the Ferry research group. The assay was performed in buffer containing 145 mM Tris-Cl, pH = 7.4, 10 mM $MgCl_2$, 704 mM $NH_2OH$, pH = 7.4 (KOH) and 10 mM ATP. Aliquots of cell culture supernatant (5 µL) were added to 333 µL assay buffer pre-warmed at 37$^{o}$C, and 5 µL Ack (50 mg $mL^{-1}$) was added to start the reaction. Reactions

were incubated at 37°C for 30 min. Reactions were stopped by the addition of 333 µL 10% (w/v) TCA. 333 µL the colorimetric solution, $FeCl_3$ (in 2N HCl) was added to each reaction which were then incubated at 37°C for 30. Absorbances were measured at 540 nm. Acetate concentrations were determined by plotting absorbances against a standard curve generated using potassium acetate.

*RNA isolation.* For each RNA sample, 10 mL of cell culture was collected, chilled immediately on ice and centrifuged at 6000 rpm for 10 min to pellet the cells. Cell pellets were stored at -80°C until RNA isolation. RNA isolation was carried out essentially as described (39).

*DNA microarray analysis.* RNA samples were checked for purity and concentration using a NanoDrop spectrophotometer and RNA quality was assessed using an Agilent Bioanalyzer RNA 6000 Nano assay. RNA samples were labeled with the Message Amp II - Bacteria kit (Ambion Inc., Austin, TX) according to the manufacturer's instruction with the use of amino allyl UTP in place of biotin modified nucleotides. Briefly, 500 ng of total RNA was polyadenylated and subsequently reverse transcribed with T7oligo(dT)VN primer. Second strand cDNA synthesis was performed and the resulting dsDNA was used as a template for in vitro transcription. Amino allyl modified UTP was incorporated into the resulting cRNA. 20 µg of this modified aRNA was coupled with Cy3 or Cy5 using the CyDye Post Labeling Reactive Dye Pack (GE Healthcare, Buckinghamshire, England) according to the Amino Allyl Message Amp II kit instructions (Ambion, Austin, TX). Samples were hybridized to NimbleGen 4-plex arrays (Catalog number: A7240-00-01; Design Name: 080303 MacetC2A EXP X4). Two color hybridizations were performed and 2 µg of each sample was hybridized to an

array. Array hybridization, washing, scanning and data acquisition were performed according to the manufacturer's instruction (Roche NimbleGen Inc., Madison, WI ). All data analysis was carried out using the ArrayStar (v3) software package (DNA Star, Madison, WI). Robust Multichip Averaging (RMA) and quantile normalization (9, 26, 27) were applied to the entire data set which consisted of four biological replicates and two technical replicates (dye swap) for each growth phase. Statistical analyses were carried out on the normalized data using a moderated *t*-test with FDR multiple testing correction (Benjamini-Hochberg) to determine differential transcript abundance. Changes in transcript abundance were considered significant if they met the following criteria: 1) ≥2.5-fold change abundance; 2) *P*-values < 0.05; 3) $Log_2$ transcript abundance >10.5 in the condition with greater abundance. The *Z*-test with FDR multiple testing correction (Benjamini-Hochberg) was used to assess the statistical significance of gene sets with with correlations in pattern of expression.

## Acknowledgements

Thanks to Craig Praul and Haikun Zhang of the Penn State Genomics Core Facility for carrying out RNA labeling, hybridization and microarray scanning and all members of the Ferry and Murakami labs for helpful support and discussions. This work was funded by the Pew Scholar's Program in the Biomedical Sciences to KSM and by grants from the National Science Foundation and Department of Energy to JGF.

## References


1. **Aceti, D. J., and J. G. Ferry.** 1988. Purification and characterization of acetate kinase from acetate-grown Methanosarcina thermophila. Evidence for regulation of synthesis. J Biol Chem **263:**15444-8.
2. **Alber, B. E., and J. G. Ferry.** 1996. Characterization of heterologously produced carbonic anhydrase from Methanosarcina thermophila. J Bacteriol **178:**3270-4.
3. **Allen, M. A., F. M. Lauro, T. J. Williams, D. Burg, K. S. Siddiqui, D. De Francisci, K. W. Chong, O. Pilak, H. H. Chew, M. Z. De Maere, L. Ting, M. Katrib, C. Ng, K. R. Sowers, M. Y. Galperin, I. J. Anderson, N. Ivanova, E. Dalin, M. Martinez, A. Lapidus, L. Hauser, M. Land, T. Thomas, and R. Cavicchioli.** 2009. The genome sequence of the psychrophilic archaeon, Methanococcoides burtonii: the role of genome evolution in cold adaptation. Isme J **3:**1012-35.
4. **Anderson, K. L., E. E. Apolinario, S. R. MacAuley, and K. R. Sowers.** 2009. A 5' leader sequence regulates expression of methanosarcinal CO dehydrogenase/acetyl coenzyme A synthase. J Bacteriol **191:**7123-8.
5. **Apolinario, E. E., K. M. Jackson, and K. R. Sowers.** 2005. Development of a plasmid-mediated reporter system for in vivo monitoring of gene expression in the archaeon Methanosarcina acetivorans. Appl Environ Microbiol **71:**4914-8.
6. **Baresi, L., R. A. Mah, D. M. Ward, and I. R. Kaplan.** 1978. Methanogenesis from acetate: enrichment studies. Appl Environ Microbiol **36:**186-97.

7. **Baronofsky, J. J., W. J. Schreurs, and E. R. Kashket.** 1984. Uncoupling by Acetic Acid Limits Growth of and Acetogenesis by Clostridium thermoaceticum. Appl Environ Microbiol **48:**1134-1139.

8. **Beauclerk, A. A., H. Hummel, D. J. Holmes, A. Bock, and E. Cundliffe.** 1985. Studies of the GTPase domain of archaebacterial ribosomes. Eur J Biochem **151:**245-55.

9. **Bolstad, B. M., R. A. Irizarry, M. Astrand, and T. P. Speed.** 2003. A comparison of normalization methods for high density oligonucleotide array data based on variance and bias. Bioinformatics **19:**185-93.

10. **Bose, A., G. Kulkarni, and W. W. Metcalf.** 2009. Regulation of putative methyl-sulphide methyltransferases in Methanosarcina acetivorans C2A. Mol Microbiol **74:**227-38.

11. **Bose, A., and W. W. Metcalf.** 2008. Distinct regulators control the expression of methanol methyltransferase isozymes in Methanosarcina acetivorans C2A. Mol Microbiol **67:**649-61.

12. **Bose, A., M. A. Pritchett, M. Rother, and W. W. Metcalf.** 2006. Differential Regulation of the Three Methanol Methyltransferase Isozymes in Methanosarcina acetivorans C2A. J Bacteriol **188:**7274-83.

13. **Buan, N. R., and W. W. Metcalf.** 2009. Methanogenesis by Methanosarcina acetivorans involves two structurally and functionally distinct classes of heterodisulfide reductase. Mol Microbiol.

14. **Cellini, A., G. L. Scoarughi, P. Poggiali, I. Santino, R. Sessa, P. Donini, and C. Cimmino.** 2004. Stringent control in the archaeal genus Sulfolobus. Res Microbiol **155:**98-104.

15. **Chang, D. E., D. J. Smalley, and T. Conway.** 2002. Gene expression profiling of Escherichia coli growth transitions: an expanded stringent response model. Mol Microbiol **45:**289-306.

16. **Cimmino, C., G. L. Scoarughi, and P. Donini.** 1993. Stringency and relaxation among the halobacteria. J Bacteriol **175:**6659-62.

17. **Deppenmeier, U., A. Johann, T. Hartsch, R. Merkl, R. A. Schmitz, R. Martinez-Arias, A. Henne, A. Wiezer, S. Baumer, C. Jacobi, H. Bruggemann, T. Lienard, A. Christmann, M. Bomeke, S. Steckel, A. Bhattacharyya, A. Lykidis, R. Overbeek, H. P. Klenk, R. P. Gunsalus, H. J. Fritz, and G. Gottschalk.** 2002. The genome of Methanosarcina mazei: evidence for lateral gene transfer between bacteria and archaea. J Mol Microbiol Biotechnol **4:**453-61.

18. **Ding, Y. H., S. P. Zhang, J. F. Tomb, and J. G. Ferry.** 2002. Genomic and proteomic analyses reveal multiple homologs of genes encoding enzymes of the methanol:coenzyme M methyltransferase system that are differentially expressed in methanol- and acetate-grown Methanosarcina thermophila. FEMS Microbiol Lett **215:**127-32.

19. **Ebbighausen, H., B. Weil, and R. Krämer.** 1991. Carrier-mediated acetate uptake in *Corynebacterium glutamicum*. Archives of Microbiology **155:**505-510.

20. **Ferry, J. G.** 1992. Methane from acetate. J Bacteriol **174:**5489-95.

21. **Ferry, J. G., and K. A. Kastead.** 2007. Methanogenesis, p. 288-314. *In* R. Cavicchioli (ed.), Archaea: Molecular and Cellular Biology. ASM Press, Washington, DC.

22. **Galagan, J. E., C. Nusbaum, A. Roy, M. G. Endrizzi, P. Macdonald, W. FitzHugh, S. Calvo, R. Engels, S. Smirnov, D. Atnoor, A. Brown, N. Allen, J. Naylor, N. Stange-Thomann, K. DeArellano, R. Johnson, L. Linton, P. McEwan, K. McKernan, J. Talamas, A. Tirrell, W. Ye, A. Zimmer, R. D. Barber, I. Cann, D. E. Graham, D. A. Grahame, A. M. Guss, R. Hedderich, C. Ingram-Smith, H. C. Kuettner, J. A. Krzycki, J. A. Leigh, W. Li, J. Liu, B. Mukhopadhyay, J. N. Reeve, K. Smith, T. A. Springer, L. A. Umayam, O. White, R. H. White, E. Conway de Macario, J. G. Ferry, K. F. Jarrell, H. Jing, A. J. Macario, I. Paulsen, M. Pritchett, K. R. Sowers, R. V. Swanson, S. H. Zinder, E. Lander, W. W. Metcalf, and B. Birren.** 2002. The genome of M. acetivorans reveals extensive metabolic and physiological diversity. Genome Res **12:**532-42.

23. **Gerstmeir, R., V. F. Wendisch, S. Schnicke, H. Ruan, M. Farwick, D. Reinscheid, and B. J. Eikmanns.** 2003. Acetate metabolism and its regulation in Corynebacterium glutamicum. J Biotechnol **104:**99-122.

24. **Guss, A. M., G. Kulkarni, and W. W. Metcalf.** 2009. Differences in hydrogenase gene expression between Methanosarcina acetivorans and Methanosarcina barkeri. J Bacteriol **191:**2826-33.

25. **Hovey, R., S. Lentes, A. Ehrenreich, K. Salmon, K. Saba, G. Gottschalk, R. P. Gunsalus, and U. Deppenmeier.** 2005. DNA microarray analysis of

Methanosarcina mazei Go1 reveals adaptation to different methanogenic substrates. Mol Genet Genomics **273:**225-39.

26. **Irizarry, R. A., B. M. Bolstad, F. Collin, L. M. Cope, B. Hobbs, and T. P. Speed.** 2003. Summaries of Affymetrix GeneChip probe level data. Nucleic Acids Res **31:**e15.

27. **Irizarry, R. A., B. Hobbs, F. Collin, Y. D. Beazer-Barclay, K. J. Antonellis, U. Scherf, and T. P. Speed.** 2003. Exploration, normalization, and summaries of high density oligonucleotide array probe level data. Biostatistics **4:**249-64.

28. **Jarrell, K. F., and M. J. McBride.** 2008. The surprisingly diverse ways that prokaryotes move. Nat Rev Microbiol **6:**466-76.

29. **Kell, D. B., M. W. Peck, G. Rodger, and J. G. Morris.** 1981. On the permeability to weak acids and bases of the cytoplasmic membrane of Clostridium pasteurianum. Biochem Biophys Res Commun **99:**81-8.

30. **Krzycki, J. A., R. H. Wolkin, and J. G. Zeikus.** 1982. Comparison of unitrophic and mixotrophic substrate metabolism by acetate-adapted strain of Methanosarcina barkeri. J Bacteriol **149:**247-54.

31. **Kulkarni, G., D. M. Kridelbaugh, A. M. Guss, and W. W. Metcalf.** 2009. Hydrogen is a preferred intermediate in the energy-conserving electron transport chain of Methanosarcina barkeri. Proc Natl Acad Sci U S A **106:**15915-20.

32. **Kvint, K., L. Nachin, A. Diez, and T. Nystrom.** 2003. The bacterial universal stress protein: function and regulation. Curr Opin Microbiol **6:**140-5.

33. **Latimer, M. T., and J. G. Ferry.** 1993. Cloning, sequence analysis, and hyperexpression of the genes encoding phosphotransacetylase and acetate kinase from Methanosarcina thermophila. J Bacteriol **175:**6822-9.

34. **Lee, S. J., M. Surma, W. Hausner, M. Thomm, and W. Boos.** 2008. The role of TrmB and TrmB-like transcriptional regulators for sugar transport and metabolism in the hyperthermophilic archaeon Pyrococcus furiosus. Arch Microbiol **190:**247-56.

35. **Lessner, D. J., L. Li, Q. Li, T. Rejtar, V. P. Andreev, M. Reichlen, K. Hill, J. J. Moran, B. L. Karger, and J. G. Ferry.** 2006. An unconventional pathway for reduction of CO2 to methane in CO-grown Methanosarcina acetivorans revealed by proteomics. Proc Natl Acad Sci U S A **103:**17921-6.

36. **Li, L., Q. Li, L. Rohlin, U. Kim, K. Salmon, T. Rejtar, R. P. Gunsalus, B. L. Karger, and J. G. Ferry.** 2007. Quantitative proteomic and microarray analysis of the archaeon Methanosarcina acetivorans grown with acetate versus methanol. J Proteome Res **6:**759-71.

37. **Li, Q., L. Li, T. Rejtar, B. L. Karger, and J. G. Ferry.** 2005. Proteome of Methanosarcina acetivorans Part I: an expanded view of the biology of the cell. J Proteome Res **4:**112-28.

38. **Li, Q., L. Li, T. Rejtar, B. L. Karger, and J. G. Ferry.** 2005. Proteome of Methanosarcina acetivorans Part II: comparison of protein levels in acetate- and methanol-grown cells. J Proteome Res **4:**129-35.

39. **Li, Q., L. Li, T. Rejtar, D. J. Lessner, B. L. Karger, and J. G. Ferry.** 2006. Electron transport in the pathway of acetate conversion to methane in the marine archaeon Methanosarcina acetivorans. J Bacteriol **188:**702-10.

40. **Moran, J. J., C. H. House, J. M. Vrentas, and K. H. Freeman.** 2008. Methyl sulfide production by a novel carbon monoxide metabolism in Methanosarcina acetivorans. Appl Environ Microbiol **74:**540-2.

41. **Nelson, M. J., and J. G. Ferry.** 1984. Carbon monoxide-dependent methyl coenzyme M methylreductase in acetotrophic Methosarcina spp. J Bacteriol **160:**526-32.

42. **Oelgeschlager, E., and M. Rother.** 2009. In vivo role of three fused corrinoid/methyl transfer proteins in Methanosarcina acetivorans. Mol Microbiol **72:**1260-72.

43. **Paiva, S., F. Devaux, S. Barbosa, C. Jacq, and M. Casal.** 2004. Ady2p is essential for the acetate permease activity in the yeast Saccharomyces cerevisiae. Yeast **21:**201-10.

44. **Rohlin, L., and R. P. Gunsalus.** Carbon-dependent control of electron transfer and central carbon pathway genes for methane biosynthesis in the Archaean, Methanosarcina acetivorans strain C2A. BMC Microbiol **10:**62.

45. **Rother, M., E. Oelgeschlager, and W. M. Metcalf.** 2007. Genetic and proteomic analyses of CO utilization by Methanosarcina acetivorans. Arch Microbiol **188:**463-72.

46. **Smith, K. S., and C. Ingram-Smith.** 2007. Methanosaeta, the forgotten methanogen? Trends Microbiol.

47. **Smith, M. R., and R. A. Mah.** 1978. Growth and methanogenesis by Methanosarcina strain 227 on acetate and methanol. Appl Environ Microbiol **36:**870-9.

48. **Sowers, K. R., J. E. Boone, and R. P. Gunsalus.** 1993. Disaggregation of Methanosarcina spp. and Growth as Single Cells at Elevated Osmolarity. Appl Environ Microbiol **59:**3832-3839.

49. **Sowers, K. R., T. T. Thai, and R. P. Gunsalus.** 1993. Transcriptional regulation of the carbon monoxide dehydrogenase gene (cdhA) in Methanosarcina thermophila. J Biol Chem **268:**23172-8.

50. **Terlesky, K. C., M. J. Nelson, and J. G. Ferry.** 1986. Isolation of an enzyme complex with carbon monoxide dehydrogenase activity containing corrinoid and nickel from acetate-grown Methanosarcina thermophila. J Bacteriol **168:**1053-8.

51. **Thauer, R. K., A. K. Kaster, H. Seedorf, W. Buckel, and R. Hedderich.** 2008. Methanogenic archaea: ecologically relevant differences in energy conservation. Nat Rev Microbiol **6:**579-91.

52. **Tzschoppe, K., A. Augstein, R. Bauer, S. D. Kohlwein, and G. Barth.** 1999. trans-dominant mutations in the GPR1 gene cause high sensitivity to acetic acid and ethanol in the yeast Yarrowia lipolytica. Yeast **15:**1645-56.

53. **Veit, K., C. Ehlers, A. Ehrenreich, K. Salmon, R. Hovey, R. P. Gunsalus, U. Deppenmeier, and R. A. Schmitz.** 2006. Global transcriptional analysis of Methanosarcina mazei strain Go1 under different nitrogen availabilities. Mol Genet Genomics.

54. **Welander, P. V., and W. W. Metcalf.** 2005. Loss of the mtr operon in Methanosarcina blocks growth on methanol, but not methanogenesis, and reveals an unknown methanogenic pathway. Proc Natl Acad Sci U S A **102:**10664-9.

55. **Wilkinson, S. P., and A. Grove.** 2006. Ligand-responsive transcriptional regulation by members of the MarR family of winged helix proteins. Curr Issues Mol Biol **8:**51-62.

56. **Zhang, W., D. E. Culley, L. Nie, and F. J. Brockman.** 2006. DNA microarray analysis of anaerobic Methanosarcina barkeri reveals responses to heat shock and air exposure. J Ind Microbiol Biotechnol **33:**784-90.

57. **Zimmerman, S. A.** 2007. Understanding the Biochemistry and Physiology of Gamma Carbonic Anhydrases in Methanosarcina Thermophila. The Pennsylvania State University, University Park, PA.

58. **Zinder, S. H.** 1993. Physiological Ecology of Methanogens, p. 128-206. *In* J. G. Ferry (ed.), Methanogenesis: Ecology, Physiology, Biochemistry and Genetics, vol. I. Chapman and Hall, New York, NY.

59. **Zinder, S. H., and A. F. Elias.** 1985. Growth substrate effects on acetate and methanol catabolism in Methanosarcina sp. strain TM-1. J Bacteriol **163:**317-23.

# Chapter 5

# Identification of MA3302, a putative regulator of acetate metabolism in *Methanosarcina acetivorans*


## Summary

A complete understanding of transcriptional regulation in *M. acetivorans* requires an understanding of how its eukaryal-like transcriptional machinery interacts with bacterial-like transcription factors. Thus, it is of enormous importance to first identify the individual transcription factors regulating particular cellular processes. MA3302, a putative transcription factor homologous TrmB-family of transcription factors was previously shown and corroborated by this analysis to be up-regulated during growth on acetate suggesting a role regulating acetate metabolism. Orthologs with greater than 97% identity to MA3302 are found in *Methanosarcina* species consistent with a conserved role in other acetate-utilizing methanogens. Furthermore, a deletion mutant strain for MA3302 exhibited severely impaired growth with acetate suggesting an *in vivo* role on this substrate. Three additional less similar homologs of MA3302 found in the *M. acetivorans* genome showed elevated transcript or protein during growth on methanol suggesting diverse roles for this family of proteins in regulating various metabolic

pathways. Future work will attempt to identify target genes for regulation by MA3302 and to characterize the biochemical properties of the MA3302 protein.

## Introduction

The ability of an organism to adapt to changing environmental conditions is key to its survival in a competitive environment. Unlike the majority of the methanogenic archaea, members of the *Methanosarcina* genus are unique in possessing metabolic diversity with regard to methanogenesis (12, 39). Furthermore, it has been demonstrated that the various methanogenic pathways utilized by *Methanosarcina* species are subject to tight regulation in response to growth substrate (1, 8, 11, 15, 18, 23-25, 35, 36), and it was discovered in chapter 3 three that the ability of *M. acetivorans* to adapt from energetically rich methylotrophic substrates to the energetically poor substrate, acetate is compromised when either of the minor TBP orthologs, *tbp2* or *tbp3* is deleted consistent with perturbations in the global regulatory network for the acetate metabolic pathway. Doubtless, this acetate metabolic regulatory network contains numerous additional gene-specific transcription factors yet to be characterized. Therefore, a deeper understanding of this acetate metabolic regulatory network will require the identification and characterization of these unknown transcription factors.

One particularly interesting aspect pertaining to transcription in the *Archaea* is the mosaic of bacterial-like and eukaryal-like components comprising the basic transcriptional machinery. The archaeal RNAP and the GTFs, TBP and TFB are each

orthologous to eukaryal proteins whereas most known gene specific transcription factors are orthologous to bacterial proteins (4, 29). Thus, it is of great interest to investigate how these eukaryal-like and bacterial-like proteins interact in the context of an archaeal cell.

In addition to having three TBP homologs, the *M. acetivorans* genome is estimated to encode approximately 160 transcriptional regulatory proteins (13, 29). However, barring a few notable exceptions (6, 7, 38), the roles of these putative regulatory proteins remain elusive. In the transcription profiling of *M. acetivorans* diauxic growth with methanol and acetate described in chapter 4, many of these putative transcription factors exhibited growth and/or substrate-dependent expression patterns consistent with functional involvement in these processes. This chapter details the initial investigation into the physiological role of one such putative transcription factor, MA3302 and its possible role in regulating acetate metabolism.

## Results

### Analysis of MA3302 gene expression

Transcriptional profiling of *M. acetivorans* diauxic growth with methanol and acetate described in chapter 4 identified elevated transcript abundance for MA3302 following the methanol utilization phase of growth. Highly elevated transcript abundance of MA3302 was confirmed using qRT-PCR at mid-log phase during growth on acetate

**Table 5-1. Relative transcript abundance for MA3302 during growth on acetate, methanol or TMA.**

| Fold increase transcript abundance on acetate | |
|---|---|
| ***versus* methanol** | ***versus* TMA** |
| 11.1 ± 1.4 [a] | 19.9 ± 2.4 |

[a] Values represent the average and standard deviation of triplicate measurements. Relative transcript abundances were calculated using the $\Delta\Delta C_t$ method with the 16s rRNA gene used as an invariant control. The $\Delta C_t$ values for acetate cells were used as the calibrator.

alone *versus* methanol alone or TMA alone (Table 5-1). These observations are consistent with previous proteomics analyses which identified peptides specific to MA3302 with elevated abundance in acetate- *versus* methanol- or CO-grown *M. acetivorans* (22, 25) and transcriptional profiling of the related species, *M. mazei* in which a highly conserved ortholog of MA3302, MM0138 exhibited elevated transcript abundance in acetate- *versus* methanol-grown cells (15). The expression pattern of MA3302 and MM0138 was largely overlooked in these reports due to original annotations as hypothetical proteins. However, sequence analysis revealed that the MA3302 gene product contains a conserved domain for the COG4738 family of predicted transcriptional regulators (Fig. 5-1). Other members of this family have been annotated as TrmB (*Thermococcus* regulator of maltose binding) transcription factors which have been shown to regulate the metabolism of various sugars in members of the *Archaea* domain (17, 19-21, 32). Sequence analysis of MA3302 reveals homology to the N-terminal DNA-binding domain of archaeal TrmB proteins. Both MA3302 and TrmB have a similar secondary structure consisting of 4 α-helices and 2 β-sheets (Fig. 5-1). However, MA3302 lacks the C-terminal ligand domain for TrmB consistent with a

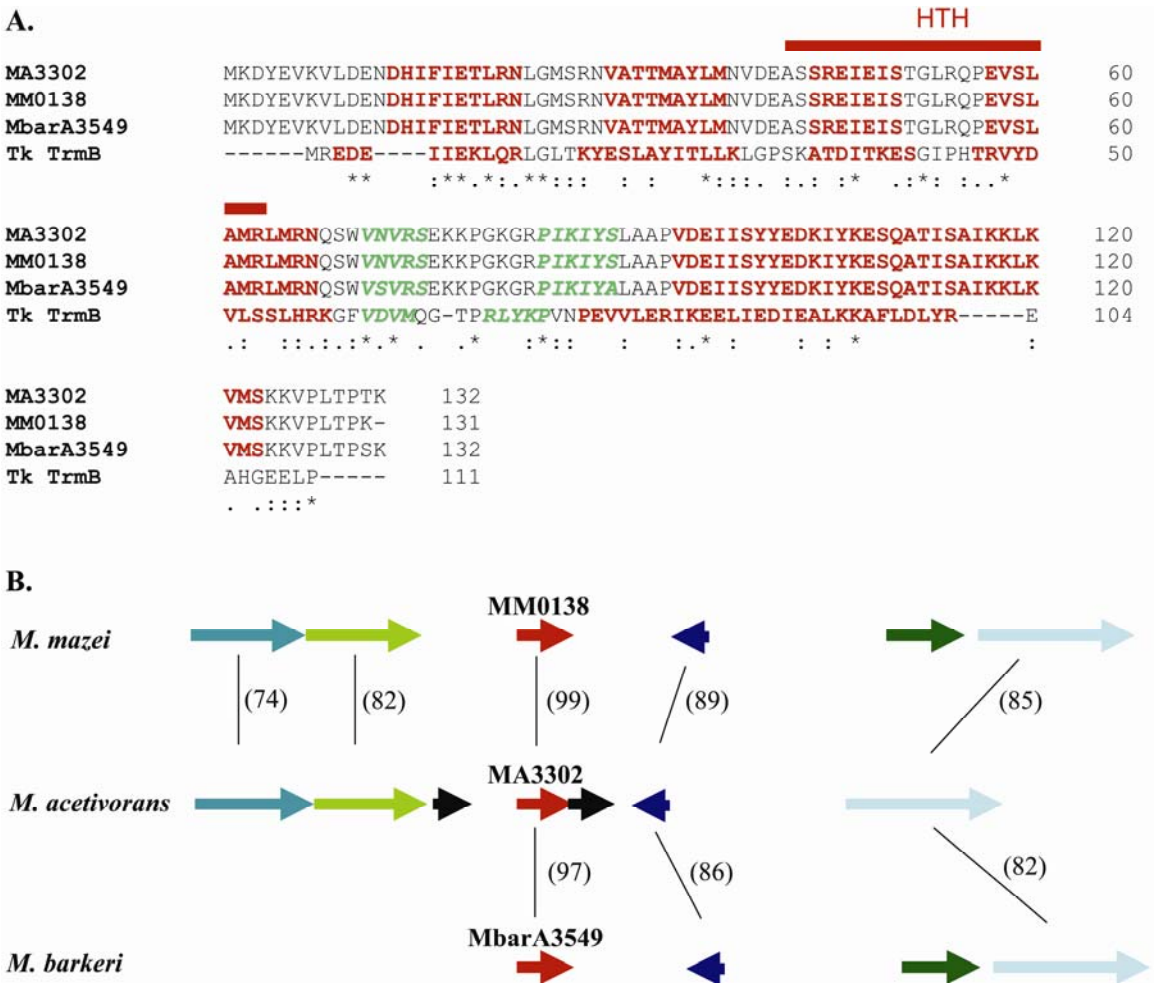


**Figure 5-1. MA3302 sequence alignment and genomic arrangement.** (A) MA3302 plus *M. mazei* and *M. barkeri* orthologs aligned against the N-terminal DNA-binding domain of *Thermococcus kodakaraensis* TrmB. Alignments were performed with ClustalW. The first 7 and first 21 residues from MA3302 and MM0138 respectively which likely misannotated in the original genome sequence have been omitted from the alignment. Conserved residues are denoted with asterisks. Similar residues are denoted with dots. Residues forming predicted α-helices and β-sheets depicted in red and green with italics respectively. Secondary structure prediction was performed using Jpred 3 (10). The residues forming the putative helix turn helix (HTH) motif from the *T. kodakaraensis* TrmB are denoted with a solid red line. (B) Comparison of the *M. acetivorans* MA3302 gene cluster (MA3305-3299; left to right) with the *M. mazei* (MM0140-0135) and *M. barkeri* (MbarA3549-3546) gene clusters. Genes and direction of transcription are denoted with arrows. Orthologous genes are depicted in the same color. Genes colored black have no orthologs. The numbers in parentheses are percent identities between the *M. mazei* and *M. barkeri* proteins with their *M. acetivorans* orthologs.

functional divergence from the canonical TrmB. Together, these results suggest a role for MA3302 in the regulation of *M. acetivorans* transcription during growth on acetate.

Orthologs of MA3302 in *M. mazei* (MM0138) and *M. barkeri* (MbarA3549) have greater than 97% identity to the putative MA3302 protein and similar gene arrangement suggesting a conserved function for these proteins in all three acetate-utilizing species (Fig. 5-1A). The nucleotide sequence upstream of these genes is also highly conserved including the putative TATA box and BRE signatures upstream the TSS identified for MM0138 (Fig. 5-2) (16) suggesting similar expression for the three genes. MA3302 and MM0138 have annotations for 7 and 21 additional amino acids at their respective N-termini which are not conserved in MbarA3549. These additional N-terminal extensions are most likely the result of genomic misannotations based on the following: 1) the sequence conservation of these N-terminal extensions is poor in relation to the rest of the protein; 2) both annotated orfs initiate translation from a TTG the start codon which is utilized infrequently in *Methanosarcina* species (37); 3) the ATG annotated for MbarA3549 is conserved in MA3302 and MM0138 as is the sequence upstream sequence corresponding to a putative ribosome binding site (Fig. 5-2); and 4) no sequences resembling a putative ribosome binding are present upstream of the annotated TTG start codons.

In addition to MbarA3549, *M. barkeri* has a second homolog of MA3302, MbarA3027 which encodes a protein with 88% sequence identity to MA3302 consistent with a possible conserved role for this gene as well. However, unlike MbarA3549, the promoter region for MbarA3027 is dissimilar to that for MA3302 consistent with a possible divergent expression pattern.


**Figure 5-2. Promoter alignment for MA3302 with *M. mazei* and *M. barkeri* orthologs.** Alignments were performed using ClustalW. Conserved bases are denoted with asterisks. The TSS identified for the *M. mazei* gene, MM0138 is denoted with a hooked arrow above the corresponding base. The putative start codon for the corresponding proteins is denoted with a boxed arrow. Annotated TTG start codons for MA3302 and MM0138 are also denoted with boxed arrows. The putative TATA-boxes, BREs and ribosome binding sites are boxed.

Three less well conserved homologs of MA3302 are present in the *M. acetivorans* genome, MA1671, MA3129 and MA3130 each of which is also conserved in *M. mazei* and *M. barkeri*. Interestingly, MA1671 and MA3130 each exhibited significantly elevated transcript abundance in the mid methanol *versus* the mid acetate phase of diauxic growth with methanol and acetate (Table 4-1) and peptides specific to MA3129 were found in elevated abundance in methanol- *versus* CO- or acetate-grown *M. acetivorans* (22) suggesting roles for these three proteins in the regulation of methanol metabolism.

**Construction and characterization of MA3302 deletion mutant strain**

To investigate its physiological role, MA3302 was deleted in the *M. acetivorans* WWM75 strain (14) by homologous recombination-mediated gene replacement and selection for puromycin resistance during growth on TMA as outlined in Chapter 3. Strain WWM75 (14) and the plasmid shuttle vector pJK301 (27) were used to enable future removal of the resistance markers by the previous described markerless exchange technique (31) and to enable site-specific integration by the ΦC31 integrase at an inserted attB locus (14). Potential mutants were screened for $Pur^R$ and $8ADP^S$, and mutant genotypes were confirmed by PCR analysis of the mutant chromosomes and sequencing of positive PCR reactions (Fig. 5-3). These results revealed that MA3302 is dispensable for growth on TMA.

For the mutant strains described in the preceding chapters, the more time consuming Southern blot analysis had been used as the primary means of genotype verification due to difficulty in amplifying the *pac* cassettes by PCR either from genomic DNA or from a plasmid template (data not shown). Use of the highly sensitive FailSafe PCR System (Epicentre, Madison, WI) designed to amply difficult templates alleviated this problem.

To identify growth substrate-dependent phenotypes associated with the deletion of MA3302, growth parameters were compared for ΔMA3302 *versus* its parental strain, WWM75 on cells cultured with 125 mM methanol, 50 mM TMA or 100 mM acetate (Fig. 5-4, Table 5-2). Growth of both strains was indistinguishable with methanol or TMA (Fig. 5-4, Table 5-2) suggesting minimal involvement for MA3302 in the

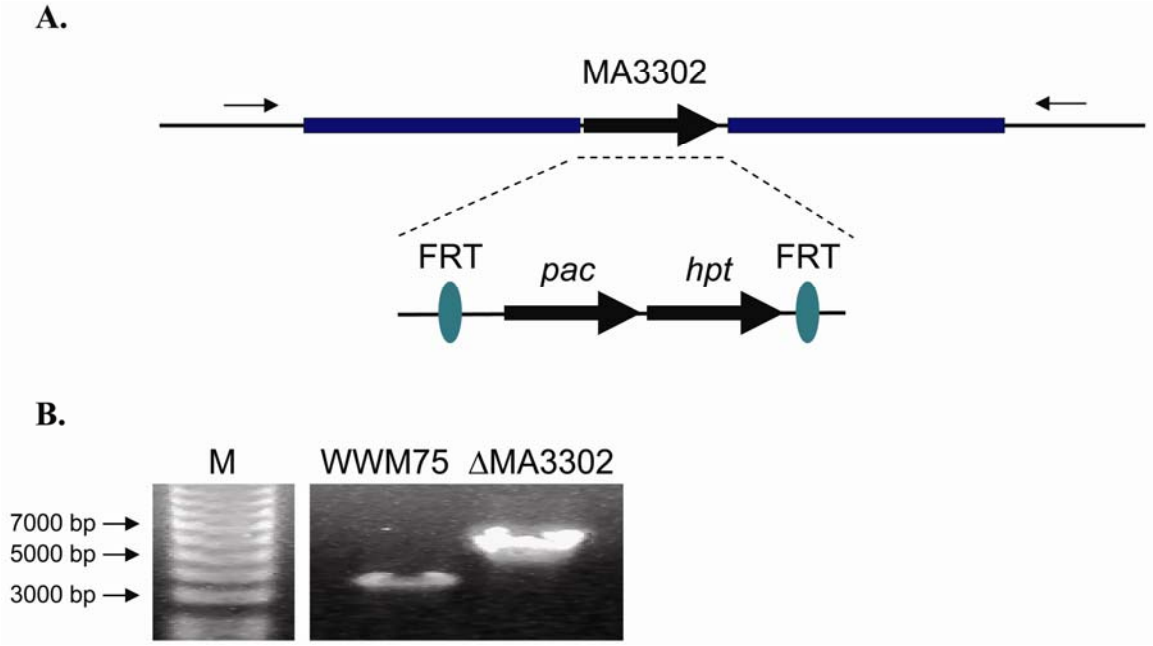


**Figure 5-3: Construction of a *M. acetivorans* ΔMA3302 deletion mutant strain.** (A) Depicts the MA3302 positioning on the *M. acetivorans* WWM75 chromosome. Large arrows denote genes and direction of transcription. Green oval denote Flp recombinase recognition targets. The broken line depicts the genomic region replaced by the *pac-hpt* cassette in the ΔMA3302 strain. Blue boxes denote genomic regions cloned into the knockout shuttle vector for homologous recombination. Small arrows denote primers used in PCR screening if potential mutants. (B) The genomic structures of ΔMA3302 was verified by PCR analysis using the primers shown in panel A and genomic DNA from WWM75 or ΔMA3302 *M. acetivorans* strains. The molecular weight marker is shown in lane M with band sizes indicated on the left.

methylotrophic pathway. However, significantly reduced growth was observed for the ΔMA3302 strain *versus* WWM75 cultured with acetate suggesting MA3302 is required for wild-type growth on this substrate (Fig. 5-4, Table 5-2).

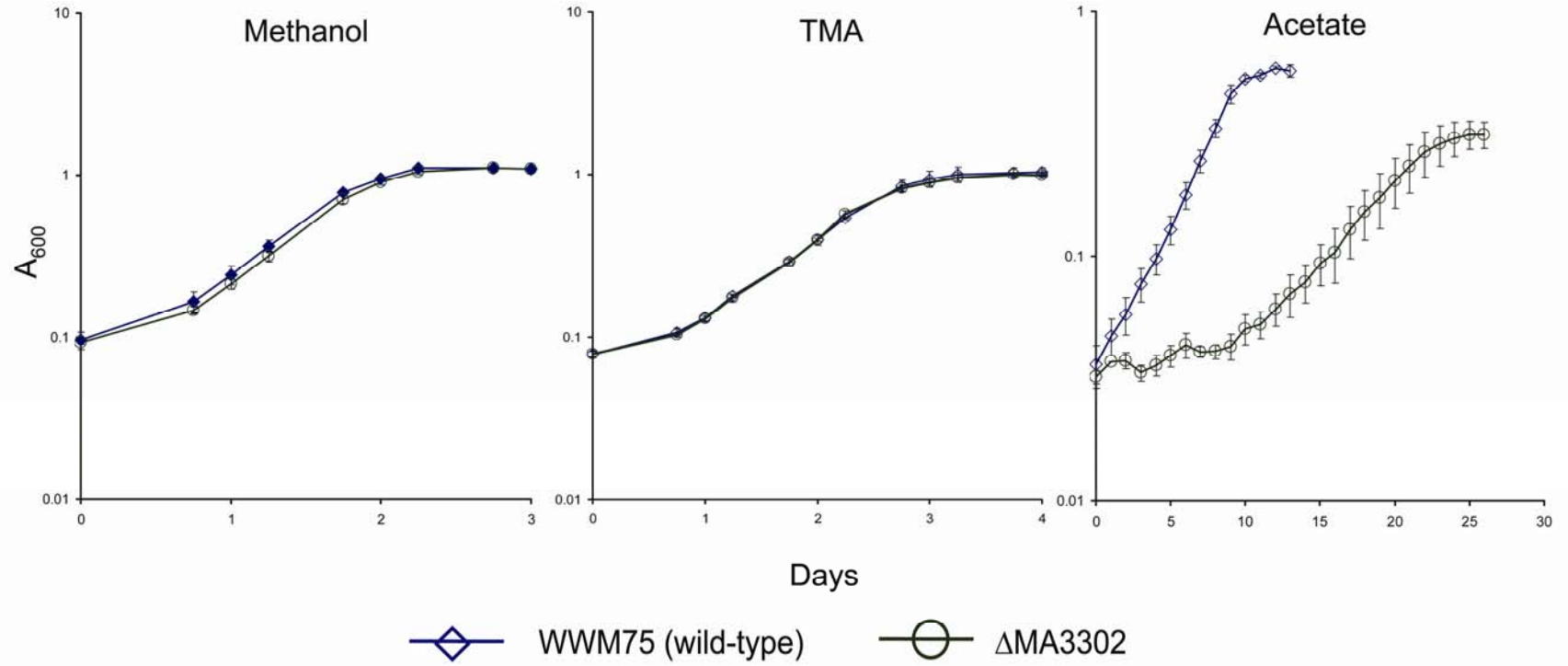


**Figure 5-4. Growth of WWM75 and ΔMA3302 *M. acetivorans* strains cultured on methanol, TMA or acetate.** Values for methanol and TMA are the average and standard deviation of triplicate cultures. Values for acetate are the average and standard deviation of five replicate cultures.

**Table 5-2. Growth parameters of WWM75 and ΔMA3302 *M. acetivorans* strains cultured with methanol, TMA and acetate [a].**

| Substrate | WWM75 | | | ΔMA3302 | | |
|---|---|---|---|---|---|---|
| | Doubling time (hours) | Maximum $A_{600}$ | Lag [d] (days) | Doubling time (hours) | Maximum $A_{600}$ | Lag (days) |
| **Methanol [b]** | 10.6 ± 0.8 | 1.11 ± 0.01 | 1.48 ± 0.03 | 10.4 ± 0.2 | 1.11 ± 0.02 | 1.56 ± 0.03 |
| **TMA [c]** | 14.9 ± 0.8 | 1.04 ± 0.08 | 2.21 ± 0.07 | 14.1 ± 0.4 | 1.00 ± 0.02 | 2.16 ± 0.05 |
| **Acetate [b]** | 51.8 ± 3.5 | 0.592 ± 0.012 | 7.59 ± 0.26 | 99.0 ± 6.8 | 0.328 ± 0.032 | 18.8 ± 1.6 |

[a] Values for methanol and TMA are the average and standard deviation of triplicate cultures. Values for acetate are the average and standard deviation of five replicate cultures.

[b] Strains were cultured on these substrates for ≥ 30 generations prior to measurement of growth parameters.

[c] Mutant strain was constructed in cells cultured on TMA and was fully adapted to this substrate.

[d] Time required to reach one half maximum $A_{600}$ value.

## Discussion

To date, little information pertaining to the factors involved in the transcriptional regulation of methanogenesis genes is known. The work presented here has identified and provided a preliminary *in vivo* characterization of MA3302, the first transcriptional regulatory protein implicated in the acetate pathway of methanogenesis.

The results presented here clearly suggest a role in acetate metabolism. However, a deeper understanding of MA3302 function will require identification the genes that are regulated by MA3302. It is plausible that MA3302 is required to activate the expression of genes involved in the conversion of acetate to methane. Candidate genes include the two *cdh/acs* operons, MA1011-1016 and MA3860-3865 (35) encoding for the CO dehydrogenase/acetyl-CoA synthase enzyme complexes, the *ack/pta* operon, MA3606-3607 (33) encoding for the enzymes acetate kinase and phosphotransactylase. In addition to having essential roles in acetate metabolism, these genes exhibited a very similar expression pattern to MA3302 during diauxic growth with methanol and acetate as described in chapter 4. Like these genes, MA3302 exhibited a sharp increase in transcript abundance in the late methanol phase followed by a decrease in the transition phase and followed again by increase in the mid acetate phase. However, the ΔMA3302 strain was still able to growth on acetate suggesting that MA3302 cannot be the sole transcription regulator in driving the expression of *ack/pta* or *cdh/acs*. Another possibility is the negative regulation of genes involved in the oxidative branch of the methylotrophic pathway such as the *fpo* operon (MA1494-1507) encoding the $F_{420}H_2$ dehydrogenase, the *fmd* operon (MA0305-0308) encoding formylmethanofuran dehydrogenase, *ftr*

(MA0010) encoding formylmethanofuran-tetrahydromethanopterin N-formyltransferase, *mch* (MA1710) encoding methenyltetrahydromethanopterin cyclohydrolase, *mtd* (MA4430) encoding methylenetetrahydromethanopterin dehydrogenase, and *mer* (MA3733) encoding $F_{420}$-dependent $N^5$,$N^{10}$-methylene-tetrahydromethanopterin reductase. Excess production of these unnecessary enzymes could compromise the cell's capacity for efficient growth on acetate.

The mechanics of putative MA3302-mediated gene regulation are not apparent from this analysis. Homology with TrmB proteins might suggest a similar mode of action of binding DNA in the absence of a ligand (maltose in the case of TrmB; possibly acetate, methanol or TMA in the case of MA3302) but not in the presence of that ligand. However, the absence of the TrmB C-terminal ligand-binding domain in MA3302 makes it unclear how MA3302 could function in this fashion. Perhaps a second protein which interacts with MA3302 is required for ligand binding.

The strict conservation of MA3302 orthologs in *M. acetivorans, M. mazei* and *M. barkeri* at the level of gene arrangement, amino acid sequence and in promoter architecture suggest the conserved function of MA3302 across these three acetotrophic species. MA3302 is far less conserved in the other acetotrophic methanogen, *Methanosaeta thermophila*. Four MA3302 homologs are present in the *M. thermophila* genome, but they have much less sequence similarity with MA3302 (43-53% identity) than the *M. mazei* or *M. barkeri* proteins, and they have dissimilar genomic arrangement and putative promoter architecture consistent with divergent function. This may reflect the fact that unlike the metabolically versatile *Methanosarcina* species, *M. thermophila* is an obligate acetotroph. In *M. thermophila,* genes involved in acetoclastic

methanogenesis are essential for growth and are presumably expressed constitutively. Therefore, it is probable that MA3302 homologs in *M. thermophila* regulate functions other than acetoclastic methanogenesis.

It is also unlikely that the three additional *M. acetivorans* MA3302 homologs, MA1671, MA3129 and MA3130 function in acetoclastic methanogenesis. The expression patterns of these genes suggest a functional role during growth on methanol. Interestingly, the MA3129 and MA3130 genes are located adjacent to and transcribed divergently from the operon encoding the ABC-type heterodisulfide reductase isozyme 1 (*hdrA1B1C1*) which has been previously implicated in methylotrophic methanogenesis (9). This placement could be indicative of roles for MA3129 and/or MA3130 in the regulation of *hdrA1B1C1* although this is yet to be tested experimentally. More importantly, the potential involvement of MA1671, MA3129 and MA3130 in methylotrophic methanogenesis is consistent with a broader role for this protein family in the regulation of diverse metabolic pathways.

Indeed, the COG4738 family of proteins is widespread in the kingdom, *Euryarchaeota* (Fig. 5-5) consistent with diverse functions in gene regulation across these species. No members of this protein family have been characterized. Therefore, the characterization of MA3302 could have broad implications for the understanding transcription regulation across this kingdom.

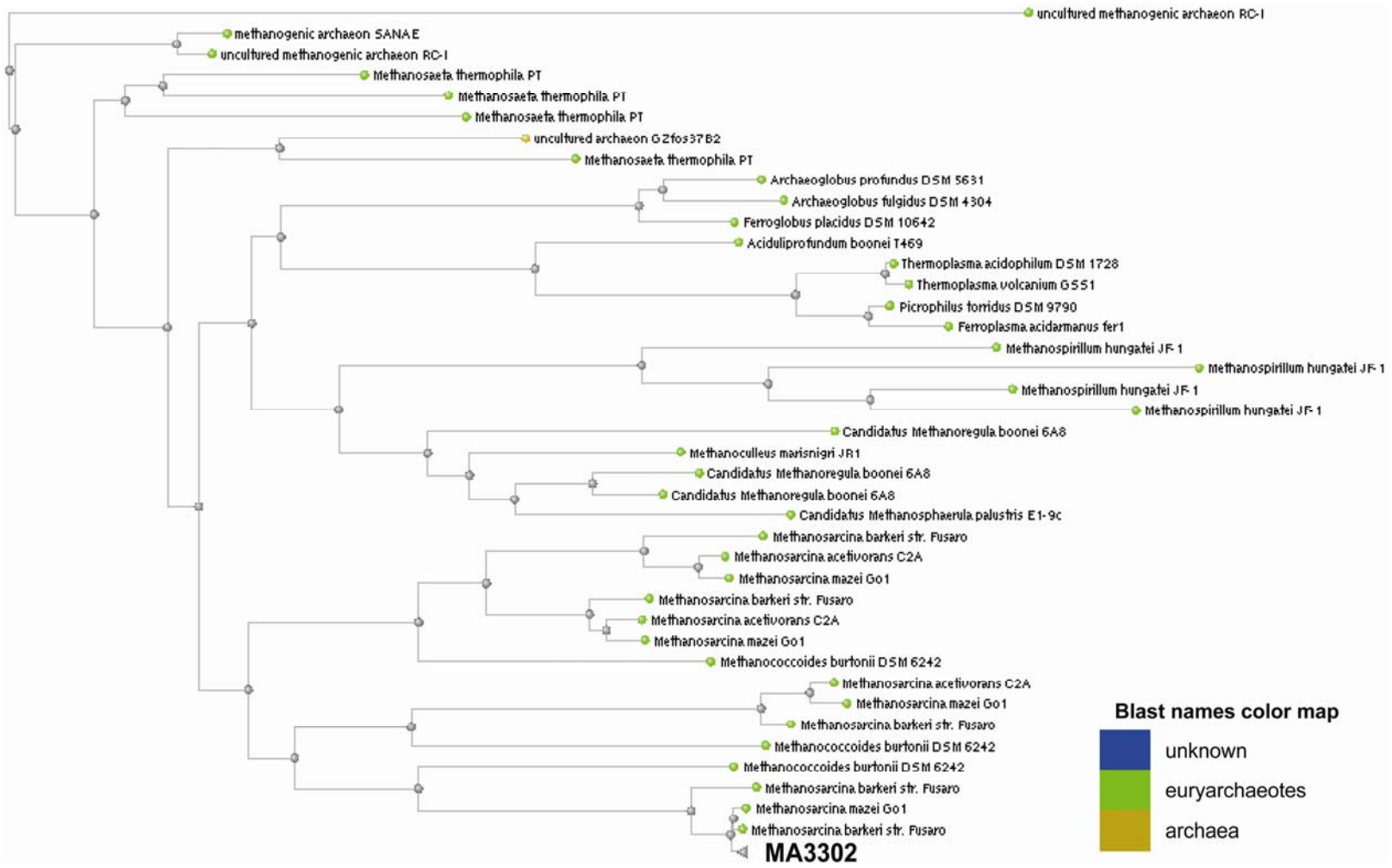


**Figure 5-5. Phylogenetic tree of MA3302 and COG4738 family members.** Tree was generated using the COBALT multiple alignment tool on the NCBI BLAST server (http://blast.ncbi.nlm.nih.gov/Blast.cgi) (28). Sequences for alignment were retrieved using blastp algorithm with MA3302 against the non-redundant database (2, 3).

## Future Directions

Both the gene expression pattern and phenotypic analysis of the ΔMA3302 strain provide compelling evidence for a functional role of the MA3302 protein in regulating acetate metabolism. Future studies will be aimed at identifying genes that are regulated by MA3302. Target genes will first be identified through comparative transcriptional analyses of the WWM75 and ΔMA3302 *M. acetivorans* cultured with acetate and global analyses such DNA microarrays or RNA-seq technologies (16), and verification of targets genes can be carried out using qRT-PCR.

Additionally, the protein encoded by MA3302 will be over-produced and purified from *E. coli,* and the DNA-binding capacity of the purified protein will be tested by electrophoretic mobility shift assay (EMSA). The purified protein can also be used for the generation of polyclonal antisera directed against MA3302 to carry out the ChiP assay described below. Lastly, the purified MA3302 protein may be an interesting candidate for 3-D structural determination by X-ray crystallography since no structural information is available for members of the COG4738 family. Structural information may prove valuable in assessing the mode of action for MA3302 since the oligomeric state of many transcription factors is known to influence function.

If the MA3302 protein is indeed found to be a true DNA-binding protein implicated in the regulation of genes involved in acetate metabolism, the next appropriate step will be to map its distribution across the chromosome using ChIP coupled with microarray analysis or direct sequencing. Cross-linked MA3302-DNA complexes will be precipitated using either antisera directed against the protein MA3302 or by expressing a His-tagged MA3302 and using antibodies directed against the His-tag.

## Materials and Methods

*Cell Growth.* Growth and harvesting of *M. acetivorans* C2A (DSM 800) in single cell morphology (34) cultured on high-salt (HS) broth medium with acetate, methanol and TMA was as previously described (22). Growth was monitored by measuring the optical density at 600 nm.

*RNA Isolation.* All *M. acetivorans* RNA samples were isolated from using an RNeasy Total RNA Mini kit (QIAGEN). Purified RNA was treated twice with RNase-free DNase I (QIAGEN) and once with RQ1 DNase (Promega) to remove contaminating DNA.

*Taqman quantitative RT-PCR. Taq*man assays were performed as described (22, 30) using total RNA isolated from at mid-exponential phase ($A_{600}$ ~ 0.6-0.7, 0.4-0.5 or 0.6-0.7 for methanol-, acetate- or TMA-grown cells respectively). Primer and probe sequences are listed in Table C-1.

*Construction of MA3302 deletion mutant strain*. Liposome-mediated transformation and homologous recombination-mediated gene replacement were used as described (5, 26) to generate *M. acetivorans* ΔMA3302*::pac-hpt* and (hereafter designated ΔMA3302). All mutant strains were generated in a *M. acetivorans* WWM75 background. Cells were transformed with 2 μg pMR80 (Table A?) linearized by restriction digestion, and transformants were selected on HS agar media with 0.8% (w/v) agar, with 50 mM TMA and 2 μg $mL^{-1}$ puromycin (Sigma, St Louis, MO) added from sterile, anaerobic 100X stock solution. 8-aza-2,6-diaminopurine (8ADP) (Sigma, St

Louis, MO) sensitivity was tested in media containing 20 μg $mL^{-1}$ 8ADP added from sterile, anaerobic 200X stock solution.

## Acknowledgements

I thank W.W. Metcalf (University of Illinois, Urbana, IL) for the donation of all plasmids and strains used for the genetic manipulation of *M. acetivorans* and D. Grove (Penn State Genomics Core Facility – University Park, PA) for optimization of *Taq*man assays. This work was funded by the Pew Scholar's Program in the Biomedical Sciences to KSM and by grants from the National Science Foundation and Department of Energy to JGF.

## References

1. **Aceti, D. J., and J. G. Ferry.** 1988. Purification and characterization of acetate kinase from acetate-grown Methanosarcina thermophila. Evidence for regulation of synthesis. J Biol Chem **263:**15444-8.
2. **Altschul, S. F., T. L. Madden, A. A. Schaffer, J. Zhang, Z. Zhang, W. Miller, and D. J. Lipman.** 1997. Gapped BLAST and PSI-BLAST: a new generation of protein database search programs. Nucleic Acids Res **25:**3389-402.

3. **Altschul, S. F., J. C. Wootton, E. M. Gertz, R. Agarwala, A. Morgulis, A. A. Schaffer, and Y. K. Yu.** 2005. Protein database searches using compositionally adjusted substitution matrices. Febs J **272:**5101-9.

4. **Bell, S. D.** 2005. Archaeal transcriptional regulation--variation on a bacterial theme? Trends Microbiol **13:**262-5.

5. **Boccazzi, P., J. K. Zhang, and W. W. Metcalf.** 2000. Generation of dominant selectable markers for resistance to pseudomonic acid by cloning and mutagenesis of the ileS gene from the archaeon Methanosarcina barkeri fusaro. J Bacteriol **182:**2611-8.

6. **Bose, A., G. Kulkarni, and W. W. Metcalf.** 2009. Regulation of putative methyl-sulphide methyltransferases in Methanosarcina acetivorans C2A. Mol Microbiol **74:**227-38.

7. **Bose, A., and W. W. Metcalf.** 2008. Distinct regulators control the expression of methanol methyltransferase isozymes in Methanosarcina acetivorans C2A. Mol Microbiol **67:**649-61.

8. **Bose, A., M. A. Pritchett, M. Rother, and W. W. Metcalf.** 2006. Differential Regulation of the Three Methanol Methyltransferase Isozymes in Methanosarcina acetivorans C2A. J Bacteriol **188:**7274-83.

9. **Buan, N. R., and W. W. Metcalf.** 2009. Methanogenesis by Methanosarcina acetivorans involves two structurally and functionally distinct classes of heterodisulfide reductase. Mol Microbiol.

10. **Cuff, J. A., and G. J. Barton.** 2000. Application of multiple sequence alignment profiles to improve protein secondary structure prediction. Proteins **40:**502-11.

11. **Ding, Y. H., S. P. Zhang, J. F. Tomb, and J. G. Ferry.** 2002. Genomic and proteomic analyses reveal multiple homologs of genes encoding enzymes of the methanol:coenzyme M methyltransferase system that are differentially expressed in methanol- and acetate-grown Methanosarcina thermophila. FEMS Microbiol Lett **215:**127-32.

12. **Ferry, J. G., and K. A. Kastead.** 2007. Methanogenesis, p. 288-314. *In* R. Cavicchioli (ed.), Archaea: Molecular and Cellular Biology. ASM Press, Washington, DC.

13. **Galagan, J. E., C. Nusbaum, A. Roy, M. G. Endrizzi, P. Macdonald, W. FitzHugh, S. Calvo, R. Engels, S. Smirnov, D. Atnoor, A. Brown, N. Allen, J. Naylor, N. Stange-Thomann, K. DeArellano, R. Johnson, L. Linton, P. McEwan, K. McKernan, J. Talamas, A. Tirrell, W. Ye, A. Zimmer, R. D. Barber, I. Cann, D. E. Graham, D. A. Grahame, A. M. Guss, R. Hedderich, C. Ingram-Smith, H. C. Kuettner, J. A. Krzycki, J. A. Leigh, W. Li, J. Liu, B. Mukhopadhyay, J. N. Reeve, K. Smith, T. A. Springer, L. A. Umayam, O. White, R. H. White, E. Conway de Macario, J. G. Ferry, K. F. Jarrell, H. Jing, A. J. Macario, I. Paulsen, M. Pritchett, K. R. Sowers, R. V. Swanson, S. H. Zinder, E. Lander, W. W. Metcalf, and B. Birren.** 2002. The genome of M. acetivorans reveals extensive metabolic and physiological diversity. Genome Res **12:**532-42.

14. **Guss, A. M., M. Rother, J. K. Zhang, G. Kulkarni, and W. W. Metcalf.** 2008. New methods for tightly regulated gene expression and highly efficient

chromosomal integration of cloned genes for Methanosarcina species. Archaea **2:**193-203.

15. **Hovey, R., S. Lentes, A. Ehrenreich, K. Salmon, K. Saba, G. Gottschalk, R. P. Gunsalus, and U. Deppenmeier.** 2005. DNA microarray analysis of Methanosarcina mazei Go1 reveals adaptation to different methanogenic substrates. Mol Genet Genomics **273:**225-39.

16. **Jager, D., C. M. Sharma, J. Thomsen, C. Ehlers, J. Vogel, and R. A. Schmitz.** 2009. Deep sequencing analysis of the Methanosarcina mazei Go1 transcriptome in response to nitrogen availability. Proc Natl Acad Sci U S A.

17. **Kanai, T., J. Akerboom, S. Takedomi, H. J. van de Werken, F. Blombach, J. van der Oost, T. Murakami, H. Atomi, and T. Imanaka.** 2007. A global transcriptional regulator in Thermococcus kodakaraensis controls the expression levels of both glycolytic and gluconeogenic enzyme-encoding genes. J Biol Chem **282:**33659-70.

18. **Kratzer, C., P. Carini, R. Hovey, and U. Deppenmeier.** 2009. Transcriptional profiling of methyltransferase genes during growth of Methanosarcina mazei on trimethylamine. J Bacteriol **191:**5108-15.

19. **Krug, M., S. J. Lee, K. Diederichs, W. Boos, and W. Welte.** 2006. Crystal structure of the sugar binding domain of the archaeal transcriptional regulator TrmB. J Biol Chem **281:**10976-82.

20. **Lee, S. J., A. Engelmann, R. Horlacher, Q. Qu, G. Vierke, C. Hebbeln, M. Thomm, and W. Boos.** 2003. TrmB, a sugar-specific transcriptional regulator of

the trehalose/maltose ABC transporter from the hyperthermophilic archaeon Thermococcus litoralis. J Biol Chem **278:**983-90.

21. **Lee, S. J., M. Surma, W. Hausner, M. Thomm, and W. Boos.** 2008. The role of TrmB and TrmB-like transcriptional regulators for sugar transport and metabolism in the hyperthermophilic archaeon Pyrococcus furiosus. Arch Microbiol **190:**247-56.

22. **Lessner, D. J., L. Li, Q. Li, T. Rejtar, V. P. Andreev, M. Reichlen, K. Hill, J. J. Moran, B. L. Karger, and J. G. Ferry.** 2006. An unconventional pathway for reduction of CO2 to methane in CO-grown Methanosarcina acetivorans revealed by proteomics. Proc Natl Acad Sci U S A **103:**17921-6.

23. **Li, Q., L. Li, T. Rejtar, B. L. Karger, and J. G. Ferry.** 2005. Proteome of Methanosarcina acetivorans Part I: an expanded view of the biology of the cell. J Proteome Res **4:**112-28.

24. **Li, Q., L. Li, T. Rejtar, B. L. Karger, and J. G. Ferry.** 2005. Proteome of Methanosarcina acetivorans Part II: comparison of protein levels in acetate- and methanol-grown cells. J Proteome Res **4:**129-35.

25. **Li, Q., L. Li, T. Rejtar, D. J. Lessner, B. L. Karger, and J. G. Ferry.** 2006. Electron transport in the pathway of acetate conversion to methane in the marine archaeon Methanosarcina acetivorans. J Bacteriol **188:**702-10.

26. **Metcalf, W. W., J. K. Zhang, E. Apolinario, K. R. Sowers, and R. S. Wolfe.** 1997. A genetic system for Archaea of the genus Methanosarcina: liposome-mediated transformation and construction of shuttle vectors. Proc Natl Acad Sci U S A **94:**2626-31.

27. **Oelgeschlager, E., and M. Rother.** 2009. In vivo role of three fused corrinoid/methyl transfer proteins in Methanosarcina acetivorans. Mol Microbiol **72:**1260-72.

28. **Papadopoulos, J. S., and R. Agarwala.** 2007. COBALT: constraint-based alignment tool for multiple protein sequences. Bioinformatics **23:**1073-9.

29. **Perez-Rueda, E., and S. C. Janga.** Identification and genomic analysis of transcription factors in archaeal genomes exemplifies their functional architecture and evolutionary origin. Mol Biol Evol.

30. **Reichlen, M. J., K. S. Murakami, and J. G. Ferry.** Functional Analysis of the Three TBP Homologs in Methanosarcina acetivorans. J Bacteriol.

31. **Rother, M., and W. W. Metcalf.** 2005. Genetic technologies for Archaea. Curr Opin Microbiol **8:**745-51.

32. **Schmid, A. K., D. J. Reiss, M. Pan, T. Koide, and N. S. Baliga.** 2009. A single transcription factor regulates evolutionarily diverse but functionally linked metabolic pathways in response to nutrient availability. Mol Syst Biol **5:**282.

33. **Singh-Wissmann, K., and J. G. Ferry.** 1995. Transcriptional regulation of the phosphotransacetylase-encoding and acetate kinase-encoding genes (pta and ack) from Methanosarcina thermophila. J Bacteriol **177:**1699-702.

34. **Sowers, K. R., J. E. Boone, and R. P. Gunsalus.** 1993. Disaggregation of Methanosarcina spp. and Growth as Single Cells at Elevated Osmolarity. Appl Environ Microbiol **59:**3832-3839.

35. **Sowers, K. R., T. T. Thai, and R. P. Gunsalus.** 1993. Transcriptional regulation of the carbon monoxide dehydrogenase gene (cdhA) in Methanosarcina thermophila. J Biol Chem **268:**23172-8.

36. **Terlesky, K. C., M. J. Nelson, and J. G. Ferry.** 1986. Isolation of an enzyme complex with carbon monoxide dehydrogenase activity containing corrinoid and nickel from acetate-grown Methanosarcina thermophila. J Bacteriol **168:**1053-8.

37. **Torarinsson, E., H. P. Klenk, and R. A. Garrett.** 2005. Divergent transcriptional and translational signals in Archaea. Environ Microbiol **7:**47-54.

38. **Weidenbach, K., C. Ehlers, J. Kock, A. Ehrenreich, and R. A. Schmitz.** 2008. Insights into the NrpR regulon in Methanosarcina mazei Go1. Arch Microbiol **190:**319-32.

39. **Zinder, S. H.** 1993. Physiological Ecology of Methanogens, p. 128-206. *In* J. G. Ferry (ed.), Methanogenesis: Ecology, Physiology, Biochemistry and Genetics, vol. I. Chapman and Hall, New York, NY.

# Chapter 6

# Ongoing and future approaches toward a refined understanding of TBP orthologs and regulation of transcription in *Methanosarcina acetivorans*

This chapter describes various approaches to further understand the *in vivo* roles for the three TBP *M. acetivorans* in homologs. This section describes unfinished projects and preliminary experimental results. Therefore, although it may be premature to formulate any conclusions based on these results, it is hoped that this work can serve as a starting point for future investigations pertaining to the *M. acetivorans* TBP genes.

## Introduction

The third chapter of this dissertation describes an investigation of the functional roles for the three *M. acetivorans* TBP homologs (20). It was concluded that TBP1 is the primary TBP utilized during *M. acetivorans* growth based on its high level of expression relative to that for *tbp2* and *tbp* and the strict conservation of *tbp1* orthologs in the genomes of other *Methanosarcina* species. Furthermore, the lack of growth following the conditional inactivation of the *tbp1* promoter indicated that *tbp1* is essential for *M. acetivorans* growth. Contrary to *tbp1*, *tbp2* and *tbp3* could be individually deleted from

the *M. acetivorans* chromosome without affecting cell viability indicating that neither is required for any vital cellular functions. Although not essential for growth, the Δ*tbp2* and Δ*tbp3* strains each exhibited a prolonged lag *versus* wild-type *M. acetivorans* when transitioning from growth on energetically rich methylotrophic substrates to growth on the least energetically favorable substrate acetate. These deletion strains also exhibited reduced growth when cultured with ecologically relevant growth-limiting concentrations of acetate as opposed to high concentrations typically utilized in a laboratory setting. Furthermore, DNA microarray analysis detected a ≥2-fold perturbation in transcription for a total of 137 genes *versus* wild-type *M. acetivorans* for the Δ*tbp2* and/or Δ*tbp3* strains suggesting functional roles for TBP2 and TBP3 in optimizing gene expression.

Based on these findings, it is apparent that all three TBP homologs are indeed required for optimal fitness of *M. acetivorans*. Still, the extent to which the three isomers differ functionally is unclear. Phenotypic effects in the Δ*tbp2* and Δ*tbp3* strains were similar and numerous genes were found to have altered transcription in both of these mutants consistent with the possibility for at least partial functional overlap between TBP2 and TBP3. If this is indeed the case, these similar phenotypic effects should be exacerbated in a double mutant for both *tbp2* and *tbp3*.

A second unresolved issue is the requirement of *tbp1* for growth. Due to the low level expression of *tbp2* and *tbp3* relative to *tbp1,* it is unclear whether this requirement stems from an inherent difference in TBP1 *versus* TBP2 or TBP3-mediated transcription or if it is simply a consequence of an insufficient level of TBP2 or TBP3 to overcome the loss of *tbp1*. Thus, it would be of interest to determine whether the requirement for *tbp1*

can be overcome if the level of *tbp2* or *tbp3* expression induced to a level comparable to *tbp1*.

Finally, transcriptional profiling revealed numerous candidate genes for TBP2- and/or TBP3-mediated regulation. However, a major drawback to DNA microarray analysis is that it does not allow a distinction to be made between genes that are directly regulated by TBP2 or TBP3 and those that are indirectly regulated. Furthermore, because a *tbp1* knockout was not obtained, no assessment of its role in transcription was made. The use of techniques such as chromatin immunoprecipitation (ChIP) (5, 12, 14) or affinity precipitation (13) which can directly measure the occupancy of each TBP isomer at a given DNA locus could greatly aid in determining the specific roles for TBP1, TBP2 and TBP3 in gene regulation. Because antibodies with high specificity to each TBP isomer are not available, a ChIP assay cannot be performed in wild-type *M. acetivorans*. Thus, the strategy to circumvent this problem is described in the upcoming sections.

## Results and Discussion

### Experimental design for construction of a double mutant strain for *tbp2* and *tbp3*

The construction of a Δ*tbp2* Δ*tbp3* double mutant strain is required to examine the physiological consequences arising from the simultaneous deletion of both minor TBPs and to test whether or not *tbp1* alone is sufficient to support growth. Because puromycin is the only commercially antibiotic with a functional selectable marker in *M. acetivorans*

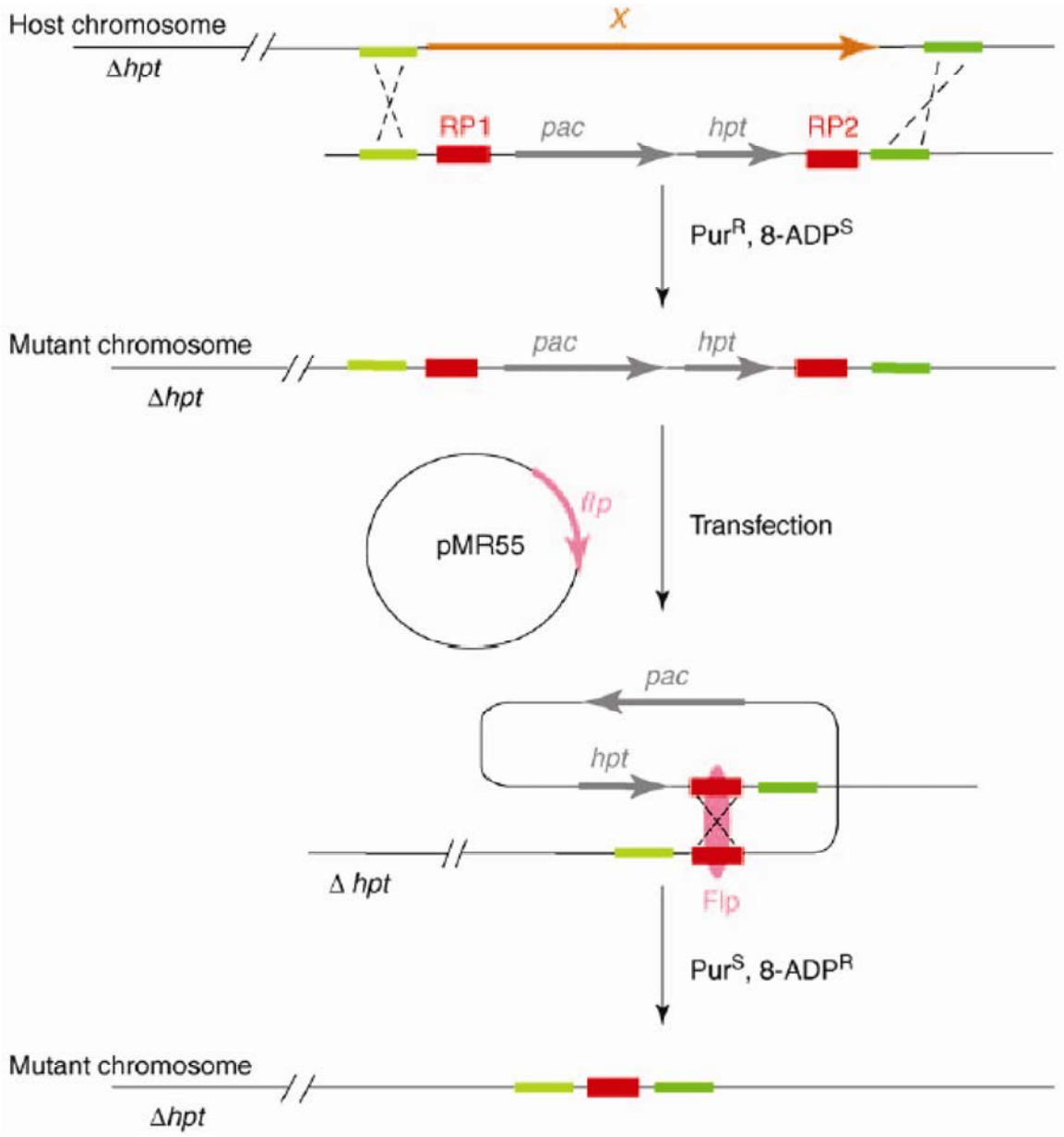


**Figure 6-1. Schematic of the markerless disruption method.** Reproduced from source[1]. Linear DNA that contains an artificial *pac–hpt* operon flanked by Flp recombinase recognition sites (RP1 and RP2) and regions homologous to the target gene (green boxes) is transformed into an *M. acetivorans* Δ*hpt* strain. Strains that replace the target gene by homologous recombination (shown by dotted lines) are selected as puromycin-resistant recombinants. Subsequently, the *pac–hpt* operon is removed by site-specific recombination between RP1 and RP2, which is catalyzed by Flp recombinase encoded on the non-replicating plasmid pMR55.

[1] **Rother, M. and W.W. Metcalf.** 2005. Genetic technologies for Archaea. Curr. Opin. Micorbiol. **8:**745-51.

(21), a Δ*tbp2* Δ*tbp3* double mutant strain cannot be constructed using either of the previously described single mutants. However, multiple rounds of selection in *M. acetivorans* can be performed using a recently developed markerless exchange technique (19, 21) (Fig. 6-1). Markerless exchange in *M. acetivorans* requires the use of a parental strain in which *hpt* (encodes hypoxanthine phosphoribosyl transferase) has been knocked out conferring resistance to the normally toxic purine analog 8ADP (8-aza-2,6-diaminopurine). The two step knockout strategy depicted in Fig. 6-1 is similar to well known bacterial gene knockout systems (7). The gene is knocked out in the first step by homologous recombination and replacement with a *pac-hpt* cassette flanked by targets for site-specific recombination by the yeast enzyme flippase (Flp) recombinase (1), and mutants are selected for $Pur^R$ and $8ADP^S$. The *pac-hpt* cassette is removed in the second step by transformation with a non-replicating plasmid carrying a constitutively expressed copy of *flp* and selection for $8ADP^R$ and $Pur^S$.

This strategy has been implemented in an attempt to construct unmarked *tbp2* and *tbp3* deletion mutants. Although construction of both Δ*tbp2::pac-hpt* and Δ*tbp3::pac-hpt* (designated Δ*tbp2** and Δ*tbp3** respectively) mutants in the WWM1 parental strain (C2A Δ*hpt*) (19) has been completed (Fig. 6-2), repeated attempts to remove the *pac-hpt* cassette with Flp have been unsuccessful. Transformation with the non-replicating plasmid carrying *flp* and selection for $8ADP^R$ typically yields large numbers of $8ADP^R$ colonies. However, all colonies were also $Pur^R$ and still in possession of the *pac-hpt* cassette (data not shown) indicating the acquisition of spontaneous $8ADP^R$.

It has been previously shown that *M. acetivorans* develops resistance to 8ADP with high frequency (19). This suggests that the reasons for previous failures to remove

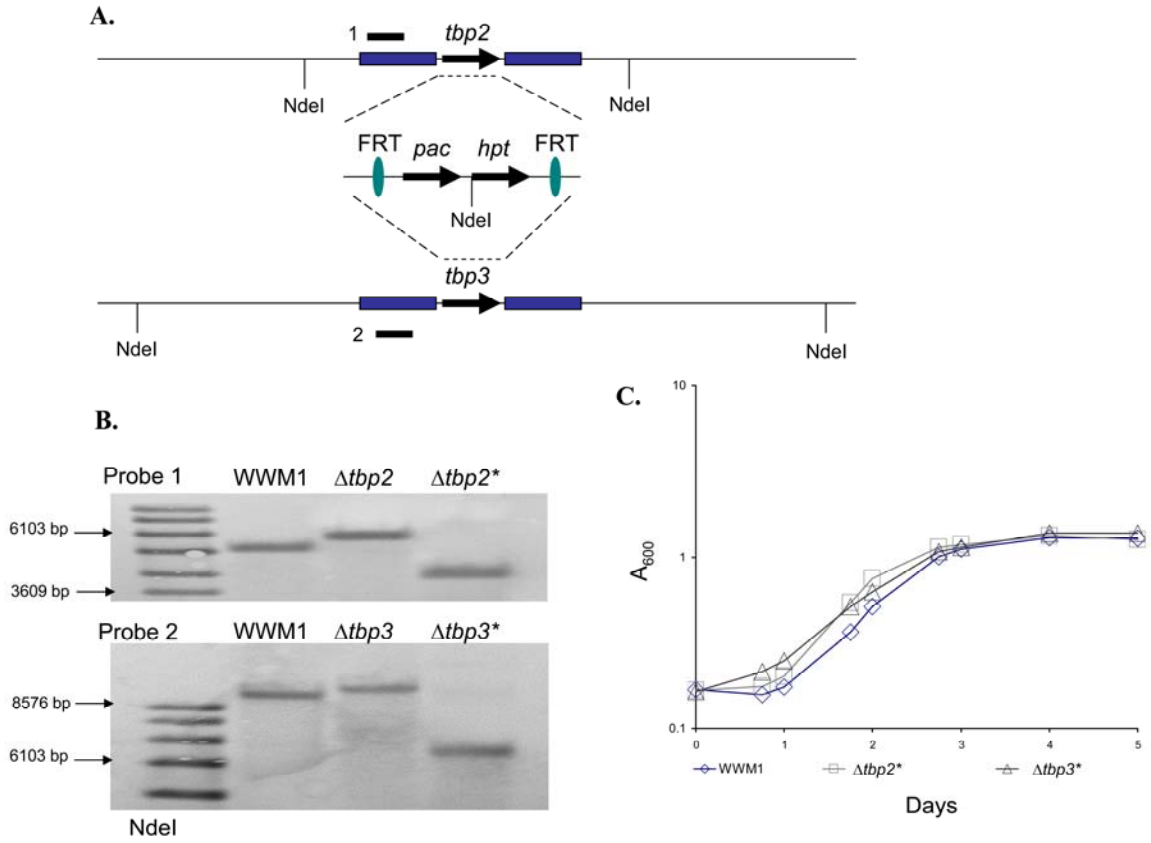


**Figure 6-2. Construction and verification of *M. acetivorans* mutants with *tbp2* or *tbp3* deleted and replaced with *pac-hpt*.** (A) Shows the *tbp2* and *tbp3* gene arrangements on the *M. acetivorans* C2A chromosome. Arrows denote genes and direction of transcription. Broken lines denote regions replaced with a *pac-hpt* cassette in deletion mutant strains. The heavy lines labeled 1 and 2 identify the PCR products used as probes for Southern hybridizations depicted in panel B. NdeI cut sites are indicated on the chromosome. Ovals denote Flp recognition targets. (B) The genomic structures of Δ*tbp2**, Δ*tbp3** were verified by Southern hybridizations of NdeI digested genomic DNA from WWM1 (lane 1), Δ*tbp2/3::pac* (lane 2) and Δ*tbp2/3::pac-hpt* (lane 3) *M. acetivorans* strains with DIG-labeled probes 1 or 2. The molecular weight marker is shown in lane M with band sizes indicated on the left. (C) Depicts growth of WWM1, Δ*tbp2** and Δ*tbp3* M. acetivorans* strains on 50 mM TMA (single replicate).

the *pac-hpt* cassette stem from poor transformation efficiency of the plasmid harboring *flp* or from poor expression of *flp* during the recovery stage of the transformation. In any event, this technical obstacle will need to be resolved to move forward in this experimental procedure and in other experiments described in the upcoming sections in which use this system for markerless exchange is required.

**Construction and characterization of conditional *tbp2* and *tbp3* expression strains**

A common alternative to the knockout approach for studying gene function is to assess the physiological affects resulting from the ectopic expression of that gene. Since the basal expression levels for *tbp2* and *tbp3* relative to *tbp1* are very low, it was reasoned that examining the consequences of the artificial induction of *tbp2* and *tbp3* could provide useful insights into their functional roles. Such approaches have been successfully applied in archaeal, bacterial and eukaryotic systems respectively to investigate the function of the multiple GTF isomers (8), alternative sigma factors (27) and TRF proteins (6).

The strategy for ectopic expression of *tbp2* and *tbp3* involved replacing the native promoters for these genes with the chimeric promoter P*mcrB*(tetO1) (10) which was used in chapter 3 to construct a conditional *tbp1* expression strain. These ΔP*tbp2::*P*mcrB*(tetO1)-*tbp2* and ΔP*tbp3::*P*mcrB*(tetO1)-*tbp3* strains were constructed by homologous recombination-mediated gene replacement and selection for puromycin resistance during growth on TMA. Mutant genotypes were confirmed by Southern blot

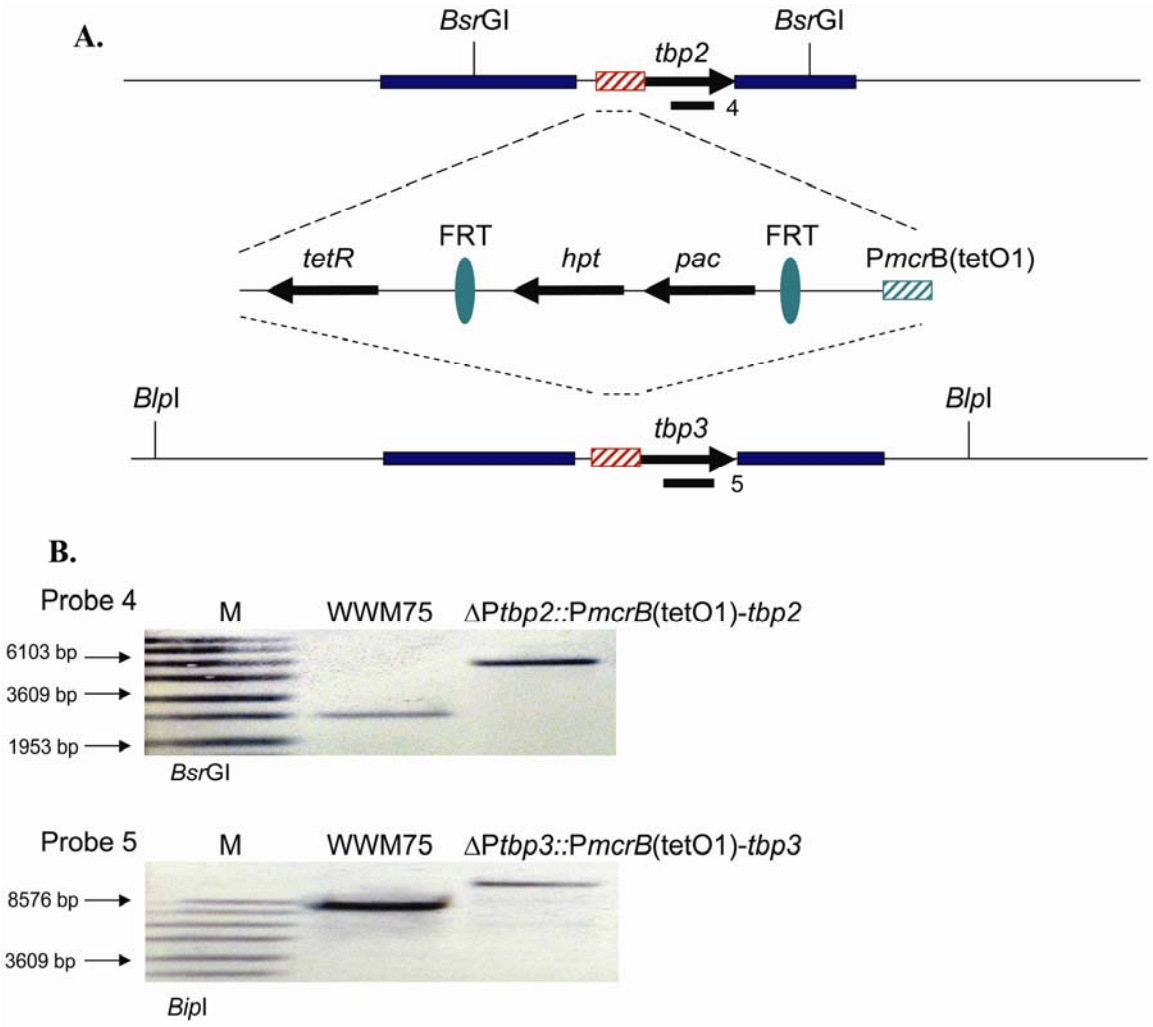


**Figure 6-3. Construction of *M. acetivorans* mutants with native P*tbp2* or P*tbp3* replaced with P*mcrB*(tetO1).** (A) Shows the *tbp2* and *tbp3* gene arrangements on the *M. acetivorans* WWM75 chromosome. Arrows denote genes and direction of transcription. The boxes denote promoter sequences (P*tbp2* red striped; P*mcrB*(tetO1) green striped). Broken lines denote regions replaced in the mutant strains. Ovals denote Flp recognition targets. The heavy lines labeled 4 and 5 identify the PCR products used as probes for Southern hybridizations depicted in panel B. BsrGI and BlpI cut sites are indicated. (B) The genomic structures of ΔP*tbp2::*P*mcrB*(tetO1)-*tbp2* and ΔP*tbp3::*P*mcrB*(tetO1)-*tbp3* were verified by Southern hybridizations of BsrGI or BlpI digested genomic DNA from WWM75, ΔP*tbp2::*P*mcrB*(tetO1)-*tbp2* or ΔP*tbp3::*P*mcrB*(tetO1)-*tbp3 M. acetivorans* strains with DIG-labeled probes 4 or 5 (Table C-1). The molecular weight marker is shown in lane M with band sizes indicated on the left.

(Fig. 6-3) and PCR screening to ensure the TBP and P*mcrB*(tetO1) sequences were intact.

Previous analyses of the ΔP*tbp1::*P*mcrB*(tetO1)-*tbp1* strain revealed that the transcript abundances for *tbp1* are comparable when expressed from either the native P*tbp1* or from P*mcrB*(tetO1) in the presence of tetracycline (Table 3-3). In wild-type *M. acetivorans,* transcript abundances for *tbp2* and *tbp3* are at least 20-fold less than those for *tbp1*under all conditions examined (Table 3-3). Under the control of tetracycline-induced P*mcrB*(tetO1), expression levels of *tbp2* and *tbp3* should, in theory, approximate the natural levels for *tbp1*.

A preliminary growth analysis of the ΔP*tbp2::*P*mcrB*(tetO1)-*tbp2* and ΔP*tbp3::*P*mcrB*(tetO1)-*tbp3* strains was carried out on cells cultured with 50 mM TMA in the presence (100 μg $mL^{-1}$) or absence of tetracycline. In the presence of tetracycline, transcription of *tbp2* and *tbp3* were indeed induced to levels comparable to the wild-type level for *tbp1* in the ΔP*tbp2::*P*mcrB*(tetO1)-*tbp2* strain and the ΔP*tbp3::*P*mcrB*(tetO1)-*tbp3* strain respectively (Table 6-1). Neither strain exhibited grossly different growth parameters in media with tetracycline *versus* media without tetracycline (Fig. 6-4) suggesting that the artificial induction of either *tbp2* or *tbp3* does not severely affect growth on TMA (no other growth substrates have been tested). Transcript abundances for *tbp2* and *tbp3* during growth of these mutants in the absence of tetracycline were roughly equivalent to the wild-type transcript abundances of these genes (data not shown) suggesting that TetR does not completely repress *tbp2* and *tbp3* transcription. At this juncture, it is not clear whether this is simply the basal level of transcription through

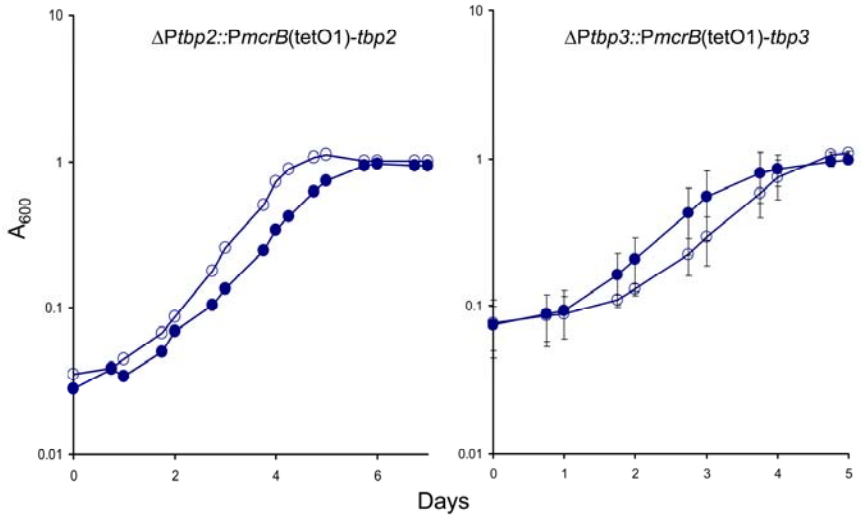


**Figure 6-4. Depicts growth of ΔP*tbp2*::P*mcrB*(tetO1)-*tbp2* and ΔP*tbp3*::P*mcrB*(tetO1)-*tbp3*.** Strains were cultured on 50 mM TMA in the presence (filled circles) or absence (open circles) of 100 µg $mL^{-1}$ of tetracycline. The ΔP*tbp3*::P*mcrB*(tetO1)-*tbp3* curve represents the average and standard deviation of triplicate cultures. Replicates were not made for the ΔP*tbp2*::P*mcrB*(tetO1)-*tbp2* strain.

**Table 6-1. Relative *tbp1*, *tbp2* and *tbp3* transcript abundance in the ΔP*tbp2*::P*mcrB*(tetO1)-*tbp2* and ΔP*tbp3*::P*mcrB*(tetO1)-*tbp3* during growth with and without tetracycline.**

| Gene | ΔP*tbp2*::P*mcrB*(tetO1)-*tbp2* [b] | | ΔP*tbp3*::P*mcrB*(tetO1)-*tbp3* [c] | |
|---|---|---|---|---|
| | 0 µg $mL^{-1}$ Tetracycline | 100 µg $mL^{-1}$ Tetracycline | 0 µg $mL^{-1}$ Tetracycline | 100 µg $mL^{-1}$ Tetracycline |
| ***tbp1*** | 1.02 ± 0.22 [a] | 0.868 ± 0.527 | 1.00 ± 0.16 | 0.0565 ± 0.0132 |
| ***tbp2*** | 1.00 ± 0.07 | 23.7 ± 2.6 | 1.00 ± 0.19 | 0.811 ± 0.113 |
| ***tbp3*** | 1.00 ± 0.06 | 0.875 ± 0.068 | 1.00 ± 0.41 | 55.9 ± 6.9 |

[a] Relative transcript abundances were calculated using the $\Delta\Delta C_t$ method with the 16s rRNA gene used as an invariant control. The $\Delta C_t$ values for 0 µg $mL^{-1}$ tetracycline treatment samples were used as the calibrator for each strain.

[b] Values represent the average and standard deviation of two technical replicates each assayed in triplicate.

[c] Values represent the average and standard deviation of three biological replicates each assayed in triplicate..

repressed P*mcrB*(tetO1) or if mutations were acquired enabling wild-type levels of *tbp2* and *tbp3* transcription.

Interestingly, following the induction of *tbp3* in theΔP*tbp3::*P*mcrB*(tetO1)-*tbp3* strain, a robust decrease in *tbp1* transcript abundance was observed (Table 6-1) indicating that during growth in the presence of tetracycline, *tbp3* is the most highly transcribed TBP gene in the ΔP*tbp3::*P*mcrB*(tetO1)-*tbp3* strain (Table 6-1). However, induction of *tbp3* had no effect on the transcription of *tbp2* (Table 6-1). In contrast, induction of *tbp2* in the ΔP*tbp2::*P*mcrB*(tetO1)-*tbp2* strain did not significantly affect either *tbp1* transcription or *tbp3* transcription.

Although preliminary, the implications of these data are intriguing. The repression of *tbp1* transcription during the artificial induction of *tbp3* implies the existence of a cellular mechanism to control the intracellular TBP pool, possibly via a negative feedback loop, perhaps by TBP3 itself. Furthermore, that the cell evolved a mechanism to control the level of *tbp1* in response to the level of *tbp3* expression implies that natural conditions exist wherein expression from wild-type P*tbp3* is induced to this level. Although to date, natural induction of *tbp3* has not been observed. Additionally, since no change in growth was observed, it implies that TBP3 is fully capable of functionally replacing *tbp1* and that, under these conditions, it may be possible to construct a *tbp1* knockout. If a *tbp1* knockout can be made in a strain artificially inducing *tbp3,* it would indicate that *tbp1* is essential for growth merely because basal level *tbp3* expression is too low to support growth in the absence of *tbp1*. Still, it is curious that if TBP3 is in fact capable of functionally replacing TBP1, why then, was *tbp3* expression not induced to compensate for the loss of *tbp1* in the

ΔP*tbp1::*P*mcrB*(tetO1)-*tbp1* strain during growth in the absence of tetracycline (see Table 3-3)? Additional work will be required to resolve these issues.

Concerning the ΔP*tbp2::*P*mcrB*(tetO1)-*tbp2* strain, additional biological replicates must be run before any assessment of the effect of *tbp2* expression on *tbp1* and *tbp3* can be made.

## Strategies for *in vivo* expression of His-tagged TBP1, TBP2 and TBP3

A direct approach to addressing the roles of each TBP homolog in gene expression is to map the distribution of the TBP proteins on the chromosome using chromatin immunoprecipitation (ChIP) coupled with DNA microarrays or direct DNA sequencing. This technique requires the use antibodies directed against the protein of interest to pull the DNA-bound TBP complex out of solution following cross-linking. Unfortunately, the anti-TBP1 and anti-TBP3 antisera used for Western blot analysis in chapter 3 exhibited high cross reactivity against all three *M. acetivorans* TBP proteins making their use in ChIP experiments impractical. The strategy that has been implemented to circumvent this problem is to express each TBP homolog in *M. acetivorans* carrying a C-terminal hexa-histidine tag and to use monoclonal antibodies directed against the His-tag for immunoprecipitation. Progress on this front has been made by expressing plasmid-based His-tagged copies of each of the three TBP genes from the promoter for the methanol-specific MT1 isozyme 2 operon, P*mtaCB2* (4) which is highly expressed during growth on methanol and repressed during growth on TMA.

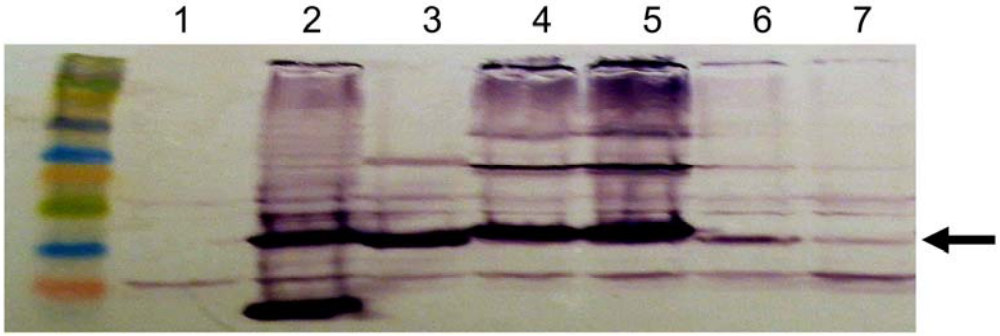


**Figure 6-5. Detection of TBP1-his$_6$, TBP2-his$_6$ and TBP3-his$_6$ in methanol-grown *M. acetivorans* cell lysate by Western blot.** Blots were probed with anti-His(C-term) monoclonal antibodies. Lanes: 1, pWM321; 2/3, pMR52/52B(TBP1); 4/5, pMR62/62B(TBP2); 6/7, pMR64/64B(TBP3). Arrow denotes the band corresponding to TBP. The additional band in lane 2 represents a truncated form of TBP1 that arose due to a mutation in the *tbp1* coding frame on pMR52.

**Table 6-2. Relative *tbp1, tbp2* and *tbp3* transcript abundance in *M. acetivorans* cells transformed with plasmids for P*mtaCB2*-based TBP1-his$_6$, TBP2-his$_6$ and TBP3-his$_6$ expression during growth on methanol or TMA.**

| | pWM321 [a] | | P*mtaCB2::tbp1-his$_6$* | | P*mtaCB2::tbp2-his$_6$* | | P*mtaCB2::tbp3-his$_6$* | |
|---|---|---|---|---|---|---|---|---|
| **Gene** | **TMA** | **Methanol** | **TMA** | **Methanol** | **TMA** | **Methanol** | **TMA** | **Methanol** |
| ***tbp1*** | 1.00 ± 0.09 [b] | 1.04 ± 0.13 | 1.01 ± 0.04 | 58.2 ± 1.1 | 0.973 ± 0.145 | 1.44 ± 0.08 | 0.914 ± 0.047 | 0.469 ± 0.073 |
| ***tbp2*** | 1.00 ± 0.07 | 1.27 ± 0.05 | 1.18 ± 0.03 | 1.00 ± 0.08 | 15.6 ± 1.3 | 1360 ± 20 | 1.00 ± 0.06 | 0.745 ± 0.033 |
| ***tbp3*** | 1.00 ± 0.10 | 1.37 ± 0.05 | 1.10 ± 0.04 | 1.10 ± 0.06 | 0.978 ± 0.092 | 1.59 ± 0.09 | 4.34 ± 0.41 | 4.27 ± 0.18 |

[a] Base vector into which all P*mtaCB2::tbp* fusion were cloned.

[b] Relative transcript abundances were calculated using the $\Delta\Delta C_t$ method with the 16s rRNA gene used as an invariant control. The $\Delta C_t$ values for pWM321 during growth on TMA were used as the calibrator.

Following transformation into TMA-grown cells, selection for $Pur^R$ and screening clones for the presence of the appropriate plasmid, expression of the TBP promoter fusions were induced by inoculating these strains into media with methanol. Expression of the TBPs was monitored by Western blot (Fig. 6-5) and qRT-PCR (Table 6-2). The C-terminally His-tagged TBP1, TBP2 and TBP3 proteins were readily detectible in lysate from strains carrying these plasmids (Fig. 6-5). However, before ChIP experiments are performed, protocols for a more controlled induction of *tbp1* and *tbp2* and for higher expression of *tbp3* will need to be established. The high level expression for *PmtaCB2::tbp1-his*$_6$ and *PmtaCB2::tbp2-his*$_6$ (approximately 60- and 1000-fold respectively above the wild-type levels for *tbp1* and *tbp2*) (Table 6-2) during growth on methanol hinders growth possibly as a consequence of high proportion of TBP relative to the other component of the transcriptional machinery. However, it should be possible to significantly reduce the expression level from *PmtaCB2* by adding TMA to the growth media as has been reported previously (4). Another solution is to use a weaker promoter such as P*mcrB*(tetO1) which has a maximum expression at a level close to the wild-type level for P*tbp1*. The reasons for the poor expression of P*mtaCB2::tbp3* are unclear. One explanation is acquisition of a mutation preventing expression, although it is apparently not the result of a cis-mutation in *tbp3* or P*mtaCB2* based on sequence analysis of plasmids recovered following growth methanol. Another possibility is that *tbp3* itself is inherently preventing the induction of this promoter. The *mtaCB2* operon did exhibit an approximately 2-fold decreased transcript abundance in the Δ*tbp3* strain *versus* wild-type *M. acetivorans* (20) consistent with an involvement of TBP3 in the regulation of *mtaCB2*.

Whether or not this merely coincidental is yet to be resolved. In the end, the simplest solution to improving *tbp3-his*$_6$ expression may also be to use an alternative promoter.

## Establishment of *M. acetivorans* strain libraries

The study of transcription in the *Archaea* is particularly attractive due to the strong resemblance of components of the archaeal transcriptional apparatus to those utilized in eukaryotes. Because of this relatedness, the findings from investigations of archaeal transcription systems can be extrapolated to provide insights into problems relevant to human biology and disease. Not surprisingly, the majority of the research on archaeal transcription has been undertaken to address unresolved issues common to both archaea and eukaryotes. Much less attention has been devoted to understanding the key differences in transcription in the *Archaea versus* the *Eukarya*. In particular, little is known regarding the interplay between the eukaryotic-like core archaeal transcriptional machinery and the bacterial-like gene specific transcription factors to explain how these organisms coordinate large scale changes in gene expression within the confines of the archaeal cell. Thus, investigations into this aspect of archaeal transcription could uncover invaluable insight regarding the evolution of transcriptional regulation in all three domains of life and contribute to broader research efforts such as the ENCODE (Encyclopedia of DNA elements) project (http://genome.gov/Site/index.html).

The development of gene knockout and knockin strain libraries for a variety of bacterial and eukaryotic model organisms (e.g. *E. coli* and *S. cerevisiae*) (2, 15)

(http://www-sequence.stanford.edu/group/yeast_deletion_project/deletions3.html) has proven a powerful tool for the study different facets of cellular biology. However, to date, no such strain libraries have been developed for any organisms in the *Archaea* domain. Thus, the establishment of knockout and knockin libraries for key archaeal model organisms would be of tremendous benefit to the archaeal research community. Because of its importance as a model organism and the availability of sophisticated genetic tools, *M. acetivorans* is a strong candidate for strain library development. Ideally, this would involve the systematic deletion and/or overexpression of all 4540 (9) *M. acetivorans* open reading frames. However, the slow growth and specialized culturing conditions required for this organism makes this a monumental task for the few laboratories with the technical know how to do so. Instead, I propose the development of smaller scale strain libraries focusing strictly on the components of the *M. acetivorans* transcriptional machinery (i.e. the RNA polymerase, GTFs and all putative gene specific transcription factors). This proposal involves the construction of three independent libraries constructed in a versatile Δ*hpt*::P*mcrB*-*tetR*-φC31-*int*-attP background (10) which will be made available to the research community. These libraries will greatly assist in performing a comprehensive analysis of the transcriptional machinery of a key archaeal model organism.

First, I propose the establishment of a *M. acetivorans* transcription factor knockout library constructed for the purpose of assessing the *in vivo* requirements for each component of the transcriptional machinery for growth. A recent bioinformatic analysis identified 158 putative gene specific DNA-binding transcription factors in the *M. acetivorans* genome (18). Attempts will be made to individually delete each of these

genes by homologous recombination-mediated gene replacement. Attempts will also be made to delete other known abundant DNA-binding proteins that have been shown to influence transcription (e.g. the archaeal histone and the nonhistone chromosomal protein MC1) (22, 24-26) and components of the core transcription machinery with poorly defined and/or non-essential roles in other organisms (e.g. TFE, TFS, NusG, NusA, RpoF) (11). All genes will be replaced with a constitutively expressed *pac-hpt* operon flanked by targets sites for site-specific recombination by Flp recombinase (10) to enable future removal of markers when desired. For the genes that cannot be knocked out by this method, conditional expression strains will be constructed wherein their native promoters are replaced with P*mcrB*(tetO1) as explained in chapter 3.

Next, I propose the establishment of a *M. acetivorans* transcription factor affinity tagged strain library constructed for the purpose of identifying the key protein-protein and protein-DNA interactions for each component of the transcriptional machinery. Here, a copy of each gene described above will be integrated into the *M. acetivorans* chromosome at the recognition site for the φC31 site-specific recombinase, attP (10). Each open reading will contain both a hexa histidine ($His_6$-tag) and hemagglutin (HA-tag) at the C-terminus, and expression of each gene will be driven by the P*mcrB*(tetO1) promoter (10) enabling it to be readily switched on and off. Tagged copies will also be generated for components of the core transcriptional machinery (e.g. a subset of RNA polymerase subunits, TFB, TBP1) which are almost certain to be essential for cell viability, and thus, will be unable to be knocked out by homologous recombination. These tagged proteins can be affinity purified or immunoprecipitated using antibodies directed against either the $His_6$-tag or HA-tag allowing for assessments of the *in vivo*

protein-protein interactions and DNA-binding sites for each component of the transcription machinery. Protein-protein interactions can be determined by subjecting the proteins that co-purified with each component to mass spectrometry. DNA binding sites on the *M. acetivorans* can be determined by chromatin immunoprecipitation coupled with DNA microarrays or next generation sequencing.

Lastly, I propose the establishment of a *M. acetivorans* transcription factor reporter gene library constructed for the purpose of assessing the conditions under which each component of the transcriptional machinery is expressed *in vivo*. Here the promoters (~1000 bp DNA sequence extending upstream from the gene start codon or the start codon for the first gene in any putative operons) for each of these genes will be fused to the *uidA* encoding for β-glucuronidase from *E. coli.* Expression levels for each promoter can be assessed under any growth condition by measuring β-glucuronidase activity from whole cell lysate (19).

## Statement of personal reflection

In reflecting on my graduate career, I feel there are two achievements for which I feel the greatest sense of accomplishment. The first of these was my success in implementing the use of genetic techniques in *M. acetivorans.* I am proud of this accomplishment because it required both considerable dedication on my part and because its mastery proved extremely beneficial to the both lab groups. When I began my graduate career, I had little previous experience in bacterial genetics. Additionally, I

chose a research project in which one the primary goals was to knockout a number of poorly characterized genes in an organism in for which genetic manipulation is inherently difficult. Since no one from either the Ferry or Murakami groups was actively performing genetics on *M. acetivorans*, I had to essentially self-teach myself how to master these techniques. Because of this, I spent the better part of a year and half going through trail and error before I finally got a handle on the system. In the end, these toils eventually paid off as I was not only able to use these tools to address problems pertinent to my own projects, but I was also able to use what I learned to successfully train other lab members in the use of these techniques. Thus, in my tenure, the lab has gone from the point of doing no genetics to where these techniques are being done more or less routinely.

My second noteworthy achievement was the recent characterization of the MA3302 gene described in chapter 5. I found this work to be important in shaping my graduate career for two reasons. The first and most important is that findings from this project significantly contribute to the overall understanding of this organism and how it regulates its differing metabolic pathways. Second, this was a project which largely designed on my own without first seeking the input from either Dr. Murakami or Dr. Ferry. I identified this gene as potentially interesting, took the initiative to design a series of experiments to characterize it and then carried these experiments out in a relatively short time frame. This is significant because it illustrated to me that I had acquired the requisite knowledge to shape my own research as opposed to simply carrying out a set of experiments that someone else had designed. Thus far, this project has yielded one manuscript describing the preliminary characterization of MA3302 that is currently in

preparation. Perhaps more importantly, this initial investigation has paved the way for numerous different follow up projects that could serve as a research projects for new graduate students or postdocs.

## Materials and Methods

*Cell Growth.* Growth and harvesting of *M. acetivorans* strains in single cell morphology (23) cultured on high-salt (HS) broth medium with methanol and TMA was as previously described (16). Growth was monitored by measuring the optical density at 600 nm.

*RNA Isolation.* All *M. acetivorans* RNA samples were isolated from using an RNeasy Total RNA Mini kit (QIAGEN). Purified RNA was treated twice with RNase-free DNase I (QIAGEN) and once with RQ1 DNase (Promega) to remove contaminating DNA.

*Taqman quantitative RT-PCR. Taq*man assays were performed as described (16, 20) using total RNA isolated from at mid-exponential phase ($A_{600}$ ~ 0.6). Primer and probe sequences are listed in Table C-1.

*Construction of MA3302 deletion mutant strain*. Liposome-mediated transformation and homologous recombination-mediated gene replacement were used as described (3, 17) to generate *M. acetivorans* Δ*tbp2::pac-hpt,* Δ*tbp3::pac-hpt* (hereafter designated Δ*tbp2** and Δ*tbp3** respectively), Δ*tbp2::*P*mcrB*(tetO1)-*tbp2* and Δ*tbp3::*P*mcrB*(tetO1)-*tbp3*. The Δ*tbp2** and Δ*tbp3** mutant strains were generated in a

*M. acetivorans* WWM1 (19) background, and the ΔP*tbp2::*P*mcrB*(tetO1)-*tbp2* and ΔP*tbp3::*P*mcrB*(tetO1)-*tbp3* strains were generated in a *M. acetivorans* WWM75 (10) background. Cells used to construct the four respective strains were transformed with 2 μg pMR37, pMR38, pMR59 or pMR60 (Table C-1) linearized by restriction digestion, and transformants were selected on HS agar media with 0.8% (w/v) agar, with 50 mM TMA and 2 μg $mL^{-1}$ puromycin (Sigma, St Louis, MO) added from sterile, anaerobic 100X stock solution. 8-aza-2,6-diaminopurine (8ADP) (Sigma, St Louis, MO) sensitivity was tested in media containing 20 μg $mL^{-1}$ 8ADP added from sterile, anaerobic 200X stock solution. Plasmids pWM321, pMR52/52B, pMR62/62B and pMR64/64B (Table C-1) which carry His-tagged TBP transformed into *M. acetivorans* C2A by liposome-mediated transformation and selection for resistance to puromycin on HS agar media with 0.8% (w/v) agar, with 50 mM TMA and 2 μg $mL^{-1}$ puromycin (Sigma, St Louis, MO) added from sterile, anaerobic 100X stock solution..

*Western blot analysis.* To prepare *M. acetivorans* cell lysate, cells were collected at mid-log phase by centrifugation, resuspended in SDS denaturing buffer (62.5 mM Tris-HCl [pH = 6.8], 2% SDS, 10% glycerol, 1% β-ME, 0.005% Bromophenol Blue) and lysed by incubation at 95$^{o}$C for 5 min. *M. acetivorans* cell extract proteins were separated by SDS-PAGE on 12% gels and electrotransferred to a polyvinylidene difluoride membrane (Sequi-Blot™ PVDF Membrane; Bio-Rad) following manufacturer's guidelines. Additional protein binding sites were blocked by incubating the membrane overnight at room temperature under constant agitation in TBS-T buffer (10 mM Tris-HCl [pH 8.0], 150 mM NaCl and 0.1% Tween 20) with the addition of 3% BSA. Following blocking membrane was incubated 3 hours at room temperature in a

1:5000 dilution of anti-His(C-term) alkaline phosphatase-conjugated mouse monoclonal antibodies (Invitrogen, Carlsbad, CA) in TBS-T. The antibody/antigen complexes were detected using the BCIP®/NBT Liquid Substrate System (Sigma) following manufacturer's guidelines.

## Acknowledgements

I thank W.W. Metcalf (University of Illinois, Urbana, IL) for the donation of all plasmids and strains used for the genetic manipulation of *M. acetivorans* and D. Grove (Penn State Genomics Core Facility – University Park, PA) for optimization of *Taq*man assays. This work was funded by the Pew Scholar's Program in the Biomedical Sciences to KSM and by grants from the National Science Foundation and Department of Energy to JGF.

## References

1. **Andrews, B. J., G. A. Proteau, L. G. Beatty, and P. D. Sadowski.** 1985. The FLP recombinase of the 2 micron circle DNA of yeast: interaction with its target sequences. Cell **40:**795-803.
2. **Baba, T., T. Ara, M. Hasegawa, Y. Takai, Y. Okumura, M. Baba, K. A. Datsenko, M. Tomita, B. L. Wanner, and H. Mori.** 2006. Construction of

Escherichia coli K-12 in-frame, single-gene knockout mutants: the Keio collection. Mol Syst Biol **2:**2006 0008.

3. **Boccazzi, P., J. K. Zhang, and W. W. Metcalf.** 2000. Generation of dominant selectable markers for resistance to pseudomonic acid by cloning and mutagenesis of the ileS gene from the archaeon Methanosarcina barkeri fusaro. J Bacteriol **182:**2611-8.

4. **Bose, A., M. A. Pritchett, M. Rother, and W. W. Metcalf.** 2006. Differential Regulation of the Three Methanol Methyltransferase Isozymes in Methanosarcina acetivorans C2A. J Bacteriol **188:**7274-83.

5. **Buck, M. J., and J. D. Lieb.** 2004. ChIP-chip: considerations for the design, analysis, and application of genome-wide chromatin immunoprecipitation experiments. Genomics **83:**349-60.

6. **Chong, J. A., M. M. Moran, M. Teichmann, J. S. Kaczmarek, R. Roeder, and D. E. Clapham.** 2005. TATA-binding protein (TBP)-like factor (TLF) is a functional regulator of transcription: reciprocal regulation of the neurofibromatosis type 1 and c-fos genes by TLF/TRF2 and TBP. Mol Cell Biol **25:**2632-43.

7. **Fabret, C., S. D. Ehrlich, and P. Noirot.** 2002. A new mutation delivery system for genome-scale approaches in Bacillus subtilis. Mol Microbiol **46:**25-36.

8. **Facciotti, M. T., D. J. Reiss, M. Pan, A. Kaur, M. Vuthoori, R. Bonneau, P. Shannon, A. Srivastava, S. M. Donohoe, L. E. Hood, and N. S. Baliga.** 2007. General transcription factor specified global gene regulation in archaea. Proc Natl Acad Sci U S A **104:**4630-5.

9. **Galagan, J. E., C. Nusbaum, A. Roy, M. G. Endrizzi, P. Macdonald, W. FitzHugh, S. Calvo, R. Engels, S. Smirnov, D. Atnoor, A. Brown, N. Allen, J. Naylor, N. Stange-Thomann, K. DeArellano, R. Johnson, L. Linton, P. McEwan, K. McKernan, J. Talamas, A. Tirrell, W. Ye, A. Zimmer, R. D. Barber, I. Cann, D. E. Graham, D. A. Grahame, A. M. Guss, R. Hedderich, C. Ingram-Smith, H. C. Kuettner, J. A. Krzycki, J. A. Leigh, W. Li, J. Liu, B. Mukhopadhyay, J. N. Reeve, K. Smith, T. A. Springer, L. A. Umayam, O. White, R. H. White, E. Conway de Macario, J. G. Ferry, K. F. Jarrell, H. Jing, A. J. Macario, I. Paulsen, M. Pritchett, K. R. Sowers, R. V. Swanson, S. H. Zinder, E. Lander, W. W. Metcalf, and B. Birren.** 2002. The genome of M. acetivorans reveals extensive metabolic and physiological diversity. Genome Res **12:**532-42.

10. **Guss, A. M., M. Rother, J. K. Zhang, G. Kulkarni, and W. W. Metcalf.** 2008. New methods for tightly regulated gene expression and highly efficient chromosomal integration of cloned genes for Methanosarcina species. Archaea **2:**193-203.

11. **Hirata, A., T. Kanai, T. J. Santangelo, M. Tajiri, K. Manabe, J. N. Reeve, T. Imanaka, and K. S. Murakami.** 2008. Archaeal RNA polymerase subunits E and F are not required for transcription in vitro, but a Thermococcus kodakarensis mutant lacking subunit F is temperature-sensitive. Mol Microbiol **70:**623-33.

12. **Horak, C. E., and M. Snyder.** 2002. ChIP-chip: a genomic approach for identifying transcription factor binding sites. Methods Enzymol **350:**469-83.

13. **Ishikawa, S., Y. Ogura, M. Yoshimura, H. Okumura, E. Cho, Y. Kawai, K. Kurokawa, T. Oshima, and N. Ogasawara.** 2007. Distribution of stable DnaA-binding sites on the Bacillus subtilis genome detected using a modified ChIP-chip method. DNA Res **14:**155-68.

14. **Jiang, C., and B. F. Pugh.** 2009. Nucleosome positioning and gene regulation: advances through genomics. Nat Rev Genet **10:**161-72.

15. **Kitagawa, M., T. Ara, M. Arifuzzaman, T. Ioka-Nakamichi, E. Inamoto, H. Toyonaga, and H. Mori.** 2005. Complete set of ORF clones of Escherichia coli ASKA library (a complete set of E. coli K-12 ORF archive): unique resources for biological research. DNA Res **12:**291-9.

16. **Lessner, D. J., L. Li, Q. Li, T. Rejtar, V. P. Andreev, M. Reichlen, K. Hill, J. J. Moran, B. L. Karger, and J. G. Ferry.** 2006. An unconventional pathway for reduction of CO2 to methane in CO-grown Methanosarcina acetivorans revealed by proteomics. Proc Natl Acad Sci U S A **103:**17921-6.

17. **Metcalf, W. W., J. K. Zhang, E. Apolinario, K. R. Sowers, and R. S. Wolfe.** 1997. A genetic system for Archaea of the genus Methanosarcina: liposome-mediated transformation and construction of shuttle vectors. Proc Natl Acad Sci U S A **94:**2626-31.

18. **Perez-Rueda, E., and S. C. Janga.** Identification and genomic analysis of transcription factors in archaeal genomes exemplifies their functional architecture and evolutionary origin. Mol Biol Evol.

19. **Pritchett, M. A., J. K. Zhang, and W. W. Metcalf.** 2004. Development of a markerless genetic exchange method for Methanosarcina acetivorans C2A and its

use in construction of new genetic tools for methanogenic archaea. Appl Environ Microbiol **70:**1425-33.

20. **Reichlen, M. J., K. S. Murakami, and J. G. Ferry.** Functional Analysis of the Three TATA Binding Protein Homologs in Methanosarcina acetivorans. J Bacteriol **192:**1511-7.

21. **Rother, M., and W. W. Metcalf.** 2005. Genetic technologies for Archaea. Curr Opin Microbiol **8:**745-51.

22. **Sandman, K., and J. N. Reeve.** 2006. Archaeal histones and the origin of the histone fold. Curr Opin Microbiol **9:**520-5.

23. **Sowers, K. R., J. E. Boone, and R. P. Gunsalus.** 1993. Disaggregation of Methanosarcina spp. and Growth as Single Cells at Elevated Osmolarity. Appl Environ Microbiol **59:**3832-3839.

24. **Weidenbach, K., J. Gloer, C. Ehlers, K. Sandman, J. N. Reeve, and R. A. Schmitz.** 2008. Deletion of the archaeal histone in Methanosarcina mazei Go1 results in reduced growth and genomic transcription. Mol Microbiol **67:**662-71.

25. **Wilkinson, S. P., M. Ouhammouch, and E. P. Geiduschek.** Transcriptional activation in the context of repression mediated by archaeal histones. Proc Natl Acad Sci U S A.

26. **Xie, Y., and J. N. Reeve.** 2004. Transcription by an archaeal RNA polymerase is slowed but not blocked by an archaeal nucleosome. J Bacteriol **186:**3492-8.

27. **Zhao, K., M. Liu, and R. R. Burgess.** 2005. The global transcriptional response of Escherichia coli to induced sigma 32 protein involves sigma 32 regulon

activation followed by inactivation and degradation of sigma 32 in vivo. J Biol Chem **280:**17758-68.

# Appendix A

# An unconventional pathway for reduction of $CO_2$ to methane in CO-grown *Methanosarcina acetivorans* revealed by proteomics

## Personal contribution to manuscript

The paper reproduced in this appendix describes a collaborative research effort between the groups of Dr. James G. Ferry (The Pennsylvania State University, University Park, PA) and the Barry L. Karger (Northeastern University, Boston, MA). The paper was published in *The Proceedings of the National Academy of Sciences*[1]. My contributions to this manuscript included cell growth and RNA harvesting for qRT-PCR analysis and transcriptional mapping and transcription start site determination for the *fpo* operon.

---

[1] **Lessner, D.J., Li, L., Li, Q., Rejtar, T., Andreev, V.P., Reichlen, M., Hill, K., Moran, J.J., Karger, B.L. and J.G. Ferry.** 2006. An unconventional pathway for the reduction of $CO_2$ to methane in CO-grown *Methanosarcina acetivorans* revealed by proteomics. PNAS. **103**(47):17921-6.

# An unconventional pathway for reduction of $CO_2$ to methane in CO-grown *Methanosarcina acetivorans* revealed by proteomics

Daniel J. Lessner*, Lingyun Li†, Qingbo Li*‡, Tomas Rejtar†, Victor P. Andreev†, Matthew Reichlen*, Kevin Hill*, James J. Moran§, Barry L. Karger†¶, and James G. Ferry*¶

*Department of Biochemistry and Molecular Biology and Center for Microbial Structural Biology, Pennsylvania State University, 205 South Frear Laboratory, University Park, PA 16802; †Barnett Institute and Department of Chemistry, Northeastern University, Boston, MA 02115; and §Department of Geosciences and Penn State Astrobiology Research Center, Pennsylvania State University, 220 Deike Building, University Park, PA 16802

Communicated by Lonnie O. Ingram, University of Florida, Gainesville, FL, October 5, 2006 (received for review June 27, 2006)

***Methanosarcina acetivorans*** **produces acetate, formate, and methane when cultured with CO as the growth substrate [Rother M, Metcalf WW (2004)** ***Proc Natl Acad Sci USA*** **101:16929–16934], which suggests novel features of CO metabolism. Here we present a genome-wide proteomic approach to identify and quantify proteins differentially abundant in response to growth on CO versus methanol or acetate. The results indicate that oxidation of CO to $CO_2$ supplies electrons for reduction of $CO_2$ to a methyl group by steps and enzymes of the pathway for $CO_2$ reduction determined for other methane-producing species. However, proteomic and quantitative RT-PCR results suggest that reduction of the methyl group to methane involves novel methyltransferases and a coenzyme $F_{420}H_2$:heterodisulfide oxidoreductase system that generates a proton gradient for ATP synthesis not previously described for pathways reducing $CO_2$ to methane. Biochemical assays support a role for the oxidoreductase, and transcriptional mapping identified an unusual operon structure encoding the oxidoreductase. The proteomic results further indicate that acetate is synthesized from the methyl group and CO by a reversal of initial steps in the pathway for conversion of acetate to methane that yields ATP by substrate level phosphorylation. The results indicate that** ***M. acetivorans*** **utilizes a pathway distinct from all known $CO_2$ reduction pathways for methane formation that reflects an adaptation to the marine environment. Finally, the pathway supports the basis for a recently proposed primitive CO-dependent energy-conservation cycle that drove and directed the early evolution of life on Earth.**

anaerobic | Archaea | carbon monoxide

Carbon monoxide (CO), an atmospheric pollutant that binds tightly to hemoglobin, is held below toxic levels in part by both aerobic and anaerobic microbes (1). The microbial metabolism of CO is an important component of the global carbon cycle (1, 2), and CO is believed to have been present in the atmosphere of early Earth that fueled the evolution of primitive metabolisms (3–7). Investigations of aerobic species from the Bacteria domain have contributed important insights into microbial CO oxidation (8, 9), as have investigations of anaerobes from the Bacteria domain that conserve energy by coupling CO oxidation to $H_2$ evolution (10–12). Further understanding has been derived from studies of CO-using anaerobes from the Bacteria domain that conserve energy by oxidizing CO and reducing $CO_2$ to acetate (13, 14) or reducing sulfate to sulfide (15). Far less is known for pathways of the few CO-using species in the Archaea domain that have been described. *Methanothermobacter thermautotrophicus*, *Methanosarcina barkeri*, and *Methanosarcina acetivorans* obtain energy for growth by converting CO to methane (16–20). Although methane formation from CO first was reported in 1947 (21), a comprehensive understanding of the overall pathway for any species has not been reported. It is postulated that *M. barkeri* oxidizes CO to $H_2$, and the $H_2$ is reoxidized to provide electrons for reducing $CO_2$ to methane (16). It is postulated further that $H_2$ production is essential for ATP synthesis during growth on CO (16, 22, 23). *M. acetivorans* was isolated from marine sediments where giant kelp is decomposed to methane (24). The flotation bladders of kelp contain CO that is a presumed substrate for *M. acetivorans* in nature. *M. acetivorans* produces acetate and formate in addition to methane during CO-dependent growth (17), the first report of any product in addition to methane and $CO_2$ during growth of methane-producing species. Further, $H_2$ was not detected during growth on CO (17). These unorthodox characteristics suggest that the pathway for metabolism of CO and mechanisms for energy conservation by *M. acetivorans* are unique among methane-producing Archaea. Here we describe a global proteomic analysis of CO metabolism in *M. acetivorans*. The results suggest that the pathway for methane formation involves novel methyltransferases and a mechanism for energy conservation not previously reported for $CO_2$-reducing pathways. Finally, the results provide support for the basis of a recent proposal that acetate formation from CO in *M. acetivorans* is the vestige of a primitive energy-conservation cycle that drove and directed the early evolution of life on Earth (7).

## Results and Discussion

Fig. 1 shows the time course obtained for CO-dependent growth of *M. acetivorans*. Acetate, formate, methane, and $CO_2$ were end products, and $H_2$ was not detected (limit of detection = 0.008%). These results are consistent with the previous report for CO-dependent growth of *M. acetivorans* (17) except that production of methane significantly exceeded acetate throughout growth and only minor amounts of formate was produced (Fig. 1). The after-growth carbon balance indicated that no other reduced products were synthesized. These results indicate that $CO_2$ reduction to methane plays a prominent role in supporting CO-dependent growth of *M. acetivorans*.

A high-sensitivity liquid chromatography/mass spectrometry analysis, using a hybrid linear ion trap/Fourier-transform ion cyclotron resonance (LTQ/FTICR)-MS, was used to identify, quantify, and compare individual proteins from CO-grown cells metabolically labeled with $^{14}N$ with separately methanol-grown and acetate-grown cells labeled with $^{15}N$. Abundance ratios of 1,023 proteins were obtained for CO versus methanol grown cells and 846 proteins for CO versus acetate grown cells, corresponding to a total of 1,125 unique proteins (Table 4, which is

Author contributions: B.L.K. and J.G.F. designed research; D.J.L., L.L., Q.L., T.R., M.R., K.H., and J.J.M. performed research; D.J.L., L.L., T.R., V.P.A., B.L.K., and J.G.F. analyzed data; and D.J.L., B.L.K., and J.G.F. wrote the paper.

The authors declare no conflict of interest.

Abbreviations: THMPT, tetrahydromethanopterin; MF, methanofuran; CoB, coenzyme B; CoM, coenzyme M.

‡Present address: Center for Pharmaceutical Biotechnology and Department of Microbiology and Immunology, University of Illinois, Chicago, IL 60607-7173.

¶To whom correspondence may be addressed. E-mail: jgf3@psu.edu or b.karger@neu.edu.

© 2006 by The National Academy of Sciences of the USA

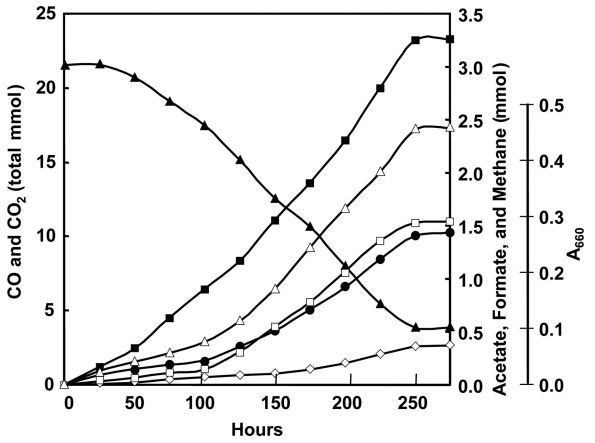


**Fig. 1.** Time course of growth by *Methanosarcina acetivorans* C2A with CO as the sole source of carbon and energy. Each point is the mean of five replicate cultures. ●, $CO_2$; ▲, CO; ■, $CH_4$; □, acetate; △, $A_{660}$; ◇, formate.

published as supporting information on the PNAS web site), representing 25% of the 4,524 genes reported in the genome (25). Of these unique proteins, 99 were found to have ≥3-fold differential abundance between CO- and methanol-grown cells and 176 between CO- and acetate-grown cells. Of the 1,125 proteins in Table 4, many were annotated for functions in pathways for methane formation from the dismutation of methanol, reduction of $CO_2$, and fermentation of acetate (Table 1). The function of these proteins and their differential abundance (Table 1) lead to the pathway for conversion of CO to acetate and methane shown in Fig. 2. No evidence has been reported for the mechanism of formate production (17), and the proteomic analyses reported here yield no clues as to the mechanism; thus, a pathway for production of formate is not shown in Fig. 2.

In the pathway shown in Fig. 2, $CO_2$ is reduced to methyl-tetrahydromethanopterin (THMPT) in steps 2–6 catalyzed by paralogs of enzymes characterized from $CO_2$-reducing methanoarchaea (26). Enzymes catalyzing steps 2, 3, 5, and 6 were at least 10-fold more abundant in CO-grown versus acetate-grown *M. acetivorans*, and the enzyme catalyzing step 4 was 2-fold greater (Table 1). These steps and enzymes are not involved in acetate fermentation to methane (27); thus, the results suggest these enzymes are differentially abundant in response to CO and support roles in steps 2–6. Further, *M. acetivorans*, like other *Methanosarcina* species, utilizes a reversal of steps 2–6 in the pathway of methanol dismutation to $CO_2$ and $CH_4$ (28, 29); thus, the finding that each of the five enzymes was at approximately the same levels in CO-grown versus methanol-grown cells further supports roles in steps 2–6 (Fig. 2). Subunits of both the molybdenum (MA0304–MA0309) and tungsten (MA0832–MA0835) forms of formylmethanofuran (MF) dehydrogenase catalyzing step 2 were substantially elevated in CO-grown versus acetate-grown cells, a result suggesting both metal forms function during growth on CO. However, the relative levels between CO- and methanol- or acetate-grown cells suggest that the tungsten form is favored during growth on CO.

Pathways for methanogenesis from all substrates involve an eight-subunit methyl-THMPT:HS-coenzyme M (CoM) methyl transferase (MtrABCDEFGH) complex that contains a methyl-accepting corrinoid cofactor (30). However, several subunits of the Mtr complex encoded by MA0269–MA0276 were detected with a 9-fold mean lower abundance in CO-grown versus acetate-grown *M. acetivorans* (Table 1), suggesting down-regulation of the complex in response to growth with CO that is supported by quantitative RT-PCR results obtained for expression of MA0269, MA0272, and MA0276 (Table 2). These results were in contrast to the relative abundances of McrA (MA4546) and McrG (MA4547) from the three-subunit $CH_3$-S-CoM methyl reductase (McrABG) that is essential to all methanogenic pathways. Both McrA and McrG were approximately equal in abundance in CO-grown versus acetate- or methanol-grown cells (Table 1), a result confirming the expected role in catalyzing step 8 (Fig. 2) of the pathway for methanogenesis. Thus, the proteomic and RT-PCR results obtained for the Mtr subunits suggest a substantially diminished role for the Mtr complex in catalyzing step 7 (Fig. 2) compared with all other pathways for methanogenesis. Although unable to grow on methanol, a mutant of *M. barkeri* disrupted in the *mtr* operon is able to produce methane from methanol (31), providing experimental evidence for an uncharacterized alternative to the Mtr complex. Thus, it was interesting that the products of MA0859 and MA4384 were robustly elevated in CO-grown versus methanol-grown and CO-grown versus acetate-grown *M. acetivorans*, respectively (Table 1). Based on sequence analysis, these genes are predicted to encode putative methyl transferases (25) and are annotated as corrinoid proteins (www.tigr.org) consistent with this function. Quantitative RT-PCR analyses (Table 2) showed MA0859 and MA4384 substantially up-regulated in CO-grown versus acetate-grown cells. MA4558, encoding a third putative methyl transferase (25) and annotated as encoding a corrinoid protein (www.tigr.org), was up-regulated in CO-grown versus acetate-grown cells (Table 2). Further, the products of MA0859, MA4384, and MA4558 have >55% sequence identity to each other, and all three putative methyl transferases contain a C-terminal domain not found in other corrinoid-containing proteins. These results encourage investigation to determine whether the products of MA0859, MA4384, and MA4558 function in step 7 (Fig. 2).

The genome is annotated (www.tigr.org) with several CO dehydrogenases that have the potential to catalyze step 1a, providing $CO_2$ and electrons for steps 2, 5, 6, 8, 9, and 10 in the pathway for methanogenesis (Fig. 2). MA1309 and MA3282 are annotated as encoding CooS, the CO dehydrogenase first described in *Rhodospirillum rubrum* (32). The products of MA1309 and MA3282 were not detected in CO-grown cells (Table 4), although quantitative RT-PCR analysis (Table 2) indicated modest up-regulation of MA1309 in CO-grown versus acetate-grown cells consistent with a role for this CO dehydrogenase in the oxidation of CO. Although the CooS paralog in *R. rubrum* reduces ferredoxin (33), the enzyme in *M. acetivorans* has not been investigated, and the electron acceptor is unknown. The genome also is annotated (www.tigr.org) with duplicate gene clusters (MA1011–MA1016 and MA3860–MA3865), each encoding paralogs of a five-subunit CO dehydrogenase/acetyl-CoA synthase (CdhABCDE) complex first described in *Methanosarcina thermophila* (34, 35). Three subunits (MA1014–MA1016 and MA3860–MA3862) from each complex were detected and found to be elevated an average of 20-fold in CO-grown versus methanol-grown cells in contrast to an ≈2-fold differential abundance versus acetate-grown cells (Table 1). The Cdh complex is not involved in the pathway for conversion of methanol to methane but is central to the pathway for conversion of acetate to methane of *Methanosarcina* species (26); thus, the relative levels in CO-grown versus methanol- or acetate-grown *M. acetivorans* suggest a role for the duplicate CdhABCDE complexes during growth on CO. Although the CdhABCDE complex of *Methanosarcina* species oxidizes CO and reduces ferredoxin (36, 37), consistent with a role in steps 1a and 1b (Fig. 2), a more certain function is catalysis of step 11 as described below.

Regardless which CO dehydrogenase functions in step 1a (Fig. 2), reduction of ferredoxin (step 1b) is most likely essential when considering ferredoxin has been proposed as the direct electron donor for formyl-MF dehydrogenases (38, 39) (step 2). Further, reduced coenzyme $F_{420}$ is the direct electron donor for characterized enzymes (26) catalyzing steps 5 and 6 (Fig. 2); thus, a mechanism for reducing $F_{420}$ also is expected (step 1c). Characterization of the CooS CO dehydrogenase from any methanogen has

**Table 1. Relative abundance of selected proteins in CO-grown versus methanol-grown and CO-grown versus acetate-grown *M. acetivorans* strain C2A**

| | | | ME/CO | | AC/CO | |
|---|---|---|---|---|---|---|
| Step* | Loci | Annotation† | Unique peptides‡ | Differential abundance | Unique peptides‡ | Differential abundance |
| 1a, 11 | 1014 | CO dehydrogenase/acetyl-CoA synthetase subunit, CdhC | 4 | 0.05 ± 0.01 | 28 | 1.40 ± 0.05 |
| 1a, 11 | 1015 | CO dehydrogenase/acetyl-CoA synthetase subunit, CdhB | 4 | 0.05 ± 0.01 | 11 | 4.1 ± 0.2 |
| 1a, 11 | 1016 | CO dehydrogenase/acetyl-CoA synthetase subunit, CdhA | 6 | 0.06 ± 0.01 | 44 | 2.8 ± 0.1 |
| 1a, 11 | 3860 | CO dehydrogenase/acetyl-CoA synthetase subunit, CdhA | 7 | 0.04 ± 0.01 | 17 | 0.32 ± 0.01 |
| 1a, 11 | 3861 | CO dehydrogenase/acetyl-CoA synthetase subunit, CdhB | 6 | 0.05 ± 0.01 | 9 | 0.60 ± 0.03 |
| 1a, 11 | 3862 | CO dehydrogenase/acetyl-CoA synthetase subunit, CdhC | 2 | 0.06 ± 0.01 | 36 | 0.43 ± 0.03 |
| 2 | 0304 | (Mo) formyl-methanofuran dehydrogenase subunit, FmdE | 4 | 1.9 ± 0.3 | ND | ND |
| 2 | 0305 | (Mo) formyl-methanofuran dehydrogenase subunit, FmdF | 5 | 1.8 ± 0.3 | 4 | 0.13 ± 0.04 |
| 2 | 0306 | (Mo) formyl-methanofuran dehydrogenase subunit, FmfA | 4 | 2.0 ± 0.3 | ND | ND |
| 2 | 0307 | (Mo) formyl-methanofuran dehydrogenase subunit, FmfC | 8 | 1.6 ± 0.2 | 2 | 0.14 ± 0.03 |
| 2 | 0308 | (Mo) formyl-methanofuran dehydrogenase subunit, FmfD | 6 | 2.0 ± 0.2 | 3 | 0.14 ± 0.01 |
| 2 | 0309 | (Mo) formyl-methanofuran dehydrogenase subunit, FmdB | 4 | 2.1 ± 0.7 | 2 | 0.11 ± 0.01 |
| 2 | 0832 | (W) formyl-methanofuran dehydrogenase subunit, FwdC | 2 | 0.22 ± 0.02 | 4 | 0.014 ± 0.001 |
| 2 | 0833 | (W) formyl-methanofuran dehydrogenase subunit, FwdA | 4 | 0.26 ± 0.03 | 2 | 0.015 ± 0.001 |
| 2 | 0834 | (W) formyl-methanofuran dehydrogenase subunit, FwdB | 3 | 0.29 ± 0.04 | 2 | 0.01 ± 0.002 |
| 2 | 0835 | (W) formyl-methanofuran dehydrogenase subunit, FwdD | 3 | 0.19 ± 0.02 | 2 | 0.011 ± 0.003 |
| 3 | 0010 | Formyl-methanofuran:THMPT formyltransferase | 5 | 1.1 ± 0.3 | 6 | 0.11 ± 0.01 |
| 4 | 1710 | Methenyl-THMPT cyclohydrolase | 11 | 1.4 ± 0.1 | 11 | 0.51 ± 0.01 |
| 5 | 4430 | Methylene-THMPT dehydrogenase | 20 | 0.55 ± 0.15 | 5 | 0.010 ± 0.001 |
| 6 | 3733 | Methylene-THMPT reductase ($F_{420}$-dependent) | 21 | 0.60 ± 0.2 | 22 | 0.093 ± 0.003 |
| 7 | 0269 | Methyl-THMPT:CoM methyltransferase subunit, MtrH | 5 | 3.1 ± 0.7 | 10 | 8.0 ± 0.3 |
| 7 | 0270 | Methyl-THMPT:CoM methyltransferase subunit, MtrG | 3 | 3.2 ± 0.2 | 2 | 9.4 ± 0.5 |
| 7 | 0272 | Methyl-THMPT:CoM methyltransferase subunit, MtrA | 6 | 2.8 ± 0.4 | 10 | 7.9 ± 0.2 |
| 7 | 0273 | Methyl-THMPT:CoM methyltransferase subunit, MtrB | 3 | 3.4 ± 0.3 | 2 | 11 ± 1 |
| 7 | 0274 | Methyl-THMPT:CoM methyltransferase subunit, MtrC | 2 | 3.1 ± 0.7 | 2 | 10 ± 1 |
| 7 | 0859 | Hypothetical protein | 2 | 0.02 ± 0.005 | ND | ND |
| 7 | 4384 | Hypothetical protein | ND | ND | 2 | 0.02 ± 0.002 |
| 8 | 4546 | Methyl-CoM reductase subunit, McrA | 12 | 0.90 ± 0.2 | 29 | 1.41 ± 0.05 |
| 8 | 4547 | Methyl-CoM reductase subunit, McrG | 14 | 0.83 ± 0.3 | 20 | 1.41 ± 0.03 |
| 8 | 4550 | Methyl-CoM reductase subunit, McrB | 15 | 1.1 ± 0.3 | 21 | 1.6 ± 0.1 |
| 9 | 0687 | Heterodisulfide reductase subunit, HdrE | 3 | 0.5 ± 0.2 | 4 | 0.86 ± 0.2 |
| 9 | 0688 | Heterodisulfide reductase subunit, HdrD | 8 | 0.52 ± 0.1 | 14 | 0.75 ± 0.02 |
| 10 | 1495 | $F_{420}H_2$ dehydrogenase, subunit FpoA | 3 | 0.88 ± 0.04 | 2 | 0.014 ± 0.002 |
| 10 | 1496 | $F_{420}H_2$ dehydrogenase subunit, FpoB | 1 | 0.43 | 3 | 0.03 ± 0.002 |
| 10 | 1497 | $F_{420}H_2$ dehydrogenase subunit, FpoC | 4 | 0.66 ± 0.05 | 7 | 0.025 ± 0.002 |
| 10 | 1498 | $F_{420}H_2$ dehydrogenase subunit, FpoD | 5 | 0.52 ± 0.11 | 5 | 0.01 ± 0.001 |
| 10 | 1499 | $F_{420}H_2$ dehydrogenase subunit, FpoH | 6 | 0.6 ± 0.2 | 6 | 0.02 ± 0.002 |
| 10 | 1500 | $F_{420}H_2$ dehydrogenase subunit, FpoI | 3 | 0.5 ± 0.1 | 3 | 0.01 ± 0.002 |
| 10 | 1503 | $F_{420}H_2$ dehydrogenase subunit, FpoK | 1 | 0.5 | 1 | 0.02 |
| 10 | 1504 | $F_{420}H_2$ dehydrogenase subunit, FpoL | 1 | 0.56 | 1 | 0.02 |
| 10 | 1505 | $F_{420}H_2$ dehydrogenase subunit, FpoM | 1 | 0.5 | ND | ND |
| 10 | 1506 | $F_{420}H_2$ dehydrogenase subunit, FpoN | 3 | 0.47 ± 0.04 | 2 | 0.01 ± 0.002 |
| 10 | 1507 | $F_{420}H_2$ dehydrogenase subunit, FpoO | 3 | 0.26 ± 0.02 | 2 | 0.01 ± 0.002 |
| 12 | 3607 | Phosphotransacetylase | 12 | 0.47 ± 0.11 | 19 | 4.4 ± 0.2 |
| 13 | 3606 | Acetate kinase | 4 | 0.15 ± 0.01 | 20 | 4.3 ± 0.2 |

ND, although the signals in CO-grown cells were robust, the ratio could not be determined because of signals below background for peptides from either acetate- or methanol-grown cells. ME, methanol-grown cells. CO, CO-grown cells. AC, acetate-grown cells.
*See Fig. 1.
†Annotations are listed at www.tigr.org.
‡Number of unique peptides used for quantitation.

not been reported, and the electron acceptor is unknown. Although ferredoxin is the electron acceptor for CooS from *Rhodospirillum rubrum* (33), reduction of $F_{420}$ by the CooS homolog from *M. acetivorans* cannot be ruled out. None of the proteins detected in the proteome of CO-grown *M. acetivorans* (Tables 1 and 4) have the potential to oxidize ferredoxin and reduce $F_{420}$, and the mechanism by which $F_{420}$ is reduced is unknown.

In all known methanogenic pathways, the reduction of $CH_3$-S-CoM with coenzyme B (HS-CoB) (step 8) produces the heterodisulfide of CoM-S-S-CoB, which requires reduction of the disulfide bond by a heterodisulfide reductase (step 9) to regenerate the sulfhydryl forms of the cofactors (Fig. 2). Both subunits of the HdrDE heterodisulfide reductase (MA0688 and MA0687) were present in CO-grown cells, which approximated the amounts in methanol- or acetate-grown cells (Table 1). HdrDE functions in the pathway for conversion of methanol to methane in all *Methanosarcina* species investigated (40) and is proposed to function in the pathway for conversion of acetate to methane in *M. thermophila*

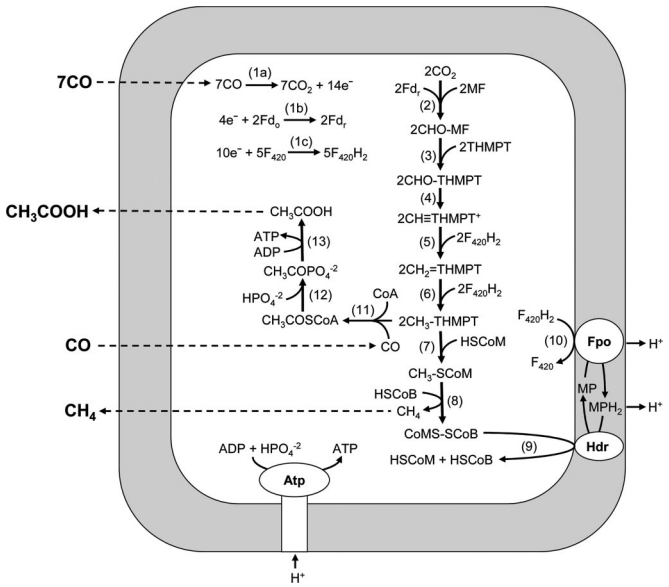


**Fig. 2.** Pathway proposed for the conversion of CO to acetate and methane by *M. acetivorans*. Proposed enzymes catalyzing steps 1–13 are indicated in Table 1. $Fd_o$, oxidized ferredoxin; $Fd_r$, reduced ferredoxin; $F_{420}$, coenzyme $F_{420}$; MF, methanofuran; THMPT, tetrahydromethanopterin; HSCoM, coenzyme M; HSCoB, coenzyme B; Fpo, $F_{420}H_2$ dehydrogenase complex; MP, methanophenazine; Hdr, heterodisulfide reductase.

(41) and *M. barkeri* (42). Thus, the relative levels of HdrDE in CO-grown versus acetate- or methanol-grown cells (Table 1) support a role for HdrDE in step 9 of the pathway for conversion of CO to methane by *M. acetivorans* (Fig. 2). In obligate $CO_2$-reducing methanogens, reduction of CoM-S-S-CoB is accomplished by the HdrABC-type of heterodisulfide reductase, and electrons are supplied to it from $H_2$ catalyzed by the MvhAGD hydrogenase (43). *M. acetivorans* is unable to grow by reducing $CO_2$ to methane with $H_2$ (24), and genes encoding the MvhAGD hydrogenase are absent from the genome (www.tigr.org). Thus, a major role for HdrABC is improbable during growth with CO.

The electron donor to the membrane-bound HdrDE in all *Methanosarcina* species previously investigated is methanophenazine, a membrane-bound quinone-like electron carrier that pumps protons to the outside upon reduction and oxidation (40). In the methanol pathway, methanophenazine transfers electrons from the $F_{420}H_2$ dehydrogenase complex (FpoABC-DHIJKLMNO) to HdrDE (40). The 12-subunit Fpo complex is membrane-bound and also functions as a proton pump. The genome of *M. acetivorans* is annotated with a gene cluster (MA1495–MA1507) encoding a Fpo complex for which the products of 11 subunits were found in CO-grown *M. acetivorans* at approximately the same levels as in methanol-grown cells (Table 1). Furthermore, the amounts were considerably more abundant in CO-grown versus acetate-grown cells where the Fpo complex does not function (27). $F_{420}H_2$:CoB-S-S-CoM oxidoreductase activity in cell extracts of CO-grown *M. acetivorans* was approximately 2- and 10-fold greater than for methanol- and acetate-grown cells, respectively (Table 3). Although unprecedented in pathways for the reduction of $CO_2$ to methane, these results support a role for the Fpo complex, methanophenazine, and HdrDE in generation of a proton gradient that drives ATP synthesis in the pathway for CO-dependent reduction of $CO_2$ to methane by *M. acetivorans* (Fig. 2, step 10). Transcriptional mapping indicated that the Fpo complex is encoded in an operon of 14 genes (Fig. 3*A*) containing duplicate *fpoJ* genes and an additional ORF (MA1494) annotated as a predicted protein (www.tigr.org), unique to *M. acetivorans*, that we designate here as *fpoP* (Fig. 3*A*). The sequence upstream of MA1494 contained a typical archaeal TATA-box (Fig. 3*B*), and a transcription start site was identified 22 nucleotides downstream of the TATA-box. Quantitative RT-PCR showed that MA1494 is up-regulated in CO-grown versus acetate-grown cells consistent with the differential abundances of other Fpo subunits encoded in the operon (Table 1). These results suggest that the Fpo complex of CO-grown *M. acetivorans* may have an unique subunit composition compared with other characterized Fpo complexes.

As discussed above, the relative abundances of subunits from two CdhABCDE complexes in CO-grown versus methanol- and acetate-grown *M. acetivorans* (Table 1) suggest a role during growth on CO. Although oxidation of CO to $CO_2$ is one potential role, the most probable function is synthesis of acetyl-CoA from methyl-THMPT, CO, and CoA in step 11 (Fig. 2). The first CdhABCDE complex to be described was isolated from acetate-grown *M. thermophila* where it functions to cleave acetyl-CoA (34), the reverse of step 11 (Fig. 2). However, the reported synthesis of acetyl-CoA from CO, $CH_3I$, and CoA by the Cdh complex from *M. thermophila* (44) supports a role for the Cdh complex as shown in step 11 of the pathway for CO conversion to acetate by *M. acetivorans* (Fig. 2). The duplicate CdhABCDE complexes encoded by MA1011–MA1016 and MA3860–MA3865 of *M. acetivorans* share >90% amino acid sequence identity (www.tigr.org), consistent with a similar function. A remarkable feature of the genomic sequence of *M. acetivorans* and *Methanosarcina mazei* is the extensive gene redundancy that has raised questions regarding the expression of duplicated genes (25, 45). As discussed above, the differential abundances for subunits of the duplicate CdhABCDE complexes in CO-grown versus methanol- or acetate-grown *M. acetivorans* (Table 1) indicate that both complexes are present in high amounts in CO-grown cells.

**Table 2. Expression ratios of genes in acetate-grown versus CO-grown *M. acetivorans* determined by quantitative RT-PCR**

| Step* | Gene | Annotation† | Ratio (AC/CO) |
|---|---|---|---|
| 1a | MA1309 | CO dehydrogenase CooS | 0.35 ± 0.04 |
| 1a | MA3282 | CO dehydrogenase CooS | 3.6 ± 0.7 |
| 7 | MA0269 | Methyl-THMPT:CoM Methyltransferase subunit, MtrH | 6.6 ± 1.5 |
| 7 | MA0272 | Methyl-THMPT:CoM Methyltransferase subunit, MtrA | 9.6 ± 1.3 |
| 7 | MA0276 | Methyl-THMPT:CoM Methyltransferase subunit, MtrE | 7.1 ± 1.4 |
| 7 7 | MA0859 | Corrinoid protein | 0.035 ± 0.010 |
| 7 | MA4384 | Corrinoid protein | 0.0012 ± 0.0005 |
| 10 | MA4558 | Corrinoid protein | 0.0092 ± 0.0005 |
| | MA1494 | Predicted protein | 0.25 ± 0.04 |

AC, acetate-grown. CO, CO-grown.
*See Fig. 1.
†Annotations are listed at www.tigr.org.

**Table 3. Coenzyme $F_{420}H_2$:CoB-S-S-CoM oxidoreductase activity in cell extracts of CO-, methanol-, and acetate-grown *M. acetivorans***

| Growth substrate | Specific activity* |
|---|---|
| CO | 60.9 ± 4.5 |
| Methanol | 32.0 ± 3.6 |
| Acetate | 6.6 ± 0.8 |

Assays were performed in triplicate as described in the text. Each assay contained 30–50 μg of cell extract and 20 μM $F_{420}H_2$. Assays were initiated by addition of CoB-S-S-CoM (90 μM).
*Expressed as nmol/min per mg of protein.

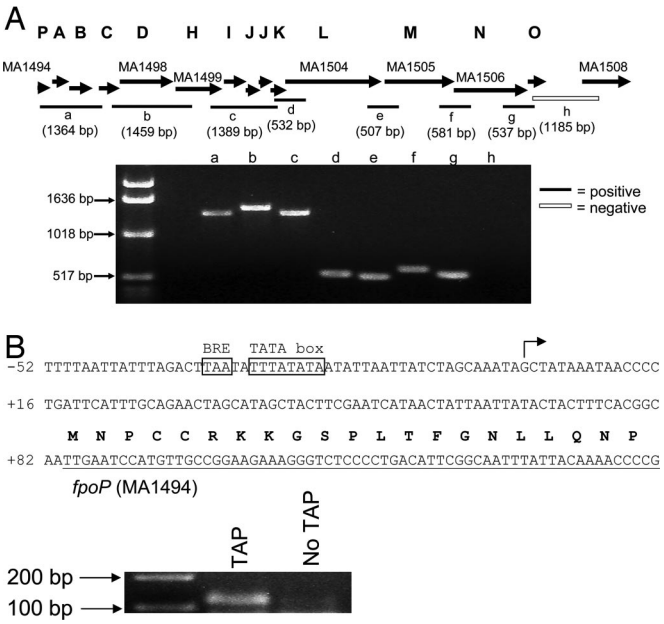


**Fig. 3.** Transcriptional mapping of the *fpoPABCDHIJJKLMNO* operon of *M. acetivorans*. (*A*) Cotranscription determined by RT-PCR. Uppercase letters refer to subunits encoded by the genes represented by arrows showing the direction of transcription. Predicted RT-PCR products are represented by lines under the genes and are labeled with lowercase letters. Predicted RT-PCR product sizes are shown in parentheses. Letters above the gel lanes correspond to predicted RT-PCR products. RT-PCR was performed with total RNA from CO-grown *M. acetivorans*. (*B*) Transcription start site identified by RNA ligation-mediated RT-PCR. The coding region for MA1494 is underlined, and the deduced sequence of the first 21 aa is shown in bold above the nucleotide sequence. The boxed sequences indicate the putative TATA-box and TFB recognition element (BRE). RT-PCRs performed with RNA templates treated and untreated with tobacco acid pyrophosphatase (TAP) are shown in gel lanes labeled "TAP" and "No TAP," respectively. The RT-PCR product amplified exclusively in the TAP-treated RNA sample was isolated and sequenced. The junction site between the exogenous oligonucleotide sequence and *M. acetivorans* sequence identified the transcription start site (G at +1) denoted by the arrow.

A role for phosphotransacetylase (MA3607) and acetate kinase (MA3606) in the pathway for conversion of CO to acetate (Fig. 2, steps 12 and 13) was demonstrated previously (17). Both enzymes were ≈4-fold less abundant in CO-grown versus acetate-grown cells (Table 1); however, 50- and 18-fold greater amounts of acetate kinase and phosphotransacetylase are reported for acetate-grown versus methanol-grown *M. acetivorans* (27), suggesting substantial amounts of both enzymes in acetate-grown cells. Thus, although lower amounts were detected in CO-grown versus acetate grown cells (Table 1), the levels of acetate kinase and phosphotransacetylase have the potential to supply adequate amounts for synthesis of acetate from acetyl-CoA during growth on CO. These results are consistent with a previous report (17) and suggest that the production of acetate yields ATP via a substrate level phosphorylation. Thus, ATP is synthesized by substrate level phosphorylation (Fig. 2, step 13) and driven by a proton gradient coupled to electron transport from $F_{420}H_2$ to CoB-S-S-CoM (Fig. 2, steps 9 and 10). The pathway in Fig. 2 provides support for the basis of the recent proposal that CO conversion to acetate in methanogens is the vestige of a primitive energy conservation cycle that was the dominant force that drove and directed the early evolution of life, including methanogenic pathways (7).

It has been proposed that CO-dependent growth of methanogens other than *M. acetivorans* involves oxidation of CO to $H_2$ and reoxidation of the $H_2$ to supply electrons for the reduction of $CO_2$ to methane (16). The pathway shown in Fig. 2 is independent of $H_2$ and consistent with the report that $H_2$ is not a metabolite during CO-dependent growth of *M. acetivorans* (17). The only mechanism reported for energy conservation in the $CO_2$-reduction pathway for methanogenesis is the reduction of CoB-S-S-CoM with $H_2$, which generates a proton gradient driving ATP synthesis (46). The $H_2$:CoB-S-S-CoM oxidoreductase system is composed of the MvhAGD hydrogenase (43) and the HdrABC-type of heterodisulfide reductase (47). As previously discussed, the evidence presented here suggests neither enzyme functions in the pathway for $CO_2$ reduction to methane during CO-dependent growth of *M. acetivorans*. Instead, it appears *M. acetivorans* has adopted a $H_2$-independent mechanism for energy conservation from the pathway for conversion of methanol to methane wherein the $F_{420}H_2$:CoB-S-S-CoM system shown in Fig. 2 (steps 9 and 10) also functions to pump protons for energy conservation. However, based on the transcriptional analysis presented above, it is tempting to speculate that adoption of the $F_{420}H_2$:CoB-S-S-CoM system for growth on CO may have required the addition of another subunit encoded by MA1494. The inability of *M. acetivorans* to metabolize $H_2$ suggests that CO-dependent reduction of $CO_2$ to formyl-MF (Fig. 2, step 2) also is different from previously characterized $CO_2$-reduction pathways of methanogens. The oxidation of $H_2$ and reduction of $CO_2$ to produce formyl-MF is endergonic, and it has been shown that *M. barkeri* employs the Ech hydrogenase complex to catalyze the oxidation of $H_2$ that is driven by an ion gradient (39, 48). The genome of *M. acetivorans* does not encode a functional Ech hydrogenase (25) (www.tigr.org); however, the reduction of $CO_2$ to formyl-MF with CO as the electron donor is exergonic and does not require $H_2$ and the Ech hydrogenase to drive the reaction (38). The $H_2$-independent pathway in Fig. 2 also is consistent with the marine environment from which *M. acetivorans* was isolated (24). In marine environments sulfate-reducing microbes outcompete methanogens for $H_2$ (49); thus, if $H_2$ was an intermediate in metabolism, it could be lost to sulfate reducers. Indeed, it was shown recently that the electron transport chain in acetate-grown *M. acetivorans* does not involve $H_2$ (27) in contrast to acetate-grown freshwater *Methanosarcina* species for which it is proposed that $H_2$ and the Ech hydrogenase plays an essential role in electron transport and energy conservation (39, 48).

## Conclusions

A highly sensitive proteomic analysis has identified proteins differentially abundant in CO-grown versus methanol- and acetate-grown *M. acetivorans*, revealing steps and enzymes in the decidedly unusual pathway of CO conversion to acetate and methane. Although the pathway involves reduction of $CO_2$ to $CH_3$-THMPT, similar to known $CO_2$-reduction pathways, subsequent reduction of the methyl group from $CH_3$-THMPT to methane appears to involve novel methyltransferases and a mechanism for energy conservation different from known pathways for $CO_2$ reduction to methane. This unusual pathway is consistent with the idea that marine methanogens have evolved pathways independent of $H_2$. Finally, the results support the basis for a recent proposal that the pathway for acetate formation from CO is the vestige of an ancient energy-conservation mechanism that directed the early evolution of life including the $CO_2$-reduction and acetate fermentation pathways for methanogenesis.

## Materials and Methods

**Growth of *M. acetivorans* and Preparation of Samples for MS Analysis.** *M. acetivorans* C2A (DSM 804) was grown in high-salt media (50) with one of three growth substrates: (*i*) 1.0 atm of CO (1 atm = 101.3 kPa), (*ii*) 100 mM acetate, or (*iii*) 250 mM methanol. For the methanol and acetate-grown cultures, $^{14}NH_4Cl$ was substituted with $^{15}NH_4Cl$ (98%) (Sigma, St. Louis, MO). Cells were harvested in the midexponential phase of growth at an $A_{660}$ of 0.3 (CO-grown), 0.8 (acetate-grown), and 0.6 (methanol-grown) as previously described (28, 29). Headspace gases and acetate were

quantified by gas chromatographical analysis as described in ref. 51. Formate quantification was performed as described in ref. 52.

**Protein Identification and Abundance Ratio Determinations.** Protein identification and quantitation is described in detail in a separate publication (53). Briefly, extracted proteins were combined in a 1:1 mass ratio to generate two samples: CO versus methanol and CO versus acetate. Then, these samples were separated by SDS/PAGE and each gel lane was cut into 10 bands of approximately similar density. Each band was in-gel-digested with trypsin, as described in ref. 54. Each sample was analyzed by liquid chromatography-tandem MS by using the Ultimate LC system (Dionex, Sunnyvale, CA) coupled to linear ion trap/Fourier-transform (LTQ-FT)-MS instrument (Thermo Electron, Waltham, MA), followed by separate sequential Sequest (55) searches for $^{15}N$ and $^{14}N$ peptides against the National Center for Biotechnology Information's database of *M. acetivorans* C2A (downloaded June 2005). Peptides with cross correlation values (Xcorr) >1.5 (1+), 2.0 (2+), and 2.5 (3+) and precursor mass within ±15 ppm of the theoretical mass initially were selected. Then, a protein list was composed, and proteins associated with probabilities >0.9 as calculated by ProteinProphet (56) were accepted as correct identifications. The protein abundance ratios were calculated based on areas of chromatographic peaks corresponding to individual peptides by using an in-house developed program, QN (53). For the most part, protein ratios were determined from at least two unique peptides. The average coefficient of variance of the observed protein abundance ratios was 9%, and approximately one-half of all proteins was quantitated with a coefficient of variance of <5%.

**$F_{420}H_2$:CoB-S-S-CoM Oxidoreductase Assay.** Activity was monitored spectrophotometrically with a Beckman (Fullerton, CA) DU-7400 inside an anaerobic chamber (Coy Laboratory Products, Grass Lake MI) with a screw-cap cuvette. $F_{420}$ was chemically reduced with $NaBH_4$ as described in ref. 57. $F_{420}H_2$ oxidation was assayed under nitrogen in 0.3 ml of 50 mM Hepes, pH 7.5, containing 2 mM dithioerythritol and 20 $\mu$M $F_{420}H_2$. After adding 30–50 $\mu$g of cell extract, the cuvette was incubated for 5 min until a stable baseline was reached. The reaction was started by addition of 2 $\mu$l of CoB-S-S-CoM (final concentration, 90 $\mu$M) and followed spectrophotometrically at 420 nm. The reaction rate was calculated from an extinction coefficient of 42.5 $mM^{-1}$ $cm^{-1}$ for $F_{420}$ at 420 nm.

**Transcriptional Mapping.** Total RNA was isolated from CO-grown *M. acetivorans* cells and RT-PCR was performed as described in ref. 27. RNA ligation-mediated (RLM) RT-PCR was performed as described in ref. 58 except that RT-PCR was carried out with an Access RT-PCR kit (Promega, Madison, WI). Primers used are listed in Table 5, which is published as supporting information on the PNAS web site.

**Quantitative RT-PCR.** *Taq*man assays were performed by using total RNA isolated from acetate-, methanol-, or CO-grown *M. acetivorans* C2A cells harvested at midexponential phase. *Taq*man primers and probes were designed with Primer Express 1.0 (Applied Biosystems, Foster City, CA). Primers were synthesized on the Bioautomation MerMade 12 (Plano, TX) at the Nucleic Acid Facility of the Pennsylvania State University. Probes were synthesized by Biosearch Technologies (Novato, CA) and were labeled with the reporter dye 6-carboxyfluorescein (6′-FAM) at the 5′ end and with the quencher dye Black Hole Quencher at the 3′ end. Primers and probes are summarized in Table 6, which is published as supporting information on the PNAS web site. cDNA was prepared by using the ABI High Capacity RT kit (Applied Biosystems) and was amplified and quantified on the ABI 7300 Real-Time PCR System (Applied Biosystems). Thermal cycling conditions were as follows: 2 min at 50°C, 10 min at 95°C, followed by 40 cycles of 15 s at 95°C and 1 min at 60°C. Relative abundances of each gene during growth on acetate, methanol, and CO were determined by using the ΔΔCT method (Applied Biosystems) using the 16s rRNA gene for normalization.

We thank Lacy Daniels (Texas A & M University, Kingsville, TX) for generously supplying $F_{420}$, Jan Keltjens (Radboud University Nijmegen, Nijmegen, The Netherlands) for providing CoB-S-S-CoM, and Deb Grove for assistance with *Taq*man assays. This work was supported by National Science Foundation Grant MCB-0110762 (to J.G.F.), a contract from Advanced Research International (to J.G.F.), and National Institutes of Health Grant GM15847 (to B.L.K.). This article is contribution number 885 from the Barnett Institute.

1. Conrad R (1996) *Microbiol Rev* 60:609–640.
2. Conrad R, Seiler W (1980) *Appl Environ Microbiol* 40:437–445.
3. Huber C, Wachtershauser G (1998) *Science* 281:670–672.
4. Miyakawa S, Yamanashi H, Kobayashi K, Cleaves HJ, Miller SL (2002) *Proc Natl Acad Sci USA* 99:14628–14631.
5. Kasting JF (1993) *Science* 259:920–926.
6. Russell MJ, Martin W (2004) *Trends Biochem Sci* 29:358–363.
7. Ferry JG, House CH (2006) *Mol Biol Evol* 23:1286–1292.
8. Meyer O, Frunzke K, Gadkari D, Jacobitz S, Hugendieck I, Kraut M (1990) *FEMS Microbiol Rev* 87:253–260.
9. Dobbek H, Svetlitchnyi V, Gremer L, Huber R, Meyer O (2001) *Science* 293:1281–1285.
10. Uffen RL (1981) *Enzyme Microb Technol* 3:197–206.
11. Ludden PW, Roberts GP, Kerby RL, Spangler N, Fox J, Shelver D, He Y, Watt R (1996) in *Microbial Growth on C1 Compounds*, eds Lidstrom ME, Tabita FR (Kluwer, Dordrecht, The Netherlands), pp 183–190.
12. Wu M, Ren Q, Durkin AS, Daugherty SC, Brinkac LM, Dodson RJ, Madupu R, Sullivan SA, Kolonay JF, Nelson WC, *et al*. (2005) *PLoS Genet* 1:e65.
13. Ljungdahl LG (1994) in *Acetogenesis*, ed Drake HL (Chapman & Hall, New York), pp 63–87.
14. Muller V, Gottschalk G (1994) in *Acetogenesis*, ed Drake HL (Chapman & Hall, New York), pp 127–156.
15. Parshina SN, Kijlstra S, Henstra AM, Sipma J, Plugge CM, Stams AJ (2005) *Appl Microbiol Biotechnol* 68:390–396.
16. O'Brien JM, Wolkin RH, Moench TT, Morgan JB, Zeikus JG (1984) *J Bacteriol* 158:373–375.
17. Rother M, Metcalf WW (2004) *Proc Natl Acad Sci USA* 101:16929–16934.
18. Krzycki JA, Wolkin RH, Zeikus JG (1982) *J Bacteriol* 149:247–254.
19. Daniels L, Fuchs G, Thauer RK, Zeikus JG (1977) *J Bacteriol* 132:118–126.
20. Zeikus JG, Kerby R, Krzycki JA (1985) *Science* 227:1167–1173.
21. Kluyver AJ, Schnellen CGTP (1947) *Arch Biochem* 14:57–70.
22. Bott M, Thauer RK (1987) *Eur J Biochem* 168:407–412.
23. Bott M, Thauer RK (1989) *Eur J Biochem* 179:469–472.
24. Sowers KR, Baron SF, Ferry JG (1984) *Appl Environ Microbiol* 47:971–978.
25. Galagan JE, Nusbaum C, Roy A, Endrizzi MG, Macdonald P, FitzHugh W, Calvo S, Engels R, Smirnov S, Atnoor D, *et al*. (2002) *Genome Res* 12:532–542.
26. Ferry JG (2003) in *Biochemistry and Physiology of Anaerobic Bacteria*, eds Ljungdahl LG, Adams MW, Barton LL, Ferry JG, Johnson MK (Springer, New York), pp 143–156.
27. Li Q, Li L, Rejtar T, Lessner DJ, Karger BL, Ferry JG (2006) *J Bacteriol* 188:702–710.
28. Li Q, Li L, Rejtar T, Karger BL, Ferry JG (2005) *J Proteome Res* 4:129–136.
29. Li Q, Li L, Rejtar T, Karger BL, Ferry JG (2005) *J Proteome Res* 4:112–128.
30. Gottschalk G, Thauer RK (2001) *Biochim Biophys Acta* 1505:28–36.
31. Welander PV, Metcalf WW (2005) *Proc Natl Acad Sci USA* 102:10664–10669.
32. Kerby RL, Hong SS, Ensign SA, Coppoc LJ, Ludden PW, Roberts GP (1992) *J Bacteriol* 174:5284–5294.
33. Ensign SA, Ludden PW (1991) *J Biol Chem* 266:18395–18403.
34. Terlesky KC, Nelson MJK, Ferry JG (1986) *J Bacteriol* 168:1053–1058.
35. Maupin-Furlow JA, Ferry JG (1996) *J Bacteriol* 178:6849–6856.
36. Fischer R, Thauer RK (1990) *FEBS Lett* 269:368–372.
37. Terlesky KC, Ferry JG (1988) *J Biol Chem* 263:4075–4079.
38. Stojanowic A, Hedderich R (2004) *FEMS Microbiol Lett* 235:163–167.
39. Meuer J, Kuettner HC, Zhang JK, Hedderich R, Metcalf WW (2002) *Proc Natl Acad Sci USA* 99:5632–5637.
40. Deppenmeier U (2004) *J Bionenerg Biomembr* 36:55–64.
41. Simianu M, Murakami E, Brewer JM, Ragsdale SW (1998) *Biochemistry* 37:10027–10039.
42. Heiden S, Hedderich R, Setzke E, Thauer RK (1993) *Eur J Biochem* 213:529–535.
43. Stojanowic A, Mander GJ, Duin EC, Hedderich R (2003) *Arch Microbiol* 180:194–203.
44. Abbanat DR, Ferry JG (1990) *J Bacteriol* 172:7145–7150.
45. Deppenmeier U, Johann A, Hartsch T, Merkl R, Schmitz RA, Martinez-Arias R, Henne A, Wiezer A, Baumer S, Jacobi C, *et al*. (2002) *J Mol Microbiol Biotechnol* 4:453–461.
46. Deppenmeier U (2002) *Prog Nucleic Acid Res Mol Biol* 71:223–283.
47. Hedderich R, Berkessel A, Thauer RK (1990) *Eur J Biochem* 193:255–261.
48. Hedderich R (2004) *J Bionenerg Biomembr* 36:65–75.
49. Zinder S (1993) in *Methanogenesis*, ed Ferry JG (Chapman & Hall, New York), pp 128–206.
50. Sowers KR, Boone JE, Gunsalus RP (1993) *Appl Environ Microbiol* 59:3832–3839.
51. Ferry JG, Wolfe RS (1976) *Arch Microbiol* 107:33–40.
52. Grant WM (1948) *Anal Chem* 20:267–269.
53. Andreev VP, Li L, Rejtar T, Li Q, Ferry JG, Karger BL (2006) *J Proteome Res* 5:2039–2045.
54. Shevchenko A, Wilm M, Vorm O, Mann M (1996) *Anal Chem* 68:850–858.
55. Eng JK, McCormack AL, Yates JR (1994) *J Am Soc Mass Spectrom* 5:976–989.
56. Nesvizhskii AI, Keller A, Kolker E, Aebersold R (2003) *Anal Chem* 75:4646–4658.
57. Deppenmeier U, Blaut M, Mahlmann A, Gottschalk G (1990) *FEBS Lett* 261:199–203.
58. Bensing BA, Meyer BJ, Dunny GM (1996) *Proc Natl Acad Sci USA* 93:7794–7799.

# Appendix B

# *Methanolobus zinderi* sp. nov., a methylotrophic methanogen isolated from a deep subsurface coal seam

## Personal contribution to manuscript

The paper reproduced in this appendix describes a collaborative research effort between the groups of Dr. James G. Ferry (The Pennsylvania State University, University Park, PA) and the J. Craig Venter institute (Rockville, MD). The paper was published in *The International Journal of Systematic and Evolutionary Microbiology*[1]. My contributions to this manuscript included assisting with plating and isolation of the clonal population of SD-1 from the original methylotrophic enrichment culture, all DNA purification, guanasine plus cytosine content determination, deposition of the strain in culture collections and writing of the materials and methods and results and discussion sections of the manuscript.

---

[1] **Doerfert, S.N.†, Reichlen, M.†, Iyer, P., Wang, M., and J.G. Ferry.** 2009. *Methanolobus zinderi* sp. nov., a methylotrophic methanogen isolated from a deep subsurface coal seem. IJSEM. **59:**1064-9.

† These authors contributed equally to this work.

*International Journal of Systematic and Evolutionary Microbiology* (2009), **59**, 1064–1069 **DOI** 10.1099/ijs.0.003772-0

# *Methanolobus zinderi* sp. nov., a methylotrophic methanogen isolated from a deep subsurface coal seam

Sebastian N. Doerfert,[1]† Matthew Reichlen,[1]† Prabha Iyer,[2] Mingyu Wang[1] and James G. Ferry[1]

Correspondence
James G. Ferry
jgf3@psu.edu

[1]Department of Biochemistry and Molecular Biology, Pennsylvania State University, University Park, PA 16802, USA

[2]J. Craig Venter Institute, Rockville, MD 20850, USA

A methanogenic organism from the domain *Archaea* (SD1$^T$) was isolated from saline water released from a coal seam located 926 m below the surface via a methane-producing well near Monroe, Louisiana, USA. Growth and methanogenesis were supported with methanol, monomethylamine, dimethylamine or trimethylamine, but not with dimethylsulfide, formate, acetate or $H_2/CO_2$. Cells grew in high-salt minimal medium but growth was stimulated with yeast extract or tryptone. Cells were single, non-motile, irregular coccoids 0.5–1.0 μm in diameter and the cell wall contained protein. Conditions for the maximum rate of growth were 40–50 °C, 0.2–0.6 M NaCl, 100–⩾200 mM $MgCl_2$, and pH 7.0–8.0. The G+C content of the genomic DNA was 42±1 mol%. A comparison of 16S rRNA gene sequences indicated that strain SD1$^T$ was most closely related to *Methanolobus oregonensis* DSM 5435$^T$ with 96% gene sequence similarity. It is proposed that strain SD1$^T$ represents a novel species, *Methanolobus zinderi* sp. nov. The type strain is SD1$^T$ (=ATCC BAA-1601$^T$=DSM 21339$^T$).

Deep subsurface coal deposits are habitats with potential for anaerobic methanogenic consortia that convert coal to methane within abundant water-filled natural fractures called cleats. Stable carbon isotope analyses from Permian coal beds in Australia (Smith & Pallasser, 1996) and Wilcox coal beds in northern Louisiana, USA (McIntosh *et al.*, 2007), indicate that a portion of the coal bed methane (CBM) is biological in origin. Sequences of 16S rRNA genes obtained from the water of a coal seam in northern Japan, located between 843 and 907 m below the surface, indicated the presence of methanogenic species belonging to the genera *Methanoculleus* and *Methanolobus* (Shimizu *et al.*, 2007). Further, unidentified microbial cells have been observed in water from a coal seam in northern Louisiana (Warwick & MacIntosh, 2007). However, methane-producing isolates from coal beds have yet to be reported. Here we describe the characteristics of strain SD1$^T$, a methane-producing species isolated from water from a northern Louisiana coal seam.

†These authors contributed equally to this work.

Abbreviation: CBM, coal bed methane.

The GenBank/EMBL/DDBJ accession numbers for the 16S rRNA and *mcrA* gene sequences of *Methanolobus zinderi* sp. nov. SD1$^T$ are EU711413$^T$ and EU715818$^T$, respectively.

Graphs showing the effects of temperature, $Na^+$, $Mg^{2+}$ and pH on the growth of strain SD1$^T$ are available with the online version of this paper.

Strain SD1$^T$ was isolated from a sample of water obtained from a Wilcox coal seam via a CBM well located approximately 40 miles south of Monroe, LA, USA. The sample was taken at the well head in sterile glass jars filled to the top and then sealed to exclude air before transport to the laboratory. The coal seam is situated 926 m below the surface where the temperature is 51 °C and the associated water has a pH of 7.8 and contains 26 mM $Mg^{2+}$ and 0.87 M $Na^+$.

An anaerobic chamber (Coy Manufacturing) was used for isolation and the Hungate method (Hungate, 1969) with modifications (Miller & Wolin, 1974, Sowers *et al.*, 1984) was used for enrichment cultures and growth studies. The high-salt minimal medium was as described by Sowers *et al.* (1993) with the following substrates where indicated: 250 mM methanol, 100 mM trimethylamine, 100 mM dimethylamine, 100 mM monomethylamine, 100 mM sodium acetate or 160 kPa $H_2/CO_2$ (80 : 20) headspace gas mixture. The enrichment medium was high-salt minimal medium containing 250 mM methanol and a head space of $N_2/CO_2/H_2$ (75 : 20 : 5). The specific growth rate was determined by measuring the absorbance of cultures at 600 nm. Growth as a function of pH was determined with high-salt minimal media containing 250 mM methanol with the indicated pH range obtained by adjusting the ratio of $CO_2$ and $N_2$ contained in the head space.

 003772 © 2009 IUMS *Printed in Great Britain*

Growth experiments were performed in anaerobic culture tubes (16 × 150 mm) that contained 10 ml high-salt minimal medium with the indicated substrate and a head space of $N_2/CO_2$ (80 : 20) unless indicated otherwise. Tubes were sealed with a butyl rubber stopper that was secured with an aluminium crimp collar. Growth was monitored spectrophotometrically at 600 nm with a Bausch and Lomb Spectronic 20. Headspace gases were quantified by GC as described by Ferry & Wolfe (1976).

For DNA isolation, stationary phase cells were collected by centrifugation for 5 min at 6000 ***g*** at 4 °C. Cells were lysed by incubation for 1 h at 37 °C in buffer containing 10 mM Tris/HCl (pH 7.5), 1 mM EDTA (pH 8.0), 0.3 % (w/v) SDS and 1.5 μg $ml^{-1}$ RNase (Roche). Genomic DNA was extracted from the cell lysate using a Purgene Genomic DNA Extraction kit (Gentra Systems) following the manufacturer's guidelines. The DNA was further purified by two rounds of phenol/chloroform extraction/ethanol precipitation to remove all residual proteins.

The G + C content of the genomic DNA of strain $CD1^T$ was determined by the thermal denaturation method, essentially as described by Mandel & Marmur (1968). Purified genomic DNA was diluted in standard SSC buffer to an absorbance of 0.4 at 260 nm and was dialysed overnight against 1000 volumes SSC. The DNA melting temperature was calculated by monitoring the change in absorbance at 260 nm over increasing temperatures on a spectrophotometer (model 50; Varian Cary) in combination with a Peltier thermostat-equipped accessory and an anaerobic fluorescence cuvette [2 mm × 1 cm (path length)] (Starna). Genomic DNA from *Escherichia coli* K-12 served as a standard.

For phylogenetic analyses, the 16S rRNA gene was amplified using the *Archaea*-specific primer 3f (5′-TCCGGTTGATCCTGCCGG-3′) and the universal primer 1423r [5′-ACGGN(AT)ACCTTGTTACGAGTT-3′] (McInerney *et al.*, 1995) and an Advantage HF2 PCR kit (BD Biosciences). The amplified PCR product was sequenced directly using an ABI 3100 automated DNA sequencer. The above mentioned PCR primers were utilized for sequencing. The sequence between positions 64 and 1401 was obtained in this fashion. A modified inverse PCR approach was employed to sequence the 5′ and 3′ ends of the 16S rRNA gene. Genomic DNA was cleaved using the blunt cutter *Pst*I and the fragments were self-ligated to form circular molecules. PCR amplification using outward facing primers complementary to the ends of the sequenced portion of the 16S rRNA gene above produced two PCR products of 1.2 kb and 2.2 kb, respectively. The ends of these PCR fragments were sequenced as above using the PCR primers for sequencing. The 2.2 kb fragment yielded the 5′ and 3′ ends of the 16S rRNA gene. A 745 bp segment of the methyl coenzyme M reductase (*mcrA*) gene was amplified using the primer set ME1[5′-C(AC)ATGCA(AG)AT(ACT)GG(AT)ATGTC-3′] and ME2 [5′-TCAT(GT)GC(AG)TAGTT(AGT)GG(AG)TAGT-3′] as described previously (Hales & Winstanley, 1996) and was sequenced directly as described above for the 16S rRNA gene.

The sequences of 1332 bases of the 16S rRNA gene and 490 bases of the *mcrA* gene from various species were aligned using CLUSTAL_X (Thompson *et al.*, 1997). Phylogenetic trees were deduced using the neighbour-joining algorithm (Saitou & Nei, 1987). Bootstrap values were calculated using the neighbour-joining method and 1000 replicate datasets and re-evaluated using the SEQBOOT, DNAPARS and CONSENSE programs implemented within the PHYLIP package.

## Results and Discussion

Methanogens were enriched using high-salt minimal medium (Sowers *et al.*, 1993) containing 250 mM methanol as the growth substrate. A 5 ml water sample taken from a deep subsurface coal seam was added to 100 ml medium in a 160 ml stoppered serum vial (Miller & Wolin, 1974) containing a head space of $N_2/CO_2/H_2$ (75 : 20 : 5) and incubated at 37 °C. After methane production subsided, subcultures were established with a 5 ml inoculum from which isolates were obtained by plating on solid medium containing 2 % Nobel agar (Difco) in an anaerobic chamber (Coy Manufacturing). Plates were incubated in an atmosphere of $N_2/CO_2$ (80 : 20) at 37 °C. Cells from plates containing a single colony type were cultured in 10 ml liquid medium under a head space of $N_2/CO_2$ (80 : 20) at 37 °C. When methane production subsided, serial dilutions were replated and incubated as described above. An isolated colony, containing cells of uniform morphology, was cultured in the liquid medium as described above and designated strain $SD1^T$.

Colonies on agar plates appeared after 5 days and reached a diameter of 2–3 mm after 14 days. The opaque colonies were circular, raised with a smooth surface and entire margins, opaque, dark yellow to light brown in colour and dry in texture. Cells were non-motile, irregular coccoids of 0.5–1.0 μm in diameter (Fig. 1a, b) that stained Gram-negative. Aggregates were not observed. Thin-section transmission electron microscopy showed features resembling vacuoles (Fig. 1c) and a cell envelope similar to that of other methanogens containing a protein S-layer adjacent to the cell membrane (Fig. 1d). Cell lysis occurred immediately following the addition of SDS (final concentration 0.1 %) to the growth medium, consistent with the presence of a protein cell wall.

Growth studies were conducted in high-salt minimal medium (Sowers *et al.*, 1993) containing the indicated substrate and a head space of $N_2/CO_2$ (80 : 20). Growth was monitored at 600 nm and methane was detected by GC. Strain $SDI^T$ grew and produced methane with 250 mM methanol, 100 mM monomethylamine, 100 mM dimethylamine and 100 mM trimethylamine as carbon and energy sources in the absence of $H_2$. Dimethylsulfide (100 mM), acetate (100 mM), formate (100 mM) and $H_2/CO_2$ (80 : 20) were not utilized by strain $SDI^T$. Although not

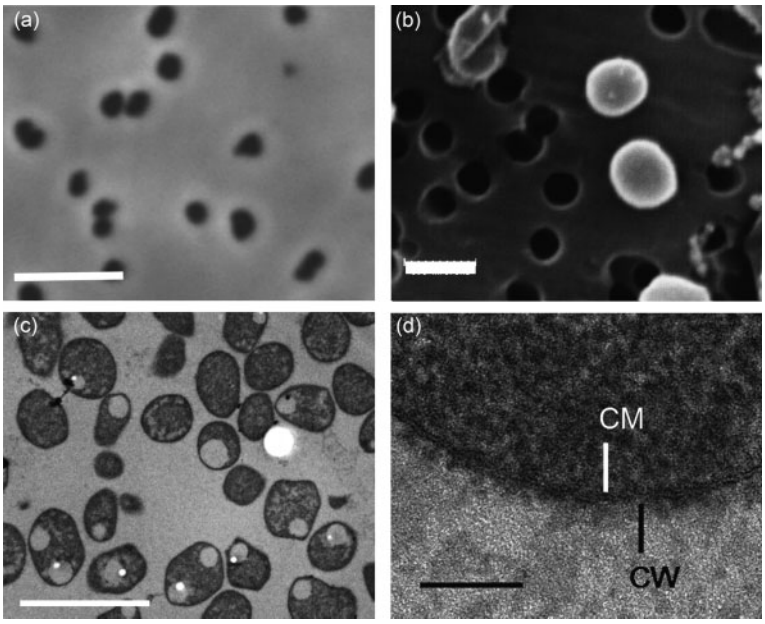


**Fig. 1.** Morphology of cells of strain SD1$^T$. (a) Phase-contrast micrograph of whole cells. Bar, 5 μm. (b) Scanning electron micrograph of whole cells. Bar, 0.5 μm. (c) Thin-section transmission electron micrograph showing vacuole-like structures. Bar, 2 μm. (d) Thin-section electron micrograph depicting the cell wall (CW) and cytoplasmic membrane (CM). Bar, 0.1 μm.

required, growth was stimulated by tryptone or acetate. The following growth experiments were conducted in high-salt medium (Sowers *et al.*, 1993) containing 250 mM methanol as the substrate and a head space of $N_2/CO_2$ (80 : 20). The temperature range for growth was 25–50 °C, with the maximum rate between 40 and 50 °C (see Supplementary Fig. S1a in IJSEM Online). Growth was not observed at 55 °C. Sodium chloride was required for growth, was supported at concentrations of 0.05–1.8 M NaCl and the maximum growth rate occurred at concentrations between 0.2 and 0.6 M NaCl (Supplementary Fig. S1b in IJSEM Online). Growth was poor with no added $MgCl_2$ (Supplementary Fig. S1c). The optimal conditions for growth were between 10 and $\geqslant$200 mM $MgCl_2$, with the maximum rate between 100 and $\geqslant$200 mM (Supplementary Fig. S1c). Growth was supported between pH 6.0 and 9.0, with the maximum rate between pH 7.0 and 8.0 (Supplementary Fig. S1d).

The G+C content of the genomic DNA of strain was SD1$^T$ determined to be 42±1 mol%. Comparison of the 16S rRNA gene sequence against GenBank using the BLAST search tool revealed that strain SD1$^T$ was most closely related to the methylotrophic species *Methanolobus oregonensis* (96 %), *Methanolobus taylorii* (96 %), *Methanolobus vulcani* (95 %), *Methanolobus bombayensis* (94 %) and several uncultured clones from a biodegraded oil well (97 %). Other methylotrophic methanogenic species related to strain SD1$^T$ included *Methanomethylovorans thermophila* (95 %), *Methanomethylovorans hollandica* strain ZB (94 %), *Methanococcoides burtonii* (93 %) and *Methanohalophilus mahii* (93 %). A phylogenetic tree constructed using 16S rRNA gene sequences showed that strain SD1$^T$ clustered with members of the genus *Methanolobus*, although bootstrap analysis indicated a clear branching of strain SD1$^T$ from the recognized species of the genus *Methanolobus* (Fig. 2). This branching occurred in 100 % of trees generated by the neighbour-joining or maximum-parsimony methods. The partial nucleotide sequence of the *mcrA* gene of strain SD1$^T$ was most closely related to those of *Methanolobus bombayensis* (94 %), *Methanolobus vulcani* (93 %), *Methanolobus tindarius* (92 %) and *Methanolobus taylorii* (91 %). The deduced partial amino acid sequence of the methyl-coenzyme M methylreductase from strain SD1$^T$ was most similar to that from *Methanococcoides burtonii* (90 %). Neighbour-joining trees of partial *mcrA* sequences indicated that the gene sequence of strain SD1$^T$ was closest to that of *Methanolobus taylorii* and clustered with other sequences from species of the genus *Methanolobus* (Fig. 2). However, it was clearly separated from other species of the genus *Methanolobus* with the branch occurring in 87 % of all trees.

The results of DNA distance matrix analyses of the 16S rRNA and partial *mcrA* gene sequences suggested that strain SD1$^T$ was most closely related to organisms in the genus *Methanolobus*. Springer *et al.* (1995) compared 16S rRNA and *mcrA* gene sequence distances between members of the same genus or different genera within the family *Methanosarcinaceae* and found 16S rRNA gene distances between members of the same genus to be 0.0214±0.0065, whereas distances between members of different genera were 0.0807±0.0096. Although these standards did not immediately suggest an unequivocal genus assignment for strain SD1$^T$, the novel strain was closely related to members of the genus *Methanolobus* with a 16S rRNA gene sequence distance of 0.0351±0.0037. Similarly, Springer *et al.* (1995) found that *mcrA* gene distances within a given genus were 0.0937±0.0313, while distances

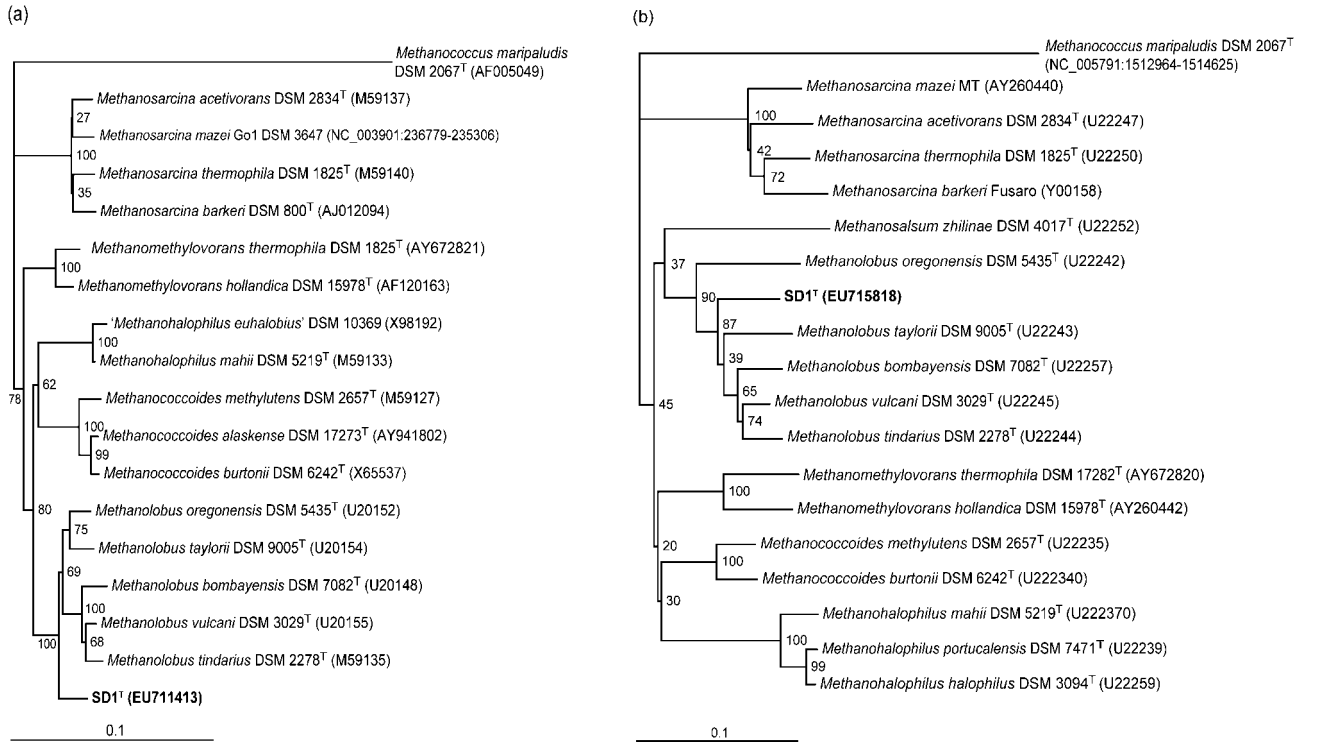


**Fig. 2.** Phylogenetic trees of 16S rRNA (a) and *mcrA* (b) gene sequences showing the relationship between strain SD1$^T$ and members of the genera *Methanosarcina*, *Methanomethylovorans*, *Methanohalophilus*, *Methanococcoides* and *Methanolobus*, constructed using the neighbour-joining algorithm. The sequences were obtained from GenBank and accession numbers are shown in parentheses. Bars, 0.1 substitutions per nucleotide position.

between genera were $0.245 \pm 0.038$. Applying these standards, it can be seen that strain SD1$^T$ clearly represents a novel species.

Analyses of 16S rRNA genes suggest that a diversity of novel methanogens are present in a variety of deep subsurface environments which include faults (Moser *et al.*, 2005), thermal aquifers (Kimura *et al.*, 2005) rock aquifers (Chapelle *et al.*, 2002, Kotelnikova *et al.*, 1998), shales (Takai *et al.*, 2003), petroleum deposits (Cheng *et al.*, 2007, Grabowski *et al.*, 2005, Orphan *et al.*, 2000), methane gas fields (Mochimaru *et al.*, 2007a, b) and coal beds (Shimizu *et al.*, 2007). However, relatively few methanogens have been isolated from these environments and none have been isolated from coal beds. A better understanding of the microbiology of deep subsurface environments is essential to grasp the extent of the Earth's prokaryotic diversity and share of Earth's living protoplasm. The microbiology of coal beds contributes to this understanding and has the added benefit of enabling on-going efforts for the development of processes for microbial enhancement of CBM. Indeed, it is estimated that an increase of 16 % in CBM reserves could be generated by the microbial conversion of only 0.01 % of US coal (Scott, 1999). Furthermore, it is anticipated that the estimated $10^{14}$ m$^3$ CBM present in deep coal seams worldwide will contribute substantially to future energy sources (Shimada, 1995). Although several species of methanogens have been isolated from oilfields (Belyaev *et al.*, 1983; Cheng *et al.*, 2007; Ni & Boone, 1991; Nilsen & Torsvik, 1996; Ollivier *et al.*, 1997), isolates from methane gas fields or methane-producing coal beds have not been reported. The temperature, pH and salinity of the sampled coal water coincided with optimal conditions for growth of strain SD1$^T$, indicating that this strain is well adapted to its environment. The results provide direct microbiological evidence supporting the 16S rRNA gene sequence, isotopic and chemical analyses (McIntosh *et al.*, 2007; Scott, 1999; Shimizu *et al.*, 2007) that suggest that biogenic methane is produced in deep subsurface coal beds by anaerobic microbial consortia.

The results presented here are an important first step in defining the *in situ* microbial populations and processes necessary to develop methods for the microbial enhancement of CBM. The methylotrophic substrates used by strain SD1$^T$ are characteristic of the genus *Methanolobus* and indicate that one-carbon compounds derived from coal, by either biogenic or thermogenic processes, are potentially important precursors to biogenic CBM. This proposal is supported by 16S rRNA gene sequences obtained from deep coal bed water in Japan that indicated a major presence of uncultured species of the genus *Methanolobus* (Shimizu *et al.*, 2007).

### Description of *Methanolobus zinderi* sp. nov.

*Methanolobus zinderi* (zin′der.i. N.L. gen. masc. n. *zinderi* of Zinder, named in honour of Stephen H. Zinder for his outstanding contributions to our understanding of the microbiology and ecology of methanogenesis).

Cells are irregular coccoids, 1.0–2.0 μm in diameter. Cells are lysed by detergents. Gram-negative. Non-motile. Cells grow by forming methane from methanol and methylamines. Cells are unable to grow with $H_2/CO_2$ or acetate. The maximum rate of growth is between 40–50 °C, 0.2–0.6 M NaCl, 100–$\geqslant$200 mM $MgCl_2$ and pH 7.0–8.0. No organic compounds are required for growth.

The type strain, SD1$^T$ (=ATCC BAA-1601$^T$=DSM 21339$^T$), was isolated from a coal seam near Monroe, LA, USA. The G+C content of the genomic DNA of the type strain is 42±1 mol%.

## Acknowledgements

This work was supported by a grant from the Pennsylvania State University and EnCana. We thank Robert Downey for the collection of water samples and Missy Hazen and Ruth Haldeman for assistance with electron microscopy.

## References

**Belyaev, S. S., Wolkin, R., Kenealy, W. R., Deniro, M. J., Epstein, S. & Zeikus, J. G. (1983).** Methanogenic bacteria from the bondyuzhskoe oil field: general characterization and analysis of stable-carbon isotopic fractionation. *Appl Environ Microbiol* **45**, 691–697.

**Chapelle, F. H., O'Neill, K., Bradley, P. M., Methe, B. A., Ciufo, S. A., Knobel, L. L. & Lovley, D. R. (2002).** A hydrogen-based subsurface microbial community dominated by methanogens. *Nature* **415**, 312–315.

**Cheng, L., Qiu, T. L., Yin, X. B., Wu, X. L., Hu, G. Q., Deng, Y. & Zhang, H. (2007).** *Methermicoccus shengliensis* gen. nov., sp. nov., a thermophilic, methylotrophic methanogen isolated from oil-production water, and proposal of *Methermicoccaceae* fam. nov. *Int J Syst Evol Microbiol* **57**, 2964–2969.

**Ferry, J. G. & Wolfe, R. S. (1976).** Anaerobic degradation of benzoate to methane by a microbial consortium. *Arch Microbiol* **107**, 33–40.

**Grabowski, A., Nercessian, O., Fayolle, F., Blanchet, D. & Jeanthon, C. (2005).** Microbial diversity in production waters of a low-temperature biodegraded oil reservoir. *FEMS Microbiol Ecol* **54**, 427–443.

**Hales, B. A. & Winstanley, C. (1996).** Sequencing of (dA:dT) cloned mixed PCR products from microbial populations. *Methods Mol Biol* **65**, 209–218.

**Hungate, R. E. (1969).** A roll tube method for cultivation of strict anaerobes. *Methods Microbiol* **3B**, 117–132.

**Kimura, H., Sugihara, M., Yamamoto, H., Patel, B. K., Kato, K. & Hanada, S. (2005).** Microbial community in a geothermal aquifer associated with the subsurface of the Great Artesian Basin, Australia. *Extremophiles* **9**, 407–414.

**Kotelnikova, S., Macario, A. J. & Pedersen, K. (1998).** *Methanobacterium subterraneum* sp. nov., a new alkaliphilic, eurythermic and halotolerant methanogen isolated from deep granitic groundwater. *Int J Syst Bacteriol* **48**, 357–367.

**Mandel, M. & Marmur, J. (1968).** Use of ultraviolet absorbance-temperature profile for determining the guanine plus cytosine content of DNA. *Methods Enzymol* **12B**, 195–206.

**McInerney, J. O., Wilkinson, M., Patching, J. W., Embley, T. M. & Powell, R. (1995).** Recovery and phylogenetic analysis of novel archaeal rRNA sequences from a deep-sea deposit feeder. *Appl Environ Microbiol* **61**, 1646–1648.

**McIntosh, J. C., Warwick, P. D., Martini, A. M. & Osborn, S. G. (2007).** Coupled hydrology and biogeochemistry of Paleocene-Eocene coal beds, northern Gulf of Mexico, abstract. In *Geological Society of America Abstracts with Programs*, 257.

**Miller, T. L. & Wolin, M. J. (1974).** A serum bottle modification of the Hungate technique for cultivating obligate anaerobes. *Appl Microbiol* **27**, 985–987.

**Mochimaru, H., Uchiyama, H., Yoshioka, H., Imachi, H., Hoaki, T., Tamaki, H., Nakamura, K., Sekiguchi, Y. & Kamagata, Y. (2007a).** Methanogen diversity in deep subsurface gas-associated water at the Minami-Kanto gas field in Japan. *Geomicrobiol J* **24**, 93–100.

**Mochimaru, H., Yoshioka, H., Tamaki, H., Nakamura, K., Kaneko, N., Sakata, S., Imachi, H., Sekiguchi, Y., Uchiyama, H. & Kamagata, Y. (2007b).** Microbial diversity and methanogenic potential in a high temperature natural gas field in Japan. *Extremophiles* **11**, 453–461.

**Moser, D. P., Gihring, T. M., Brockman, F. J., Fredrickson, J. K., Balkwill, D. L., Dollhopf, M. E., Lollar, B. S., Pratt, L. M., Boice, E. & other authors (2005).** *Desulfotomaculum* and *Methanobacterium* spp. dominate a 4- to 5-kilometer-deep fault. *Appl Environ Microbiol* **71**, 8773–8783.

**Ni, S. S. & Boone, D. R. (1991).** Isolation and characterization of a dimethyl sulfide-degrading methanogen, *Methanolobus siciliae* HI350, from an oil well, characterization of *M. siciliae* T4/MT, and emendation of *M. siciliae*. *Int J Syst Bacteriol* **41**, 410–416.

**Nilsen, R. K. & Torsvik, T. (1996).** *Methanococcus thermolithotrophicus* isolated from North Sea oil field reservoir water. *Appl Environ Microbiol* **62**, 728–731.

**Ollivier, B., Cayol, J. L., Patel, B. K., Magot, M., Fardeau, M. L. & Garcia, J. L. (1997).** *Methanoplanus petrolearius* sp. nov., a novel methanogenic bacterium from an oil-producing well. *FEMS Microbiol Lett* **147**, 51–56.

**Orphan, V. J., Taylor, L. T., Hafenbradl, D. & Delong, E. F. (2000).** Culture-dependent and culture-independent characterization of microbial assemblages associated with high-temperature petroleum reservoirs. *Appl Environ Microbiol* **66**, 700–711.

**Saitou, N. & Nei, M. (1987).** The neighbor-joining method: a new method for reconstructing phylogenetic trees. *Mol Biol Evol* **4**, 406–425.

**Scott, A. R. (1999).** Improving coal gas recovery with microbially enhanced coalbed methane. In *Coalbed Methane: Scientific, Environmental and Economic Evaluation*, pp. 89–110. Edited by M. Mastalerz, M. Glikson & S. D. Golding. Dordrecht: Kluwer.

**Shimada, M. (1995).** State of the art of coalbed methane development. *J Min Mater Process Inst Jpn* **111**, 135–143.

**Shimizu, S., Akiyama, M., Naganuma, T., Fujioka, M., Nako, M. & Ishijima, Y. (2007).** Molecular characterization of microbial communities in deep coal seam groundwater of northern Japan. *Geobiology* **5**, 423–433.

**Smith, J. W. & Pallasser, R. J. (1996).** Microbial origin of Australian coalbed methane. *Am Assoc Pet Geol Bull* **80**, 891–897.

**Sowers, K. R., Baron, S. F. & Ferry, J. G. (1984).** *Methanosarcina acetivorans* sp. nov., an acetotrophic methane-producing bacterium isolated from marine sediments. *Appl Environ Microbiol* **47**, 971–978.

**Sowers, K. R., Boone, J. E. & Gunsalus, R. P. (1993).** Disaggregation of *Methanosarcina* spp. and growth as single cells at elevated osmolarity. *Appl Environ Microbiol* **59**, 3832–3839.

**Springer, E., Sachs, M. S., Woese, C. R. & Boone, D. R. (1995).** Partial gene sequences for the A subunit of methyl-coenzyme M reductase (*mcr*I) as a phylogenetic tool for the family *Methanosarcinaceae*. *Int J Syst Bacteriol* **45**, 554–559.

**Takai, K., Mormile, M. R., McKinley, J. P., Brockman, F. J., Holben, W. E., Kovacik, W. P., Jr & Fredrickson, J. K. (2003).** Shifts in archaeal communities associated with lithological and geochemical variations in subsurface Cretaceous rock. *Environ Microbiol* **5**, 309–320.

**Thompson, J. D., Gibson, T. J., Plewniak, F., Jeanmougin, F. & Higgins, D. G. (1997).** The CLUSTAL_X windows interface: flexible strategies for multiple sequence alignment aided by quality analysis tools. *Nucleic Acids Res* **25**, 4876–4882.

**Warwick, P. D. & MacIntosh, J. C. (2007).** Microbial origin of Wilcox group gas in northern Louisiana. In *Geological Society of America Abstracts with Programs*, 256.

# Appendix C

## Bacterial strains, primers and plasmids used

**Table C-1. Bacterial strains, primers and plasmids used.**

| ***Methanosarcina* strains used:** | | |
|---|---|---|
| **name:** | **genotype:** | **source:** |
| C2A | Wild-type *M. acetivorans* | (5) |
| WWM1 | Δ*hpt* | (3) |
| WWM75 | Δ*hpt::*P*mcrB-tetR*-φC31-*int*-attP | (1) |
| Δ*tbp2* | Δ*tbp2::pac* | This study |
| Δ*tbp3* | Δ*tbp3::pac* | This study |
| Δ*tbp2** | Δ*hpt,* Δ*tbp2::pac-hpt* | This study |
| Δ*tbp3** | Δ*hpt,* Δ*tbp3::pac-hpt* | This study |
| ΔP*tbp1*::P*mcrB*(tetO1)-*tbp1* | Δ*hpt::*P*mcrB-tetR*-φC31-*int*-attP, ΔP*tbp1*::P*mcrB*(tetO1)-*tbp1-pac-hpt-tetR* | This study |
| ΔP*tbp2*::P*mcrB*(tetO1)-*tbp2* | Δ*hpt::*P*mcrB-tetR*-φC31-*int*-attP, ΔP*tbp2*::P*mcrB*(tetO1)-*tbp2-pac-hpt-tetR* | This study |
| ΔP*tbp3*::P*mcrB*(tetO1)-*tbp3* | Δ*hpt::*P*mcrB-tetR*-φC31-*int*-attP, ΔP*tbp3*::P*mcrB*(tetO1)-*tbp3-pac-hpt-tetR* | This study |
| ΔMA3302 | Δ*hpt::*P*mcrB-tetR*-φC31-*int*-attP, ΔMA3302*::pac-hpt* | This study |

| **Cloning primers:** | |
|---|---|
| **name:** | **sequence (5'-3'):** |
| TBP2a-R-XhoI | AAAACTCGAGGTTCTCTATAGTTATTGTGGGTTCCATAC |
| TBP2b-F-SpeI | AAAAACTAGTGGCCTTCGGATCATCAAAACACAGTTG |
| TBP2b-R-NotI | AAAAGCGGCCGCCGGGATTTTTTCAGCAGCAGCTATCAGC |
| TBP3a-F-ApaI | AAAAGGGCCCCATACTGTTTTGCAGGCACGGTTCATG |
| TBP3a-R-XhoI | AAAACTCGAGGCCACCACGTTCTCTATAGTTATTGTG |
| TBP3b-F-SpeI | AAAAACTAGTGAGTTCGACAACTTAGGACTTCTCTG |
| TBP3b-R-NotI | AAAAGCGGCCGCCTGGTTGTAAACAGGATCAGCGTGC |
| TetR-1a-F-NcoI | AAAAAACCATGGCCAGAAAATGGACCTGAGGA |
| TetR-1a-R-ApaI | AAAAAAGGGCCCGGCGCCAGTAAATTCAAAAA |
| TetR-1b-F-NdeI | TAATCATATGAGACGAATCTAGCATTAAATTG |
| TetR-1b-R | TCTGCCTGTTTTTCTCCTGAA |
| TetR-2a-F-NcoI | AAAAAACCATGGTCCCGAAATTGTTCGTGTTT |
| TetR-2a-R-ApaI | ATATATGGGCCCTCAAGCTGGTTTTTCTCATCG |
| TetR-2b-F-NdeI | TAATCATATGGAACCCACAATAACTATAGAG |
| TetR-2b-R | CGTTTCGAGACGCATAGTCA |
| TetR-3a-F-Bsu361 | AAAAAACCTTAGGTGACGAGCGTTAAAATTTGG |
| TetR-3a-R-ApaI | AAAAAAGGGCCCGGCCAAAATTGAAGGTGACT |
| TetR-3b-F-NdeI | TAATCATATGGAATCCACAATAACTATAGAG |
| TetR-3b-R-HindIII | AAAAAAAAGCTTCAATGAAGGAGATGCTGGTTG |

| | |
|---|---|
| 3302A-F-ApaI | GAGCTTTCTGGGCGTATGAG |
| 3302A-R-XhoI | ATATATCTCGAGCGGTAATTATGCCCAGACCT |
| 3302B-F-SpeI | ATATATACTAGTGGCTCTCCAAAAGGGTTAGC |
| 3302B-R-NotI | ATATATGCGGCCGCGGGCACCATAAAAACGAAAA |
| PmtaC2F-SphI | AAAAGCATGCTAGTCGGAATAAGGGACAAATTAAAG |
| PmtaC2R-NdeI | AAAACATATGTTAACCTCCATTTTAATAATGAAGCGA |
| | AAAAAAGCATGCTTAGTGGTGGTGGTGGTGGTGTAAAAGTCCC |
| TBP1-R-His-SphI | ATGTTATCAAGCT |
| | AAAAAAGCATGCTTAGTGGTGGTGGTGGTGGTGATAAAGAAGT |
| TBP2-R-His-SphI | CCTAAGTTGTCCA |
| | AAAAAAGCATGCTTAGTGGTGGTGGTGGTGGTGACAGAGAAGT |
| TBP3-R-His-SphI | CCTAAGTTGTCGA |

| **Southern Blot Probe primers:** | |
|---|---|
| **name:** | **sequence (5'-3'):** |
| **Probe 1** | |
| TBP2up-F | GACCCCGTCCTCACGATAC |
| TBP2up-R | CACACCCATAGCCGGATTAC |
| **Probe 2** | |
| TBP3up-F | TTTTGCTGTGAAGCTGAGGA |
| TBP3up-R | AAGGCCAAAATTGAAGGTGA |
| **Probe 3** | |
| TBP1in-F | TCGCTGAAGAGTTTGATTTAACTG |
| TBP1in-R | TCGATATTTTCAAGCCCAAGCCC |
| **Probe 4** | |
| TBP2in-F | GAGAACAGCCGCATAGCTCTT |
| TBP2in-R | TAACRCGTCCTTAAGTTTGCG |
| **Probe 5** | |
| TBP3in-F | AATAATGCCCATAAAGCCATAAC |
| TBP3in-R | TACCTTGGGAGCCTCGACTC |

| **RT-PCR primers:** | |
|---|---|
| **name:** | **sequence (5' - 3'):** |
| **Fig. 3-1** | |
| TBP1F | CGCTGAAGAGTTTGATTTAACTG |
| TBP1R | TCGATATTTTCAAGCCCAAGCCC |
| TBP2F | GAGAACAGCCGCATAGCTCTTTT |
| TBP2R | TAAACTCGTCCTTAAGTTTGCGG |
| TBP3F | AATAATGCCCATAAAGCCATAAC |
| TBP3R | TACCTTGGGAGCCTCGACTC |
| **Fig. 3-3** | |
| TBP1-F | CGCTGAAGAGTTTGATTTAACTG |
| 4330-F | GACCTCGGTCTCAATTTCAAAGCC |
| 4330-R | GCCCGCAAGAAACTTGAGGACG |
| 4332-F | GGAGACCTTCTCGAAAGAATCTGTAAA |
| 4329-R | GAGTCACGTAGCAGAGGAAGTC |
| TBP2-F | GAGAACAGCCGCATAGCTCTTTT |
| TBP2-R | TAAACTCGTCCTTAAGTTTGCGG |
| TBP2-300up-F | CACATTGTAGGTTCAAAATAGTTGCAGATGC |
| 0178-R | GATAACAAGCATGGTAACTGAAAAACATAGGTCAAGAATAC |
| TBP3-R | TACCTTGGGAGCCTCGACTC |
| 0277-F | GATATATAATTCTATAGATCCTACACTTTCC |
| 0277-100up-F | GATCTTTATTTCTATCGGGGTTCGGTC |
| **Fig. 3-4** | |
| TBP1-TAP | GAACTCGGATTCAATCACAGTTAAATC |

| | |
|---|---|
| TBP2-TAP | CAGTATCTATCTATTTTTTATCAAACATGGAGG |
| TBP3-TAP | GCCCAGAATCCATTATTTTTACCAAGTCG |
| 0277-TAP | GGATATCTGGGATCAGCTGCGAAATAG |
| TFB-TAP | TATGACCTGACCTGTGCAGC |
| TAP-RNA | GGUAUUGCGGUACCCUUGUACGC |
| TAP-DNA | GGTATTGCGGTACCCTTGTACGC |

| **Taqman primers and probes:** | |
|---|---|
| **name:** | **sequence (5'-3'):** |
| tbp1-F | GCACACCATCCTTAACCTCAATG |
| tbp1-R | GCTCGGGTTCATATTCGATATTTT |
| tbp1-probe | FAM-AATTGCCATCGGGCTTGGGCTT-BHQ |
| tbp2-F | TTCCGCAAACTTAAGGACGAGT |
| tbp2-R | CGACGTTTTCCACGCCA |
| tbp2-probe | FAM-ACCTGAACGCCGTTTTGAGCGC-BHQ |
| tbp3-F | GCGACAGAATTCGACTTGGTAA |
| tbp3-R | GCCTGGGAACTTCGTTTTGTT |
| tbp3-probe | FAM-TGGATTCTGGGCTGGAAGGTGCA-BHQ |
| 3302-F | TTCATCCCGCGAAATTGAA |
| 3302-R | CAGGACTGGTTCCGCATCA |
| 3302-probe | FAM-TGAGGCAACCCGAAGTAAGTCTTGCAA-BHQ |

| **Plasmids:** | |
|---|---|
| **name:** | **source/construction:** |
| pJK3 | (2) |
| pJK301 | (4) |
| pGK050A | (1) |
| pWM321 | (2) |
| pSC-A | StrataClone™ TA-cloning vector (Stratagene, La Jolla, CA) |
| pMR15 | ApaI/XhoI digested PCR product amplified from *M. acetivorans* genomic DNA using TBP2a-F-ApaI and TBP2a-R-XhoI cloned into ApaI/XhoI digested pJK3 |
| pMR16 | ApaI/XhoI digested PCR product amplified from *M. acetivorans* genomic DNA using TBP3a-F-ApaI and TBP3a-R-XhoI cloned into ApaI/XhoI digested pJK3 |
| pMR18 | SpeI/NotI digested PCR product amplified from *M. acetivorans* genomic DNA using TBP2b-F-SpeI and TBP2b-R-NotI cloned into SpeI/NotI digested pMR15 |
| pMR19 | SpeI/NotI digested PCR product amplified from *M. acetivorans* genomic DNA using TBP3b-F-SpeI and TBP3b-R-NotI cloned into SpeI/NotI digested pMR16 |
| pMR34 | ApaI/XhoI digested PCR product amplified from *M. acetivorans* genomic DNA using TBP2a-F-ApaI and TBP2a-R-XhoI cloned into ApaI/XhoI digested pJK301 |
| pMR35 | ApaI/XhoI digested PCR product amplified from *M. acetivorans* genomic DNA using TBP3a-F-ApaI and TBP3a-R-XhoI cloned into ApaI/XhoI digested pJK301 |
| pMR37 | SpeI/NotI digested PCR product amplified from *M. acetivorans* genomic DNA using TBP2b-F-SpeI and TBP2b-R-NotI cloned into SpeI/NotI digested pMR34 |
| pMR38 | SpeI/NotI digested PCR product amplified from *M. acetivorans* genomic DNA using TBP3b-F-SpeI and TBP3b-R-NotI cloned into SpeI/NotI digested pMR35 |
| pMR54 | NcoI/ApaI digested PCR product amplified from *M. acetivorans* genomic DNA using TetR-1a-F-NcoI and TetR-1a-R-ApaI cloned into NcoI/ApaI digested pGK050A |
| pMR58 | NdeI/HindIII digested PCR product amplified from *M. acetivorans* genomic DNA using TetR-1b-F-NdeI and TetR-1b-R cloned into NdeI/HindIII digested pMR54 |
| pMR56 | NcoI/ApaI digested PCR product amplified from *M. acetivorans* genomic DNA using TetR-2a-F-NcoI and TetR-2a-R-ApaI cloned into NcoI/ApaI digested pGK050A |
| pMR59 | NdeI/BsrGI digested PCR product amplified from *M. acetivorans* genomic DNA using TetR-2b-F-NdeI and TetR-2b-R cloned into NdeI/BsrGI digested pMR56 |
| pMR57 | Bsu361/ApaI digested PCR product amplified from *M. acetivorans* genomic DNA using TetR-3a-F-Bsu361 and TetR-1a-R-ApaI cloned into Bsu361/ApaI digested pGK050A |
| pMR60 | NdeI/HindIII digested PCR product amplified from *M. acetivorans* genomic DNA using TetR-3b-F-NdeI and TetR-3b-R-HindIII cloned into NdeI/HindIII digested pMR57 |
| pMR53 | PCR product amplified using PmtaC2F-SphI and PmtaC2R-NdeI cloned into pSC-A by |

| | |
|---|---|
| | TA cloning |
| pMR48 | NdeI/SphI digested PCR product amplified from *M. acetivorans* genomic DNA using TetR-1b-F-NdeI and TBP1-R-His-SphI cloned in NdeI/SphI digested pMR53 |
| pMR49 | NdeI/SphI digested PCR product amplified from *M. acetivorans* genomic DNA using TetR-2b-F-NdeI and TBP2-R-His-SphI cloned in NdeI/SphI digested pMR53 |
| pMR50 | NdeI/SphI digested PCR product amplified from *M. acetivorans* genomic DNA using TetR-3b-F-NdeI and TBP3-R-His-SphI cloned in NdeI/SphI digested pMR53 |
| pMR52/52B | SphI digested P*mtaCB2::tbp1-his6* sub-cloned from pMR48 into SphI digested pWM321. Insert has opposite orientation in pMR52B |
| pMR62/62B | SphI digested P*mtaCB2::tbp2-his6* sub-cloned from pMR49 into SphI digested pWM321. Insert has opposite orientation in pMR62B |
| pMR64/64B | SphI digested P*mtaCB2::tbp3-his6* sub-cloned from pMR50 into SphI digested pWM321. Insert has opposite orientation in pMR64B |
| pMR76 | ApaI/XhoI digested PCR product amplified from *M. acetivorans* genomic DNA using T3302A-F-ApaI and 3302A-R-XhoI cloned into ApaI/XhoI digested pJK301 |
| pMR80 | SpeI/NotI digested PCR product amplified from *M. acetivorans* genomic DNA using 3302B-F-SpeI and 3302B-R-NotI cloned into SpeI/NotI digested pMR76 |

## References


1. **Guss, A. M., M. Rother, J. K. Zhang, G. Kulkarni, and W. W. Metcalf.** 2008. New methods for tightly regulated gene expression and highly efficient chromosomal integration of cloned genes for Methanosarcina species. Archaea **2:**193-203.
2. **Metcalf, W. W., J. K. Zhang, E. Apolinario, K. R. Sowers, and R. S. Wolfe.** 1997. A genetic system for Archaea of the genus Methanosarcina: liposome-mediated transformation and construction of shuttle vectors. Proc Natl Acad Sci U S A **94:**2626-31.
3. **Pritchett, M. A., J. K. Zhang, and W. W. Metcalf.** 2004. Development of a markerless genetic exchange method for Methanosarcina acetivorans C2A and its use in construction of new genetic tools for methanogenic archaea. Appl Environ Microbiol **70:**1425-33.
4. **Rother, M., and W. W. Metcalf.** 2005. Genetic technologies for Archaea. Curr Opin Microbiol **8:**745-51.
5. **Sowers, K. R., S. F. Baron, and J. G. Ferry.** 1984. Methanosarcina acetivorans sp. nov., an Acetotrophic Methane-Producing Bacterium Isolated from Marine Sediments. Appl Environ Microbiol **47:**971-978.

# Curriculum Vita

**Matthew James Reichlen**

## Education:

Aug 2003 - Present

Ph.D. candidate in Biochemistry Microbiology and Molecular Biology program
The Pennsylvania State University, University Park, PA.

Aug 1999 – May 2003

B.S. in Biology, B.A. in Philosophy *cum laude*
The University of Scranton, Scranton, PA.

## Research Experience:

Jan 2004 – Present

Graduate research assistant in the department of Biochemistry and Molecular Biology under the guidance of James G. Ferry and Katsuhiko Murakami

Thesis: Functional assessment of transcriptional regulation in the methanogen, *Methanosarcina acetivorans*

## Honors and Awards:

Jun 2009 – Present

Stanley Person fellowship for outstanding graduate research

## Publications:

- **Reichlen, M.J., Murakami, K.S. and J.G. Ferry.** 2010. Identification of MA3302, a putative regulator of acetate metabolism in *Methanosarcina acetivorans*. In preparation.

- **Reichlen, M.J., Murakami, K.S. and J.G. Ferry.** 2010. Genome-wide transcription profiling of *Methanosarcina acetivorans* diauxic growth on methanol and acetate. In preparation.

- **Reichlen, M.J., Murakami, K.S. and J.G. Ferry.** 2010. Functional analysis of the three TBP homologs in *Methanosarcina acetivorans*. J Bacteriol. **192**(6):1511-7.

- **Doerfert, S.N.†, Reichlen, M.†, Iyer, P., Wang, M., and J.G. Ferry.** 2009. *Methanolobus zinderi* sp. nov., a methylotrophic methanogen isolated from a deep subsurface coal seem. IJSEM. **59:**1064-9.
  † These authors contributed equally to this work.

- **Lessner, D.J., Li, L., Li, Q., Rejtar, T., Andreev, V.P., Reichlen, M., Hill, K., Moran, J.J., Karger, B.L. and J.G. Ferry.** 2006. An unconventional pathway for the reduction of $CO_2$ to methane in CO-grown *Methanosarcina acetivorans* revealed by proteomics. PNAS. **103**(47):17921-6.